



Improving thermal energy storage via storage retrofit and digital twin technology

by Lukas Kasper

A thesis for the degree of
Doctor technicae

In the
Doctoral Program in Engineering Sciences – Mechanical Engineering

At the
Faculty of Mechanical and Industrial Engineering, TU Wien

Under the supervision of
René Hofmann, TU Wien

Reviewed by
Simon Harvey

and
Martin Kozek

Author

Lukas Kasper



Supervisor

René Hofmann
TU Wien
Institute for Energy Systems and
Thermodynamics
Getreidemarkt 9/E302
1060 Wien

Reviewers

Simon Harvey
Chalmers University of Technology
Department of Space, Earth and Envi-
ronment
Division of Energy Technology
Hörsalsvägen 7B
412 96 Gothenburg, Sweden

Martin Kozek
TU Wien
Institute of Mechanics and Mechatronics
Research Unit of Control and Process
Automation
Getreidemarkt 9/E325
1060 Wien

Going to press

I confirm that going to press of this thesis needs the confirmation of the examination committee.

Affidavit

I declare in lieu of oath, that I wrote this thesis and performed the associated research myself, using only literature cited in this volume. If text passages from sources are used literally, they are marked as such. I confirm that this work is original and has not been submitted elsewhere for any examination, nor is it currently under consideration for a thesis elsewhere.

I acknowledge that the submitted work will be checked electronically-technically using suitable and state-of-the-art means (plagiarism detection software). On the one hand, this ensures that the submitted work adheres to the high-quality standards of the current rules for ensuring good scientific practice "Code of Conduct" at the Vienna University of Technology. On the other hand, a comparison with other students' theses avoids violations of my copyright.

Vienna, June 2023

Lukas Kasper

Abstract

Energy systems are currently undergoing necessary but drastic changes toward sustainability. As renewable energy sources are taking over, their intermittent nature challenges industrial energy systems to increase flexibility and energy efficiency of operation. In this context, thermal energy storage (TES) emerges as a pivotal technology by enabling balancing of energy supply and demand as needed. At the same time, rapid digitalization developments and especially digital twin (DT) technology promise a paradigm shift of automation and optimization. However, major drawbacks remain. Firstly, investment costs are a critical impediment to increasing TES capacity. Secondly, industrial-scale TES remains very complex to operate, as DT solutions have yet to mature.

To overcome the first issue, this thesis investigated a novel hybrid TES prototype. The goal of the hybrid concept is an economic and technically feasible option to retrofit widely used steam storage with phase change material (PCM), thereby increasing capacity. In this work, design guidelines for PCM arrangement were derived via numerical modeling, and the concept's potential but also engineering challenges were revealed in experimental studies.

To further improve the practical utilization of TES, this thesis introduced methods for more intelligent system operation. Digitalization applications and DT solutions provide immense capabilities for this aim but still require focused research. Therefore, a DT platform was developed that bridges the gap between the latest research and technology on DTs in computer engineering and the actual implementation and value creation in the energy sector. Equipped with powerful services on this intelligent platform, the DT can automatically adapt its virtual models to physical behavior, as demonstrated in this work. A DT was deployed on a TES test rig, emulating a use case of waste heat recovery in steel production. Experimental tests in live operation enabled qualitative and quantitative evaluation of the developed DT-based methodology. The DT approaches, developed in this work, are tailored to the requirements of industrial energy systems and are thus not bound to their application for energy storage alone.

Kurzfassung

Energiesysteme weltweit durchlaufen derzeit einen notwendigen, aber drastischen Wandel zu Gunsten höherer Nachhaltigkeit. Während die Versorgung auf erneuerbare Energiequellen umgestellt wird, verlangt deren volatiler Charakter höhere Flexibilität und Energieeffizienz industrieller Energiesysteme. Unter dieser Herausforderung erweisen sich thermische Energiespeicher (TES) als eine zentrale Technologie, die den Ausgleich von Energieversorgung und -bedarf ermöglicht. Gleichzeitig verspricht die rasante Digitalisierung mit Entwicklungen wie dem digitalen Zwilling (digital twin – DT) einen Paradigmenwechsel in Automatisierung und Optimierung. Allerdings gilt es noch einige Schwierigkeiten zu überwinden. Einesteils stellen hohe Investitionskosten eine kritische Hürde für die Erhöhung der Kapazität von TES dar. Andererseits ist der Betrieb von TES im industriellen Maßstab nach wie vor sehr komplex, da DT-Lösungen noch nicht ausgereift sind.

Um das erste Problem zu überwinden, wurde in dieser Arbeit ein neuartiger hybrider TES-Prototyp untersucht. Das Ziel des Hybridspeicherkonzepts ist eine sowohl technisch als auch wirtschaftlich sinnvolle Option zur Nachrüstung weit verbreiteter Dampfspeicher mit Phasenwechselmaterial (phase change material - PCM), um so die Kapazität zu erhöhen. In dieser Arbeit wurden mittels numerischer Modellierung Designrichtlinien für die PCM-Anordnung abgeleitet. Anschließende experimentelle Untersuchungen am entwickelten Prototyp zeigen das Potential und weitere technische Herausforderungen des Konzepts auf.

Um die praktische Verwendung von TES weiter zu verbessern, wurden in dieser Arbeit Methoden für einen intelligenteren Betrieb industrieller Energiesysteme entwickelt. Digitalisierungsanwendungen und DT-Lösungen bieten immense Möglichkeiten für dieses Ziel, erfordern aber noch gezielte Forschung. Daher wurde eine praktische DT-Plattform entwickelt, welche die Lücke zwischen der neuesten Forschung und Entwicklung zu DTs in der Informatik und der konkreten Umsetzung und Wertschöpfung in der Energietechnik schließt. Ausgestattet mit leistungsstarken Services auf dieser intelligenten Plattform, kann der DT seine virtuellen Modelle automatisch an physikalisches Verhalten anpassen. Dies wird in dieser Arbeit demonstriert. Zur Erprobung wurde ein DT für den Prüfstand eines TES implementiert, wobei ein Prozess zur effizienten Abwärmenutzung in der Stahlherzeugung den industriellen Use Case bildet. Der experimentelle Live-Betrieb des DT ermöglichte die qualitative und quantitative Evaluierung der entwickelten DT-basierten Lösungen. Die in dieser Arbeit entwickelten DT-Methoden sind auf die Anforderungen industrieller Energiesysteme zugeschnitten und daher nicht nur an die Anwendung für TES gebunden.

Acknowledgements

Four years ago, pursuing a doctoral degree did not even cross my mind. I then started out of sheer interest in the topic but soon developed a great passion for research. It was a choice I never regretted - at least never for long - and I am happy and proud to complete this thesis. However, there were many people who accompanied my journey and whose support I want to acknowledge.

First of all, I want to thank my supervisor Prof. René Hofmann. My time as Prae-Doc in his research unit was stressful, but also incredibly instructive. I am grateful for the opportunity to contribute to so many diverse research projects and also university courses, while still having some freedom for my own research interests. René, thank you for the trust you put in me from the beginning, for your encouragement, and for your many lessons which I hold in high regard.

I am very thankful to all my colleagues over the years, be they industrial partners, professors, fellow research associates, or masters students. Collaborating with so many interesting people and dismantling every minor detail in inspired discussions brings the true joy to scientific work. Here, I want to thank not exclusively but especially my colleagues Dominik, Paul, and Felix. Not only did they significantly contribute to the broader context of my thesis topic with their own respective work, but they provided great support and never turned down critical discussions on my ideas.

Most importantly, I thank my family for their support: My parents, Helga and Alfred, for the attitude to life they handed to me and for always encouraging me in my decisions. My grandmother Poldi, for spearheading my education since Kindergarten and for her loving support. And, my girlfriend Nicki, for cheering me up during rough patches, tolerating my late-night work sessions, and giving me a reason to torment myself in these studies so she can legitimately put a *Dr.* in front of my nickname. Without you, life would be dreary.

*Any sufficiently advanced technology
is indistinguishable from magic.*

ARTHUR C. CLARKE

Preface

This thesis for the degree of Doctor technicae was arranged as a cumulative dissertation. As opposed to a monograph, it consists of a series of individual contributions to scientific literature published during the timeframe of the doctorate study. In terms of academic accreditation, cumulative dissertations and monographs are subject to the same formal requirements. Therefore, this document not only contains the core publications of my scholarly work, but also a synopsis establishing the contextual link of the individual articles within the overarching scope of this thesis and expounding the coherent contribution to scientific progress. The research presented in my core publications, five journal papers, were not part of any other theses for an academic degree.

This thesis was compiled during my employment at TU Wien at the Institute of Energy Systems and Thermodynamics in the research unit Industrial Energy Systems¹ starting in July, 2019. Along my teaching activities, I had the chance to contribute to several national and international funded research projects, most notably

- HyStEPs - Hybrid storage for efficient processes² (FFG project number 868842),
- DIGI STEAM - Digitalization in the energy sector: Identification of digitalization possibilities in the energy sector especially in the field of steam supply systems³ (vgbe project number 429),
- 5DIndustrialTwin - 5D Digital Twin for Industrial Energy Systems⁴ (FFG project number 881140),
- SINFONIES - Sustainability IN Flexibly Operated reNewable Industrial Energy Systems⁵ (FFG project number 871673), and the
- IEA IETS Task XVIII on “Digitalization, Artificial Intelligence and Related Technologies for Energy Efficiency and GHG Emissions Reduction in Industry”⁶ (national funding under FFG project number 883006).

My involvement in these projects and the consequent scientific exchange significantly shaped the research for this thesis.

¹<https://www.tuwien.at/en/mwbw/iet/e302-03-research-unit-of-industrial-energy-systems>

²<https://www.nefi.at/de/projekt/hysteps>

³https://www.vgbe.energy/fe429_abschlussbericht

⁴<https://energieforschung.at/projekt/5d-digital-twin-fuer-industrielle-energiesysteme/>

⁵<https://energieforschung.at/projekt/sustainability-in-flexibly-operated-renewable-industrial-energy-systems/>

⁶<https://iea-industry.org/tasks/digitalization-artificial-intelligence-and-related-technologies-for-energy-efficiency-and-ghg-emissions-reduction-in-industry/>

Contents

List of Figures	xv
List of Tables	xv
Nomenclature	xvii
Research summary	1
1 Introduction	1
2 Context	6
2.1 Thermal energy storage	8
2.2 Digitalization and digital twin technology	14
3 Problem statement	18
4 Research approach	20
5 Conclusion and outlook	25
5.1 Scientific contribution	25
5.2 Outlook	27
References	31
Publications	45
Paper 1	46
<i>Numerical studies on the influence of natural convection under inclination on optimal aluminium proportions and fin spacings in a rectangular aluminium finned latent-heat thermal energy storage</i>	
Paper 2	64
<i>Experimental characterization, parameter identification and numerical sensitivity analysis of a novel hybrid sensible/latent thermal energy storage prototype for industrial retrofit applications</i>	
Paper 3	84
<i>Digitalization possibilities and the potential of the Digital Twin for steam supply systems</i>	
Paper 4	94
<i>Toward a Practical Digital Twin Platform Tailored to the Requirements of Industrial Energy Systems</i>	
Paper 5	124
<i>A digital twin-based adaptive optimization approach applied to waste heat recovery in green steel production: Development and experimental investigation</i>	
Further publications and other scientific contributions	151
About the author	161

List of Figures

1	Past and future global primary energy supply by source	2
2	Development of energy sources until 2050 under the current scenario “Net Zero Emissions by 2050 (NZE)” of the International Energy Agency (IEA) 2022 to accomplish the 1.5 °C global warming “target”	3
3	Electric energy systems face a “flexibility gap” gap due to the phase-out of fossil-fueled power plants and the increasing share of renewable-based generation	4
4	Results of a recent survey on the perception of digitalization in the energy sector of the United Nations Economic Commission for Europe (UNECE) 2022	7
5	Categorization and thermodynamic characteristic of sensible, latent and thermo-chemical TES	9
6	Simplified illustration of the hybrid storage concept first introduced by Dusek & Hofmann 2018	13
7	Simplified illustration of the 5D-DT modeling concept introduced by Tao et al. 2019b.	16
8	Overview of publications and their contextual embedding into this thesis .	20

List of Tables

1	Comparing of the general characteristics of the three main TES types . .	10
---	--	----

Nomenclature

Acronyms

5D	five dimensional
AI	Artificial Intelligence
CCSU	Carbon capture, storage and utilisation
DT	Digital twin
DTs	Digital twins
EAF	Electric arc furnace
GDTA	Generic digital twin architecture
GHG	Greenhouse gas
HTF	Heat transfer fluid
I4.0	Industry4.0
IEA	International Energy Agency
IoT	Internet of Things
IRENA	International Renewable Energy Agency
LHTES	Latent heat thermal energy storage
MILP	Mixed-integer linear programming
MPC	Model predictive control
OPC UA	Open Platform Communications Unified Architecture
P&I	Pipe and Instrumentation
PBTES	Packed bed thermal energy storage

PCM	Phase change material
RAMI4.0	Reference Architecture Model Industry 4.0
RQ	Research question
RSS	Ruths steam storage
SCADA	Supervisory control and data acquisition
SOC	State of charge
SQL	Structured Query Language
TES	Thermal energy storage
UC	Unit commitment
UNIDO	United Nations Industrial Development Organization

Parameters and Variables

Δl_m	Specific latent heat (kJkg^{-1})
ΔT	Temperature difference between low and high temperature level (K)
c_p	Specific heat capacity ($\text{kJkg}^{-1}\text{K}^{-1}$)
m	Mass (kg)
Q_{latent}	Latent storage heat (J)
Q_{sensible}	Sensible storage heat (J)

Research summary

This introductory chapter of my cumulative thesis provides a synopsis of its core publications and establishes the contextual link of the individual articles within the overarching scope of this thesis.

In Section 1, I explain why we need to *improve thermal energy storage* in facing human-induced global warming, one of the world's biggest challenges of the 21st century, as well as the basic considerations to achieve this. Section 2 summarizes the industrial and scientific state of the art within the subject area, which this thesis aims to extend. It further provides essential theoretical and methodical background information. The specific problem statement, which my work addresses, is given in Section 3 together with corresponding research questions. Section 4 links the publications within the overarching research framework. It explains which part of this thesis is covered in each paper and summarizes their content and results. The thesis is concluded in Section 5, where the academic contribution is discussed with regard to the stated research questions.

1 Introduction

We are currently in the middle of one of the biggest revolutions in the energy sector in history. Only three transitions before were of comparable magnitude: Firstly, the big shift from traditional biomass to fossil fuels as the primary energy source during the Industrial Revolution, beginning in the 18th century. Secondly, the period of Electrification in the late 19th century/ early 20th century, which saw the establishment of early power plants and their grid connections to homes, businesses, and industries that allowed for widespread access to electricity. Thirdly, the subsequent oil and gas revolution, triggered by advances in drilling, oil refinement, and combustion engines. From this point forward, we heavily relied on fossil fuels for heating, transportation, and electricity generation. While these energy revolutions lead to unprecedented economic growth and prosperity in large parts of the world, in retrospect, we know that they also took a huge toll on our planet's health. In 2019, approximately 79% of global greenhouse gas (GHG) emissions originated from fossil fuel consumption in the sectors of energy, industry, and transport (Intergovernmental Panel on Climate Change (IPCC) 2023). GHG emissions are the main driver for climate change which threatens ecosystems, biodiversity, and human wellbeing. Slowly, most people and governments have acknowledged the fact that we need to reduce these GHG emissions drastically and rapidly to mitigate these effects as best as possible, which is currently the main driver of change in energy systems.

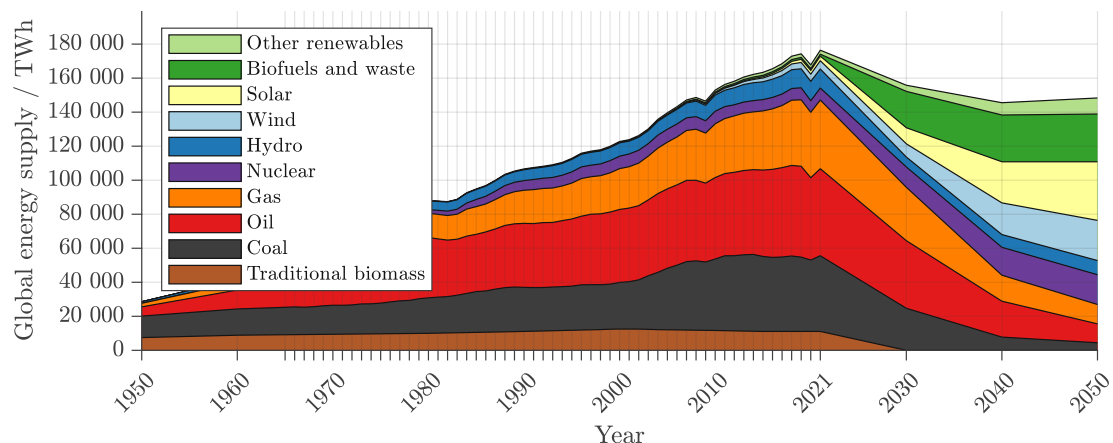


Figure 1: *Past and future global primary energy supply by source.*

Note: Historic data until 2021 from Ritchie et al. 2022 based on Smil 2017 and BP 2022. Future data corresponds to the scenario “Net Zero Emissions by 2050 (NZE)” of the International Energy Agency (IEA) 2022.

The current energy transition is marked by the continuing replacement of fossil fuels with sustainable, renewable energy sources such as solar wind, hydro, and geothermal power (see Figure 1). The International Renewable Energy Agency (IRENA) 2023 estimates that the share of renewable energy in the global primary energy supply must grow from 16 % in 2020 to 77 % in 2050 given the currently targeted 1.5 °C Scenario in the Paris Agreement (i.e., limiting global warming to a maximum increase of 1.5 °C above pre-industrial levels). However, about 37 % of total energy consumption originates from the industry sector (Wei et al. 2019), which still relies on direct fossil fuel combustion for more than 60 % of its energy supply, see Figure 2a. This slow abandonment of fossils is mainly explained by high-temperature process heat requirements, but also cost-sensitivity and the long design life of equipment (Wei et al. 2019). Worldwide, heat generation in the industry sector causes 21 % of global CO₂ emissions (Global Carbon Project 2019) to drive, often via steam, processes like fluid heating, distillation, drying, chemical reactions, or metal melting and processing (Thiel & Stark 2021). To achieve the widespread defossilisation of industrial energy supply, efficiency improvements, e.g., by excess heat utilization, but also direct electrification are key (Gerres et al. 2019). Thus, the International Renewable Energy Agency (IRENA) 2023 concluded that the global electricity generation must at least triple from 2021 to 2050, see Figure 2b. Moreover, the share of renewable energy sources in electricity generation, such as solar photovoltaic, wind, and hydropower, is expected to double from 40 % in 2021 to more than 80 % in less than 30 years, see Figure 2b. However, an electricity grid based on renewable energy sources combined with the huge demand of an electrified industry raises some obstacles. The main challenge with most renewables is their intermittent nature. For example, solar irradiation and wind speed are very volatile and, on top of that, will remain hard to predict. Future energy systems must therefore solve the balancing issue between energy supply and demand. In the past, flexibility rested primarily on the energy supply side, e.g., in the form of conventional fossil-fueled power plants. Due to their gradual phase-out, the flexibility on the supply side is decreasing.

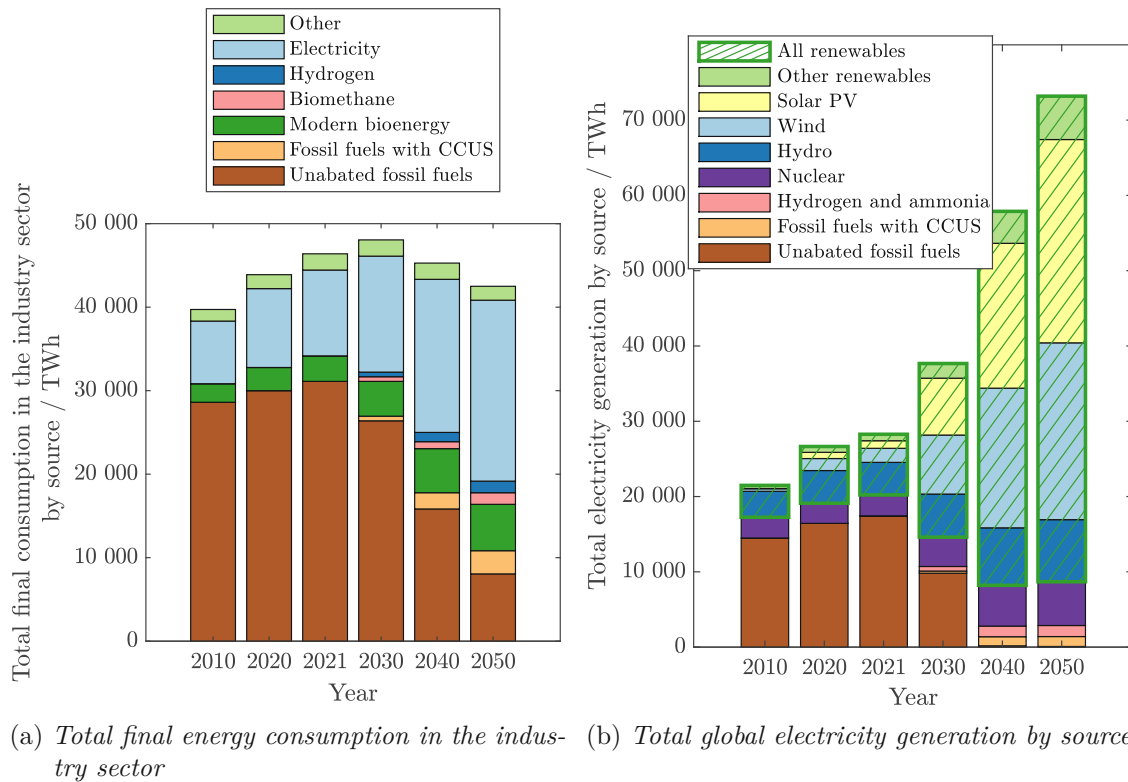


Figure 2: *Development of energy sources until 2050 under the current scenario “Net Zero Emissions by 2050 (NZE)” of the International Energy Agency (IEA) 2022 to accomplish the 1.5°C global warming “target”*

Leinauer et al. 2022 and Papaefthymiou et al. 2018 refer to this development as the “flexibility gap”, which is illustrated in Figure 3. It is therefore evident that additional flexibility on the demand side is essential (Biegel et al. 2014).

A widely acknowledged option to increase this much-needed demand-side flexibility is demand response (or demand-side management) of residential, commercial, and industrial consumers (Lund et al. 2015). While different concepts for demand response exist, the basic idea is that consumers can (or must) adjust their consumption pattern based on signals sent by the grid system operator depending on the balancing needs (Jordehi 2019). Such signals either require immediate action or announce changes in advance, e.g., day-ahead, and their response is typically rewarded via price incentives. Of course, also volatile market prices can be a natural incentive for consumer demand balancing. Especially the energy-intensive industry may significantly contribute to closing the arising flexibility gap (Leinauer et al. 2022) in energy systems, since it consumes more than 30% of the global electricity demand. Papaefthymiou et al. 2018 states that large industrial consumers, such as steel and aluminum mills, constitute not only the greatest but often also the most cost-effective potential for demand-side flexibility. In fact, industrial plants have several advantages compared to residential or commercial consumers (Fattras et al.

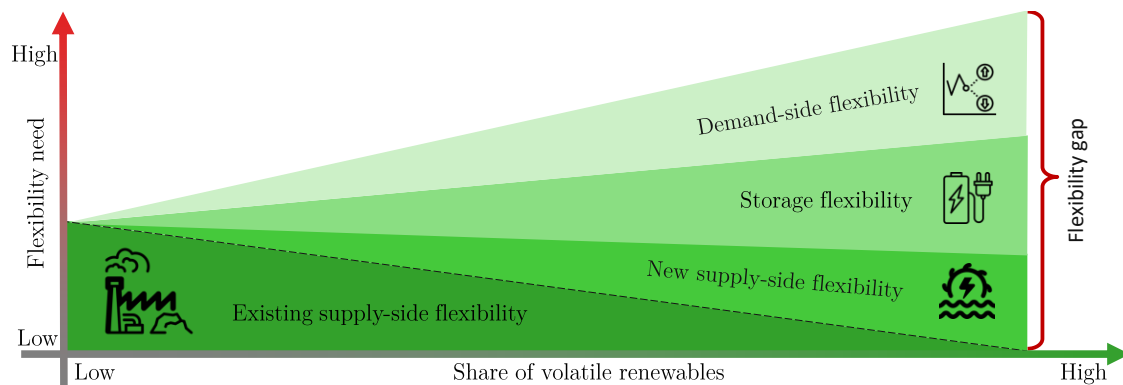


Figure 3: *Electric energy systems face a “flexibility gap” gap due to the phase-out of fossil-fueled power plants and the increasing share of renewable-based generation.*
Note: Adapted from Papaefthymiou et al. 2018.

2022). They feature, for example, large consumption volumes, and enablers like installed load monitoring devices, allowing load scheduling at high time resolution (Shoreh et al. 2016). However, a major drawback is that industrial energy demand is typically very inflexible due to process requirements (Lund et al. 2015). Olsthoorn et al. 2015 and Leinauer et al. 2022 found that, besides present regulatory shortcomings, the technical risk of operation disruption, the impact on product quality, and uncertainties about cost savings are the most relevant barriers impeding flexibility enhancement.

Out of this predicament, it is obviously pivotal to store energy on the demand side: Energy storage enables the decoupling of energy supply and demand. The clever operation of industrial sites with physical storage enables flexible consumption without obstructing process requirements. The question remains of how this storage is achieved. Lund et al. 2015 states that the demand for thermal energy dominates the global final energy use, and it is also easier to store thermal energy than electricity. In fact, high-temperature heat ($> 500\text{ }^{\circ}\text{C}$), required, e.g., in iron, steel, cement, and lime production, accounts for more than 50 % of the final energy consumption in the whole European industry sector (Naegler et al. 2015). Another big part is consumed for process heat at temperatures between $100\text{ }^{\circ}\text{C}$ and $500\text{ }^{\circ}\text{C}$, e.g., in pulp & paper, food production, and chemical industries (Naegler et al. 2015). Therefore, it is clear that the greatest industrial energy storage potential is to store heat, i.e., thermal energy, in thermal energy storage (TES). Arce et al. 2011 showed that TES can potentially reduce total CO_2 emissions in the EU by up to 6 % in the residential and industrial sector alone. Furthermore, TES typically features lower prices and higher cycle efficiency than electric battery storage (Lund et al. 2016).

Despite excellent technical options as well as the great potential for operational cost benefits for TES integration, Martin & Chiu 2022 found that TES is rarely used in industrial applications. They conclude that this has likely to do with two important aspects that impede the commercial feasibility (p. 744):

- *TES can increase complexity to processes, and thus increase the operational risk.*

- *An economically feasible TES, with payback on investment of only a few years, is still an investment that need to compete with other investments closer to the core of the business itself.*

However, they also state that the increasing cost of energy will make an investment in TES more attractive, if not necessary (Martin & Chiu 2022). In fact, the International Renewable Energy Agency (IRENA) 2020 estimated that the total installed TES capacity will increase from 234 GWh in 2019 to 800 GWh in 2030. Since profitability and short payback times are key criteria for investment decisions in the industry, cost-effective integration scenarios for TES and the best possible exploitation of available capacity are crucial. Therefore, TES technology must improve further. The International Renewable Energy Agency (IRENA) 2020 specified the most important research and innovation objectives across different TES technologies for industry in their TES Innovation Outlook of 2020 as (p. 82):

- *Develop TES materials that are more suitable for industrial application considering factors such as operating temperature ranges and discharge power.*
- *Develop systematic approaches for designing TES systems to better integrate renewable technologies in industrial processes. Enhanced system modularity could be used to address issues of scale. Emphasis should be placed on optimizing heat transfer efficiencies.*
- *Develop advanced control and operation systems for TES, to ensure storage is stable and flexible for energy-intensive industrial processes.*

Plainly spoken, we need to find ways to:

- increase TES capacity in a technically feasible and economically viable manner, and
- use that TES more intelligently.

Only if industrial energy systems have sufficient TES capacity and are able to operate it cleverly, do they have the flexibility to contribute to the sustainable energy system transition. This is the motivation for this thesis.

2 Context

Energy storage will play an important role in the current energy transition since it enables the flexibility necessary due to volatile renewable energy supply. The basic principle of energy storage is simple: Besides just maintaining energy content (idle), storage can absorb abundant energy (charging) and release energy when it is needed (discharging). The state of charge (SOC) increases through charging and decreases when discharging and is limited by the storage capacity. In reality, also conversion losses of energy during charging/discharging occur and continual losses can reduce the SOC. The storage's power, i.e., the rate at which energy can be charged and discharged, is limited and can also depend on the current SOC or other factors. Technically, energy is always stored in the form of internal, potential, or kinetic energy, but it is common practice to classify energy storage systems according to the physical form of energy stored, i.e., electrical, chemical, mechanical, and thermal energy (Sterner & Stadler 2019). For industrial application, TES is especially well suited, since on-site process heat production accounts for about 74 % of total industrial energy use (International Renewable Energy Agency (IRENA) 2020). This potential of TES has led to growing research interest. Research activity in high-quality journals has increased exponentially without stagnation since 2000 (Calderón et al. 2020).

While substantial research has been dedicated to this area, and TES technology matures more and more, its integration in energy-intensive industry still lags behind. Besides technical and physical restrictions, costs are a major barrier to the application of TES. Typically, process technologies and energy supply systems have long lifetimes of several years to decades (Gibb et al. 2018). Rathgeber et al. 2022 states that in the industry sector, high interest rates of 10 % and above and short payback periods of 5 years and below are usual. Therefore, high initial capital costs are a major impediment to TES (Therkelsen & McKane 2013). Additionally, process requirements may change frequently and retrofit approaches that feature small changes in the infrastructure of the energy system have special relevance for the current transition phase (Gibb et al. 2018). To see the tripling of global TES capacity in only 10 years until 2030, projected by the International Renewable Energy Agency (IRENA) 2020, economically and technically feasible options to increase TES capacity are needed.

Phasing out fossil fuels, as introduced in Section 1, is not the only development that is shaking up the energy sector. Vahidinasab & Mohammadi-Ivatloo 2023 state that there are four challenges in the way toward future energy systems that will solve the energy trilemma of sustainability, affordability, and security of supply: *Decarbonization*, *Decentralization*, *Digitalization*, and *Democratization*. In fact, besides the liberalization of the energy market with new participation concepts and tariffs and the spatially distributed nature of renewable electricity generation, digitalization has been a big topic for years. Accelerated by the manufacturing sector under the catchword “Industry4.0” (I4.0), this development is expected to have an immense impact on energy systems (Xu et al. 2022).

We rely on digital models of physical TES not only for design but also for operation. On the one hand, not all states within TES can be measured. On the other hand, complex

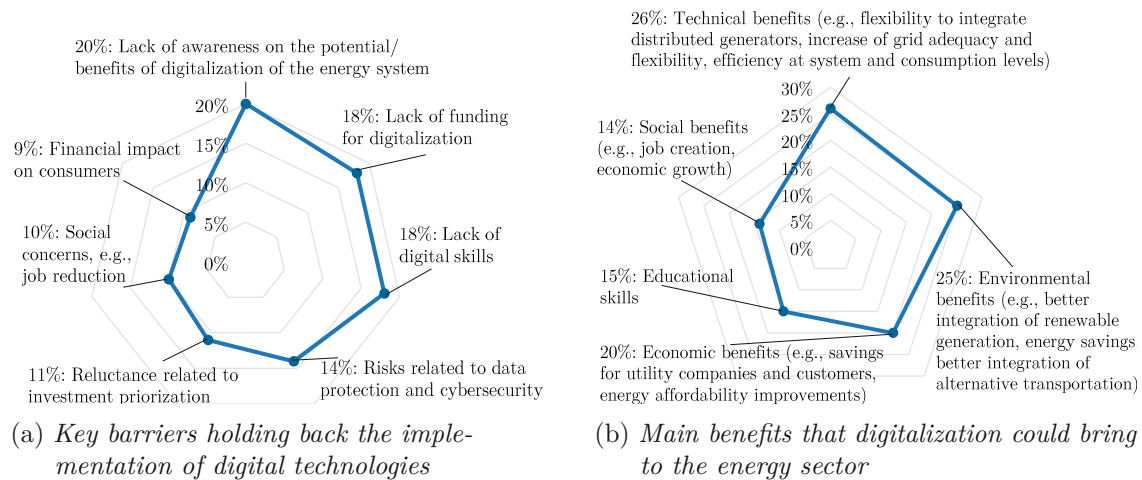


Figure 4: Results of a recent survey on the perception of digitalization in the energy sector of the United Nations Economic Commission for Europe (UNECE) 2022

industrial TES cannot be efficiently controlled by simple control strategies as, e.g., for household hot-water storage. Also, industrial energy demand is often well-known by a specified production/process schedule in advance. Thus, the ability to accurately predict TES behavior is of great value. This is where digitalization developments can make a big impact. The UNIDO 2017 stated that the sustainable energy transition and the digital transformation of industry can mutually benefit from each other. There are already a fair amount of examples attesting this symbiosis. Digitalization provides new capabilities for process optimization (Xu et al. 2019; Min et al. 2019), prediction (Prawiranto et al. 2021), monitoring (Yu et al. 2020), and control (Zabala et al. 2020), predictive maintenance, as well as fault detection and analysis (Abdrakhmanova et al. 2020), to name a few. Most importantly, digitalization has great potential in addressing the aforementioned flexibility gap. Based on a review of digital applications in the energy sector, Weigel & Fishedick 2019 concluded that, while in the past, the generation followed the demand, digitalization will enable demand to follow generation, to some extent, by providing the necessary information and control infrastructure. The International Energy Agency (IEA) 2017 projects for 2040 that energy curtailment, i.e., the forced temporal reduction of electricity production by renewables, can be limited from 7% to 1.6% by digitally enabled demand response measures and additional energy storage. This in turn would boost the share of renewable electricity generation and reduce GHG emissions. A recent survey by the United Nations Economic Commission for Europe (UNECE) 2022 found that the general perception is that digitalization could bring great technical, environmental and economic benefits to energy systems (see, Figure 4). However, at the same time, the lack of awareness of the potential and benefits of digitalization in the sector is reckoned as the most critical barrier holding back the implementation of digital technologies.

The digital twin (DT) is often seen at the pinnacle of digitalization or at least as the key enabler for realizing the widespread application of digital solutions and thus aiding the energy transition (Lu et al. 2020). A DT is, in essence, a virtual replica of a physical

object. However, a DT should be more than a model (Kritzinger et al. 2018) in that it automatically adapts to real-world changes and is able to predict and control its physical counterpart. Furthermore, a DT should offer a large number of value-generating services to the real system (Cimino et al. 2019). DTs of energy system components, such as TES, or even whole industrial energy systems, could fundamentally change the way energy systems operate (Yu et al. 2022). The adaptivity of DTs could provide major benefits for industrial TES operating in harsh conditions. DTs could also increase automation and reduce uncertainty about flexibility potentials, both of which are crucial for power grid services such as demand response (Leinauer et al. 2022). However, DT technology is still in its early development stage. Implementation requirements, frameworks, and even benefits need to be investigated. A recent review on DT technology for industrial energy management by Yu et al. 2022 resulted in eight critical future research directions, including service and maintenance applications, adaptive DT technology for real-world behavior changes, specification of DT software requirements, and, engineering of machine learning-driven techniques.

The motivation for this thesis is to counteract the growing global flexibility gap, introduced in Section 1, by improving the thermal energy storage potential of industrial energy systems. Based on the current options, I approached this problem via TES retrofit and DT technology. In the remainder of this section, relevant principles, methods, and applications for the technological aspects investigated in this thesis are outlined and set into context. At the beginning of each section, a general overview is presented before the state of the art relevant to this work is introduced in detail.

2.1 Thermal energy storage

TES can be grouped into various different categories regarding the selection criteria. For example, categorization according to temperature level, storage duration, or the storage system's heat carrier or heat-transfer fluid (HTF) (Sterner & Stadler 2019; Zhang et al. 2016). However, the most used distinction in literature is after the physical form of stored energy (Maruf et al. 2022; Gil et al. 2010). This results in three different types: Sensible, latent and thermo-chemical energy storage. The International Renewable Energy Agency (IRENA) 2020 also listed thermo-mechanical energy storage as another separate but promising TES technology. Each TES type has distinctive features regarding stored energy density, response time, cycle efficiency, or temperature range, to name a few. Choosing the best storage system primarily depends on the specific application. Sensible TES is considered the most mature technology (Barbosa et al. 2023). Latent and thermo-chemical storage systems are not commercially mature yet (Esence et al. 2017) and are more complex due to potential component corrosion, toxicity, and chemical instability (Paul et al. 2022). Maruf et al. 2022 states that sensible and latent heat storage have a high technology readiness level (TRL) of 9, while thermo-chemical energy storage technology is still in the early stages of development (TRL 4), despite its potential for long-term storage. Figure 5b illustrates the presented basic categorization together with the corresponding development stage and typical energy density. In the following paragraph, the three main TES types are briefly described.

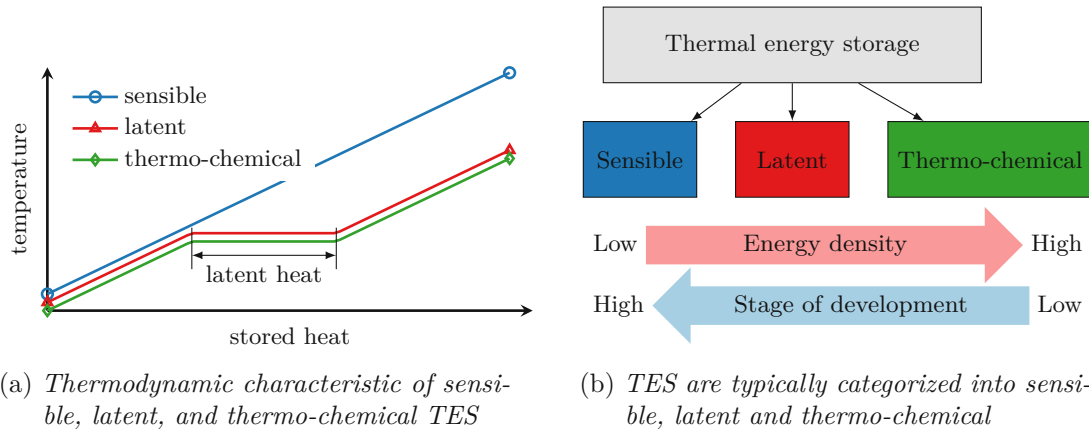


Figure 5: Categorization and thermal characteristic of sensible, latent and thermo-chemical TES. Note: Figure 5b adapted from Sterner & Stadler 2019.

Sensible thermal energy storage is based on the heat capacity of storage media. The energy that is transferred to and from the TES results in a corresponding increase or decrease of the medium's temperature. The amount of energy stored

$$Q_{\text{sensible}} = m \cdot c_p \Delta T \quad (1)$$

(in J) depends on the mass of the storage material m (kg) and its specific heat c_p ($\text{kJkg}^{-1}\text{K}^{-1}$), and is proportional to the temperature difference between low and high temperature level (see Figure 5a). Storage media can be liquid (e.g., water or oil) or solid (e.g., bricks, rock beds, or sand), but are usually selected according to their heat capacity and spatial options (Cabeza et al. 2021). Compared to latent heat, the specific heat of materials is typically 50–100 times smaller (Alva et al. 2018). To achieve similar energy storage densities, large temperature spreads are necessary. Thus, in order to minimize storage losses and increase efficiency, good heat insulation is necessary.

Latent heat thermal energy storage (LHTES) exploits the phase transition of a material. The amount of energy stored

$$Q_{\text{latent}} = m \cdot \Delta l_m \quad (2)$$

(in J) is generally given by the product of the storage material mass m (kg) and the specific latent heat (kJkg^{-1}). During operation however, also the sensible heat Q_{sensible} (1) must be considered. As illustrated in Figure 5a, a large amount of energy is stored at a constant temperature level. An LHTES storage material is usually referred to as phase change material (PCM). In the most frequent case, LHTES use solid-liquid phase change. i.e., heat is stored during melting of the PCM and it is released again during solidification. The nearly isothermal charging/discharging process together with its high energy density compared to sensible TES is often considered the major advantage of LHTES over the latter (Ibrahim et al. 2017). Cabeza et al. 2021 states that although many materials have been studied for use

as PCM, only few of them have been commercialized due to frequent problems such as phase separation, subcooling, corrosion, long-term stability, and low heat conductivity.

Thermo-chemical energy storage refers to TES systems that rely on the chemical reaction of at least two substances for heat absorption and release. Typically, there is a differentiation between three mechanisms: Reversible chemical reactions, adsorption, and absorption (Sternner & Stadler 2019). However, the common feature is that they can store large amounts of energy in a small temperature range, similar to LHTES (see Figure 5a). The subgroup of thermo-chemical TES is not relevant for this work, partly because of their low TRL level, and will not be discussed further. I refer the interested reader to a recent review by Desai et al. 2021.

Table 1 summarizes the advantages and disadvantages of individual TES types briefly introduced above. From this overview, it is clear that various forms of TES exist, at least on an experimental scale, and that they can be tailored to the respective industry sector and application. E.g., TES applications are available for a temperature range from -269°C to around 1600°C (Gasia et al. 2017). Cabeza et al. 2021 presents the main requirements for the specific design of a TES system as: high-energy density, good heat transfer between the HTF and the storage material, mechanical and chemical stability of the storage material, compatibility between the storage material and the container material, complete reversibility of a number of cycles, low thermal losses during the storage period, and easy control. Moreover, the operation strategy, the needed charging/discharging rates, and nominal temperature and enthalpy drops have a large influence. The requirements

Characteristic	Sensible TES	LHTES	Thermo-chemical TES
Energy storage density	Small ($\sim 50 \text{ kWh/m}^3$)	Moderate ($\sim 100 \text{ kWh/m}^3$)	High ($\sim 500 \text{ kWh/m}^3$)
Heat loss during storage	High	High	Minor
Charging/discharging rates	High	Medium	Medium
System complexity	Low	Low	High
Maturity	Industrial scale	Pilot-scale	Laboratory-scale
Costs	Low	Moderate	High

Table 1: Comparing of the general characteristics of the three main TES types. The color scheme indicates the weight of advantages (green) and disadvantages (red). Note: Table adapted from Desai et al. 2021 and Sadeghi 2022. The characteristics can widely differ depending on temperature and other requirements. This table should only provide an overview. For more information, I recommend the interested reader the Handbook of Thermal Energy Storage by Sternner & Stadler 2019 or Advances in Thermal Energy Storage by Cabeza 2021.

most relevant for this thesis were presented by Gasia et al. 2017 in their review on system and materials requirements for high-temperature TES. They established more than 25 requirements for both sensible and latent heat TES to handle in order to ensure optimal performance and further achieve widespread deployment. These can be grouped into chemical, kinetic, physical and thermal (from a material point of view) and environmental, economic and technological (from both material and system points of view) (Gasia et al. 2017).

Hybrid sensible/latent thermal energy storage

As previously stated, each type of TES has its own set of benefits and drawbacks, which vary depending on the particular application. This fact motivates the basic idea of combining different TES in a hybrid configuration to capitalize on their respective advantages and reduce their disadvantages. In 2021, Ding et al. 2021 presented the first-ever literature review on hybrid TES developments. They found that combinations of sensible TES and LHTES are currently the most studied and termed the integration of PCM in hot water tanks as the “classic” hybrid TES system, which was most frequently investigated. Some studies showed that with PCM, the tank volume can be reduced (Bayomy et al. 2019; Abdelsalam et al. 2017), the effective operation time can be extended (Nkwetta et al. 2014), and system efficiency can be enhanced (Zhao et al. 2018). Ding et al. 2021 concluded that more hybrid TES systems need to be explored to overcome the shortcomings such as low efficiency and low storage density of standalone systems.

Sensible hot water storage is mostly applicable in the residential sector (Tatsidjodoung et al. 2013) and for low-temperature industrial processes, e.g., in the food sector. For storage temperatures above the boiling point of water, high-temperature TES are required. Here, the Ruths steam storage (RSS) comes in as a well-known and widely applied sensible TES type in industrial steam systems (see, e.g., Steinmann & Eck 2006, González-Roubaud et al. 2017, Biglia et al. 2017, Kuravi et al. 2013). Worldwide, steam systems account for approximately 30 % of the energy used in industrial facilities (Yang & Dixon 2012). The RSS is a pressure vessel containing a two-phase mixture of liquid water and steam at the equilibrium point. It is also simply known as steam accumulator or, after its working principle, sliding pressure steam storage (Tamme et al. 2005). In general, the RSS can be charged and discharged with either liquid water or steam but typically relies on steam. During charging, superheated or saturated steam at higher pressure is introduced that instantly condenses inside the RSS and thus increases the temperature, liquid filling level, and pressure of the equilibrium. During discharging, saturated steam is released from the vessel leading to evaporation inside the RSS and a decrease in pressure (Goldstern 1970). Hence the expression “sliding pressure” storage. Since the storage medium (steam) is at the same time the HTF, no heat exchangers are required and the RSS achieves high charging and discharging rates. These high rates and fast reaction times are considered the main advantages of the RSS (González-Roubaud et al. 2017; Steinmann & Eck 2006). A disadvantage for some applications is the pressure drop during discharging, which can be circumvented by integrating additional heat sources or introducing PCM inside the

storage vessel (Steinmann & Eck 2006). A further disadvantage is that the RSS capacity is always determined by vessel volume and the allowed pressure operation range. Thus, no capacity expansion is possible during the storage lifetime. Acquiring additional RSS units is rather expensive with the price being mainly driven by the pressure vessel costs at high temperatures (Beck et al. 2021). Since steam systems are a part of almost every major industrial process today (Einstein et al. 2001), cost-effective improvements to traditional RSS technology are highly relevant. Even small increases in the efficiency of steam systems can thus account for considerable energy savings and flexibility enhancement on a global scale.

However, up to now, few research teams have considered a hybrid TES approach involving RSS. The arrangement of pressure-resistant PCM capsules inside the RSS pressure vessel was mentioned by Steinmann & Eck 2006, Buschle et al. 2006, and Tamme et al. 2008. Another proposed option is to use a tube register surrounded by PCM to extend the RSS (Buschle et al. 2006; Tamme et al. 2008). In a novel hybrid storage concept, Dusek & Hofmann 2018 proposed to place PCM-filled containers at the shell surface of the RSS. The authors state that this configuration combines the high charging and discharging rates of the RSS and the high energy density of PCM. This basic concept is illustrated in Figure 6. It is also possible to divide the outer PCM containers into several chambers, enabling the arrangement of PCM with different material properties (Dusek & Hofmann 2019). Such a mixture can lead to an increased charging rate in LHTES (Fang & Chen 2007; Li et al. 2021). Furthermore, an iterated concept of Dusek & Hofmann 2019 considers the integration of electric heating elements or heat exchangers inside the PCM containers. This could prove advantageous since pressure increase in the RSS is delayed and power-to-heat options are enabled, which become increasingly relevant (Nepustil et al. 2016). However, the most critical disadvantage for LHTES performance is the low heat conductivity of most PCM (Ibrahim et al. 2017). Various methods have been discussed to increase the heat transfer between the heat transfer medium and PCM (Merlin et al. 2016). Zayed et al. 2020 presented a recent review on this topic. The most prominent strategies include adding fins or other extended surfaces (Yang et al. 2017; Eslamnezhad & Rahimi 2017; Augspurger et al. 2018; Muhammad & Badr 2017), heat pipes (Motahar & Khodabandeh 2016), porous media (Mesalhy et al. 2005), or nanoparticles (Motahar et al. 2014; Khodadadi & Hosseinizadeh 2007) into PCM.

Leading up to my thesis, only a handful of publications studied the hybrid storage approach illustrated in Figure 6. A first numerical model of the hybrid TES was established by Dusek & Hofmann 2019, validating the RSS sub-model with data from an industrial steel plant. A simulation study of different PCM arrangements was compared and presented in Dusek et al. 2019. A non-linear design optimization tool for such hybrid TES systems was developed by Hofmann et al. 2019a to enable cost-effective retrofitting of conventional RSS. Furthermore, Niknam & Sciacovelli 2023 presented the first holistic techno-economic investigation of the discussed hybrid TES. In their simulation studies, they included capital expenditures, annual fuel, and non-fuel-related operating costs into total TES costs while taking technology lifetime into account. This investigation resulted in 5% less costs for the hybrid TES than for a conventional RSS and additional relative operational savings of about 5.5%, thus confirming previous results of Hofmann et al. 2019a. While previous

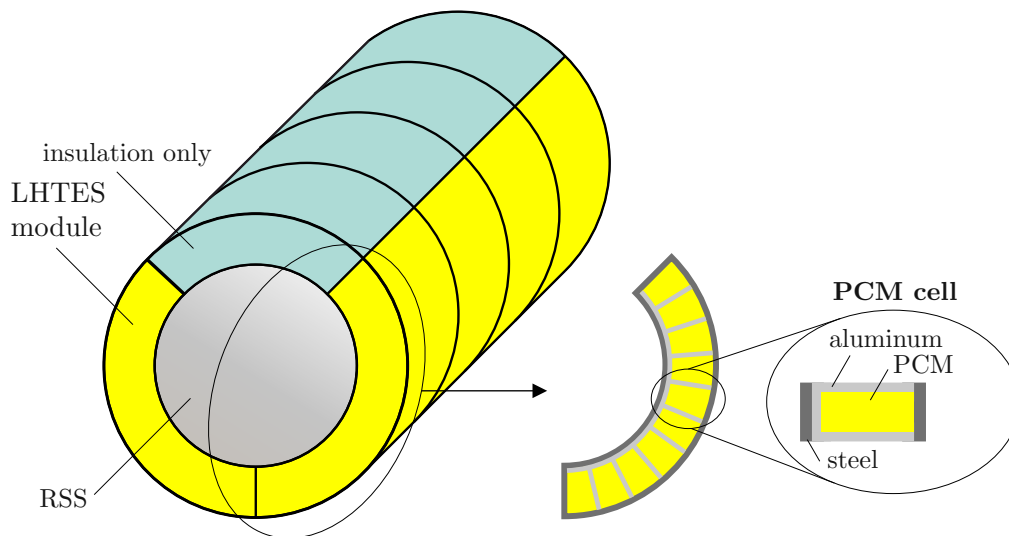


Figure 6: *Simplified illustration of the hybrid storage concept first introduced by Dusek & Hofmann 2018. Aluminium finned LHTES modules filled with PCM are retrofitted to the outer surface of an RSS. Note: Reprinted from the author's previous publication (Kasper et al. 2023b) with permission from Elsevier Ltd.*

research shows that this hybrid RSS/LHTES system could provide advantageous and cost-effective, it lacked some details concerning practical implementation. For example, Niknam & Sciacovelli 2023 modeled the LHTES part only in one dimension and assumed perfect heat transfer between both storage types. Dusek et al. 2019 provided a more detailed two-dimensional LHTES model but neglected natural convection effects. Also, a clear operating strategy for the hybrid TES is missing.

Modeling and operation of thermal energy storage

Digital, mathematical models are essential for both the efficient design and operation of TES. The control of typical TES in the residential sector and even of some industrial TES applications is often very simple, e.g., following timers or simple feedback loops via thermostats (Davis 2015). This is typically very energy-inefficient. More sophisticated strategies such as model predictive controllers (MPC)s are equipped with a model to forecast TES behavior and optimize it according to given system demands.

TES models, be they for design, observation, or control purposes, must account for the main heat transfer and phase transition phenomena occurring in TES. Heat transfer is differentiated into three types: Heat conduction, heat radiation, and convection (natural and/or forced convection). The complex combination of these thermodynamic mechanisms results in strong non-linearities in TES models. For some phenomena, no analytical solution exists, e.g., for transient phase change problems in more than one dimension (Radhakrishnan & Balakrishnan 1992). Numerous approaches were developed in the past to accurately model these effects. Physical models based on exact thermodynamic laws and

numerical discretization methods are typically reliable but require high implementation effort and computational power. Contrary to physical models, data-driven approaches require little or no information about the physical behavior and rely on historic data to find a relationship between the system state variables, e.g., input and output variables. They generally benefit from reduced computational and modeling effort but can lack robustness. Hofmann et al. 2019b presented a comparison of a physical and a hybrid physical/data-driven model, also known as a grey-box model for an industrial TES. From their study, it can be concluded that physical models remain state of the art for detailed TES design analysis. However, data-driven and grey-box models could provide huge advantages for TES operation. A review on the use of Artificial Intelligence (AI) for performance prediction, optimal design, and operational control of TES was recently provided by He et al. 2022. However, regarding operational optimization of industrial energy systems, Maruf et al. 2022 states that mathematical programming can still be considered state of the art. For short and medium-term operation planning on an industrial scale, typically unit commitment (UC) problems are solved to decide on the efficiently timed operation of energy supply, storage, and consumption (Abdi 2021). In the energy sector, this problem is often referred to as energy management (Moretti et al. 2020). Various solution methods have been proposed for energy management, such as dynamic programming, Lagrangian relaxation, simulated annealing, fuzzy logic, genetic algorithms, and linear and mixed-integer linear programming (MILP) (Pernsteiner et al. 2022). However, Moser et al. 2020 state that modern energy management is most frequently based on MILP. MILP is suitable considering runtime and accuracy (Ommen et al. 2014) and because of its inherent guarantee of finding global optima (Muschick et al. 2022).

2.2 Digitalization and digital twin technology

This section presents a brief history and some important definitions of digitalization and DT technology, which is an essential foundation to follow the state of the art in this research area.

Definitions

Digitalization is no completely new phenomenon. Weigel & Fishedick 2019 even dates it back to the 1950s. However, the International Energy Agency (IEA) 2017 found that digitalization in the energy sector is increasing rapidly, based on the analysis of global investment flows. Expenses for digital infrastructure and software already exceed investments in traditional electricity generation infrastructure in some instances.

As motivated above, the DT is often seen as a key concept in the context of extensive digital transformation. Tao et al. 2019a states that the DT concept was first introduced as early as 2003 but the first actual definition of a DT was presented in 2012 (Glaessgen & Stargel 2012). However, the DT definition remains vigorously debated and sometimes inconsistent (Cimino et al. 2019). Negri et al. 2017 and Liu et al. 2021 even presented tables of 16 and 21 separate DT definitions found in the literature. However, the characteristics most

often prescribed to a DT by research align with the refined definition given by Negri et al. 2017 and then approved in numerous reviews, e.g., by Cimino et al. 2019 and Kritzing et al. 2018:

“The DT consists of a virtual representation of a production system that is able to run on different simulation disciplines that is characterized by the synchronization between the virtual and real system, thanks to sensed data and connected smart devices, mathematical models and real time data elaboration.”

This definition for *production systems* hints at the origin of the DT in the manufacturing domain. For a more general scope, the terms physical object (Wagner et al. 2018) or physical entity are used (Josifovska et al. 2019). According to Josifovska et al. 2019, a physical entity is an abstraction of a “thing” persisting in the real world which has to be mirrored or twinned in the virtual world. Regarding energy systems, this can be a single process unit or even part of that unit, but also a whole energy system.

To further avoid some misconceptions about DTs, Kritzing et al. 2018 introduced a categorization that received mainly endorsement in the scientific community (see, e.g., Yu et al. 2022). According to them, some DTs are only digital models or digital shadows. A digital model exhibits no form of automated data exchange between the physical and virtual entity. If a model features an automated one-way data exchange from the physical to the virtual entity, one should refer to such a combination as a digital shadow. Consequently, a *real* DT should feature bidirectional automated information and data exchange. Thus, the field of DTs is about much more than just accurate mathematical descriptions of physical system behavior. Of course, DT development comprises many specific sub-problems, but the main difficulty lies in automation and intelligent algorithm-based decision-making.

Digital twin modeling

Wang et al. 2022 states that DT technology is developing rapidly, thanks to simulation and modeling capabilities, better interoperability and IoT sensors, and more available tools and computing infrastructure. Although the number of DT publications is increasing, there is still no uniform platform available for the practical implementation of a DT (Liu et al. 2021). However, numerous concepts and frameworks for DT modeling have been proposed. In a bibliometric review on DT-enabled smart industrial systems, Ciano et al. 2021 located the work of Tao et al. in the center of past research in this field. Tao et al. 2019b proposed a five dimensional (5D)-DT modeling concept, see Figure 7. Adding to the three basic aspects of (i) the physical space, (ii) the virtual space, and (iii) the connection between them, already established by Grieves 2014, they added (iv) DT data and (v) DT services (Tao et al. 2018a; Tao et al. 2019c). In the 5D-DT concept, especially the service dimension is emphasized as an important part. The functionality of the DT is encapsulated into standardized services with user-friendly interfaces for easy and on-demand usage. However, most modeling proposals are very conceptual, maintaining a high level of abstraction and leave important implementation details unaddressed (Steindl & Kastner 2021). Concrete DT implementations, on the other hand, are mostly realized with a specific application in

mind without any architectural template (Josifovska et al. 2019) or target a limited set of services (Cimino et al. 2019). There remains a significant gap in DT research, regarding how to offer a higher number of services in the same environment to support complex decision-making (Cimino et al. 2019). For a comprehensive overview of DT modeling regarding different aspects within the 5D-DT concept, I refer to the most recent work of Tao et al. 2022.

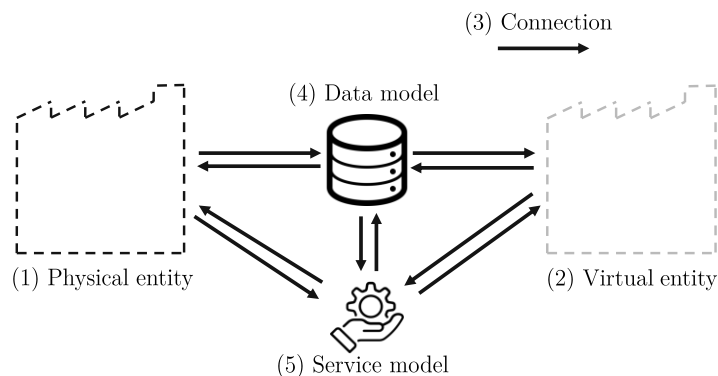


Figure 7: *Simplified illustration of the 5D-DT modeling concept introduced by Tao et al. 2019b.*

Digital twins in energy systems: state of the art

Most previous work on DT technology focused on the manufacturing domain. On a methodical level, very few DT publications targeted energy-related applications (Cioara et al. 2021). In 2019, Tao et al. 2019a found that DTs for dispatching optimization and operational control are currently completely underexplored but very promising. In a current literature review by Kaiblinger & Woschank 2022, only 5 % of evaluated DT case studies could be attributed to the energy domain, which is similar to the findings of Yu et al. 2022. However, the sector is catching up, albeit it's a very young research field. Since the second half of 2022, three comprehensive review papers were published analyzing the state of the art: Yu et al. 2022, Ghenai et al. 2022, and Sleiti et al. 2022. To the best of my knowledge, these were the first scientific reviews of DT technology specifically in the energy sector. Sleiti et al. 2022 found 21 publications addressing industrial energy supply, starting with one publication in 2018, 10 in 2019, and 9 since 2020. Ghenai et al. 2022 found 22.5 % of studies related to DT for energy storage and only one paper addressing DT of TES (which is co-author publication D of this thesis).

A crucial research gap is that the majority of proposed DT in the energy domain lack automated bidirectional connectivity between virtual and physical entity, which was observed by Yu et al. 2022. They state that most DT thus fall under the digital model or

digital shadow group. Several future research directions were proposed in the mentioned review papers to improve DT development for energy systems. A selection is given here:

- Fast, guaranteed connectivity within the DT and its physical entity, to guarantee availability and the foundation for real-time decision-making (Ghenai et al. 2022).
- Parallel simulation with physics-based and data-driven models to enhance results and allow interpretation of data-driven processes (Sleiti et al. 2022).
- Hybrid physics-based/data-driven modeling approaches to provide more robustness for failure prediction and corrective actions than pure data-driven approaches (Sleiti et al. 2022).
- Localized high-fidelity simulations of system components as a foundation for data-driven anomaly detection purposes (Sleiti et al. 2022).
- Continuous system parameter update via measurements or state parameter estimation approaches to cope with degradation of physical system components (Sleiti et al. 2022).
- Self-adaptive DT technology to recalibrate to degradation, state changes, or reconfiguration of the physical entity (Yu et al. 2022).
- Specification of software artefacts and standardized languages to support interoperability (Yu et al. 2022).
- Research on automated AI model incorporation into DT processes such as AI optimization algorithms or machine learning models (Yu et al. 2022).

3 Problem statement

TES must be improved very quickly in the coming years to cope with the increasing volatility in energy supply and future flexibility requirements of industrial processes, as explained in the Introduction. Of course, this involves several specific issues that need to be treated, partly in parallel. For example, this includes optimal design, integration, and operation of TES systems, as well as affordable investment and maintenance, and longevity of the technology. Therefore, the overarching key objective of this thesis can be formulated as:

Key Objective: Increase the flexibility of industrial energy systems by improving thermal energy storage

On the one hand, this means that more TES capacity is needed. On the other hand, the intelligent operation of TES is crucial. To address both of these challenges, this thesis focuses on (1) the feasibility of economic TES capacity retrofit, and (2) DT technology to improve the system's operational optimization and consequently energy storage. Based on the current challenges and the state of the art, two main research questions and corresponding sub-questions tackling the key objective are stated below.

Thermal energy storage retrofit: As presented in the state of the art summarized in Section 2, numerous types of TES exist for industrial applications. A major hurdle for their practical implementation is the investment costs for new TES capacity. Dusek & Hofmann 2018 presented a promising concept for the economic retrofit of RSS capacity with PCM. Leading up to this thesis, several publications studied this concept (see Section 2.1). However, many questions critical to the technical feasibility of this concept remained. For example, the influence of natural convection on the behavior of the PCM containers was never considered. However, this effect can be significant and needs to be examined in detail to account for it in design considerations and operational methods. But above all, the concept lacked experimental confirmation. These research gaps lead to one main research question of this thesis and corresponding sub-questions:

RQ 1: How can the technical feasibility of the hybrid TES concept for RSS retrofit be achieved for actual implementation?

RQ 1.1: What is the optimal design of PCM modules for RSS retrofit, considering the influence of natural convection?

RQ 1.2: Which parameters are the most critical to hybrid TES performance?

A high-fidelity model of the PCM part of the hybrid TES is used for detailed numerical design studies considering natural convection. Furthermore, the first-of-a-kind functional lab-scale prototype of the hybrid storage, built by a project consortium I was part of, provided the test rig for experimental validation of PCM module design and the interaction between RSS and PCM parts.

Digital twin technology for energy system operation: It is expected that DTs have a great potential to increase the operational efficiency of industrial energy systems and thus also TES utilization. However, reliable case studies are scarce and the potential of digitalization applications and DTs for energy supply and storage needs to be evaluated, to shape targeted future research directions. Another problem is that most previous DT research can be ascribed to the manufacturing domain (Jones et al. 2020), following different requirements than those relevant to energy systems. As just one example of such sectoral differences, energy systems feature multiple continuous processes as opposed to manufacturing with a high share of discrete states during operation. This makes the practical application of DTs in energy systems considerably lag behind other fields since important concepts and methods are missing. Essential architectural patterns have to be established and tested, regarding, e.g., the connectivity between physical and virtual system, data integration and knowledge management, and modeling frameworks. Technical implementation barriers in this interdisciplinary field have to be addressed by providing practical and easily transferable solutions. Furthermore, the majority of previous research did not develop comprehensive DT technology for fully bidirectional information exchange (Yu et al. 2022).

This assessment leads to the following main research question and connected sub-questions:

RQ 2: *What is an appropriate way to implement a DT for industrial energy system operation and what are its qualitative and quantitative benefits?*

RQ 2.1: *What is the potential of digitalization and DT technology for optimizing energy supply and storage operation?*

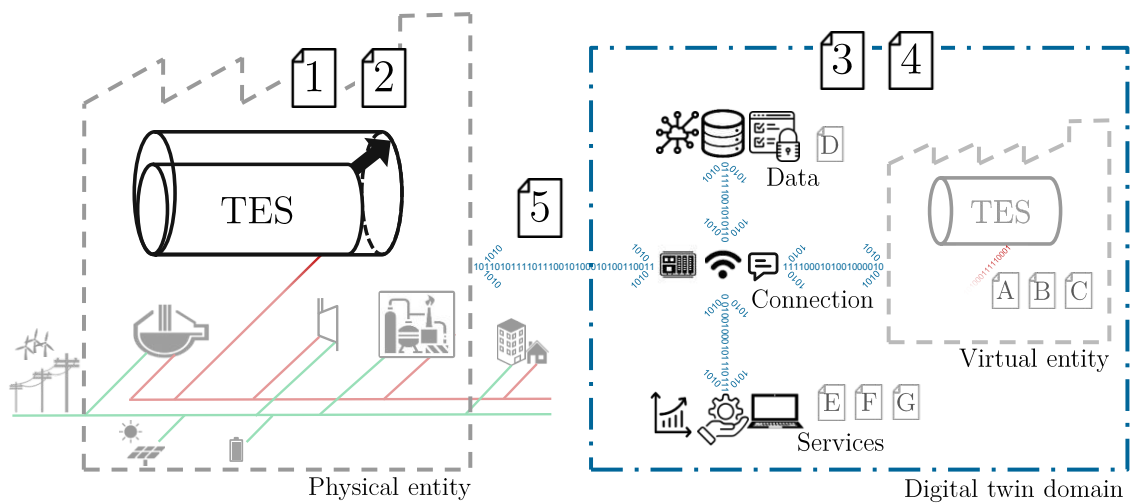
RQ 2.2: *What are the requirements on DT implementation for industrial energy systems and how can these be met?*

For this second research question, a well-founded literature review, establishing the current state of the art, is necessary, to draw legitimate conclusions and develop pertinent methods on this basis. Additionally, a DT is not comprehensively tested until it is bidirectionally connected to its physical counterpart in live operation. For this aim, an existing sensible TES test rig, a packed bed thermal energy storage (PBTES) located at TU Wien laboratories, was used. An industrial use case of waste heat recovery in a steel production plant provided the means for experimental testing of DT-based TES model adaption and optimization.

4 Research approach

This work contributes to the state of the art in different areas, pursuing the research questions stated in Section 3. In this section, the approach to solve these questions is explained and the contributing work presented in the individual published articles is summarized. Figure 8 provides an overview of my core publications and relevant co-author publications and illustrates their contextual embedding into this thesis. Papers 1 and 2 focused on research question *RQ 1* by numerical and experimental investigation of a novel hybrid TES concept for storage capacity retrofit. Papers 3, 4 and 5 targeted research question *RQ 2*. The DT platform, first conceptualized in Paper 3, and published comprehensively in Paper 4, was evaluated on the experimental operation of a TES in Paper 5. The listed publications that I co-authored further contributed to the impact of this work. While Papers A, B and C presented methods for state observation and control of the specific hybrid TES concept, these approaches could also be implemented as virtual entity models in the DT platform. In Paper D, a fundamental DT architecture was presented, with a special focus on a smart data service and virtual entity instances. Papers E, F and G developed automation approaches for model adaptation, soft sensor creation, and MILP linearization, respectively, which can all be integrated as services within a DT and contribute powerful functionality to TES operation.

The combined overarching purpose of all my published work was to *improve thermal energy storage* and thus make industrial energy systems more flexible and efficient.



Core publications

Paper **1**: Numerical design study for TES retrofit

Paper **2**: Experimental investigation of hybrid TES

Paper **3**: Potential analysis of DT for energy systems

Paper **4**: Practical DT platform tailored to requirements

Paper **5**: DT-based optimization of TES operation

Further publications

Paper **A**: Co-simulation methodology of hybrid TES

Paper **B**: Data-based LHTES model reduction

Paper **C**: LHTES state estimation concept

Paper **D**: Generic DT architecture for industrial energy systems

Paper **E**: Framework for automated TES model adaptation

Paper **F**: DT-based soft sensor automation for TES

Paper **G**: Heuristic for TES model linearization to MILP

Figure 8: Overview of publications and their contextual embedding into this thesis.

Research question *RQ* 1 of this thesis called for the detailed investigation of the hybrid RSS/LHTES storage retrofit concept first introduced by Dusek & Hofmann 2018. The background and state of the art regarding this concept were given in Section 2.1. The intended benefit of this retrofit concept is twofold: Firstly, increasing storage capacity in an economic manner, and secondly, extending the application range of the common RSS. After the concept's initial discussion in scientific literature in 2018, it was the subject of a series of publications. These provided a more detailed analysis of the hybrid TES, aiming for an optimal design from both the thermodynamic and the techno-economic perspectives. These early investigations laid the foundation for my work in this thesis.

An important effect that all previous studies of the hybrid TES neglected is heat transfer via natural convection within the liquid PCM of the LHTES part. Depending on the material properties, the geometry of the PCM cavities, and the operating scenario, natural convection can have a significant influence on the charging/discharging speed of the LHTES. Therefore, I conducted numerical studies with a high-fidelity model of the PCM cavities that considers heat transfer by both conduction and natural convection pursuing research question *RQ* 1.1. This resulted in the first published study of the combined effects of (i) aluminum proportions, (ii) fin spacing, and (iii) cavity orientation on the charging/discharging speed of this type of PCM cavity arrangement (Paper 1). The methodology for these design studies was thus established and optimal design parameters were calculated for a wide parameter range. Thus, well-founded decisions for PCM module design for RSS retrofit can be made.

After the design of the hybrid TES was studied in detail via numerical simulation, the logical next step in following research question *RQ* 1 were experimental investigations. Luckily, the construction of the first prototype was funded within the project HyStEPs (*HyStEPs / NEFI* 2023). While the basic concept, illustrated in Figure 6, implies a very simple design and construction of the hybrid TES, its implementation is not straightforward. The actual design is bound to a number of thermodynamic, economic, and safety requirements. For well over a year, several construction ideas for LHTES modules were debated within the project consortium and analyzed via thermodynamic models, mechanical stress analysis, material characterization, and economic calculations. Also, the targeted ability of an easy technology scale-up and budgetary restrictions were constraints to possible realizations. Optimization of all the, partly opposing, aspects is impossible and we had to tolerate some trade-offs. We finally built a fully functional lab-scale RSS and the corresponding LHTES container modules to retrofit the RSS. The full test rig was set up at the steel production facility of project partner voestalpine Stahl Donawitz GmbH in Leoben, Austria to be supplied with high-pressure saturated steam. I presented the construction considerations, the full experimental set-up, and the subsequent investigation in Paper 2.

Various charging/discharging experiments were performed with the test rig. After some baseline tests where only the RSS was insulated and characterized, the LHTES modules were mounted to the RSS (just as they would be in an industrial retrofit) and insulated. The fact that we increased the RSS capacity by 30 % was a success in itself. However, irregular heat transfer between the two storage types proved to strongly impede the storage performance. For an in-depth investigation of the observed effects, I identified uncertain

parameters in the simulation model of the LHTES part. The strong deviation between the heat transfer coefficients between the RSS wall and individual LHTES modules matched experimental observations. With the help of the now validated model, I performed a sensitivity analysis of the critical parameters of charging/discharging performance. These results provide the answer to research question *RQ* 1.2 and indicate that LHTES storage power could be increased by up to 10 times compared to the achieved results, with realistic adjustment of heat transfer between RSS and LHTES part.

The finding that natural convection effects in the PCM cavities can significantly influence heat transfer and thus the overall hybrid TES behavior (see Paper 1), led to further research. The hybrid TES retrofit approach could only ever be successful if efficient operation could be guaranteed. However, the convective heat transfer complicates SOC measurement and control in a LHTES even more. On top of that, Paper 1 found that the PCM cavities' position on the RSS, i.e., the angular orientation, influences the charging speed. Given this highly complex state system, new methods for optimal control of hybrid TES operation had to be found. These developments culminated in co-author publications A, B, and C that I contributed to.

The first step was a co-simulation methodology we developed, coupling the high-fidelity conduction/convection PCM model with a one-dimensional two-phase equilibrium model of the RSS (Paper A). To reduce computational effort, we implied a strategy to optimally aggregate the high number of PCM cells at the circumference of the RSS into several sectors. Thus, only one representative cell simulation for each sector is needed.

Despite the clever aggregation approach, the developed co-simulation is only suitable for design analysis and would be too slow for operational purposes. Therefore, we further worked on real-time capability of the PCM simulation model. We developed an approach to circumvent the laborious solving of Navier-Stokes equations via data-based model reduction based on the observation of dominant flow patterns (Paper B). This provides a reliable simulation method, including convective effects, but by orders of magnitude faster than the previous model.

With the data-based reduced order model, we could tackle the problem of real-time state estimation that is necessary for optimal control of the hybrid TES. The work published in Paper C established a robust observation methodology where the higher-order PCM cell model is linearized around the current operation trajectory and implemented in a well-known extended Kalman filter. We proved that this state observation method can estimate both the SOC, as well as the location and shape of the PCM cell's melting front with high accuracy.

The findings of my work on research question *RQ* 1 primarily provide answers for the design of the hybrid TES. Even if some developed methods enable much more accurate TES operation, their standardized application is not straightforward. Thus, partly in parallel to my work on the hybrid TES, I pursued scientific gaps in energy system operation (research question *RQ* 2). Recent digital innovations provide the potential to massively surpass current operational strategies but still require more research. Especially, to achieve

widespread implementation of promising DT technology, which is a cornerstone of energy systems' adaption to I4.0.

Thus, I started out by reviewing the current options offered by digitalization and the involved technological aspects. A literature review of the history and definition of the DT was important to avoid any misconceptions and establish the basic idea and purpose of DT modeling. I also introduced this review to my work in the IEA's IETS Task XVIII on "Digitalization, Artificial Intelligence and Related Technologies for Energy Efficiency and GHG Emissions Reduction in Industry". The reports of my colleagues and me on this topic are listed under Scientific reports in this thesis. The discussions within the scientific community helped to sharpen the definitions, and the expertise of industry participants facilitated the assessment of the current obstacles and needs. I found a general lack of in-depth research on DT modeling, despite the attention the topic received in recent years. For example, there is an urgent need to standardize interfaces and communication protocols. Proven DT modeling approaches were rare, and most previous research had been done in manufacturing, differing from the needs of the energy domain. As a consequence, a first DT implementation concept for a steam generator was developed, based on the 5D-DT model introduced by Tao et al. 2018b. The 5D-DT scheme was received well in previous literature. It can be viewed as a high-abstraction implementation guideline for DTs. The goal of my work was to present how this concept could be used for industrial energy systems and their components. Therefore, recommendations for approaching each DT dimension were developed. A first qualitative assessment of the benefits of the DT was conducted via use cases from relevant literature and an application concept of the DT. This work was presented in Paper 3.

After this first DT conceptualization, I worked with colleagues from the Institute of Computer Engineering at TU Wien on a more detailed DT architecture, demonstrating the application of semantic web technologies as part of a smart data service. This work on a "Generic Digital Twin Architecture" (GDTA) for industrial energy systems was published in co-author publication D.

Since the work from Paper 3 left only a DT concept with specific recommendations, and the GDTA is a technology-independent implementation architecture, focusing on the data and virtual entity dimension, more research on a practical, holistic DT implementation was necessary. On reviewing further literature, I found that there are some distinct barriers that impede DT development in the energy sector. Following a requirements engineering approach, I established a list of DT requirements to help DTs overcome the current implementation barriers (see, Paper 4). Equipped with this knowledge, a DT platform tailored to the identified requirements was developed. To facilitate the implementation of the platform, concrete implementation issues were addressed, and universal, yet specific, approaches for resolving these issues were proposed. The alignment of the technological aspects with the requirements was then qualitatively validated and the DT platform's benefits were discussed.

To also assess the quantitative benefits of the DT (as part of research question *RQ 2*), it was instantiated for a PBTES test-rig acting as the physical entity. In the evaluation use case, automatically created soft sensors act as surrogates for damaged sensor values in

order to reduce error propagation to, e.g., SOC observation. The DT platform was set up as developed in Paper 4. The SCADA system, as part of the physical entity, was realized with the software XAMControl of evon Automation. An existing ontology was extended with context information on the test rig. Furthermore, four services and corresponding DT workflows were developed and integrated into the platform. This setup and the following evaluation was documented in co-author publication F. The DT workflow of automated soft sensor creation was evaluated in experimental tests and we could quantify its benefit.

After the platform's first successful validation, I worked on another option to test the benefits of DT modeling, which is documented in Paper 5. An excess heat recovery process in steel production constituted the industrial reference case, with a PBTES integrated to balance the fluctuating excess heat and steam generation. Since the high dust load in the off-gas leads to a gradual pressure drop in the PBTES system and thus decreases charging/discharging power, this system provided a great example for DT implementation. State-of-the-art operational optimization of this system via MILP modeling would overestimate the decreasing power and lead to non-optimal operation schedules. Thus, we developed and implemented several DT micro-services and workflows to guarantee that (1) deviations between virtual entity models and physical entity behavior are detected, (2) the models are updated, (3) subsequently linearized to suit the MILP approach and (4) used for live operational optimization. The approach was tested in experiments on the PBTES test rig, where the actual power was scaled to the PBTES size in the virtual energy system use case.

5 Conclusion and outlook

The current drastic changes within energy systems require the efficient utilization of TES. Therefore, this thesis investigated options and methods to improve TES. On the one hand, a promising hybrid TES concept was studied via numerical and experimental studies. On the other hand, possibilities for intelligent system operation offered by digitalization technologies were analyzed. Based on this, a DT platform, tailored to the requirements of industrial energy systems, was developed and experimentally tested for the operation of a TES.

This section concludes my research summary by highlighting the scientific contribution to the state of the art of the individual publications constituting this thesis (Section 5.1) while reflecting on the problem statement presented in Section 3. Finally, an outlook on further research and development is given (Section 5.2).

5.1 Scientific contribution

Research question *RQ* 1.1 was pursued via detailed numerical studies. To find an appropriate design of PCM modules for the RSS retrofit in the hybrid TES concept, the influence of several factors was analyzed with a high-fidelity model of the PCM behavior. This resulted in the first numerical investigation that studied the combined effects of (i) aluminum proportions, (ii) fin spacing, and (iii) cavity orientation on the charging/discharging speed of this type of PCM cavity arrangement. This work was published in Paper 1. Significant angular dependency of the cavity orientation on charging behavior was observed. Contrary to that, the orientation had a negligible impact on the discharging behavior, which agrees with the literature. As expected, the convective enhancement factor, quantifying the relative increase in charging power compared to negligible convection, generally increases with both the angle of cavity inclination and the fin spacing. Interestingly, convective enhancement factors of up to 2 were observed for downwards-facing cavities, given a critical fin spacing width was exceeded. The choice of volumetric aluminum ratio to increase heat flux in the PCM cavity always presents a trade-off between fast charging time and overall storage capacity. Therefore, guideline values for the optimal volumetric aluminum ratio of about 15 % were found. Furthermore, optimal choices for fin spacing were found, each for a particular aluminum ratio and cavity orientation. Thus, a well-founded decision on uniform fin spacing can be made, or even different fin spacings in dependence on a cavity's orientation on the retrofitted RSS could be considered. These results summarized here provided the answer to research question *RQ* 1.1 for the specific hybrid TES retrofit concept in focus. On top of that, the studied configurations are frequently found in PCM applications even in completely different domains. The findings thus provide at least qualitative evidence for a wide range of applications.

The first functional prototype of the hybrid TES made it possible to properly address research question *RQ* 1.2 and ultimately also *RQ* 1. The experimental characterization and sensitivity analysis of the test rig was presented in Paper 2. This presented a vital

step in verifying the novel retrofit concept. The numerical models could be validated with satisfactory results. It was a success that the targeted retrofitted storage capacity of 30 % could be reached. However, only approximately 26 % of the stored enthalpy in the LHTES could be recovered to the RSS during a discharging period of 8.5 h. The reason for this can be ascribed to relatively low heat transfer values between the RSS and LHTES part of the storage. The comparison of measurement results of the individual LHTES modules' estimated power showed large differences, which reflects in the identified heat transfer coefficients. Presumably, small air gaps between the two storage types account for that. While this fact is hard to determine, the measurement results were a clear indication of it and could be confirmed via optical inspection. Thus, the most critical parameter of the hybrid TES concept (*RQ 1.2*) is heat transfer between the two storage types, which proved harder to manage than expected. The sensitivity analysis, also carried out in Paper 2, gave insight into the hybrid TES potential, given that reasonable adjustments are made.

To achieve the technical feasibility of the hybrid TES concept (*RQ 1*), the heat transfer between RSS and the retrofitted LHTES must be improved. The design of the LHTES part must be optimized taking natural convection into account, as demonstrated in Paper 1. Furthermore, intelligent simulation, estimation, and control methods, such as those presented in co-author publications A, B and C, must be applied to capitalize on the storage's full potential.

The work on the second main objective of this thesis (*RQ 2*) was published over the course of several publications.

After a first literature review that clarified the basic definitions of digitalization applications and summarized the relevant state of the art, research question *RQ 2.1* could be approached. Within the reviewed digitalization aspects, my analysis in Paper 3 found that DT technology is especially promising for operation and maintenance in the energy sector. Many methods and applications for improving the operational performance of components of industrial energy systems, e.g., based on mathematical modeling or machine learning, already exist. However, the major benefit of the DT approach is the tight integration and interaction of all these smart services. DTs facilitate the integration of otherwise stand-alone digital services such as, e.g., condition monitoring, predictive maintenance, and operational optimization. The DT serves as a platform for these services that gives them access to a common knowledge base and bi-directional communication with the physical entity. Therefore, DTs can maximize the added value from individual solutions by exploiting synergies, while increasing interoperability, robustness, and scalability. This potential was outlined for a use case in the area of steam supply systems. Also, a first conceptual DT implementation was presented and recommendations were drawn.

To develop not just one DT solution, but DT technology that is tailored to the application in industrial energy systems, research question *RQ 2.2* was established. The specific requirements for DT implementation for industrial energy systems were presented based on a detailed literature review of current implementation barriers in energy systems and requirements given in other domains. Building on previous literature concepts and my work in co-author publication D, a practical DT platform was developed. The description of

this platform provides solutions to various implementation issues that were not addressed in previous concepts while meeting the established requirements. The work on this topic was presented in Paper 4 and also answered how DTs are appropriately implemented for industrial energy system operation (research question *RQ 2*).

This thesis also discussed the benefits of DT implementation (*RQ 2*). On a qualitative level, DTs define clear interfaces to separate the work of energy system engineers and informatics experts. Through the efficient service encapsulation of the proposed DT platform, energy domain experts can focus their work on service development, virtual entity models, and the optimal operation of energy systems. At the same time, computer scientists can leverage their expertise on the scalability, reliability, and security of the DT platform and on establishing interoperability on a technical, syntactical, semantical, and operational level (see Paper 3 and Paper 4). On the one hand, this facilitates the widespread application of novel methods straight from applied research in only a short amount of development time. On the other hand, more industrial facilities can leverage these complex methods by facilitating their implementation via DT technology. Quantitative benefits are created by the tight integration of individual digitalization solutions together with semantic web technology in the data and connection dimension of DTs. Thus, the use of existing methods can be improved. This was experimentally validated via different application use cases involving TES. Co-author publication F presented how a DT, equipped with the capability to automatically create soft sensors, can effectively eliminate the error in SOC calculation of a TES introduced by temperature sensor failures. Thus, the cost- and energy-efficient operation of the system is undisturbed. Furthermore, Paper 5 presented a methodology for automatic model adaptation and linearization services integrated on a DT platform. Using these DT services ensures that efficient operational optimization is not impaired by outdated component models.

5.2 Outlook

The first ever prototype of a hybrid RSS/LHTES storage concept and its goal of retrofitting 30 % of TES capacity was realized. However, the heat transfer between the two storage types was too low to call it technically efficient, yet. In the developed construction concept, direct contact between the RSS and the LHTES containers is essential for efficient storage operation. Fixed, permanent mounting to the RSS shell was disregarded due to technical and safety restrictions (see, Paper 2). Unfortunately, the metallic springs, intended to ensure a tight fit of LHTES containers to the RSS surface, proved inadequate. Additionally, heat insulation proved to be worse than expected. Future iterations of the prototype must assess the option to avoid some thermal bridges to the environment, such as the hoses, designated to remove eventual exhaust gases from liquified PCM.

To conclude, the hybrid TES construction concept must be revisited. Some possible options were discussed in Paper 2. The application of, e.g., silicon-based, heat conductivity pastes or the use of flexible, elastomer-based PCM encapsulations seem most promising to increase heat transfer between the two storage types. Of course, economic assessments of the retrofit concept, previously presented by Hofmann et al. 2019a and Niknam & Sciacovelli 2023 should also be revisited under new circumstances. The conducted numerical studies of the

PCM cavities demonstrated the importance of considering natural convection in LHTEs design and operation. Since the studied aluminum-finned geometry is very common, the analysis provides at least qualitative findings for a wide range of PCM applications. If the exhibited engineering challenges are solved and the developed methods are put to use, the hybrid TES retrofit could provide a valuable addition to TES technology for industrial energy systems.

DTs are a great result of rapid digitalization and I4.0 developments. After an initial hype, DTs could soon see their widespread application in industrial energy systems. The DT platform presented in this thesis provides a scalable implementation template for that. However, DT services that incorporate verified methods are essential for DTs to generate added value. While service integration and scalability are facilitated in DT platforms, methodical research on energy system services must continue. Important research aspects relating thereto, independent of the specific application, are automation and reliability.

For example, most data-based modeling methods still rely on manual verification of training data or at least expertise-based specification of respective historic time windows. Thus, the reliable automation of such model training tasks within DTs is highly relevant. The same holds for fault detection services. The detection of deviations and faults as well as their classification is a challenging topic even when manually conducted. For their automation, e.g., ontology-based reasoning approaches could prove appropriate. The automatic generation of such information models from existing Pipe and Instrumentation (P&I) diagrams was already demonstrated and could provide a powerful tool to foster automation (Sierla et al. 2020). Based on ontologies, dynamic data-driven models of energy systems can be identified fully automatically (Steindl & Kastner 2020). It would be desirable to apply this approach for automated optimization model identification. In recent years, several research teams introduced modular MILP-based energy management approaches (see, e.g., Krien et al. 2020, Halmschlager & Hofmann 2021, and Moser et al. 2020). This provides a foundation for further automation via ontology-based model identification, hence facilitating the still cumbersome development of optimization models even more. However, the further development of specific ontologies and related approaches will require interdisciplinary work between computer scientists and energy system experts for years to come.

DTs could also provide a great platform for transfer learning and energy system control via reinforcement learning (see, e.g., Tubeuf et al. 2023). On the one hand, an accurate digital representation provides the clear advantage that less or even no training of these machine learning methods on the physical entity is necessary. On the other hand, model adaption based on the newest operating data and deployment of these models for actual control is facilitated by a DT platform. This could also foster faster development of reliable fault detection services. However, the first feasibility studies on this approach with experimental validation are necessary to guide future research. In this context, hybrid physical and data-driven modeling methods as well as reduced order models are very promising.

We need to continue our work on the optimal design and utilization of TES since it is an indispensable necessity for enabling the flexibility of industrial energy systems. Of course,

improving TES integration options and TES operation are not the only way to aid the energy transition and reduce GHG emissions. However, they are definitely key aspects. I am certain, that worldwide TES capacity will grow substantially and that DT technology will mature and thrive in the coming years. But I can only hope, that we'll make these adaptations fast enough.

References

- Abdelsalam, M., P. Sarafraz, J. Cotton & M. Lightstone (2017). “Heat transfer characteristics of a hybrid thermal energy storage tank with Phase Change Materials (PCMs) during indirect charging using isothermal coil heat exchanger”. In: *Solar Energy* 157, pp. 462–476. ISSN: 0038-092X.
DOI: 10.1016/j.solener.2017.08.043
- Abdi, H. (2021). “Profit-based unit commitment problem: A review of models, methods, challenges, and future directions”. In: *Renewable and Sustainable Energy Reviews* 138, p. 110504. ISSN: 1364-0321.
DOI: 10.1016/j.rser.2020.110504
- Abdrakhmanova, K. N., A. V. Fedosov, K. R. Idrisova, N. K. Abdrakhmanov & R. R. Valeeva (2020). “Review of modern software complexes and digital twin concept for forecasting emergency situations in oil and gas industry”. In: *IOP Conference Series: Materials Science and Engineering* 862.3, p. 032078.
DOI: 10.1088/1757-899x/862/3/032078
- Alva, G., Y. Lin & G. Fang (2018). “An overview of thermal energy storage systems”. In: *Energy* 144, pp. 341–378. ISSN: 0360-5442.
DOI: 10.1016/j.energy.2017.12.037
- Arce, P., M. Medrano, A. Gil, E. Oró & L. F. Cabeza (2011). “Overview of thermal energy storage (TES) potential energy savings and climate change mitigation in Spain and Europe”. In: *Applied Energy* 88.8, pp. 2764–2774. ISSN: 0306-2619.
DOI: 10.1016/j.apenergy.2011.01.067
- Augspurger, M., K. Choi & H. Udaykumar (2018). “Optimizing fin design for a PCM-based thermal storage device using dynamic Kriging”. In: *International Journal of Heat and Mass Transfer* 121, pp. 290–308. ISSN: 0017-9310.
DOI: 10.1016/j.ijheatmasstransfer.2017.12.143
- Barbosa, E. G., M. E. V. de Araujo, A. C. L. de Oliveira & M. A. Martins (2023). “Thermal energy storage systems applied to solar dryers: Classification, performance, and numerical modeling: An updated review”. In: *Case Studies in Thermal Engineering* 45, p. 102986. ISSN: 2214-157X.
DOI: 10.1016/j.csite.2023.102986
- Bayomy, A., S. Davies & Z. Saghir (2019). “Domestic Hot Water Storage Tank Utilizing Phase Change Materials (PCMs): Numerical Approach”. In: *Energies* 12.11. ISSN: 1996-1073.
DOI: 10.3390/en12112170
- Beck, A., A. Sevault, G. Drexler-Schmid, M. Schöny & H. Kauko (2021). “Optimal Selection of Thermal Energy Storage Technology for Fossil-Free Steam Production in the Processing Industry”. In: *Applied Sciences* 11.3. ISSN: 2076-3417.
DOI: 10.3390/app11031063
- Biegel, B., L. H. Hansen, J. Stoustrup, P. Andersen & S. Harbo (2014). “Value of flexible consumption in the electricity markets”. In: *Energy* 66, pp. 354–362. ISSN: 0360-5442.
DOI: 10.1016/j.energy.2013.12.041
- Biglia, A., L. Comba, E. Fabrizio, P. Gay & D. Ricauda Aimonino (2017). “Steam batch thermal processes in unsteady state conditions: Modelling and application to a case

- study in the food industry”. In: *Applied Thermal Engineering* 118, pp. 638–651. ISSN: 1359-4311.
DOI: 10.1016/j.applthermaleng.2017.03.004
- BP (2022). *Statistical Review of World Energy*. Available at: <https://www.bp.com/en/global/corporate/energy-economics/statistical-review-of-world-energy.html>.
- Buschle, J., W.-D. Steinmann & R. Tamme (2006). “Latent heat storage for process heat applications”. In: *10th International Conference on thermal Energy Storage ECOSTOCK 2006*. Vol. 31, pp. 1–8.
URL: <https://elib.dlr.de/55379/>
- Cabeza, L. F. (2021). *Advances in Thermal Energy Storage Systems (Second Edition)*. Second Edition. Woodhead Publishing. ISBN: 978-0-12-819885-8.
DOI: 10.1016/B978-0-12-819885-8.00030-9
- Cabeza, L. F., I. Martorell, L. Miró, A. I. Fernández, C. Barreneche, L. F. Cabeza, A. I. Fernández & C. Barreneche (2021). “1 - Introduction to thermal energy storage systems”. In: *Advances in Thermal Energy Storage Systems (Second Edition)*. Ed. by L. F. Cabeza. Second Edition. Woodhead Publishing Series in Energy. Woodhead Publishing, pp. 1–33. ISBN: 978-0-12-819885-8.
DOI: 10.1016/B978-0-12-819885-8.00001-2
- Calderón, A., C. Barreneche, K. Hernández-Valle, E. Galindo, M. Segarra & A. I. Fernández (2020). “Where is Thermal Energy Storage (TES) research going? – A bibliometric analysis”. In: *Solar Energy* 200. Special Issue on The 14th International Conference on Energy Storage - EnerSTOCK2018., pp. 37–50. ISSN: 0038-092X.
DOI: 10.1016/j.solener.2019.01.050
- Ciano, M. P., R. Pozzi, T. Rossi & F. Strozzi (2021). “Digital twin-enabled smart industrial systems: a bibliometric review”. In: *International Journal of Computer Integrated Manufacturing* 34.7-8, pp. 690–708.
DOI: 10.1080/0951192X.2020.1852600
- Cimino, C., E. Negri & L. Fumagalli (2019). “Review of digital twin applications in manufacturing”. In: *Computers in Industry* 113, p. 103130. ISSN: 01663615.
DOI: 10.1016/j.compind.2019.103130
- Cioara, T., I. Anghel, M. Antal, I. Salomie, C. Antal & A. G. Ioan (2021). *An Overview of Digital Twins Application Domains in Smart Energy Grid*. to be submitted to an IEEE conference. arXiv: 2104.07904 [eess.SY].
- Davis, P. (2015). “16 - Monitoring and control of thermal energy storage systems”. In: *Advances in Thermal Energy Storage Systems*. Ed. by L. F. Cabeza. Woodhead Publishing Series in Energy. Woodhead Publishing, pp. 419–440. ISBN: 978-1-78242-088-0.
DOI: 10.1533/9781782420965.4.419
- Desai, F., J. Sunku Prasad, P. Muthukumar & M. M. Rahman (2021). “Thermochemical energy storage system for cooling and process heating applications: A review”. In: *Energy Conversion and Management* 229, p. 113617. ISSN: 0196-8904.
DOI: 10.1016/j.enconman.2020.113617
- Ding, Z., W. Wu & M. Leung (2021). “Advanced/hybrid thermal energy storage technology: material, cycle, system and perspective”. In: *Renewable and Sustainable Energy Reviews*

- 145, p. 111088. ISSN: 1364-0321.
DOI: 10.1016/j.rser.2021.111088
- Dusek, S. & R. Hofmann (2018). “A hybrid energy storage concept for future application in industrial processes”. In: *Thermal Science* 22, pp. 2235–2242. ISSN: 5.
DOI: 10.2298/TSCI171230270D
- (2019). “Modeling of a Hybrid Steam Storage and Validation with an Industrial Ruths Steam Storage Line”. In: *Energies* 12.6. ISSN: 1996-1073.
DOI: 10.3390/en12061014
- Dusek, S., R. Hofmann & S. Gruber (2019). “Design analysis of a hybrid storage concept combining Ruths steam storage and latent thermal energy storage”. In: *Applied Energy* 251, p. 113364. ISSN: 0306-2619.
DOI: 10.1016/j.apenergy.2019.113364
- Einstein, D., E. Worrell & M. Khrushch (2001). “Steam systems in industry: Energy use and energy efficiency improvement potentials”. In: *Lawrence Berkeley National Laboratory*. Retrieved from <https://escholarship.org/uc/item/3m1781f1>.
- Esence, T., A. Bruch, S. Molina, B. Stutz & J.-F. Fourmigué (2017). “A review on experience feedback and numerical modeling of packed-bed thermal energy storage systems”. In: *Solar Energy* 153, pp. 628–654. ISSN: 0038-092X.
DOI: 10.1016/j.solener.2017.03.032
- Eslamnezhad, H. & A. B. Rahimi (2017). “Enhance heat transfer for phase-change materials in triplex tube heat exchanger with selected arrangements of fins”. In: *Applied Thermal Engineering* 113, pp. 813–821. ISSN: 1359-4311.
DOI: 10.1016/j.applthermaleng.2016.11.067
- Fang, M. & G. Chen (2007). “Effects of different multiple PCMs on the performance of a latent thermal energy storage system”. In: *Applied Thermal Engineering* 27.5, pp. 994–1000. ISSN: 1359-4311.
DOI: 10.1016/j.applthermaleng.2006.08.001
- Fatras, N., Z. Ma & B. N. Jørgensen (2022). “Process-to-market matrix mapping: A multi-criteria evaluation framework for industrial processes’ electricity market participation feasibility”. In: *Applied Energy* 313, p. 118829. ISSN: 0306-2619.
DOI: 10.1016/j.apenergy.2022.118829
- Gasia, J., L. Miró & L. F. Cabeza (2017). “Review on system and materials requirements for high temperature thermal energy storage. Part 1: General requirements”. In: *Renewable and Sustainable Energy Reviews* 75, pp. 1320–1338. ISSN: 1364-0321.
DOI: 10.1016/j.rser.2016.11.119
- Gerres, T., J. P. Chaves Ávila, P. L. Llamas & T. G. San Román (2019). “A review of cross-sector decarbonisation potentials in the European energy intensive industry”. In: *Journal of Cleaner Production* 210, pp. 585–601. ISSN: 0959-6526.
DOI: 10.1016/j.jclepro.2018.11.036
- Ghenai, C., L. A. Husein, M. Al Nahlawi, A. K. Hamid & M. Bettayeb (2022). “Recent trends of digital twin technologies in the energy sector: A comprehensive review”. In: *Sustainable Energy Technologies and Assessments* 54, p. 102837. ISSN: 2213-1388.
DOI: 10.1016/j.seta.2022.102837
- Gibb, D., M. Johnson, J. Romani, J. Gasia, L. F. Cabeza & A. Seitz (2018). “Process integration of thermal energy storage systems – Evaluation methodology and case

- studies”. In: *Applied Energy* 230, pp. 750–760. ISSN: 0306-2619.
DOI: 10.1016/j.apenergy.2018.09.001
- Gil, A., M. Medrano, I. Martorell, A. Lázaro, P. Dolado, B. Zalba & L. F. Cabeza (2010). “State of the art on high temperature thermal energy storage for power generation. Part 1—Concepts, materials and modellization”. In: *Renewable and Sustainable Energy Reviews* 14.1, pp. 31–55. ISSN: 1364-0321.
DOI: 10.1016/j.rser.2009.07.035
- Glaessgen, E. & D. Stargel (2012). “The Digital Twin Paradigm for Future NASA and U.S. Air Force Vehicle”. In: *53rd AIAA/ASME/ASCE/AHS/ASC Structures, Structural Dynamics and Materials Conference*, pp. 1–14.
DOI: 10.2514/6.2012-1818
- Global Carbon Project (2019). *Supplemental data of Global Carbon Budget 2019 (Version 1.0) [Data set]. Global Carbon Project*.
DOI: 10.18160/gcp-2019
- Goldstern, W. (1970). *Steam Storage Installations: Construction, Design, and Operation of Industrial Heat Accumulators*. Vol. 4. Pergamon.
- González-Roubaud, E., D. Pérez-Osorio & C. Prieto (2017). “Review of commercial thermal energy storage in concentrated solar power plants: Steam vs. molten salts”. In: *Renewable and Sustainable Energy Reviews* 80, pp. 133–148. ISSN: 1364-0321.
DOI: 10.1016/j.rser.2017.05.084
- Grieves, M. (2014). “Digital twin: Manufacturing excellence through virtual factory replication”. In: *White paper*, pp. 1–7.
URL: https://www.researchgate.net/publication/275211047_Digital_Twin_Manufacturing_Excellence_through_Virtual_Factory_Replication
- Halmschlager, V. & R. Hofmann (2021). “Assessing the potential of combined production and energy management in Industrial Energy Hubs – Analysis of a chipboard production plant”. In: *Energy* 226, p. 120415. ISSN: 0360-5442.
DOI: 10.1016/j.energy.2021.120415
- He, Z., W. Guo & P. Zhang (2022). “Performance prediction, optimal design and operational control of thermal energy storage using artificial intelligence methods”. In: *Renewable and Sustainable Energy Reviews* 156, p. 111977. ISSN: 1364-0321.
DOI: 10.1016/j.rser.2021.111977
- Hofmann, R., S. Dusek, S. Gruber & G. Drexler-Schmid (2019a). “Design Optimization of a Hybrid Steam-PCM Thermal Energy Storage for Industrial Applications”. In: *Energies* 12.5. ISSN: 1996-1073.
DOI: 10.3390/en12050898
- Hofmann, R., V. Halmschlager, M. Koller, G. Scharinger-Urschitz, F. Birkelbach & H. Walter (2019b). “Comparison of a physical and a data-driven model of a Packed Bed Regenerator for industrial applications”. In: *Journal of Energy Storage* 23, pp. 558–578. ISSN: 2352-152X.
DOI: 10.1016/j.est.2019.04.015
- HyStEPs* / *NEFI* (2023).
URL: <https://www.nefi.at/en/project/hysteps> (visited on 06/08/2023)
- Ibrahim, N. I., F. A. Al-Sulaiman, S. Rahman, B. S. Yilbas & A. Z. Sahin (2017). “Heat transfer enhancement of phase change materials for thermal energy storage applications:

- A critical review”. In: *Renewable and Sustainable Energy Reviews* 74, pp. 26–50. ISSN: 1364-0321.
DOI: 10.1016/j.rser.2017.01.169
- Intergovernmental Panel on Climate Change (IPCC) (2023). *Synthesis Report of the IPCC Sixth Assessment Report (AR6)*. Available at: <https://www.ipcc.ch/report/sixth-assessment-report-cycle/>. Geneva, Switzerland.
- International Energy Agency (IEA) (2017). *Digitalisation and Energy*. Available at: <https://www.iea.org/reports/digitalisation-and-energy>. Paris.
- (2022). *World Energy Outlook 2022 Free Dataset*. Available at: <https://www.iea.org/data-and-statistics/data-product/world-energy-outlook-2022-free-dataset>. Licence: Creative Commons Attribution CC BY-NC-SA 4.0.
- International Renewable Energy Agency (IRENA) (2020). *Innovation Outlook: Thermal Energy Storage*. Available at: https://www.irena.org/-/media/Files/IRENA/Agency/Publication/2020/Nov/IRENA_Innovation_Outlook_TES_2020.pdf. Abu Dhabi.
- (2023). *World Energy Transitions Outlook 2023: 1.5 °C Pathway*. Available at: <https://www.irena.org/Publications/2023/Mar/World-Energy-Transitions-Outlook-2023>. This publication is a preview of the forthcoming report. Abu Dhabi.
- Jones, D., C. Snider, A. Nassehi, J. Yon & B. Hicks (2020). “Characterising the Digital Twin: A systematic literature review”. In: *CIRP Journal of Manufacturing Science and Technology* 29, pp. 36–52. ISSN: 1755-5817.
DOI: 10.1016/j.cirpj.2020.02.002
- Jordehi, A. R. (2019). “Optimisation of demand response in electric power systems, a review”. In: *Renewable and Sustainable Energy Reviews* 103, pp. 308–319. ISSN: 1364-0321.
DOI: 10.1016/j.rser.2018.12.054
- Josifovska, K., E. Yigitbas & G. Engels (2019). “Reference Framework for Digital Twins within Cyber-Physical Systems”. In: *2019 IEEE/ACM 5th International Workshop on Software Engineering for Smart Cyber-Physical Systems (SEsCPS)*. Institute of Electrical and Electronics Engineers Inc, pp. 25–31.
DOI: 10.1109/SEsCPS.2019.00012
- Kaiblinger, A. & M. Woschank (2022). “State of the Art and Future Directions of Digital Twins for Production Logistics: A Systematic Literature Review”. In: *Applied Sciences* 12.2.
DOI: 10.3390/app12020669
- Kasper, L., T. Bacher, F. Birkelbach & R. Hofmann (2020). “Digitalization possibilities and the potential of the Digital Twin for steam supply systems”. In: *VGB PowerTech* 11/2020, pp. 45–52.
URL: <https://www.vgb.org/vgbmultimedia/PT202011HOFMANN-p-16462.pdf>
- Kasper, L., F. Birkelbach, P. Schwarzmayr, G. Steindl, D. Ramsauer & R. Hofmann (2022). “Toward a Practical Digital Twin Platform Tailored to the Requirements of Industrial Energy Systems”. In: *Applied Sciences* 12.14. Section “Energy Science and Technology”. Special Issue “Industry 4.0 Technologies Supporting the Energy Transition”. ISSN: 2076-3417.
DOI: 10.3390/app12146981

- Kasper, L., D. Pernsteiner, M. Koller, A. Schirrer, S. Jakubek & R. Hofmann (Jan. 2021). “Numerical studies on the influence of natural convection under inclination on optimal aluminium proportions and fin spacings in a rectangular aluminium finned latent-heat thermal energy storage”. In: *Applied Thermal Engineering* 190, p. 116448. ISSN: 13594311.
DOI: 10.1016/j.applthermaleng.2020.116448
- Kasper, L., D. Pernsteiner, A. Schirrer, S. Jakubek & R. Hofmann (2023a). “Experimental characterization, parameter identification and numerical sensitivity analysis of a novel hybrid sensible/latent thermal energy storage prototype for industrial retrofit applications”. In: *Applied Energy* 344, p. 121300. ISSN: 0306-2619.
DOI: 10.1016/j.apenergy.2023.121300
- Kasper, L., P. Schwarzmayr, F. Birkelbach, F. Javernik, M. Schwaiger & R. Hofmann (2023b). “A digital twin-based adaptive optimization approach applied to waste heat recovery in green steel production: Development and experimental investigation”. In: *Applied Energy*. Submitted for publication on 2023-06-30.
- Khodadadi, J. & S. Hosseinizadeh (2007). “Nanoparticle-enhanced phase change materials (NEPCM) with great potential for improved thermal energy storage”. In: *International Communications in Heat and Mass Transfer* 34.5, pp. 534–543. ISSN: 0735-1933.
DOI: 10.1016/j.icheatmasstransfer.2007.02.005
- Krien, U., P. Schönfeldt, J. Launer, S. Hilpert, C. Kaldemeyer & G. Pleßmann (2020). “oemof.solph—A model generator for linear and mixed-integer linear optimisation of energy systems”. In: *Software Impacts* 6, p. 100028. ISSN: 2665-9638.
DOI: 10.1016/j.simpa.2020.100028
- Kritzinger, W., M. Karner, G. Traar, J. Henjes & W. Sihn (2018). “Digital Twin in manufacturing: A categorical literature review and classification”. In: *IFAC-PapersOnLine* 51.11, pp. 1016–1022. ISSN: 2405-8963.
DOI: 10.1016/j.ifacol.2018.08.474
- Kuravi, S., J. Trahan, D. Y. Goswami, M. M. Rahman & E. K. Stefanakos (2013). “Thermal energy storage technologies and systems for concentrating solar power plants”. In: *Progress in Energy and Combustion Science* 39.4, pp. 285–319. ISSN: 0360-1285.
DOI: 10.1016/j.pecs.2013.02.001
- Leinauer, C., P. Schott, G. Fridgen, R. Keller, P. Ollig & M. Weibelzahl (2022). “Obstacles to demand response: Why industrial companies do not adapt their power consumption to volatile power generation”. In: *Energy Policy* 165, p. 112876. ISSN: 0301-4215.
DOI: 10.1016/j.enpol.2022.112876
- Li, W., Y. Zhang, X. Zhang & J. Zhao (2021). “Studies on performance enhancement of heat storage system with multiple phase change materials”. In: *Journal of Energy Storage*, p. 103585. ISSN: 2352-152X.
DOI: 10.1016/j.est.2021.103585
- Liu, M., S. Fang, H. Dong & C. Xu (2021). “Review of digital twin about concepts, technologies, and industrial applications”. In: *Journal of Manufacturing Systems* 58, pp. 346–361. ISSN: 0278-6125.
DOI: 10.1016/j.jmsy.2020.06.017
- Lu, Y., C. Liu, K. I.-K. Wang, H. Huang & X. Xu (2020). “Digital Twin-driven smart manufacturing: Connotation, reference model, applications and research issues”. In:

- Robotics and Computer-Integrated Manufacturing* 61, p. 101837. ISSN: 0736-5845.
DOI: 10.1016/j.rcim.2019.101837
- Lund, H., P. A. Østergaard, D. Connolly, I. Ridjan, B. V. Mathiesen, F. Hvelplund, J. Z. Thellufsen & P. Sorknæs (2016). “Energy Storage and Smart Energy Systems”. In: *International Journal of Sustainable Energy Planning and Management* 11, pp. 3–14.
DOI: 10.5278/ijsepm.2016.11.2
- Lund, P. D., J. Lindgren, J. Mikkola & J. Salpakari (2015). “Review of energy system flexibility measures to enable high levels of variable renewable electricity”. In: *Renewable and Sustainable Energy Reviews* 45, pp. 785–807. ISSN: 1364-0321.
DOI: 10.1016/j.rser.2015.01.057
- Martin, V. & N. J. Chiu (2022). “Industrial Applications of Thermal Energy Storage Systems”. In: *Advances in Energy Storage*. John Wiley & Sons, Ltd. Chap. 32, pp. 729–747. ISBN: 9781119239390.
DOI: 10.1002/9781119239390.ch32
- Maruf, M. N. I., G. Morales-España, J. Sijm, N. Helistö & J. Kiviluoma (2022). “Classification, potential role, and modeling of power-to-heat and thermal energy storage in energy systems: A review”. In: *Sustainable Energy Technologies and Assessments* 53, p. 102553. ISSN: 2213-1388.
DOI: 10.1016/j.seta.2022.102553
- Merlin, K., D. Delaunay, J. Soto & L. Traonvouez (2016). “Heat transfer enhancement in latent heat thermal storage systems: Comparative study of different solutions and thermal contact investigation between the exchanger and the PCM”. In: *Applied Energy* 166, pp. 107–116. ISSN: 0306-2619.
DOI: 10.1016/j.apenergy.2016.01.012
- Mesalhy, O., K. Lafdi, A. Elgafy & K. Bowman (2005). “Numerical study for enhancing the thermal conductivity of phase change material (PCM) storage using high thermal conductivity porous matrix”. In: *Energy Conversion and Management* 46.6, pp. 847–867. ISSN: 0196-8904.
DOI: 10.1016/j.enconman.2004.06.010
- Min, Q., Y. Lu, Z. Liu, C. Su & B. Wang (2019). “Machine Learning based Digital Twin Framework for Production Optimization in Petrochemical Industry”. In: *International Journal of Information Management* 49, pp. 502–519. ISSN: 0268-4012.
DOI: 10.1016/j.ijinfomgt.2019.05.020
- Moretti, L., E. Martelli & G. Manzolini (2020). “An efficient robust optimization model for the unit commitment and dispatch of multi-energy systems and microgrids”. In: *Applied Energy* 261, p. 113859. ISSN: 0306-2619.
DOI: 10.1016/j.apenergy.2019.113859
- Moser, A., D. Muschick, M. Göllés, P. Nageler, H. Schranzhofer, T. Mach, C. Ribas Tugores, I. Leusbrock, S. Stark, F. Lackner & A. Hofer (2020). “A MILP-based modular energy management system for urban multi-energy systems: Performance and sensitivity analysis”. In: *Applied Energy* 261, p. 114342. ISSN: 0306-2619.
DOI: 10.1016/j.apenergy.2019.114342
- Motahar, S. & R. Khodabandeh (2016). “Experimental study on the melting and solidification of a phase change material enhanced by heat pipe”. In: *International*

- Communications in Heat and Mass Transfer* 73, pp. 1–6. ISSN: 0735-1933.
DOI: 10.1016/j.icheatmasstransfer.2016.02.012
- Motahar, S., N. Nikkam, A. A. Alemrajabi, R. Khodabandeh, M. S. Toprak & M. Muhammed (2014). “A novel phase change material containing mesoporous silica nanoparticles for thermal storage: A study on thermal conductivity and viscosity”. In: *International Communications in Heat and Mass Transfer* 56, pp. 114–120. ISSN: 0735-1933.
DOI: 10.1016/j.icheatmasstransfer.2014.06.005
- Muhammad, M. & O. Badr (2017). “Performance of a finned, latent-heat storage system for high temperature applications”. In: *Applied Thermal Engineering* 116, pp. 799–810. ISSN: 1359-4311.
DOI: 10.1016/j.applthermaleng.2017.02.006
- Muschick, D., S. Zlabinger, A. Moser, K. Lichtenegger & M. Göllés (2022). “A multi-layer model of stratified thermal storage for MILP-based energy management systems”. In: *Applied Energy* 314, p. 118890. ISSN: 0306-2619.
DOI: 10.1016/j.apenergy.2022.118890
- Naegler, T., S. Simon, M. Klein & H. C. Gils (2015). “Quantification of the European industrial heat demand by branch and temperature level”. In: *International Journal of Energy Research* 39.15, pp. 2019–2030.
DOI: 10.1002/er.3436
- Negri, E., L. Fumagalli & M. Macchi (2017). “A Review of the Roles of Digital Twin in CPS-based Production Systems”. In: *Procedia Manufacturing* 11, pp. 939–948.
DOI: 10.1016/j.promfg.2017.07.198
- Nepustil, U., D. Laing-Nepustil, D. Lodemann, R. Sivabalan & V. Hausmann (2016). “High Temperature Latent Heat Storage with Direct Electrical Charging – Second Generation Design”. In: *Energy Procedia* 99. 10th International Renewable Energy Storage Conference, IRES 2016, 15-17 March 2016, Düsseldorf, Germany, pp. 314–320. ISSN: 1876-6102.
DOI: 10.1016/j.egypro.2016.10.121
- Niknam, P. H. & A. Sciacovelli (2023). “Hybrid PCM-steam thermal energy storage for industrial processes – Link between thermal phenomena and techno-economic performance through dynamic modelling”. In: *Applied Energy* 331, p. 120358. ISSN: 0306-2619.
DOI: 10.1016/j.apenergy.2022.120358
- Nkwetta, D. N., P.-E. Vouillamoz, F. Haghghat, M. El Mankibi, A. Moreau & K. Desai (2014). “Phase change materials in hot water tank for shifting peak power demand”. In: *Solar Energy* 107, pp. 628–635. ISSN: 0038-092X.
DOI: 10.1016/j.solener.2014.05.034
- Olsthoorn, M., J. Schleich & M. Klobasa (2015). “Barriers to electricity load shift in companies: A survey-based exploration of the end-user perspective”. In: *Energy Policy* 76, pp. 32–42. ISSN: 0301-4215.
DOI: 10.1016/j.enpol.2014.11.015
- Ommen, T., W. B. Markussen & B. Elmegaard (2014). “Comparison of linear, mixed integer and non-linear programming methods in energy system dispatch modelling”. In:

- Energy* 74, pp. 109–118. ISSN: 0360-5442.
DOI: 10.1016/j.energy.2014.04.023
- Papaefthymiou, G., E. Haesen & T. Sach (2018). “Power System Flexibility Tracker: Indicators to track flexibility progress towards high-RES systems”. In: *Renewable Energy* 127, pp. 1026–1035. ISSN: 0960-1481.
DOI: 10.1016/j.renene.2018.04.094
- Paul, A., F. Holy, M. Textor & S. Lechner (2022). “High temperature sensible thermal energy storage as a crucial element of Carnot Batteries: Overall classification and technical review based on parameters and key figures”. In: *Journal of Energy Storage* 56, p. 106015. ISSN: 2352-152X.
DOI: 10.1016/j.est.2022.106015
- Pernsteiner, D., V. Halmschlager, A. Schirrer, R. Hofmann & S. Jakubek (2022). “Efficient Sensitivity-Based Cooperation Concept for Hierarchical Multilayer Process Automation of Steam-Powered Plants”. In: *IEEE Access* 10, pp. 66844–66861.
DOI: 10.1109/ACCESS.2022.3178436
- Prawiranto, K., J. Carmeliet & T. Defraeye (2021). “Physics-Based Digital Twin Identifies Trade-Offs Between Drying Time, Fruit Quality, and Energy Use for Solar Drying”. In: *Frontiers in Sustainable Food Systems* 4. ISSN: 2571-581X.
DOI: 10.3389/fsufs.2020.606845
- Radhakrishnan, K. & A. Balakrishnan (1992). “Heat transfer analysis of thermal energy storage using phase change materials”. In: *Heat Recovery Systems and CHP* 12.5, pp. 427–435. ISSN: 0890-4332.
DOI: 10.1016/0890-4332(92)90064-0
- Rathgeber, C., E. Lävemann & A. Hauer (2022). “Economy of Thermal Energy Storage Systems in Different Applications”. In: *Advances in Energy Storage*. John Wiley & Sons, Ltd. Chap. 33, pp. 749–760. ISBN: 9781119239390.
DOI: 10.1002/9781119239390.ch33
- Ritchie, H., M. Roser & P. Rosado (2022). “Energy”. In: *Our World in Data*.
URL: <https://ourworldindata.org/grapher/global-energy-substitution> (visited on 06/08/2023)
- Sadeghi, G. (2022). “Energy storage on demand: Thermal energy storage development, materials, design, and integration challenges”. In: *Energy Storage Materials* 46, pp. 192–222. ISSN: 2405-8297.
DOI: 10.1016/j.ensm.2022.01.017
- Shoreh, M. H., P. Siano, M. Shafie-khah, V. Loia & J. P. Catalão (2016). “A survey of industrial applications of Demand Response”. In: *Electric Power Systems Research* 141, pp. 31–49. ISSN: 0378-7796.
DOI: 10.1016/j.epsr.2016.07.008
- Sierla, S., M. Azangoo, A. Fay, V. Vyatkin & N. Papakonstantinou (2020). “Integrating 2D and 3D Digital Plant Information Towards Automatic Generation of Digital Twins”. In: *2020 IEEE 29th International Symposium on Industrial Electronics (ISIE)*, pp. 460–467.
DOI: 10.1109/ISIE45063.2020.9152371
- Sleiti, A. K., J. S. Kapat & L. Vesely (2022). “Digital twin in energy industry: Proposed robust digital twin for power plant and other complex capital-intensive large engineering

- systems”. In: *Energy Reports* 8, pp. 3704–3726. ISSN: 2352-4847.
DOI: 10.1016/j.egy.2022.02.305
- Smil, V. (2017). *Energy Transitions: Global and National Perspectives*. 2nd expanded and updated edition. Available at: <https://vaclavsmil.com/2016/12/14/energy-transitions-global-and-national-perspectives-second-expanded-and-updated-edition/>. Praeger. ISBN: 144085324X.
- Steindl, G. & W. Kastner (2020). “Ontology-Based Model Identification of Industrial Energy Systems”. In: *2020 IEEE 29th International Symposium on Industrial Electronics (ISIE)*, pp. 1217–1223.
DOI: 10.1109/ISIE45063.2020.9152386
- (2021). “Semantic Microservice Framework for Digital Twins”. In: *Applied Sciences* 11.12. ISSN: 2076-3417.
DOI: 10.3390/app11125633
- Steinmann, W.-D. & M. Eck (2006). “Buffer storage for direct steam generation”. In: *Solar Energy* 80.10. Solar Power and Chemical Energy Systems (SolarPACES’04), pp. 1277–1282. ISSN: 0038-092X.
DOI: 10.1016/j.solener.2005.05.013
- Sterner, M. & I. Stadler (2019). *Handbook of Energy Storage: Demand, Technologies, Integration*. Springer. ISBN: 978-3-662-55504-0.
DOI: 10.1007/978-3-662-55504-0
- Tamme, R., T. Bauer, J. Buschle, D. Laing, H. Müller-Steinhagen & W.-D. Steinmann (2008). “Latent heat storage above 120°C for applications in the industrial process heat sector and solar power generation”. In: *International Journal of Energy Research* 32.3, pp. 264–271.
DOI: 10.1002/er.1346
- Thermal Energy Storage Technology for Industrial Process Heat Applications* (Aug. 2005). Vol. Solar Energy. International Solar Energy Conference, pp. 417–422.
DOI: 10.1115/ISEC2005-76250
- Tao, F., B. Xiao, Q. Qi, J. Cheng & P. Ji (2022). “Digital twin modeling”. In: *Journal of Manufacturing Systems* 64, pp. 372–389. ISSN: 0278-6125.
DOI: 10.1016/j.jmsy.2022.06.015
- Tao, F., H. Zhang, A. Liu & A. Y. C. Nee (2019a). “Digital Twin in Industry: State-of-the-Art”. In: *IEEE Transactions on Industrial Informatics* 15.4, pp. 2405–2415.
DOI: 10.1109/TII.2018.2873186
- Tao, F., M. Zhang, Y. Liu & A. Nee (2018a). “Digital twin driven prognostics and health management for complex equipment”. In: *CIRP Annals* 67.1, pp. 169–172. ISSN: 0007-8506.
DOI: 10.1016/j.cirp.2018.04.055
- (2018b). “Digital twin driven prognostics and health management for complex equipment”. In: *CIRP Annals* 67.1, pp. 169–172. ISSN: 0007-8506.
DOI: 10.1016/j.cirp.2018.04.055
- Tao, F., M. Zhang & Nee, A. Y. C. (2019b). “Chapter 3 - Five-Dimension Digital Twin Modeling and Its Key Technologies”. In: *Digital Twin Driven Smart Manufacturing*. Ed. by F. Tao, M. Zhang & A. Y. C. Nee. Academic Press, pp. 63–81. ISBN: 978-0-12-

- 817630-6.
DOI: 10.1016/B978-0-12-817630-6.00003-5
- (2019c). *Digital Twin Driven Smart Manufacturing*. Academic Press.
DOI: 10.1016/C2018-0-02206-9
- Tatsidjodoung, P., N. Le Pierrès & L. Luo (2013). “A review of potential materials for thermal energy storage in building applications”. In: *Renewable and Sustainable Energy Reviews* 18, pp. 327–349. ISSN: 1364-0321.
DOI: 10.1016/j.rser.2012.10.025
- Therkelsen, P. & A. McKane (2013). “Implementation and rejection of industrial steam system energy efficiency measures”. In: *Energy Policy* 57, pp. 318–328. ISSN: 0301-4215.
DOI: 10.1016/j.enpol.2013.02.003
- Thiel, G. & A. Stark (2021). “To decarbonize industry, we must decarbonize heat”. In: *Joule*.
DOI: 10.1016/j.joule.2020.12.007
- Tubeuf, C., F. Birkelbach, A. Maly & R. Hofmann (2023). “Increasing the Flexibility of Hydropower with Reinforcement Learning on a Digital Twin Platform”. In: *Energies* 16.4. ISSN: 1996-1073.
DOI: 10.3390/en16041796
- UNIDO (2017). *Accelerating clean energy through Industry 4.0: manufacturing the next revolution: A report of the United Nations Industrial Development Organization, Vienna, Austria*. Tech. rep. Available at: https://www.unido.org/sites/default/files/2017-08/REPORT_Accelerating_clean_energy_through_Industry_4.0.Final_0.pdf.
- United Nations Economic Commission for Europe (UNECE) (2022). “Presentation of survey results, insights, and recommendations”. In: Report of the UNECE Task Force on Digitalization in Energy. 2022-09-20. Available at: https://unece.org/sites/default/files/2022-09/Andrei_Covatariu_Digitalization_Electricity_Systems_0.pdf.
- Vahidinasab, V. & B. Mohammadi-Ivatloo (2023). *Energy systems transition: Digitalization, Decarbonization, Decentralization and Democratization*. Power Systems. Cham, Switzerland: Springer. ISBN: 978-3-031-22186-6.
DOI: 10.1007/978-3-031-22186-6
- Wagner, C., J. Grothoff, U. Epple, R. Drath, S. Malakuti, S. Grüner, M. Hoffmeister & P. Zimmermann (2018). “The role of the Industry 4.0 asset administration shell and the digital twin during the life cycle of a plant”. In: *IEEE International Conference on Emerging Technologies and Factory Automation, ETFA*, pp. 1–8.
DOI: 10.1109/ETFA.2017.8247583
- Wang, J., X. Li, P. Wang & Q. Liu (2022). “Bibliometric analysis of digital twin literature: a review of influencing factors and conceptual structure”. In: *Technology Analysis & Strategic Management* 0.0, pp. 1–15.
DOI: 10.1080/09537325.2022.2026320
- Wei, M., C. A. McMillan & S. de la Rue du Can (Dec. 2019). “Electrification of Industry: Potential, Challenges and Outlook”. In: *Current Sustainable/Renewable Energy Reports* 6.4, pp. 140–148. ISSN: 2196-3010.
DOI: 10.1007/s40518-019-00136-1

- Weigel, P. & M. Fishedick (2019). “Review and Categorization of Digital Applications in the Energy Sector”. In: *Applied Sciences* 9.24. ISSN: 2076-3417.
DOI: 10.3390/app9245350
- Xu, B., J. Wang, X. Wang, Z. Liang, L. Cui, X. Liu & A. Y. Ku (Nov. 2019). “A case study of digital-twin-modelling analysis on power-plant-performance optimizations”. In: *Clean Energy* 3.3, pp. 227–234. ISSN: 2515-4230.
DOI: 10.1093/ce/zkz025
- Xu, Q., M. Zhong & X. Li (2022). “How does digitalization affect energy? International evidence”. In: *Energy Economics* 107, p. 105879. ISSN: 0140-9883.
DOI: 10.1016/j.eneco.2022.105879
- Yang, M. & R. K. Dixon (2012). “Investing in efficient industrial boiler systems in China and Vietnam”. In: *Energy Policy* 40. Strategic Choices for Renewable Energy Investment, pp. 432–437. ISSN: 0301-4215.
DOI: 10.1016/j.enpol.2011.10.030
- Yang, X., Z. Lu, Q. Bai, Q. Zhang, L. Jin & J. Yan (2017). “Thermal performance of a shell-and-tube latent heat thermal energy storage unit: Role of annular fins”. In: *Applied Energy* 202, pp. 558–570. ISSN: 0306-2619.
DOI: 10.1016/j.apenergy.2017.05.007
- Yu, J., P. Liu & Z. Li (2020). “Hybrid modelling and digital twin development of a steam turbine control stage for online performance monitoring”. In: *Renewable and Sustainable Energy Reviews* 133, p. 110077. ISSN: 1364-0321.
DOI: 10.1016/j.rser.2020.110077
- Yu, W., P. Patros, B. Young, E. Klinac & T. G. Walmsley (2022). “Energy digital twin technology for industrial energy management: Classification, challenges and future”. In: *Renewable and Sustainable Energy Reviews* 161, p. 112407. ISSN: 1364-0321.
DOI: 10.1016/j.rser.2022.112407
- Zabala, L., J. Febres, R. Sterling, S. López & M. Keane (2020). “Virtual testbed for model predictive control development in district cooling systems”. In: *Renewable and Sustainable Energy Reviews* 129, p. 109920. ISSN: 1364-0321.
DOI: 10.1016/j.rser.2020.109920
- Zayed, M. E., J. Zhao, W. Li, A. H. Elsheikh, A. M. Elbanna, L. Jing & A. Geweda (2020). “Recent progress in phase change materials storage containers: Geometries, design considerations and heat transfer improvement methods”. In: *Journal of Energy Storage* 30, p. 101341. ISSN: 2352-152X.
DOI: 10.1016/j.est.2020.101341
- Zhang, H., J. Baeyens, G. Cáceres, J. Degrève & Y. Lv (2016). “Thermal energy storage: Recent developments and practical aspects”. In: *Progress in Energy and Combustion Science* 53, pp. 1–40. ISSN: 0360-1285.
DOI: 10.1016/j.pecs.2015.10.003
- Zhao, J., Y. Ji, Y. Yuan, Z. Zhang & J. Lu (2018). “Energy-Saving Analysis of Solar Heating System with PCM Storage Tank”. In: *Energies* 11.1. ISSN: 1996-1073.
DOI: 10.3390/en11010237

Publications

This chapter presents the publications constituting this thesis, including the core publications of this thesis – five journal papers – as well as further publications, comprising seven co-author publications and other scientific contributions.

For each core publication, the full paper, a short summary, my own contribution based on the CRediT taxonomy¹ and the bibliographic reference are provided. Further publications are also briefly described and my contribution to them is presented.

The publications are not sorted by release date but instead based on this thesis’s incremental research approach and thematic chronology.

Core publications

1	Numerical studies on the influence of natural convection under inclination on optimal aluminium proportions and fin spacings in a rectangular aluminium finned latent-heat thermal energy storage	46
2	Experimental characterization, parameter identification and numerical sensitivity analysis of a novel hybrid sensible/latent thermal energy storage prototype for industrial retrofit applications	64
3	Digitalization possibilities and the potential of the Digital Twin for steam supply systems	84
4	Toward a Practical Digital Twin Platform Tailored to the Requirements of Industrial Energy Systems	94
5	A digital twin-based adaptive optimization approach applied to waste heat recovery in green steel production: Development and experimental investigation	124

Further publications and other scientific contributions

	Paper A – Co-author publication	151
	Paper B – Co-author publication	152
	Paper C – Co-author publication	152
	Paper D – Co-author publication	153
	Paper E – Co-author publication	154
	Paper F – Co-author publication	154
	Paper G – Co-author publication	155
	Presentations	156
	Scientific reports	156
	Supervised theses	157
	Awards	158
	Teaching activity	158

¹According to the Elsevier CRediT author statement: <https://www.elsevier.com/authors/policies-and-guidelines/credit-author-statement>

Paper 1

Numerical studies on the influence of natural convection under inclination on optimal aluminium proportions and fin spacings in a rectangular aluminium finned latent-heat thermal energy storage

published in Applied Thermal Engineering in collaboration with Dominik Pernsteiner, Martin Koller, Alexander Schirrer, Stefan Jakubek, and René Hofmann

This journal paper covers the detailed design analysis of PCM modules for the hybrid TES concept. The specific goal was to address research question *RQ* 1.1 of this thesis, hence to find an optimal design with regard to charging/discharging speed. The paper explains the basic geometry considerations and modeling assumptions. The high-fidelity PCM model that was used in these numerical studies is explained in detail and its validation is presented. With the help of this model, different geometry variations of a rectangular aluminium finned PCM cavity could be analyzed. The parameter study focused on the combined effects of three main geometrical aspects: the aluminum fin spacing, the volumetric aluminium-to-PCM ratio, and the cavity orientation. All three present interesting trade-offs. Increasing the fin spacing leads to stronger effective heat flux enhancement due to natural convection. However, for small fin spacing as well as for some operating states, convective effects are small, and in such cases, the spacing should be as small as technically possible. In the paper, optimal fin spacing values for different cavity orientations are specified. The second aspect of the volumetric aluminum ratio always presents a trade-off between fast charging time and overall storage capacity. A guideline value of about 15 % could be determined. Regarding the third aspect, a significant influence of the cavity orientation on charging speed was found. The consideration of these effects in the design is essentially a techno-economic question since uniform fin spacings are easier to construct and thus cheaper in serial production. However, the effects must at least be considered in TES operation. With the results of this study, well-founded decisions on the PCM module design can be made. Furthermore, this paper enabled the subsequent work on co-simulation (Paper A), model reduction (Paper B), and storage state estimation (Paper C) to improve the hybrid TES concept.

My contribution: Conceptualization, Methodology, Validation, Investigation, Formal Analysis, Data Curation, Writing – Original Draft & Editing, Visualization

L. Kasper, D. Pernsteiner, M. Koller, A. Schirrer, S. Jakubek & R. Hofmann (Jan. 2021). “Numerical studies on the influence of natural convection under inclination on optimal aluminium proportions and fin spacings in a rectangular aluminium finned latent-heat thermal energy storage”. In: Applied Thermal Engineering 190, p. 116448. ISSN: 13594311.

DOI: 10.1016/j.applthermaleng.2020.116448



Contents lists available at [ScienceDirect](https://www.sciencedirect.com)

Applied Thermal Engineering

journal homepage: www.elsevier.com/locate/apthermeng



Numerical studies on the influence of natural convection under inclination on optimal aluminium proportions and fin spacings in a rectangular aluminium finned latent-heat thermal energy storage

Lukas Kasper^a, Dominik Pernsteiner^b, Martin Koller^c, Alexander Schirrer^b, Stefan Jakubek^b, René Hofmann^{a,*}

^a TU Wien, Institute for Energy Systems and Thermodynamics, Getreidemarkt 9/BA, 1060 Vienna, Austria

^b TU Wien, Institute of Mechanics and Mechatronics, Getreidemarkt 9/BA, 1060 Vienna, Austria

^c AIT Austrian Institute of Technology GmbH, Center for Energy, Sustainable Thermal Energy Systems, Giefinggasse 2, 1210 Vienna, Austria

ARTICLE INFO

Keywords:

Phase change material (PCM)
Latent heat thermal energy storage (LHTES)
Natural convection
Parameter study of rectangular enclosure dimensions
Computational fluid dynamics (CFD)
Angular dependency

ABSTRACT

Phase change material (PCM) is applicable in various use cases, such as in a novel hybrid steam/latent heat storage system where containers filled with PCM are placed at the shell surface of a Ruths steam storage (RSS) for retrofitting. The considered approximately rectangular PCM cavity design includes aluminium fins, which is a common choice for heat transfer enhancement. Numerical studies were conducted with two separate numerical models to analyse melting and solidification of PCM in such cavity. Varying aluminium proportions, as well as varying fin spacings were simulated under different orientations of the PCM cavity and their impact on charging/discharging speed was analysed, providing a foundation for design optimization of the considered geometry. Guideline values for optimal aluminium ratio and optimal fin spacing could be obtained. Significant angular dependency on the thermophysical behaviour could be observed during melting, whereas the effect of natural convection during solidification was found to be negligible. The results of this work provide important insight to facilitate the design process of rectangular aluminium finned PCM cavities.

1. Introduction

1.1. Motivation

As a consequence of progressive decarbonisation efforts the energy-intensive industries are required to drastically increase energy efficiency. A large increase of thermal energy storage capacity in existing industrial plants and processes is therefore required in the future. Having the advantage of high energy density, Phase Change Material (PCM) is commonly used either in stand-alone storage systems, e.g., passive climatization modules in buildings, or to retrofit existing storage systems of other types. An overview of typical PCM and their application is given in Zalba et al. [1]. Dusek and Hofmann [2] presented a novel approach to increase the storage capacity of well-established Ruths steam storages (RSS) by attaching PCM containers to its outer shell. To ensure optimal use of latent heat thermal energy storages (LHTES) it is necessary to study the exact thermodynamic behaviour of the included PCM containers.

Different types of PCM encapsulations have been developed in the past, each tailored to the specific use case of interest (for an overview see, for example, Lin et al. [3], Zayed et al. [4], or Agyenim et al. [5]). PCM is typically placed in long thin heat pipes, cylindrical containers or rectangular containers, whereby the shell and tube system are the most intensely analysed LHTES type [5]. The typically low thermal conductivity of PCM prevents rapid heat transfer during charging (melting) and discharging (solidification) processes. Various techniques were developed to improve heat transfer rates in LHTES, e.g., using extended surfaces [6–8], high thermal conductivity porous matrices [9,10], heat pipes [11], nanoparticles [12] and carbon nanotubes [13], to mention a few. A very common approach for heat transfer enhancement is to equip the encapsulations with heat conductivity enhancement structures, such as flat-plate aluminium fins [14]. The application of such fins is particularly desirable due to the effectiveness in performance, ease in fabrication, and relatively low cost of construction [5]. In the hybrid storage approach presented by Dusek and Hofmann [2], PCM cavities are arranged around the cylindrical RSS where each cavity features aluminium fins orientated in the radial-axial plane of the RSS. Due to the

* Corresponding author at: Institute for Energy Systems and Thermodynamics, TU Wien, Getreidemarkt 9/E302, 1060 Vienna, Austria.

E-mail address: rene.hofmann@tuwien.ac.at (R. Hofmann).

<https://doi.org/10.1016/j.applthermaleng.2020.116448>

Received 4 May 2020; Received in revised form 9 November 2020; Accepted 7 December 2020

Available online 19 December 2020

1359-4311/© 2020 The Authors. Published by Elsevier Ltd. This is an open access article under the CC BY license (<http://creativecommons.org/licenses/by/4.0/>).

Nomenclature	
Acronyms	
CFD	Computational Fluid Dynamics
FDM	Finite Difference Method
FEM	Finite Element Method
LHTES	Latent Heat Thermal Energy Storage
PCM	Phase Change Material
RMSE	Root Mean Square Error
RSS	Ruths Steam Storage
Index	
alu	aluminium
conduction	conduction only reference case
in	inner value
init	initial value
out	outer value
ref	reference
Parameters and variables	
α	heat transfer coefficient ($\text{W m}^{-2} \text{K}^{-1}$)
β	volumetric thermal expansion coefficient (K^{-1})
Δl_m	specific latent heat (J kg^{-1})
Δt	time step (s)
Δx_{PCM}	cavity PCM dimension in x direction (m)
Δy_{PCM}	cavity PCM dimension in y direction (m)
\dot{Q}	heat flux (W)
ϵ	mushy region temperature range (K)
\hat{H}	enthalpy per unit volume (J m^{-3})
\mathbf{f}	force density ($\text{kg m}^{-2} \text{s}^{-2}$)
\mathbf{g}	gravitational acceleration vector (ms^{-2})
\mathbf{q}	specific heat flux (W m^{-2})
\mathbf{S}_m	momentum source term
\mathbf{u}	velocity vector (m s^{-1})
μ	dynamic viscosity (N s m^{-2})
ϕ	fin segment orientation
ρ	density (kg m^{-3})
ρ_0	constant density of PCM (kg m^{-3})
a	volumetric aluminium ratio
B	momentum source term coefficient (Pa s m^{-3})
c	specific heat capacity ($\text{J kg}^{-1} \text{K}^{-1}$)
f_l	liquid fraction
h	specific enthalpy (J kg^{-1})
k	thermal conductivity ($\text{W m}^{-1} \text{K}^{-1}$)
L_x, L_y	length of PCM segment in x,y direction (m)
p	pressure (N m^{-2})
S_h	enthalpy source term
T	temperature ($^{\circ}\text{C}$)
t	time (s)
T_m	melting temperature ($^{\circ}\text{C}$)
u, v	velocity components in x,y direction (m s^{-1})
w	aluminium fin spacing (m)
x, y	space coordinates (m)
\tilde{L}	characteristic length (m)
τ	dimensionless time
A	aspect ratio
A_{mush}	mushy zone constant ($\text{kg m}^{-3} \text{s}^{-1}$)
Fo	Fourier number
H	cavity height (m)
Pr	Prandtl number
Ra	Rayleigh number
Ste	Stefan number
EF	convective enhancement factor
Symbols	
$\mathcal{D}, \partial \mathcal{D}$	spatial domain, boundary of spatial domain
∇	Nabla operator: $\nabla = (\partial/\partial x, \partial/\partial y)$

typical dimensions of the hybrid storage, these fin segments are approximately rectangular, effectively making this a flat-plate rectangular PCM cavity design (for more details, see Section 2 and Fig. 1). In this work, numerical studies were conducted to analyse the melting and solidification of PCM in such encapsulation and thus providing essential

information to enable storage design optimization.

1.2. PCM simulation methods

Analytical solutions only exist for a limited number of phase change

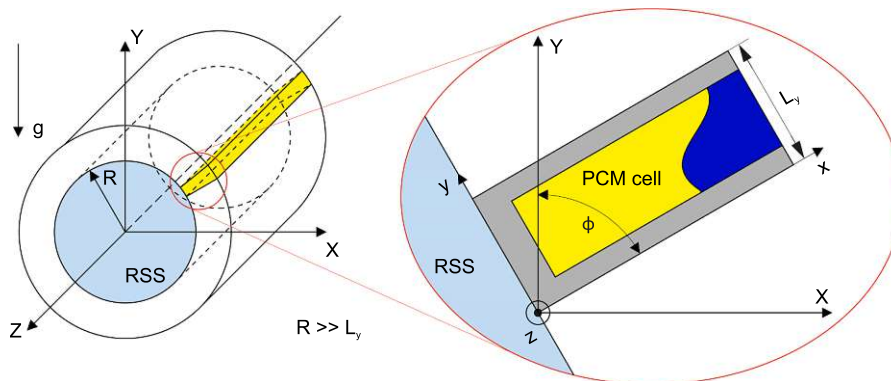


Fig. 1. The location of the PCM cells attached to a RSS is illustrated, as proposed by Dusek and Hofmann [2]. Geometry and location of the considered PCM fin segment and adjacent fin segments and orientation relative to the gravitational vector are defined. Liquid PCM is depicted in yellow, solid PCM in blue. For details on PCM cell geometry, see Fig. 2. Note: This illustration is not true to scale.

problems, as for example for the one-dimensional Stefan-problem, see for example [15]. When treating problems in more than one dimension and considering heat transfer by conduction and convection, numerical methods have to be applied. Also, the Stefan problem is complicated by the fact that in general more than one moving phase boundary occur in PCM [16]. Liu et al. [17] and Dutil et al. [18] review options for mathematical modelling and simulation of PCM. The majority of these approaches uses the enthalpy method, as for example in Voller and Prakash [19] or the effective heat capacity method, as in Tenchev et al. [20], to account for phase change.

Although finite difference (FDM) and finite volume schemes are well established in computational fluid dynamics (CFD) applications, including the well-known software package *ANSYS Fluent*, Nedjar [21] states that especially finite element methods (FEM) are able to handle complex coupled thermomechanical problems with various and complex boundary conditions. Kasper [22] pursued an approach to couple an FEM implementation of the effective heat capacity method and an adaptation of the FDM code published by Seibold [23] to solve the 2D Navier–Stokes equations arising in convection modelling. This experimentally validated and highly adaptable model was applied for the parameter studies presented in this work, alongside with the CFD software *ANSYS Fluent*.

1.3. Previous studies

When designing PCM cavities, the thermodynamic behaviour has to be assessed in detail to enable optimal storage design regarding storage capacity and charging/discharging times. Natural convection can have a significant influence on this behaviour, additionally being dependent on the cavity orientation. Furthermore, the amount of heat transfer enhancing metal structures has to be optimized. Although the installation of fins can efficiently enhance PCM melting rate [24], it also restricts natural convection and reduces PCM volume and thus lowers the overall storage capacity [25]. Thus, fin dimensions as fin spacing and width should be appropriately selected to achieve better performance of the storage application [25–27]. These aspects were investigated to some extent and for specific PCM cavity geometries in previous studies, as the following review, primarily focussing on rectangular fin geometries, shows.

One important question is how natural convection in the liquid phase of the storage material influences the phase change problem. The relative influence of natural convection depends on both geometric parameters and PCM properties. Mostafavi Tehrani et al. [28] found a critical Rayleigh number of $8 \cdot 10^5$ below which natural convection is negligible in their respective shell-and-tube configuration. Dhaidan and Khodadadi [29] give an overview on melting with natural convection in different geometries. Numerous experimental and numerical analyses have been dedicated to melting in rectangular geometries, as for example by Bareiss and Beer [30], Benard et al. [31], Duan et al. [32] or Jany and Bejan [33]. However, Vogel et al. [34] state that the findings of this research are not directly applicable to large aspect ratio cavities and high temperature inorganic PCM, like $\text{KNO}_3\text{-NaNO}_3$. In their respective work a flat plate LHTES, filled with the above-mentioned PCM, is analysed numerically, with a lab scale storage unit serving as experimental validation platform. Thereby, the influence of natural convection on the heat transfer rate was assessed by an introduced convective enhancement factor, providing a simple comparison of varying enclosure dimensions. Their results indicated that heat transfer enhancement due to natural convection increases with greater widths and smaller heights of storage material enclosures.

Many studies have already investigated the geometric and design parameters of heat transfer enhancing fins for PCM cavities [35]. Xie et al. [36,37] characterized the effects of metal structure, metal volume fraction and orientation and proposed optimized tree shape designs outperforming the flat plate designs. Xie et al. [38] suggested that their optimized tree shape structure is more superior in applications where

minimum conductive material is necessary and natural convection is significant. However, in a review on geometric and design parameters of fins employed for enhancing LHTES, Abdulateef et al. [35] state that the best enhancement is achieved using longitudinal finned configurations because of its easy design and fabrication. Lacroix and Benmadda [39] found in a numerical investigation that there is an optimum number of fins in a horizontal rectangular enclosure beyond which the melting rate decreases due to the weakening of convection currents. This was also found by Huang et al. [40] who reported that decreasing the fin spacing can impede the convective motion of liquid PCM between fins and therefore decreases the positive effect of fins. Biwole et al. [41] numerically studied the melting of paraffin in a vertical finned enclosure heated from one side. They varied number and thickness of the fins and found that using thinner but longer fins increases the heat transfer rate. Ye et al. [42] studied the effects of different cavity volume fractions of PCM on fluid flow and heat transfer behaviour. Bondareva and Sheremet [43] analysed the effect of fin height and width on convective melting intensity.

Regarding the orientation, i.e. inclination of PCM enclosures, Zhao et al. [44] theoretically and experimentally studied the contact melting of PCM in a rectangular cavity at different orientations and found that there is a unique optimal orientation to minimize melting time in the considered arrangement. Yang et al. [45] experimentally studied the effect of inclination and Yazici et al. [46] studied the combined effects of inclination angle and fin number on thermal performance of a PCM cavity, heated from their wide side. Their results revealed that the inclination angle and fin number plays a critical role on the formation of convective cells in the liquid PCM domain and consequently on the heat transfer and operating time. Sharifi et al. [47] studied the effect of orientation during outward melting from a concentrically heated rod placed inside a cylindrical enclosure. It was observed that even small tilting of the enclosure significantly affects the evolution of the melting front. In an investigation on melting of PCM in an unfinned rectangular enclosure with a specific fixed geometry for different Stefan numbers Kamkari et al. [48] found that when the orientation of the enclosure varies from 90° to 45° and 0° , the melting time reduces by 37% and 52%, respectively. In an experimental investigation, Kamkari and Groulx [49] analysed the effect of the cavity orientation on the melting rate for 1-fin and 3-fin rectangular enclosures and found small inclination angles to enhance melting in this specific enclosure geometry. This was confirmed in Karami and Kamkari [50] where this type of finned cavity was studied numerically under different inclination angles varied from 0° to 180° . Therein, the authors stress that limited attention has been given to the effect of orientation on the thermal behaviour of PCM in rectangular enclosures and that the only studies devoted to the effect of orientation on the melting process in finned PCM enclosures can be found in Kamkari and Groulx [49], Karami and Kamkari [50] and more recently in Groulx et al. [51]. Similar studies analysed the partly combined effects of fin spacing, thickness and angle on the optimum geometry for shell and tube LHTES configurations [52,53].

1.4. Main contributions

As can be seen from the above cited literature, numerous numerical and experimental studies on the effect of natural convection in PCM cavities have been published in recent years. Some of these considered different rectangular geometries, many analysed the design of heat enhancement fins and even studies of varying cavity orientation can be found, albeit very few. However, the findings of previous investigations are often difficult to exploit for different geometric characteristics. Many of the cited analyses cover rectangular enclosures heated/cooled from a wide side of the cavity, whereby this work focuses on heat transfer through one of the narrow sides of the cavity.

To the best of the authors' knowledge, no experimental or numerical investigation has been conducted to study the combined effects of (i) aluminium proportions, (ii) fin spacing and (iii) cavity orientation on

charging/discharging speed of this type of rectangular PCM cavity arrangement. Hence, we consider the following as main contributions of this work:

- The effect of natural convection on charging (melting) and discharging (solidification) of a narrow rectangular finned PCM cavity was studied for different orientations. Significant angular dependency on the thermophysical behaviour was observed during charging, while the effect of natural convection during discharging was found to be negligible regardless of the orientation.
- The influence of the aluminium proportion of the finned cavity on the charging/discharging speed was evaluated, thus giving a measure for optimized cavity design.
- The influence of the aluminium fin spacings on the charging/discharging speed was studied, leading to quantitative statements about optimized fin configuration. The influence of natural convection is expressed by a convective enhancement factor for three different fin spacing configurations and varying cavity orientations.

This work presents how aluminium ratio and fin spacing of rectangular finned PCM cavity can be systematically optimized, hence guiding the design of applications as and similar to the concept proposed by Dusek and Hofmann [2]. The here presented study is essential for construction and the upcoming experimental investigations of this storage application.

1.5. Paper structure

This paper is organised as follows: In Section 2, the numerical modelling conducted for the presented parameter study is discussed and the applied *Fluent* and FEM/FDM model are explained in reasonable detail. The validation of these models is given in Section 3. The results of the conducted parameter studies are presented and discussed in Section 4. In Section 5, the main findings are highlighted and critically assessed and their practicality evaluated. Suggestions for further research are given.

2. Numerical modelling

The numerical models for the presented investigation are based on the following assumptions:

- Heat transfer is driven by conduction and natural convection.
- Material properties are constant in each phase but they can differ for the liquid and solid phases except for the density which is assumed to be constant and equal for both phases.
- Density is assumed to be constant except for the buoyancy term (Boussinesq approximation), and the only body force arises due to the gravitational acceleration in vertical direction. The flow is therefore considered incompressible, Newtonian and also laminar.
- Phase transition takes place in a small temperature region (“mushy region”) $T \in [T_m - \varepsilon, T_m + \varepsilon]$ around the melting temperature T_m and is only dependent on T (no hysteresis, no dynamics, no rate dependency).
- The depth of the rectangular enclosure in z-direction (as defined in Figs. 1 and 2) is assumed large enough for wall boundary layer effects to be negligible, hence the problem is reduced to two dimensions (no heat flow or convection in z-direction).
- Movement of the solid phase is neglected.
- Radiation and viscous dissipation is neglected.

The assumptions made herein are the same as those applied by Vogel et al. [34], who could successfully validate their model via experimental data. Since the same material of (KNO₃-NaNO₃) was used therein as in the present study and the geometry of the PCM cavity is considered very similar, we consider these assumptions justified. For general fin

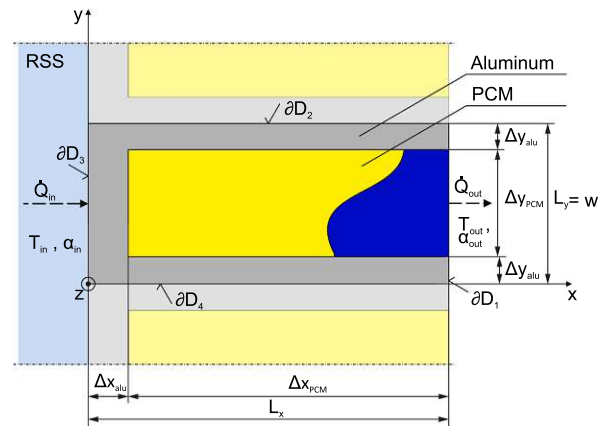


Fig. 2. Definition of geometry of the considered PCM fin segment, including boundary conditions. Liquid PCM is depicted in yellow, solid PCM in blue. (For interpretation of the references to colour in this figure legend, the reader is referred to the web version of this article.)

arrangements a three-dimensional cavity simulation might be required. However, the geometry of the regarded PCM cavities in this work, where the depth of the enclosure in z-direction is assumed large enough for wall boundary layer effects to be negligible, suggests symmetry reduction of the simulation problem to single aluminium fin segments and a two-dimensional approach. In the hybrid storage concept of Dusek and Hofmann [2] this geometry relates to an aluminium fin structure orientated in the radial-axial plane of an RSS. With a typical pressure vessel outer diameter of 2050 mm, as in Hofmann et al. [54], and the considered PCM segment length in this work of 120 mm, the fin segments exhibit an aperture angle of 5,6° for the widest considered fin spacing and of under 1,2° for more reasonable fin spacings under 20 mm. Hence, the diameter of the RSS is considered large against the width of the enclosure in y-direction, thus justifying a rectangular approximation of a fin segment. Fig. 2 illustrates the examined fin segment consisting of a rectangular aluminium enclosure filled with PCM. This segment is modelled in local coordinates (x, y) in the two-dimensional spatial domain \mathcal{D} and its boundary $\partial\mathcal{D}$, defined as follows:

$$\begin{aligned} \mathcal{D} &= \{0 \leq x \leq L_x, 0 \leq y \leq L_y\} \\ \partial\mathcal{D} &= \partial\mathcal{D}_1 \cup \partial\mathcal{D}_2 \cup \partial\mathcal{D}_3 \cup \partial\mathcal{D}_4 \\ \partial\mathcal{D}_1 &= \{x = L_x, y \in \mathcal{D}\} \\ \partial\mathcal{D}_2 &= \{x \in \mathcal{D}, y = L_y\} \\ \partial\mathcal{D}_3 &= \{x = 0, y \in \mathcal{D}\} \\ \partial\mathcal{D}_4 &= \{x \in \mathcal{D}, y = 0\} \end{aligned} \quad (1)$$

For the top and bottom walls ($\partial\mathcal{D}_2$ & $\partial\mathcal{D}_4$) adiabatic boundary conditions are applied based on the cavity’s symmetry:

$$\mathbf{q}|_{\partial\mathcal{D}_2, \partial\mathcal{D}_4} = 0 \quad (2)$$

On the left and right sides of the domain ($\partial\mathcal{D}_1$ & $\partial\mathcal{D}_3$) type-3 boundary conditions, also known as Robin boundary conditions,

$$\mathbf{q}|_{\partial\mathcal{D}_3} = \alpha_{in} \cdot (T(x, y) - T_{in}) \quad (3)$$

$$\mathbf{q}|_{\partial\mathcal{D}_1} = \alpha_{out} \cdot (T(x, y) - T_{out}) \quad (4)$$

are implemented, prescribing a heat flux dependent on the current boundary temperature $T(x, y)$, specified heat transfer coefficients α_{in} , α_{out} and ambient temperatures T_{in} , T_{out} .

Regarding the planar velocity field $\mathbf{u} = [u, v]^T$ with its spatial components $u(x, y, t)$ and $v(x, y, t)$, no-slip boundary conditions are set for the domain boundaries,

$$\mathbf{u}|_{\partial\Omega} = 0, \quad (5)$$

as well as at in-domain phase boundaries. For details on the implementation, see [22].

In this work two different transient numerical models were utilized to study the melting and solidification behaviour of the PCM segment. The main model implements the corresponding equations for convection/conduction in MATLAB® [55] using an FEM/FDM approach. The auxiliary model simulates a PCM cell in *Fluent* and is used to provide validation of the main model. In the following subsections both model implementations are described.

2.1. ANSYS Fluent model

The model developed for the investigations on a PCM segment in *Fluent* uses the finite volume approach. It is a two-dimensional model with the expansion of one single cell in z-direction (symmetry boundary conditions). It is based on the Navier–Stokes equations for energy, momentum and mass conservation.

Fluent uses an enthalpy-porosity technique developed in [19,56] to describe the melting/solidification process. Thereby the melting front is not tracked explicitly, instead a liquid fraction $f_l \in [0, 1]$ is assigned to each cell. The liquid fraction is determined in each iteration via the enthalpy balance. With this approach melting/solidification at a certain temperature point (e.g., for pure substances or eutectic mixtures) as well as melting/solidification across a temperature range (“mushy region”) can be treated. The balance equations are applied for a mixture of both phases (liquid and solid) using the liquid fraction as compound (see [57]).

With the melting/solidification approach in *Fluent*, the PCM is assumed incompressible. Density gradients due to temperature distribution are considered to drive natural convection using the Boussinesque approximation.

2.1.1. Governing equations

The governing balance equations for energy, momentum and mass conservation are (for detailed descriptions see [34] or [57]):

$$\text{energy eq. : } \rho \frac{\partial h}{\partial t} + \nabla \cdot (\rho \mathbf{u} h) = \nabla \cdot (k \nabla T) + S_h \quad (6)$$

$$\text{momentum eq. : } \rho \frac{\partial \mathbf{u}}{\partial t} + \rho (\mathbf{u} \cdot \nabla) \mathbf{u} = \mu \nabla \cdot (\nabla \mathbf{u}) - \nabla p + \mathbf{b} + \mathbf{S}_u \quad (7)$$

$$\text{continuity eq. : } \nabla \cdot \mathbf{u} = 0 \quad (8)$$

In (6)–(8) ρ represents the constant density, μ the dynamic viscosity, p the pressure and T the temperature of a cell. In the enthalpy-porosity approach the specific enthalpy h is the sum of the sensible enthalpy h_s and the latent heat Δl_m according to the liquid fraction f_l (9). In this work, ∇ and Δ are the Nabla and Laplace operators respectively. The enthalpy source term S_h (10) is introduced to discretize the energy equation as a single phase for a two-phase problem.

$$\text{enthalpy of a cell : } h = h_s + f_l \Delta l_m \quad (9)$$

$$\text{enthalpy source term : } S_h = \rho \frac{\partial (f_l \Delta l_m)}{\partial t} + \rho \nabla \cdot (\mathbf{u} f_l \Delta l_m) \quad (10)$$

$$\text{momentum source term : } \mathbf{S}_u = -B \mathbf{u} \quad (11)$$

$$\text{buoyancy term : } \mathbf{b} = \rho \beta (T - T_{\text{ref}}) \mathbf{g} \quad (12)$$

The buoyancy term \mathbf{b} from (7) is defined with the Boussinesq approximation, a reference temperature T_{ref} , the gravity vector \mathbf{g} and a volumetric thermal expansion coefficient β in (12). The momentum source term \mathbf{S}_u in (11) is a damping term for (8). This term must be zero for a

cell in liquid state but becomes very large for a cell in solid state to ensure velocities near zero. The term

$$B = A_{\text{mush}} \frac{(1 - f_l)^2}{f_l^3 + 10^{-3}} \quad (13)$$

in (11) is a function of the liquid fraction and a mushy zone constant A_{mush} , as defined in [34,58]. This is an adaption of the Carman-Kozeny equation [59]. A large mushy zone constant results in a strong damping of convection in the transition area between liquid and solid (“mushy region”). Shmueli et al. [60] investigated the influence of the value A_{mush} for a material with a mushy region and find a great variation of results with different values of A_{mush} . More recent investigations can be found in Fadl and Eames [61], Kumar and Krishna [62] or Arena et al. [63]. Although overall large influence of the parameter on the results have been obtained, Vogel et al. [34] state that with a smaller mushy region, the mushy zone constant becomes less important.

2.1.2. Discretization

The pressure-based solver SIMPLE developed by Patankar [64] is selected for pressure-velocity coupling in the balance equations. The second-order differencing scheme was used for solving the momentum and energy equations, whereas the interpolation of pressure values at the cell faces is done with the PRESTO! scheme. The temporal derivatives are discretized with a second-order implicit transient formulation. The convergence criterion for continuity, velocity components in x- and y-directions, and energy are 10^{-4} , 10^{-4} and 10^{-8} respectively. The underrelaxation factors for the velocity components, pressure correction, thermal energy and liquid fraction were 0.4, 0.8, 1 and 0.4, respectively. It has been observed that several iterations are required to obtain convergent results for an underrelaxation factor of the liquid fraction this low. Therefore the minimum number of iterations is set to 20.

2.2. FEM/FDM model

The developed FEM/FDM model used for the simulation studies in this work was developed by Kasper [22] and is outlined in the following.

2.2.1. Governing equations

The governing equations within the framework of assumptions are the energy Eq. (14), continuity Eq. (15) and Navier–Stokes Eq. (16), which are in this work implemented as follows:

$$\rho c \frac{\partial T}{\partial t} = k \nabla \cdot (\nabla T) - \rho c \nabla \cdot (T \cdot \mathbf{u}) \quad (14)$$

$$\nabla \cdot \mathbf{u} = 0 \quad (15)$$

$$\rho \left(\frac{\partial \mathbf{u}}{\partial t} + (\mathbf{u} \cdot \nabla) \mathbf{u} \right) - \mu \nabla \cdot (\nabla \mathbf{u}) + \nabla p = \mathbf{f} + \mathbf{S}_u \quad (16)$$

Therein, the temperature field $T(x, y, t)$ is treated as dependent variable in the energy Eq. (14) and the velocity field \mathbf{u} is treated as dependent variable in the Navier–Stokes Eq. (16), see [65]. The symbols denote the parameters density ρ , apparent heat capacity

$$c = \begin{cases} c_{\text{solid}} & \text{if: } T_m - \varepsilon > T, \\ \frac{\Delta l_m + c_{\text{solid}} \cdot (T_m + \varepsilon - T) + c_{\text{liquid}} \cdot (T - (T_m + \varepsilon))}{2\varepsilon} & \text{if: } T_m - \varepsilon < T < T_m + \varepsilon, \\ c_{\text{liquid}} & \text{if: } T > T_m + \varepsilon, \end{cases} \quad (17)$$

heat conductivity k and dynamic viscosity μ . The force density \mathbf{f} formulates the buoyancy force

$$\mathbf{f} = \rho \mathbf{g} = \rho_0 \mathbf{g} (1 - \beta (T - T_{\text{ref}})), \quad (18)$$

which is calculated as given in Huang et al. [66] by the volumetric thermal expansion coefficient β , the constant density ρ_0 , a reference temperature T_{ref} and the gravitational standard acceleration vector \mathbf{g} . The source term S_u as defined in (11) is added to modulate the additional viscous force with respect to the liquid fraction f_l .

2.2.2. Discretization

The FEM/FDM discretization of the governing Eqs. (14)–(16) is outlined in the following. For more details, refer to Kasper [22] or Pernsteiner et al. [67].

The energy Eq. (14) is discretised in space using a standard Galerkin FEM. Four-noded bilinear rectangular elements are used to obtain a finite element representation of the temperature field $T(x, y, t)$. Using this finite element representation and applying Galerkin's method of weighted residuals (see, for example, [68]) results in a system of ordinary differential equations. To compute the coefficient matrices, the surface and volume integrals are split into the finite element domains and are then numerically solved applying two-point Gauss–Legendre quadrature and three-point Gauss–Lobatto quadrature for the convection terms. The ordinary differential equation system is solved implicitly for the temperature field at the next time step by applying the backwards Euler method.

The velocity field components $u(x, y, t)$ and $v(x, y, t)$ and the set of incompressible 2D Navier–Stokes Eq. (16) are treated separately from the heat transfer part of the model by applying a finite difference discretization based on a MATLAB® code available on the course homepage (<http://math.mit.edu/~gs/cse/>) of “Computational Science and Engineering” at the Massachusetts Institute of Technology. This open source code, created and documented by Seibold [23] was implemented and extended to meet specific tasks in the work [22]. The main numerical concept used therein is the fractional step method [69], which is applied to split the Navier–Stokes system into equations that are significantly simpler to work with. The solution update for the velocity is then found by executing a three-step approach, (1) an explicit time step for the nonlinear convective acceleration terms, (2) an implicit time step for linear viscosity terms and (3) a pressure correction step.

The spatial discretization via the FDM is conducted using a staggered grid based on the finite element mesh, where the pressure p is defined in the element centres, u values are defined in the middle of the vertical element edges and the values of v are defined in the middle of the horizontal element edges (see [22,23]).

3. Validation

The numerical models utilized herein were validated by experimental data (see Section 3.1). Furthermore, a cross validation of the FEM/FDM model and the *Fluent* model is given based on a number of reference cases which are part of the parameter study conducted in the scope of this work (see Section 3.2). The conducted independence study of grid size and time step for the presented parameter study is discussed in Section 3.3. Details on the grid size and time step independence for the experimental validation case can be found in Kasper [22] for the FEM/FD model.

Regarding the independence study for the *Fluent* model, we found a difference of 2.6% in the liquid fraction value after 20 min between simulations with $\Delta x = \Delta y = 0.5$ mm and $\Delta x = \Delta y = 1.0$ mm. Furthermore we found a difference in the liquid fraction value of 0.03% between simulations with $\Delta t = 0.1$ s and $\Delta t = 0.01$ s. We consider the grid and time step as converged with $\Delta x = \Delta y = 1.0$ mm and $\Delta t = 0.1$ s and used these parameters for comparison with the experimental reference case.

3.1. Experimental validation

The conduction/convection models used in the here presented study

were validated with the benchmark experiment of Gau and Viskanta [70], who investigated the melting and solidification behaviour of gallium in a rectangular enclosure. Furthermore, comparison with the numerical results of Brent et al. [71], Kumar et al. [72] is given.

The mushy zone constant A_{mush} for this problem was varied between 10^5 and 10^9 $\text{kg m}^{-3}\text{s}^{-1}$. The best agreement with the experimental data was obtained for the value $A_{mush} = 10^8$ $\text{kg m}^{-3}\text{s}^{-1}$ and is given below.

Very good agreement of the simulated melted volume fraction compared to the experimental data was found for the FEM/FDM model, with a root mean squared error of below 3% (for details, see [22]). The quantitative agreement between the simulations in this work and the benchmark experimental and numerical results is reasonable for all compared times, capturing regions of different melting regimes. A comparison of the simulated and reference melting front at three different times is given in Fig. 3. A comparison of the liquid fraction is given in Fig. 4, together with the root mean square error (RMSE) calculated from the respective given melting front data. Minor quantitative deviations can be obtained therein. The melting progresses slightly slower in the FEM/FDM simulation and fits reasonably well to the experimental data. In the *Fluent* simulation, melting progresses faster, similar to the reference case by Kumar et al. [72]. It should be noted, that discrepancies between the FEM/FDM and *Fluent* model were found to be smaller for the parameter studies of $\text{KNO}_3\text{-NaNO}_3$, see Section 3.2.

Remaining deviations to the experimental data of Gau and Viskanta [70] generally arise from inconsistencies between the assumptions of selected mathematical model and the exact experimental procedure [73]. Some controversy about the flow structure for this investigation and therefore the case's adequacy as validation benchmark still remains. Some researchers suggest that the correct solution should feature multiple convective cells [73], while three-dimensional simulations showed the absence of multiple convective cells [74]. To further verify the accuracy of the present investigation, a numerical cross validation of the two developed models was conducted.

3.2. Numerical cross validation

In total 24 reference cases of the following parameter studies were simulated using both the FEM/FDM and *Fluent* models. These cases included melting and solidification, fin spacings w of 12.5 mm, 25.0 mm, 50.0 mm, aluminium volumetric ratios a of 4%, 8% and 16% and segment orientations ϕ of 0° , 45° , 90° , 135° , 180° , as well as cases considering only conduction. The maximum obtained RMSE of the simulated enthalpy change values was 15.6%. The RMSE over all 24

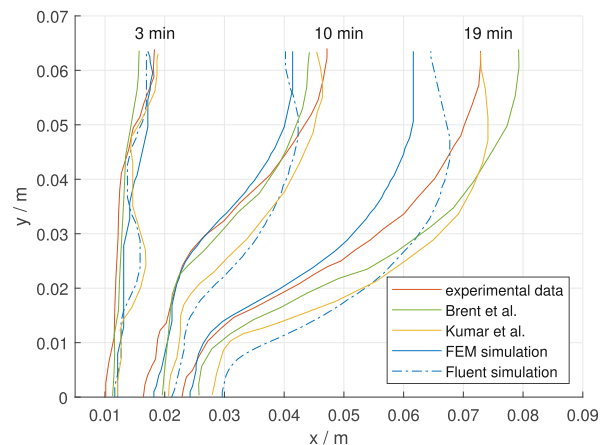


Fig. 3. Melting front results of the developed numerical models compared to experimental and numerical reference results at three different times of the melting progress.

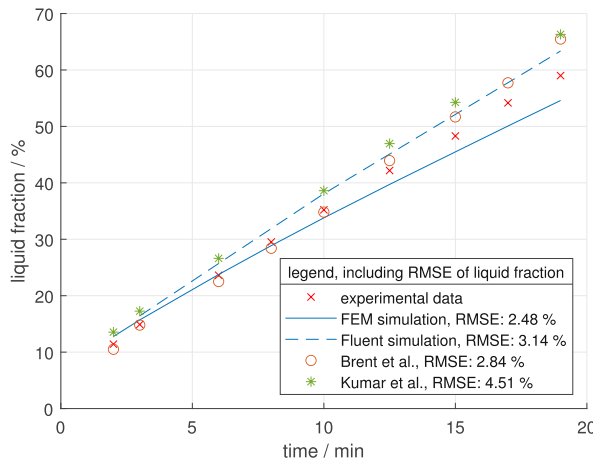


Fig. 4. Liquid fraction results of the developed numerical models compared to experimental and numerical reference results.

reference values and all logged time steps for the relative deviation of the enthalpy change values was 3.8%. We consider these as small discrepancies between the two models for the regarded simulation cases, therefore providing another verification of the conducted simulation studies in this work.

3.3. Grid size and time step independence study

The accuracy implications of the element grid and time step sizes were carefully tested to keep the computational effort in reasonable limits.

The mushy zone constant A_{mush} for this problem is chosen to be 10^6 which is in the recommended range by ANSYS® Fluent, Release 16.0 [57]. This value lies in accordance with [34], and their experimental validation while using (KNO_3-NaNO_3) .

3.3.1. ANSYS Fluent model

The geometry and mesh creation was carried out with ANSYS Workbench [75]. To ensure mesh and time step independency, convergence studies were performed. The rectangular and structured mesh consists of 240×50 elements in x- and y-direction, respectively. To achieve a volumetric mesh, one element and symmetry boundary conditions are used in z-direction. A uniform time step of $\Delta t = 0.05$ s was applied for all simulated reference cases during the numerical cross validation.

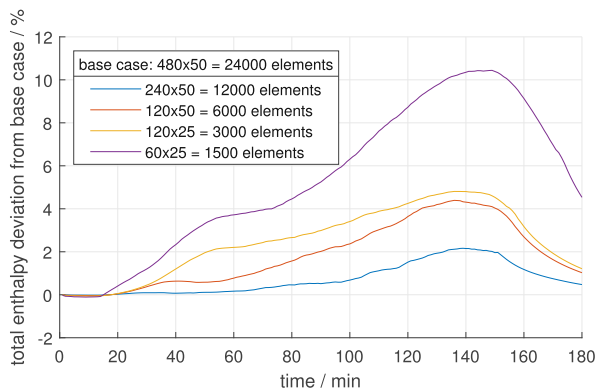


Fig. 5. Grid size sensitivity for simulation case with $w = 12.5$ mm, $a = 8\%$ and $\phi = 0^\circ$. Carried out with a time step size $\Delta t = 0.05$.

3.3.2. FEM/FDM model

For the finite element simulations, uniformly distributed grids of 12000 elements presented adequate resolution. The grid size sensitivity is illustrated for a reference simulation case in Fig. 5. Further refinement showed non-significant impact on the simulation results within the scope of this investigation, which holds true for all simulated geometries. Furthermore, the effect of time step size was investigated and a time step size of $\Delta t = 0.05$ s was selected for the simulation studies. Fig. 6 shows good convergence of the solution for this value. The selected grid and time step proved accurate and sufficient to meet the Courant-Friedrichs-Lewy (CFL) condition [76]

$$\begin{aligned} \Delta t &\leq \Delta x / |u|, \\ \Delta t &\leq \Delta y / |v|, \end{aligned} \quad (19)$$

where $\Delta x, \Delta y$ are the mesh resolutions and $|u|, |v|$ the magnitudes of the velocity in x- and y-directions. Fig. 7 illustrates the maximum CFL numbers in the liquid domain in x- and y-direction for all here investigated cases over the whole duration of the simulation.

4. Results and discussion

In this Section, the results of the parameter study regarding charging/discharging performance of the considered PCM storage design are illustrated by a number of representative results and discussed. While the considered materials' thermophysical properties remained unchanged (see Section 4.1.2), three geometrical aspects were varied, which is explained in Section 4.1.1.

4.1. Parameter study remarks

Since this work presents a foundation to thermal energy storage design optimization for industrial applications, the characteristic measure investigated herein is the total stored thermal energy, i.e. total enthalpy [54]. For further comprehension of the results, illustrations of latent enthalpy and convective enhancement are presented.

It should be noted that the obtained results highly depend on all three varied geometrical aspects. As it is not possible to study the influence of all three at the same time, the herein given results are presented in a way where at least one aspect is always constant. However, the extent of the presented results allow to fully assess the design characteristics in the considered parameter range.

Small oscillations of the calculated heat flux can be obtained, which are attributed to the nature of the finite element discretization and shape functions in combination with the apparent heat capacity method, which are known for supporting spurious oscillations [77]. However, careful comparisons of numerical errors over discretization fineness as

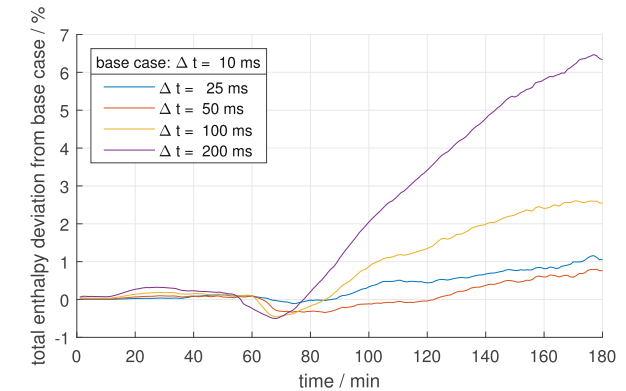


Fig. 6. Time step sensitivity for simulation case with $w = 12.5$ mm, $a = 8\%$ and $\phi = 0^\circ$. Carried out with a grid size of 12000 elements.

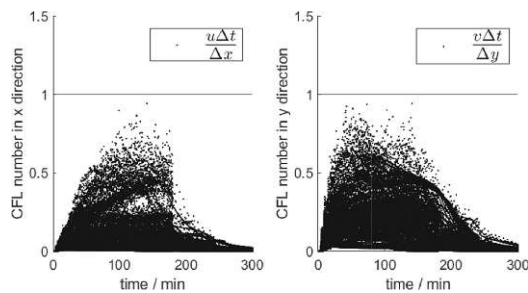


Fig. 7. Scatter plot of the maximum CFL numbers in the liquid domain for all investigated cases over the whole simulation duration.

mentioned above have been carried out to control these numerical errors. Similar oscillations can be found in other numerical investigations, as for example [41], not effecting the qualitative results.

4.1.1. Geometry

As described in Section 2, the PCM storage design of interest is that of PCM filled aluminium encapsulations including plane parallel aluminium fins. A fin segment of such cavity is illustrated in Figs. 1 and 2. The conducted parameter study presented in this work focused on three main geometrical aspects:

- (i) the aluminium fin spacing $w = L_y$,
- (ii) the aluminium-to-PCM ratio $a = 2\Delta y_{\text{alu}}/L_y$ in vol% (neglecting the aluminium share introduced by Δx_{alu}),
- (iii) the fin segment orientation ϕ , as defined in Fig. 1.

In all studies, the material properties as well as the wall thickness of the heated wall $\Delta x_{\text{alu}} = 2$ mm were held constant in this study. Also, the segment length $L_x = 120$ mm is kept constant, which is done because in previous research, this value was found optimal for the considered PCM arrangement and for a specific industrial use case with charging/discharging cycle times of about 3 h. The underlying design optimization was published in Hofmann et al. [54].

4.1.2. Material properties

The considered PCM is an eutectic mixture of potassium nitrate and sodium nitrate $\text{KNO}_3\text{-NaNO}_3$ which is commonly used for high-temperature phase change thermal storage systems [78]. Its properties were obtained from Vogel et al. [34] and are given in Table 1, including values for the liquid state (L) and solid state (S), alongside the utilized property data of the simulated aluminium encapsulation. Variable properties of specific heat capacity c and heat conductivity k are approximated in this study by different, but constant values for the liquid and solid state. A similar approach for this material was pursued

Table 1

Material properties of the considered LHTES used in this study. Source: Vogel et al. [34].

Property	PCM ($\text{KNO}_3\text{-NaNO}_3$)	Aluminium
density $\frac{\rho}{\text{kg m}^{-3}}$	2050	2700
spec. heat capacity $\frac{c}{\text{J}(\text{kgK})^{-1}}$	1350 (S) 1492 (L)	910
heat conductivity $\frac{k}{\text{W}(\text{mK})^{-1}}$	0.457 (S) 0.435 (L)	237
melting temperature $\frac{T_m}{^\circ\text{C}}$	220 (± 0.1)	–
spec. latent heat $\frac{\Delta I_m}{\text{kJ}(\text{kg})^{-1}}$	108	–
thermal expansion coefficient $\frac{\beta}{(\text{K})^{-1}}$	$3.5 \cdot 10^{-4}$	–
dynamic viscosity $\frac{\mu}{\text{Ns}(\text{m})^{-2}}$	$5.8 \cdot 10^{-4}$	–

by Vogel et al. [79], who set the properties for the charging process to the values of the solid state and for the discharging process to the value of the liquid state. The authors stated that this simplifies the model and results in better convergence of the governing equations and resulting deviations are considered to be rather small.

4.1.3. Initial and boundary conditions

The melting temperature of the simulated PCM was set to $T_m = 220$ °C, with a mushy region of $\pm \epsilon = \pm 0.1$ °C. For charging simulations, the whole storage cell was initialized at a temperature of $T_{\text{init}} = 219$ °C, and a left-hand side heating temperature of $T_{\text{in}} = 230$ °C was prescribed, with a fixed heat transfer coefficient of $\alpha_{\text{in}} = 700$ W/mK. This value of α_{in} corresponds to the heat transfer from liquid water to metal [80,81]. For discharging simulations, the initialization temperature was set to $T_{\text{init}} = 221$ °C and a left-hand side temperature of $T_{\text{in}} = 200$ °C was applied. The insulation of the PCM cell was considered perfect in the scope of transient charging/discharging simulations, hence the right-hand side was considered adiabatic corresponding to a heat transfer coefficient of $\alpha_{\text{in}} = 0$ W/mK. The duration of the simulation was in most cases 3 h, as argued above. Selected simulation cases were defined to cover a longer charging duration, to observe full liquefaction of the PCM.

4.2. Effects of angular dependency

To illustrate the angular dependency of convection effects in the PCM cavity, the progression of enthalpy per unit volume over time during charging and discharging is given in Fig. 8 for fixed cavity parameters $w = 25.0$ mm and $a = 8\%$. Five different cavity orientations were simulated and compared to the case considering only heat conduction. Fig. 8a shows significant influence for the upwards-oriented cavities (0° , 45°), whereas convection effects are small for the orientation angles 135° and 180° for this geometry. It should be noted however, that these findings differ from cases with larger fin spacings, as discussed in Section 4.4, where convection effects are very significant also for downwards orientated cavities. Furthermore, the influence of convection effects also depends on the aluminium ratio a , because the melting shape and therefore convective domains in the PCM cavity change significantly with the altered distribution of heat into the PCM.

Convective effects during solidification were found negligible, which is illustrated by Fig. 8b. This result was also found for other values of fin spacing and aluminium besides for the fixed cavity parameters $w = 25.0$ mm and $a = 8\%$ and therefore proved independent of fin spacing and aluminium. For this reason, we focused on the charging scenario in the remainder of this parameter study. It should be noted, however, that the obtained result of negligible convective effects during solidification regardless of orientation, fin spacing, or aluminium ratio is restricted to the considered cavity geometry and especially to the chosen discharging scenario. For example, results might differ for discharging scenarios starting at higher temperatures, where convection is expected to be effective in the initial cooling phase. The observed insensitivity of convective heat transfer during discharging is attributed to the effect that the PCM, with its low thermal conductivity, acts as an insulator once solidification at the aluminium fins sets in. Thereby, the temperature gradient inside the - now well insulated - liquid sub-domain is small and convection is negligible. The fact that natural convection is negligible during the discharge of LHTES was already reported by, for example, [82,83]. The only reason natural convection can affect the solidification process is very high sensible heating of the liquid or heating from the boundary. However, these effects seem negligible in the here considered PCM cavity design.

4.3. Effects of aluminium ratio

The ratio of aluminium to PCM in this cavity design has strong impact on the charging/discharging performance. Higher aluminium

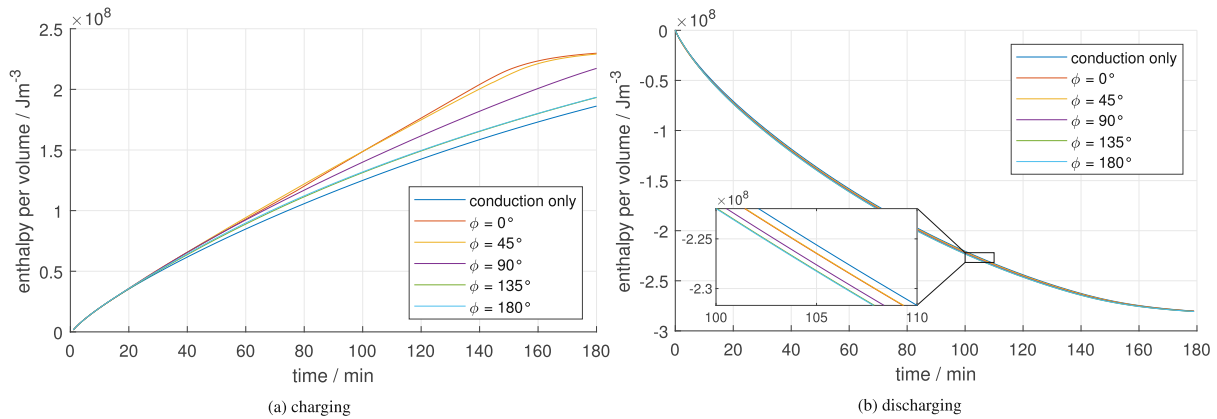


Fig. 8. Progression of enthalpy per volume over time during charging (a) and discharging (b), referenced to the starting point, for fixed fin spacing $w = 25.0$ mm, aluminium ratio $a = 8\%$ and different segment orientations ϕ compared to conduction only case.

shares result in better heat conductivity and therefore faster cavity charging/discharging, while at the same time the sum of specific heat capacity and specific latent heat per unit volume is reduced. Therefore, the choice of aluminium ratio faces a trade-off between storage capacity and charging/discharging speed. The results discussed in this work give indicators to support such decisions. The relation between the total storage capacity in the considered charging scenario of the cavity and its aluminium ratio is given in Fig. 9.

The effect of three exemplary aluminium ratios $a = 4\%$, $a = 8\%$ and $a = 16\%$ on charging speed (specific heat flux/ Wm^{-2}) is illustrated for three different fin spacings and for cavity orientation $\phi = 0^\circ$ and the case considering only conduction in Fig. 10. For the small fin spacing of $w = 12.5$ mm, we obtain only small heat flux enhancement due to convection, whereas it is significantly higher for fin spacings $w = 25.0$ mm and $w = 50.0$ mm. This effect will be discussed in detail in Section 4.4. It should also be noted that the reason of the sudden drop in heat flux towards the end of the charging process for aluminium ratios $a = 8\%$ and $a = 16\%$ is caused by the cavity reaching full liquefaction and therefore its maximum capacity. This becomes apparent by examining Fig. 11, where the change of latent heat per volume over time for the same particular charging cases is given.

Upon close examination of Fig. 10b, which shows charging speeds of cavities with fin spacing $w = 25.0$ mm, a slight but sharp increase in heat

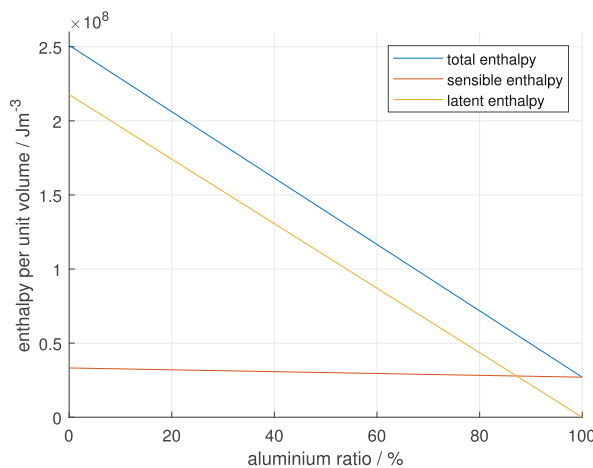


Fig. 9. Dependency of total storage capacity (enthalpy per unit volume) and its sensible and latent part on aluminium ratio for the considered cavity design and charging scenario.

flux can be obtained at around 80 min. The reason for this is an intensification of convection in the cavity as soon as the liquid PCM area reaches a critical size. After this point, the heat flux remains nearly constant until it drops again due to the previously mentioned completion of charging. The small time gap between the onset of this heat flux increase of the different aluminium ratio cases is assumed to have two reasons. Firstly, the PCM area is naturally slightly narrower for cavities with wider fins resulting of higher aluminium ratios. It therefore takes more time until the liquid PCM area reaches a critical size. Secondly, due to higher aluminium ratios also a higher amount of heat is transferred through the fins and effectively further into the cavity domain, which in turn leads to a different melting behaviour. As can be interpreted from temperature distributions of these cases, the liquid PCM area consists of rather narrow parts, where convection is limited. In contrast, cases with lower aluminium ratio develop a wide liquid PCM area near the heated wall, since heat transfer through the fins to the opposite side of the heated wall is comparatively smaller.

4.3.1. Optimal aluminium ratio

To obtain information about the optimal ratio of aluminium for the considered cavity geometry, aluminium ratios between 2% and 40% in increments of 2% were simulated for fixed fin spacing $w = 25.0$ mm and segment orientations $\phi = 0^\circ$, $\phi = 45^\circ$ and $\phi = 90^\circ$ as well as the conduction only case. Fig. 12 illustrates the results of this investigation by means of the time needed to reach particular charging levels, expressed by the enthalpy change per unit volume referenced to the starting value. From these charging levels, the relative charging level can be obtained from the relation in Fig. 9, which also shows that the charging level of $2.0 \cdot 10^8 \text{ Jm}^{-3}$ can not be reached in case of aluminium ratios above 22%, same as $1.7 \cdot 10^8 \text{ Jm}^{-3}$ for aluminium ratios above 36%.

Looking at the lower charging levels of $0.8 \cdot 10^8 \text{ Jm}^{-3}$ and $1.3 \cdot 10^8 \text{ Jm}^{-3}$ in Fig. 12, no significant difference between convection cases and conduction only case exists, except for very small aluminium ratios. For higher charging levels of $1.7 \cdot 10^8 \text{ Jm}^{-3}$ and $2.0 \cdot 10^8 \text{ Jm}^{-3}$ though, this difference is quite pronounced. These high charging levels are reached faster by segment orientations $\phi = 0^\circ$ and $\phi = 45^\circ$ compared to $\phi = 90^\circ$ and considerably faster compared to the conduction only case. This is especially distinctive for small aluminium ratios, where in some cases the chosen charging levels could not be reached within the 3 h charging scenario.

Looking at the two lower charging levels, it can be seen that aluminium ratios above 15 to 20% just lead to marginal reductions of the charging time. The same conclusion can be drawn at the two higher charging levels, where the time needed to reach the charging level even increases with the upper values of the illustrated aluminium ratios. This

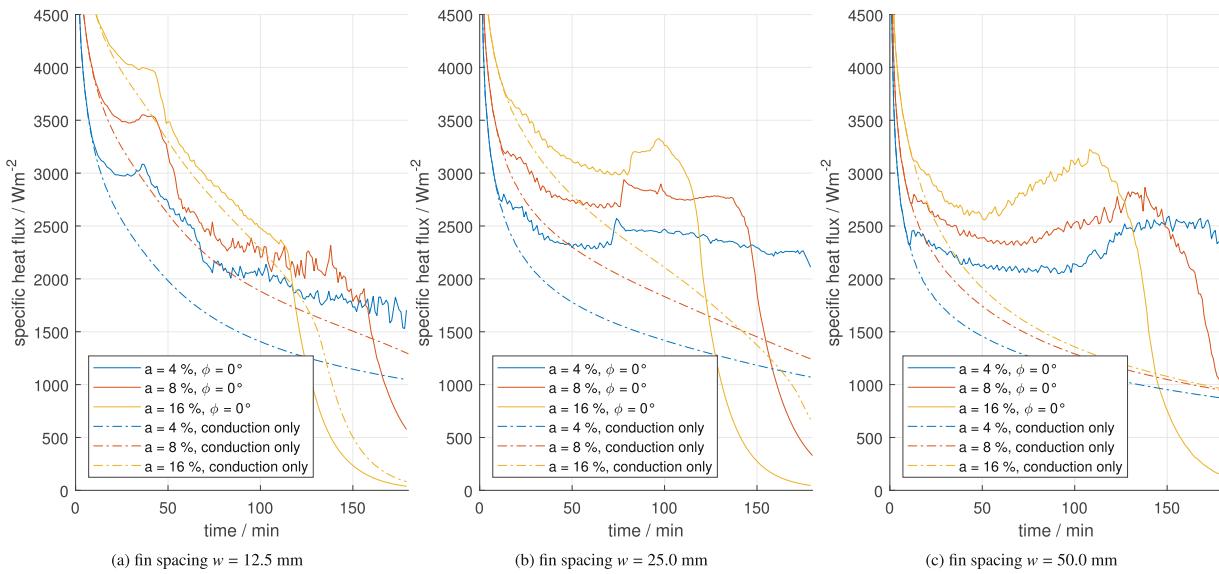


Fig. 10. Effect of different aluminium ratios on charging speed (specific heat flux) for segment fin spacings (a) $w = 12.5$ mm, (b) $w = 25.0$ mm, (c) $w = 50.0$ mm and segment orientation $\phi = 0^\circ$ compared to conduction only case.

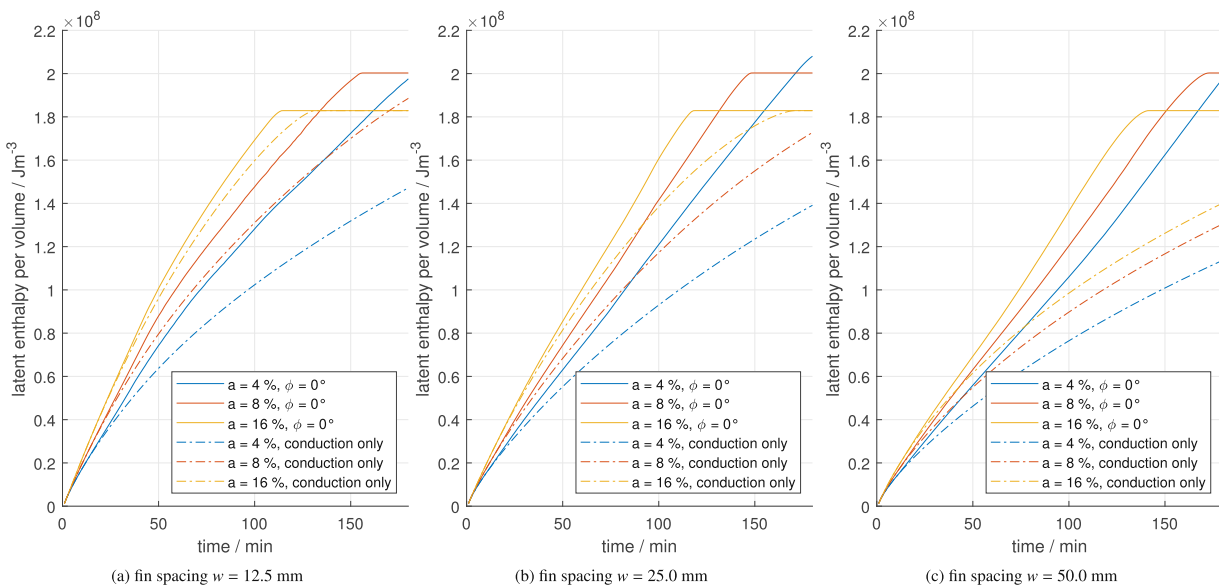


Fig. 11. Effect of different aluminium ratios on progression of latent enthalpy per volume over time during charging, referenced to the starting point, for segment fin spacings (a) $w = 12.5$ mm, (b) $w = 25.0$ mm, (c) $w = 50.0$ mm and segment orientation $\phi = 0^\circ$ compared to conduction only case.

however is of course caused by the limited storage capacity and the fact that the heat flux diminishes towards the end of charging due to the absence of high temperature gradients.

All in all, for the investigated cases and charging scenario, an aluminium ratio of about 10 to 15% appears to be the optimal choice, presenting an efficient trade-off between fast charging time and overall storage capacity.

4.4. Effects of aluminium fin spacing

Although the aluminium fin spacing should be as small as possible when neglecting the effect of natural convection, it has been shown that decreasing the fin spacing can impede the convective motion of the

liquid PCM and therefore decrease their positive effects (see, for example [39,40]). The effect of three exemplary fin spacings $w = 12.5$ mm, $w = 25.0$ mm and $w = 50.0$ mm on charging speed (specific heat flux [Wm^{-2}]) is illustrated in Fig. 13 for three different aluminium ratios $a = 4\%$, $a = 8\%$ and $a = 16\%$ and for segment orientation $\phi = 0^\circ$ and the case considering only conduction. The change of latent heat per volume over time for these charging cases is given in Fig. 14, similar to Fig. 11 in Section 4.3. Figs. 13 and 14 show that for the fin spacing $w = 12.5$ mm convection effects lead to only small enhancement in specific heat flux, with the exception of small aluminium ratio $a = 4\%$. This becomes apparent especially in the case of high aluminium ratio $a = 16\%$. Furthermore, while smaller fin spacings lead to overall higher heat flux and faster charging times in the conduction only cases and especially for

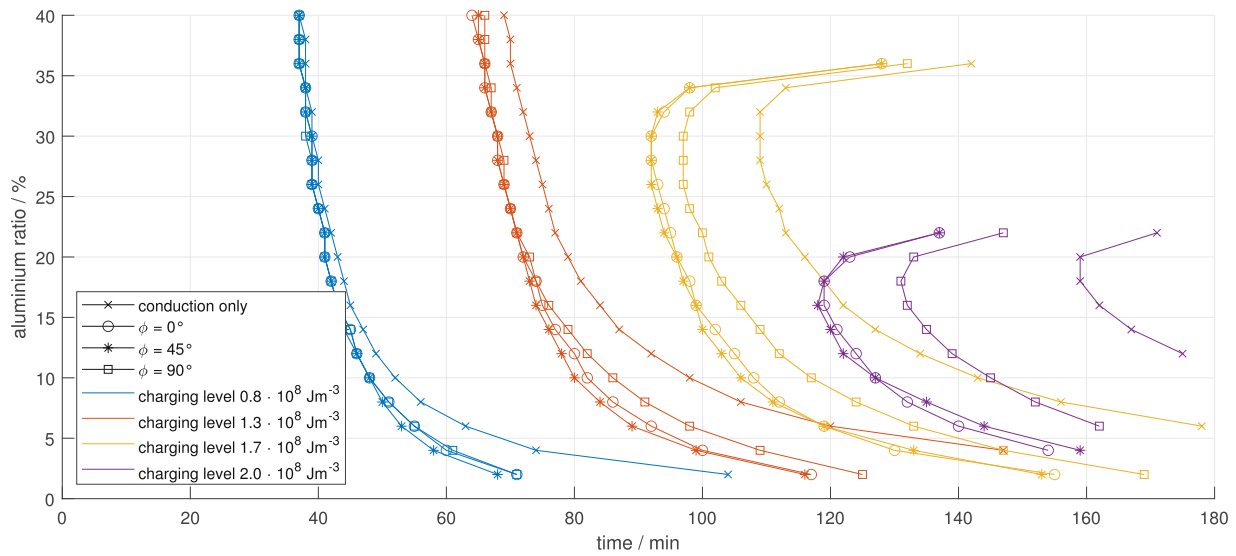


Fig. 12. Effect of different aluminium ratios on time to reach charging level (enthalpy per volume) for fixed fin spacing $w = 25.0$ mm and different segment orientations $\phi = 0^\circ$, $\phi = 45^\circ$ and $\phi = 90^\circ$ compared to conduction only case.

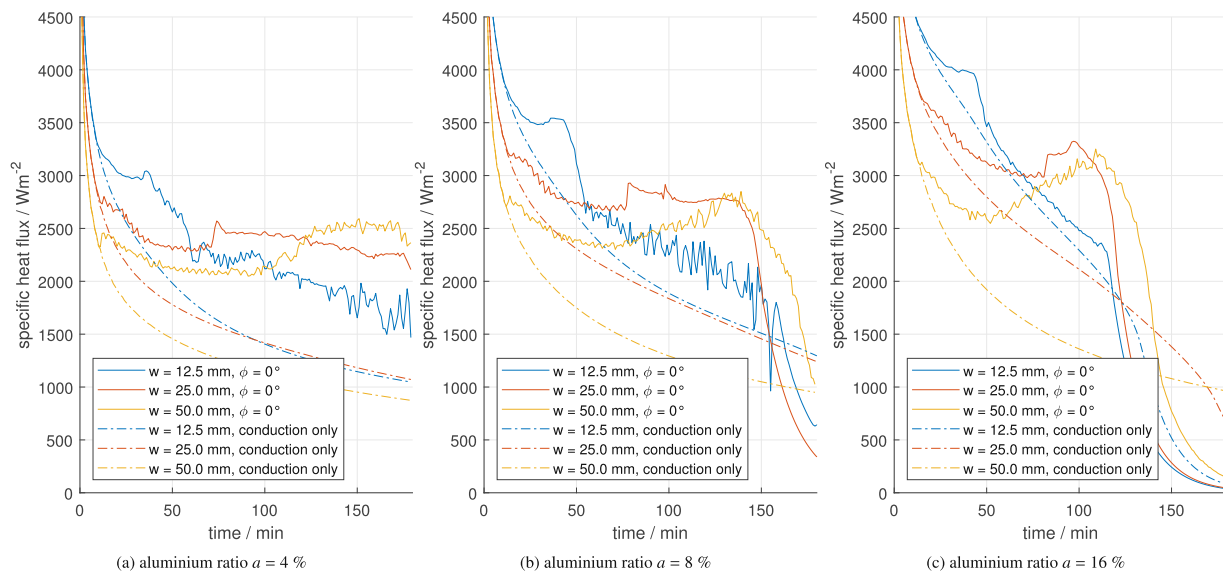


Fig. 13. Effect of different fin spacings on charging speed (specific heat flux) for aluminium ratios (a) $a = 4\%$, (b) $a = 8\%$, (c) $a = 16\%$ and segment orientation $\phi = 0^\circ$ compared to conduction only case.

high aluminium ratio, the same can not be said for the convection case with orientation $\phi = 0^\circ$. While the small fin spacings produce high heat fluxes and faster charging times compared to the cases with fin spacings of $w = 25.0$ mm and $w = 50.0$ mm in the case of high aluminium ratio $a = 16\%$, for the lower aluminium ratios $a = 4\%$ and $a = 8\%$ the charging times are almost identical. The cases with fin spacings $w = 25.0$ mm even surpass the charging speed of the small fin spacings $w = 12.5$ mm, as shown in Fig. 14a and b.

It can be concluded that the heat transfer by natural convection is substantial especially in case of large fin spacings and small aluminium ratios. To quantify this impact of natural convection on the heat transfer, the convective enhancement factor

$$EF(\hat{H}) = \frac{\dot{Q}(\hat{H})}{\dot{Q}_{\text{conduction}}(\hat{H})} \quad (20)$$

is calculated, as introduced by Vogel et al. [34]. It is defined as the ratio of the actual heat flux considering natural convection to a hypothetical heat flux by heat conduction only. Since time scale and phase front progression are different in each case, both heat flux values are evaluated at equal enthalpy per volume \hat{H} , which approximates to the liquid phase fraction f_l . The convective enhancement factors for fixed aluminium ratio $a = 8\%$ for three particular fin spacings and segment orientations ranging from 0° to 180° are illustrated in Fig. 15. Enhancement factors of up to $EF = 2$ arise in case of fin spacing $w = 12.5$

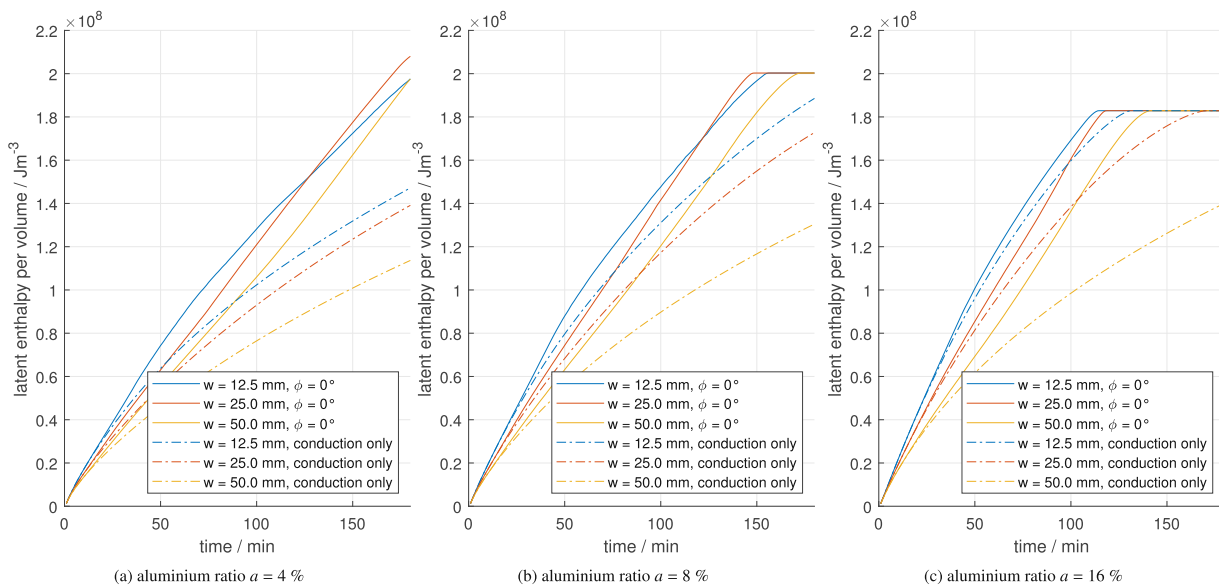


Fig. 14. Effect of different fin spacings on progression of latent enthalpy per volume over time during charging, referenced to the starting point, for aluminium ratios (a) $a = 4\%$, (b) $a = 8\%$, (c) $a = 16\%$ and segment orientation $\phi = 0^\circ$ compared to conduction only case.

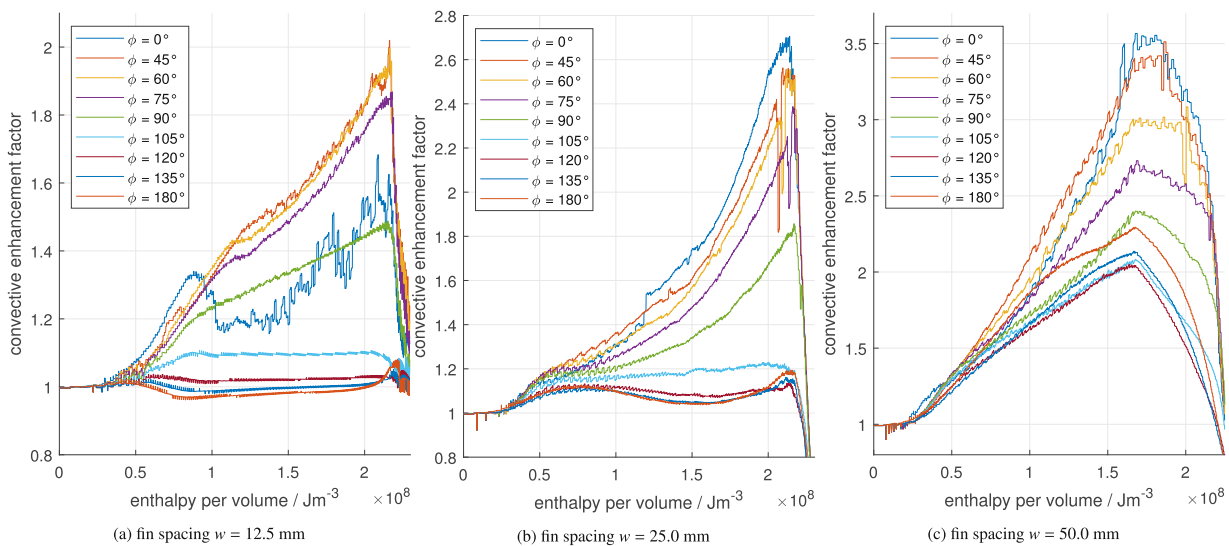


Fig. 15. Convective enhancement factor for aluminium ratio $a = 8\%$ and fin spacings (a) $w = 12.5$ mm, (b) $w = 25.0$ mm, (c) $w = 50.0$ mm for different segment orientations ϕ .

mm, while for the wider fin spacings $w = 25.0$ mm and $w = 50.0$ mm enhancement factors of up to $EF = 2.8$ and $EF = 3.6$ arise, respectively. Looking at Fig. 15a and b, low convective enhancement factors and therefore negligible influence of natural convection on heat transfer for downwards orientated segments (orientation $\phi = 105^\circ, 120^\circ, 135^\circ, 180^\circ$) can be obtained. Fig. 15c however shows convective enhancement factors of up to $EF = 2$ for these downwards orientated segments. In case of wide fin spacings, as in the case $w = 50.0$ mm, heat is thus transferred downwards through the aluminium fins and natural convection in this case transfers heat back up the segment, hence increasing the heat distribution.

Regarding the convective enhancement in upwards orientated segments, almost the same behaviour can be observed for the orientations $\phi = 0^\circ, 45^\circ, 60^\circ, 75^\circ$ in the corresponding fin spacing cases. An

exception to this is the segment orientation $\phi = 0^\circ$ for the fin spacing $w = 12.5$ mm, where the convective enhancement factor decreases after the initial charging phase and after that shows high variability and is considerably lower than that of segment orientations $\phi = 45^\circ, 60^\circ, 75^\circ$. This interesting effect can be explained by observing the velocity distribution during the charging of this segment. The liquid area in the PCM part of the segment has to reach a particular size so that convection effects become crucial. In case of the segment with small fin spacing $w = 12.5$ mm and orientation $\phi = 0^\circ$, two separate convection vortices form due to symmetry, both being too small to strongly affect the heat transfer enhancement. A slight tilt of the segment however breaks this symmetry, leading to a single convection vortex. This therefore covers a larger liquid PCM area resulting in stronger convection and heat transfer enhancement.

4.4.1. Optimal fin spacing

To investigate the optimal fin spacing for this type of PCM cavity geometry, an aluminium ratio of 8% was selected and segment orientation $\phi = 0^\circ$, $\phi = 45^\circ$ and $\phi = 90^\circ$ as well as the conduction only case were compared for different fin spacings. In a preliminary parameter study, fin spacings between 5 mm and 100 mm in increments of 6.25 mm were simulated. The results are illustrated in Fig. 16 similarly to Fig. 12 in Section 4.3. In this case the charging levels are expressed by % of the total storable enthalpy per volume of the fin segment, since this value is equal for all compared cases with all of them having the same aluminium ratio. As expected, in the conduction only case the charging time increases with increasing fin spacing, which is also true for the time to reach the charging level 30% when considering convection, since up to this point heat transfer is still dominated by conduction. For the cases considering convection though, an optimal fin spacing value can be obtained for each case. For segment orientation $\phi = 0^\circ$ a fin spacing of $w = 18.75$ mm leads to the fastest time to reach the charging levels 70% and 90%, while the charging level of 50% is reached slightly faster with a fin spacing of $w = 12.5$ mm. For segment orientations $\phi = 45^\circ$ and $\phi = 90^\circ$ fin spacings of $w = 12.5$ mm lead to the fastest charging times.

Based on the results of the preliminary study to find an optimal fin spacing, a second parameter study with refined resolution was conducted to eliminate errors and achieve improved results. Fig. 17 shows the results of this investigation, where additionally fin spacings between 5 mm and 30 mm in increments of 1.25 mm were simulated. For segment orientation $\phi = 45^\circ$ fin spacings between $w = 10$ mm and $w = 15$ mm lead to the fastest charging times. The findings of fin spacing optimum between $w = 15.0$ mm and $w = 20.0$ mm for segment orientation $\phi = 0^\circ$ and fin spacing optimum of $w = 13.75$ mm for segment orientation $\phi = 90^\circ$ accurately confirm the results of the preliminary study. Notably, another local optimum for segment orientation $\phi = 0^\circ$ can be obtained due to the refined fin spacing resolution, which is situated between $w = 7.5$ mm and $w = 8.75$ mm.

To explain the findings illustrated in Fig. 17, the velocity distribution in the liquid PCM part of the cavity has to be observed in the particular case. As addressed in the explanation of Fig. 15a, the liquid PCM area has to reach a certain size for a strong convection vortex to develop. For this reason, the segments with orientation $\phi = 90^\circ$ show an optimum in fin spacing at around $w = 13$ mm. For wider fin spacings the heat transport via the fins is less effective and convective effects cannot make up this detriment. In case of segment orientation $\phi = 0^\circ$ this optimum is

situated at wider fin spacings, because two separate convection vortices develop due to the symmetry and the necessary liquid area is therefore wider than in the case of orientation $\phi = 90^\circ$.

The local optimum for segment orientation $\phi = 0^\circ$ at fin spacings of about $w = 8$ mm is apparently caused by a breakdown in the symmetry of the liquid PCM flow in the cavity. This leads to the development of a single convection vortex, resulting in enhanced heat transfer and therefore lower charging times. For fin spacings of about $w = 10$ mm this effect subsides, since separate convection vortices develop that are less pronounced than at $w = 20$ mm due to their reciprocal disturbance. Heat transfer is therefore decreased and charging time is slowed. This interesting effect is not obtained for segment orientation $\phi = 90^\circ$ because buoyancy forces are not as significant in such wide and very low fin segments.

4.5. Remark on dimensional analysis

The results discussed above show that the melting process depends on the geometrical and thermal parameters of investigated PCM cavity. As a thorough dimensional analysis of the here presented studies would be extremely comprehensive, only the range of the relevant non-dimensional groups is given. Thus, the main aspects of the fundamental heat transfer mechanics and flow phenomena can be deduced.

The Prandtl number

$$Pr = \frac{c_p \mu}{k} = 17.1 \quad (21)$$

and Stefan number

$$Ste = \frac{c_p \Delta T}{\Delta I_m} = 0.125 \quad (22)$$

are constant throughout all simulated melting cases, where $\Delta T = T_{in} - T_m$ is the temperature difference between the heated wall and the melting temperature. The further relevant non-dimensional numbers are the Rayleigh number

$$Ra = \frac{g \beta \Delta T L^3}{\frac{k}{\rho c_p} \mu} \quad (23)$$

the Fourier number

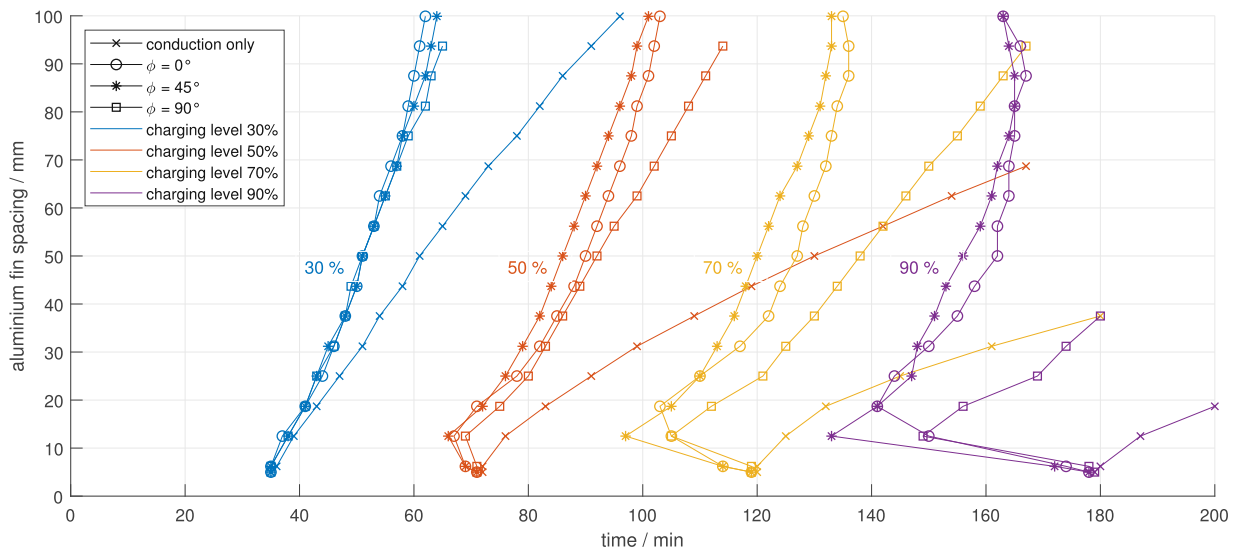


Fig. 16. Effect of different fin spacings (5 mm to 100 mm) on time to reach charging level (% of total enthalpy per volume) for fixed aluminium ratio $a = 8\%$ and different segment orientations $\phi = 0^\circ$, $\phi = 45^\circ$, $\phi = 90^\circ$ compared to conduction only case.

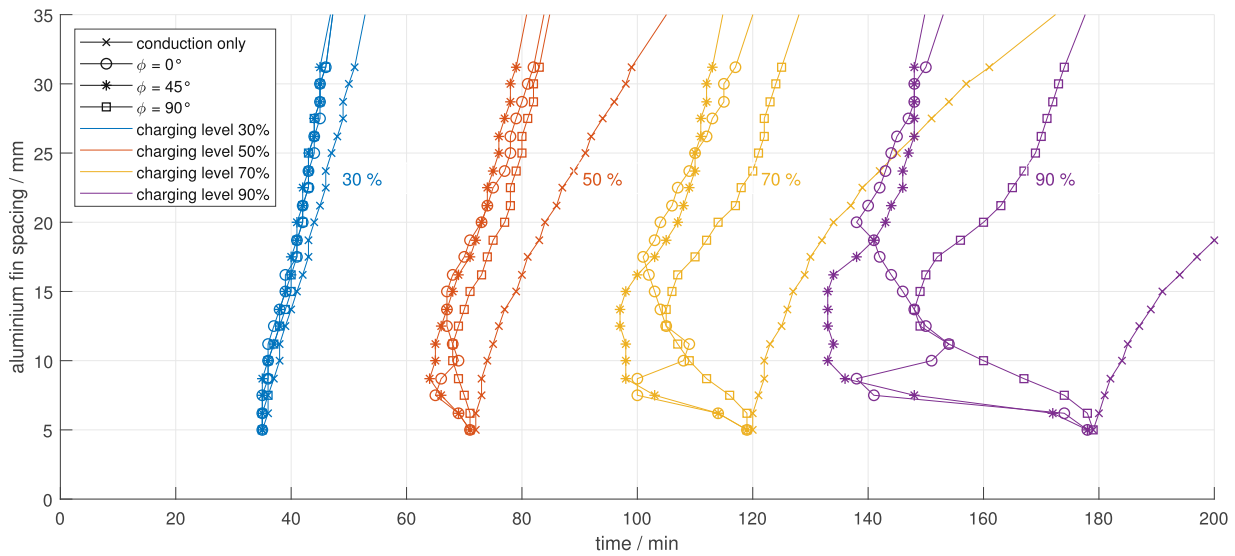


Fig. 17. Effect of different fin spacings (5 mm to 35 mm) on time to reach charging level (% of total enthalpy per volume) for fixed aluminium ratio $a = a\%$ and different segment orientations $\phi = 0^\circ$, $\phi = 45^\circ$, $\phi = 90^\circ$ compared to conduction only case.

$$Fo = \frac{\frac{k}{\rho c_p} \tau}{\tilde{L}} \quad (24)$$

and the aspect ratio

$$A = \frac{H}{w} = \frac{\Delta x_{PCM}}{w} \quad (25)$$

between the height, i.e. length of the enclosure and the width, which herein corresponds to the fin spacing w [34,84]. In phase-change heat transfer, the dimensionless time τ in the Fourier number Fo is usually the same as the product of Stefan and Fourier numbers, where Ste measures the degree of liquid superheat and Fo the time of thermal diffusion across the distance \tilde{L} [33,84].

The Rayleigh number should be related to buoyancy, hence, in case of $\phi = 90^\circ$, the characteristic length \tilde{L} can be chosen as fin spacing w , also found in literature for PCM enclosures heated from the narrow side (see, for example [85]). In this case, Rayleigh numbers range from $Ra = 9 \cdot 10^3$ to $Ra = 7 \cdot 10^7$ for the studies presented in this work. However, for $\phi = 0^\circ$, the vertical measure Δx_{PCM} should be used as characteristic length \tilde{L} , resulting in a Rayleigh number of $Ra = 1.2 \cdot 10^8$. This approach, using the enclosure height as characteristic length is also found for PCM heated from the wide enclosure side [44]. Other metrics used in literature include, for example, the half-thickness of the PCM layer [86], while it was pointed out that actually a “transient” Rayleigh number for only the liquid part should be calculated [34].

Using the non-dimensional Rayleigh and Fourier number and the aspect ratio, correlations for the liquid phase fraction, convective enhancement and Nusselt number can be obtained for specific problems. However, besides the influence of the aspect ratio, PCM cavity orientation and the varying relation between conductive and convective heat transfer introduced by different volumetric aluminium ratios would have to be considered to generalize the numerical results presented in this work. Common approaches use a modified Stefan number to account for sensible heating of both solid and liquid phases of the PCM [87,84]. Kamkari and Amlashi [48] presented a correlation for the Nusselt number and melting rate under inclination by introducing an additional function of the cavity orientation angle. In Kamkari and Shokouhmand [84], a non-dimensional correlation was presented for the effect of the number of fins on the Nusselt number.

To the best of the author’s knowledge, no dimensional analysis was

conducted to present a correlation for the combined effects of fin spacing, orientation and aluminium ratio on the thermal performance of PCM cavity design as investigated herein. Although we highlight the necessity for further research, we consider such investigation beyond the scope of this work.

5. Conclusions

5.1. Summary of the findings

In the presented parameter study of a rectangular aluminium finned PCM cavity significant angular dependency of the cavity orientation on charging behaviour was observed, whereas the orientation of the cavity was found to have no impact on the discharging behaviour. The influence of natural convection during charging was quantified by means of the convective enhancement factor EF. As could be expected, convective enhancement factors increase with fin spacing in case of upwards-orientated cavities. For downwards-orientated cavities, the impact of natural convection was found negligible for fin spacings of $w = 25$ mm and less, while convective enhancement factors of up to 2 were observed for a fin spacing of $w = 50$ mm.

The impact of aluminium ratio and fin spacing on heat flux during charging was examined in detail. Guideline values for optimal aluminium ratio of the considered cavity geometry of about 15% were found, presenting a trade-off between fast charging time and overall storage capacity. Optimal choices for fin spacing were found for a particular aluminium ratio and cavity orientations $\phi = 0^\circ$, $\phi = 45^\circ$ and $\phi = 90^\circ$. Albeit these particular optima differ, it can be assumed that the optimal fin spacings for segment orientations between $\phi = 0^\circ$ and $\phi = 90^\circ$ are situated between the respective optima and close to the optimum for $\phi = 45^\circ$ due to liquid PCM flow characteristics.

The findings of the present study highlight the crucial effects of aluminium ratio, fin spacing and inclination on the performance of rectangular, finned PCM cavities, therefore showing the importance of design optimization for industrial applications.

5.2. Scope and limitations

The obtained results are of course not directly transferable to general PCM encapsulations and load cycles. A specific geometry was considered meaning a PCM cavity of fixed length with parallel aluminium fins thus

forming narrow fin segments, which are heated from only one of the narrow side walls. Such configurations, however, are found frequently in PCM applications due to its constructional simplicity. Thus, the analysis herein provides at least qualitative findings for a wide range of PCM applications.

Only one type of PCM was investigated in the course of the parameter studies in this work. It should be noted that results for the examined characteristics might differ for other PCM, especially in case of different viscosities or thermal expansion properties. The approximation of specific heat capacity c and heat conductivity k of the studied $\text{KNO}_3\text{-NaNO}_3$ by different, but constant properties for solid and liquid state, as given in Table 1, might differ from reality. Possible quantitative deviations are considered rather small.

5.3. Further research

Since the presented results were only obtained through numerical simulation, experimental investigations should be conducted to confirm or disprove these findings. Similarly useful would be a verification by numerical models based on different methods. Comprehensive dimensional analysis of the presented findings, based on and outlined in Section 4.5 could provide the possibility to scale the results to different geometry and material properties.

To assess the optimal design of a continuous operating LHTES, investigations of a combined charging/discharging scenario are to be conducted.

In Pernsteiner et al. [67], a detailed, high-fidelity co-simulation model of the RSS/PCM segment setup also considered herein is developed. The findings herein are used to attain an efficient model structure and enable deeper design studies and model-based estimation and control tasks [88] for this hybrid storage.

Declaration of Competing Interest

The authors declare that they have no known competing financial interests or personal relationships that could have appeared to influence the work reported in this paper.

Acknowledgements

This work was carried out in the course of the project HyStEPS, grant number 868842, within the NEFI - New Energy for Industry framework and funded by the Austrian Climate Energy Fund (KLIEN).

References

- [1] B. Zalba, J.M. Marín, L.F. Cabeza, H. Mehling, Review on thermal energy storage with phase change: materials, heat transfer analysis and applications, *Appl. Therm. Eng.* 23 (2003) 251–283, [https://doi.org/10.1016/S1359-4311\(02\)00192-8](https://doi.org/10.1016/S1359-4311(02)00192-8).
- [2] S. Dusek, R. Hofmann, A hybrid energy storage concept for future application in industrial processes, *Thermal Sci.* 22 (2018) 2235–2242, <https://doi.org/10.2298/TSCI171230270D>.
- [3] Y. Lin, Y. Jia, G. Alva, G. Fang, Review on thermal conductivity enhancement, thermal properties and applications of phase change materials in thermal energy storage, *Renew. Sustain. Energy Rev.* 82 (2018) 2730–2742, <https://doi.org/10.1016/j.rser.2017.10.002>.
- [4] M.E. Zayed, J. Zhao, W. Li, A.H. Elsheikh, A.M. Elbanna, L. Jing, A. Geweda, Recent progress in phase change materials storage containers: Geometries, design considerations and heat transfer improvement methods, *J. Energy Storage* 30 (2020) 101341, <https://doi.org/10.1016/j.est.2020.101341>.
- [5] F. Agyenim, N. Hewitt, P. Eames, M. Smyth, A review of materials, heat transfer and phase change problem formulation for latent heat thermal energy storage systems (lhtess), *Renew. Sustain. Energy Rev.* 14 (2010) 615–628, <https://doi.org/10.1016/j.rser.2009.10.015>.
- [6] H. Eslamnezhad, A.B. Rahimi, Enhance heat transfer for phase-change materials in triplex tube heat exchanger with selected arrangements of fins, *Appl. Therm. Eng.* 113 (2017) 813–821, <https://doi.org/10.1016/j.applthermaleng.2016.11.067>.
- [7] M. Augspurger, K. Choi, H. Udaykumar, Optimizing fin design for a PCM-based thermal storage device using dynamic Kriging, *Int. J. Heat Mass Transf.* 121 (2018) 290–308, <https://doi.org/10.1016/j.ijheatmasstransfer.2017.12.143>.
- [8] M. Muhammad, O. Badr, Performance of a finned, latent-heat storage system for high temperature applications, *Appl. Therm. Eng.* 116 (2017) 799–810, <https://doi.org/10.1016/j.applthermaleng.2017.02.006>.
- [9] R. Baby, C. Balaji, Experimental investigations on thermal performance enhancement and effect of orientation on porous matrix filled PCM based heat sink, *Int. Commun. Heat Mass Transfer* 46 (2013) 27–30, <https://doi.org/10.1016/j.icheatmasstransfer.2013.05.018>.
- [10] A. Pourakbar, A. Rabiataj Darzi, Enhancement of phase change rate of pcm in cylindrical thermal energy storage, *Appl. Therm. Eng.* 150 (2019) 132–142, <https://doi.org/10.1016/j.applthermaleng.2019.01.009>.
- [11] S. Motahar, R. Khodabandeh, Experimental study on the melting and solidification of a phase change material enhanced by heat pipe, *Int. Commun. Heat Mass Transfer* 73 (2016) 1–6, <https://doi.org/10.1016/j.icheatmasstransfer.2016.02.012>.
- [12] S. Motahar, N. Nikkam, A.A. Alemrajabi, R. Khodabandeh, M.S. Toprak, M. Muhammed, A novel phase change material containing mesoporous silica nanoparticles for thermal storage: A study on thermal conductivity and viscosity, *Int. Commun. Heat Mass Transfer* 56 (2014) 114–120, <https://doi.org/10.1016/j.icheatmasstransfer.2014.06.005>.
- [13] X. Zhang, R. Wen, Z. Huang, C. Tang, Y. Huang, Y. Liu, M. Fang, X. Wu, X. Min, Y. Xu, Enhancement of thermal conductivity by the introduction of carbon nanotubes as a filler in paraffin/expanded perlite form-stable phase-change materials, *Energy Build.* 149 (2017) 463–470, <https://doi.org/10.1016/j.enbuild.2017.05.037>.
- [14] Y. Tao, Y.L. He, A review of phase change material and performance enhancement method for latent heat storage system, *Renew. Sustain. Energy Rev.* 93 (2018) 245–259, <https://doi.org/10.1016/j.rser.2018.05.028>.
- [15] K. Radhakrishnan, A. Balakrishnan, Heat transfer analysis of thermal energy storage using phase change materials, *Heat Recovery Syst. CHP* 12 (1992) 427–435, [https://doi.org/10.1016/0890-4332\(92\)90064-0](https://doi.org/10.1016/0890-4332(92)90064-0).
- [16] T.F. Cheng, Numerical analysis of nonlinear multiphase Stefan problems, *Comput. Struct.* 75 (2000) 225–233, [https://doi.org/10.1016/S0045-7949\(99\)00071-1](https://doi.org/10.1016/S0045-7949(99)00071-1).
- [17] S. Liu, Y. Li, Y. Zhang, Mathematical solutions and numerical models employed for the investigations of PCMs phase transformations, *Renew. Sustain. Energy Rev.* 33 (2014) 659–674, <https://doi.org/10.1016/j.rser.2014.02.032>.
- [18] Y. Dutil, D.R. Rousse, N.B. Salah, S. Lassue, L. Zalewski, A review on phase-change materials: Mathematical modeling and simulations, *Renew. Sustain. Energy Rev.* 15 (2011) 112–130, <https://doi.org/10.1016/j.rser.2010.06.011>.
- [19] V. Voller, C. Prakash, A fixed grid numerical modelling methodology for convection-diffusion mushy region phase-change problems, *Int. J. Heat Mass Transf.* 30 (1987) 1709–1719, [https://doi.org/10.1016/0017-9310\(87\)90317-6](https://doi.org/10.1016/0017-9310(87)90317-6).
- [20] R. Tenchev, J. Mackenzie, T. Scanlon, M. Stickland, Finite element moving mesh analysis of phase change problems with natural convection, *Int. J. Heat Fluid Flow* 26 (2005) 597–612, <https://doi.org/10.1016/j.ijheatfluidflow.2005.03.003>.
- [21] B. Nedjar, An enthalpy-based finite element method for nonlinear heat problems involving phase change, *Comput. Struct.* 80 (2002) 9–21, [https://doi.org/10.1016/S0045-7949\(01\)00165-1](https://doi.org/10.1016/S0045-7949(01)00165-1).
- [22] L. Kasper, Modeling of the Phase Change Material of a Hybrid Storage using the Finite Element Method, TU Wien Academic Press, Wien, 2020, <https://doi.org/10.34727/2020/isbn.978-3-85448-037-2>.
- [23] B. Seibold, A compact and fast Matlab code solving the incompressible Navier-Stokes equations on rectangular domains, Massachusetts Institute of Technology, 2008, http://math.mit.edu/gs/cse/codes/mit18086_navierstokes.pdf.
- [24] A.A. Al-Abidi, S. Mat, K. Sopian, M. Sulaiman, A.T. Mohammad, Internal and external fin heat transfer enhancement technique for latent heat thermal energy storage in triplex tube heat exchangers, *Appl. Therm. Eng.* 53 (2013) 147–156, <https://doi.org/10.1016/j.applthermaleng.2013.01.011>.
- [25] Y. Tao, Y. Liu, Y.L. He, Effects of pcm arrangement and natural convection on charging and discharging performance of shell-and-tube lhs unit, *Int. J. Heat Mass Transf.* 115 (2017) 99–107, <https://doi.org/10.1016/j.ijheatmasstransfer.2017.07.098>.
- [26] J.M. Mahdi, E.C. Nsofor, Melting enhancement in triplex-tube latent thermal energy storage system using nanoparticles-fins combination, *Int. J. Heat Mass Transf.* 109 (2017) 417–427, <https://doi.org/10.1016/j.ijheatmasstransfer.2017.02.016>.
- [27] A. Shinde, S. Arpit, P. KM, P.V.C. Rao, S.K. Saha, Heat transfer characterization and optimization of latent heat thermal storage system using fins for medium temperature solar applications, *J. Sol. Energy Eng.* 139 (2017), <https://doi.org/10.1115/1.4035517>.
- [28] S.S. Mostafavi Tehrani, G. Diarce, R.A. Taylor, The error of neglecting natural convection in high temperature vertical shell-and-tube latent heat thermal energy storage systems, *Sol. Energy* 174 (2018) 489–501, <https://doi.org/10.1016/j.solener.2018.09.048>.
- [29] N.S. Dhaidan, J. Khodadadi, Melting and convection of phase change materials in different shape containers: A review, *Renew. Sustain. Energy Rev.* 43 (2015) 449–477, <https://doi.org/10.1016/j.rser.2014.11.017>.

- [30] M. Bareiss, H. Beer, Experimental investigation of melting heat transfer with regard to different geometric arrangements, *Int. Commun. Heat Mass Transfer* 11 (1984) 323–333, [https://doi.org/10.1016/0735-1933\(84\)90060-5](https://doi.org/10.1016/0735-1933(84)90060-5).
- [31] C. Benard, D. Gobin, F. Martinez, Melting in rectangular enclosures: experiments and numerical simulations, *J. Heat Transfer* 107 (1985) 794–803, <https://doi.org/10.1115/1.3247506>.
- [32] J. Duan, Y. Xiong, D. Yang, On the melting process of the phase change material in horizontal rectangular enclosures, *Energies* 12 (2019) 3100, <https://doi.org/10.3390/en12163100>.
- [33] P. Jany, A. Bejan, Scaling theory of melting with natural convection in an enclosure, *Int. J. Heat Mass Transf.* 31 (1988) 1221–1235, [https://doi.org/10.1016/0017-9310\(88\)90065-8](https://doi.org/10.1016/0017-9310(88)90065-8).
- [34] J. Vogel, J. Felbinger, M. Johnson, Natural convection in high temperature flat plate latent heat thermal energy storage systems, *Appl. Energy* 184 (2016) 184–196, <https://doi.org/10.1016/j.apenergy.2016.10.001>.
- [35] A.M. Abdulateef, S. Mat, J. Abdulateef, K. Sopian, A.A. Al-Abidi, Geometric and design parameters of fins employed for enhancing thermal energy storage systems: a review, *Renew. Sustain. Energy Rev.* 82 (2018) 1620–1635, <https://doi.org/10.1016/j.rser.2017.07.009>.
- [36] J. Xie, H.M. Lee, J. Xiang, Numerical study of thermally optimized metal structures in a phase change material (pcm) enclosure, *Appl. Therm. Eng.* 148 (2019) 825–837, <https://doi.org/10.1016/j.applthermaleng.2018.11.111>.
- [37] J. Xie, W. Luo, W. Zhang, Z. Wu, H.M. Lee, Investigations of optimized fin structures in a compact thermal energy storage panel, *IOP Conf. Series: Earth Environ. Sci.* 467 (2020) 012006, <https://doi.org/10.1088/1755-1315/467/1/012006>.
- [38] J. Xie, K.F. Choo, J. Xiang, H.M. Lee, Characterization of natural convection in a pcm-based heat sink with novel conductive structures, *Int. Commun. Heat Mass Transf.* 108 (2019) 104306, <https://doi.org/10.1016/j.icheatmasstransfer.2019.104306>.
- [39] M. Lacroix, M. Benmadda, Analysis of natural convection melting from a heated wall with vertically oriented fins, *Int. J. Num. Methods Heat Fluid Flow* 8 (1998) 465–478, <https://doi.org/10.1108/09615539810213241>.
- [40] M. Huang, P. Eames, B. Norton, Thermal regulation of building-integrated photovoltaics using phase change materials, *Int. J. Heat Mass Transf.* 47 (2004) 2715–2733, <https://doi.org/10.1016/j.ijheatmasstransfer.2003.11.015>.
- [41] P.H. Biwole, D. Groulx, F. Souayfane, T. Chiu, Influence of fin size and distribution on solid-liquid phase change in a rectangular enclosure, *Int. J. Therm. Sci.* 124 (2018) 433–446, <https://doi.org/10.1016/j.ijthermalsci.2017.10.038>.
- [42] W.B. Ye, D.S. Zhu, N. Wang, Fluid flow and heat transfer in a latent thermal energy unit with different phase change material (pcm) cavity volume fractions, *Appl. Therm. Eng.* 42 (49–57) (2012) 2009, <https://doi.org/10.1016/j.applthermaleng.2012.03.002>, heat Powered Cycles Conference.
- [43] N.S. Bondareva, M.A. Sheremet, Conjugate heat transfer in the pcm-based heat storage system with finned copper profile: Application in electronics cooling, *Int. J. Heat Mass Transf.* 124 (2018) 1275–1284, <https://doi.org/10.1016/j.ijheatmasstransfer.2018.04.040>.
- [44] J. Zhao, J. Zhai, Y. Lu, N. Liu, Theory and experiment of contact melting of phase change materials in a rectangular cavity at different tilt angles, *Int. J. Heat Mass Transf.* 120 (2018) 241–249, <https://doi.org/10.1016/j.ijheatmasstransfer.2017.12.006>.
- [45] X. Yang, Z. Guo, Y. Liu, L. Jin, Y.L. He, Effect of inclination on the thermal response of composite phase change materials for thermal energy storage, *Appl. Energy* 238 (2019) 22–33, <https://doi.org/10.1016/j.apenergy.2019.01.074>.
- [46] M.Y. Yazici, M. Avci, O. Aydin, Combined effects of inclination angle and fin number on thermal performance of a pcm-based heat sink, *Appl. Therm. Eng.* 159 (2019) 113956, <https://doi.org/10.1016/j.applthermaleng.2019.113956>.
- [47] N. Sharifi, C.W. Robak, T.L. Bergman, A. Faghri, Three-dimensional PCM melting in a vertical cylindrical enclosure including the effects of tilting, *Int. J. Heat Mass Transf.* 65 (2013) 798–806, <https://doi.org/10.1016/j.ijheatmasstransfer.2013.06.070>.
- [48] B. Kamkari, H.J. Amlashi, Numerical simulation and experimental verification of constrained melting of phase change material in inclined rectangular enclosures, *Int. Commun. Heat Mass Transf.* 88 (2017) 211–219, <https://doi.org/10.1016/j.icheatmasstransfer.2017.07.023>.
- [49] B. Kamkari, D. Groulx, Experimental investigation of melting behaviour of phase change material in finned rectangular enclosures under different inclination angles, *Exp. Thermal Fluid Sci.* 97 (2018) 94–108, <https://doi.org/10.1016/j.expthermflusc.2018.04.007>.
- [50] R. Karami, B. Kamkari, Investigation of the effect of inclination angle on the melting enhancement of phase change material in finned latent heat thermal storage units, *Appl. Therm. Eng.* 146 (2019) 45–60, <https://doi.org/10.1016/j.applthermaleng.2018.09.105>.
- [51] D. Groulx, P.H. Biwole, M. Bhourri, Phase change heat transfer in a rectangular enclosure as a function of inclination and fin placement, *Int. J. Therm. Sci.* 151 (2020) 106260, <https://doi.org/10.1016/j.ijthermalsci.2020.106260>.
- [52] P. Wang, H. Yao, Z. Lan, Z. Peng, Y. Huang, Y. Ding, Numerical investigation of pcm melting process in sleeve tube with internal fins, *Energy Convers. Manage.* 110 (2016) 428–435, <https://doi.org/10.1016/j.enconman.2015.12.042>.
- [53] X. Cao, Y. Yuan, B. Xiang, L. Sun, Z. Xingxing, Numerical investigation on optimal number of longitudinal fins in horizontal annular phase change unit at different wall temperatures, *Energy Build.* 158 (2018) 384–392, <https://doi.org/10.1016/j.enbuild.2017.10.029>.
- [54] R. Hofmann, S. Dusek, S. Gruber, G. Drexler-Schmid, Design optimization of a hybrid steam-PCM thermal energy storage for industrial applications, *Energies* 12 (2019), <https://doi.org/10.3390/en12050898>.
- [55] MATLAB, version 9.5.0 (R2018b), The MathWorks Inc., Natick, Massachusetts, 2018.
- [56] V. Voller, C. Swaminathan, General source-based method for solidification phase change, *Num. Heat Transfer, Part B: Fundament.* 19 (1991) 175–189, <https://doi.org/10.1080/10407799108944962>.
- [57] ANSYS Fluent, Release 16.0, 2016. Theory Guide.
- [58] J. Dallaire, L. Gosselin, Numerical modeling of solid-liquid phase change in a closed 2d cavity with density change, elastic wall and natural convection, *Int. J. Heat Mass Transf.* 114 (2017) 903–914, <https://doi.org/10.1016/j.ijheatmasstransfer.2017.06.104>.
- [59] P. Carman, Fluid flow through granular beds, *Chem. Eng. Res. Des.* 75 (1997) S32–S48, [https://doi.org/10.1016/S0263-8762\(97\)80003-2](https://doi.org/10.1016/S0263-8762(97)80003-2).
- [60] H. Shmueli, G. Ziskind, R. Letan, Melting in a vertical cylindrical tube: Numerical investigation and comparison with experiments, *Int. J. Heat Mass Transf.* 53 (2010) 4082–4091, <https://doi.org/10.1016/j.ijheatmasstransfer.2010.05.028>.
- [61] M. Fadl, P.C. Eames, Numerical investigation of the influence of mushy zone parameter amush on heat transfer characteristics in vertically and horizontally oriented thermal energy storage systems, *Appl. Therm. Eng.* 151 (2019) 90–99, <https://doi.org/10.1016/j.applthermaleng.2019.01.102>.
- [62] M. Kumar, D.J. Krishna, Influence of mushy zone constant on thermohydraulics of a pcm, *Energy Procedia* 109 (2017) 314–321, doi:10.1016/j.egypro.2017.03.074. international Conference on Recent Advancement in Air Conditioning and Refrigeration, RAAR 2016, 10–12 November 2016, Bhubaneswar, India.
- [63] S. Arena, E. Casti, J. Gasia, L.F. Cabeza, G. Cau, Numerical simulation of a finned-tube lhtes system: influence of the mushy zone constant on the phase change behaviour, *Energy Procedia* 126 (2017) 517–524, <https://doi.org/10.1016/j.egypro.2017.08.237>, aTI 2017 - 72nd Conference of the Italian Thermal Machines Engineering Association.
- [64] S. Patankar, Numerical Heat Transfer and Fluid Flow, Hemisphere Publishing Corporation, 1980, URL <https://books.google.at/books?id=N2MVAQAIAAJ>. ISBN: 978-0891165224.
- [65] A.J. Chorin, Numerical solution of the Navier-Stokes equations, *Mathe. Comput.* 22 (1968) 745–762, <https://doi.org/10.1090/S0025-5718-1968-0242392-2>.
- [66] M. Huang, P. Eames, B. Norton, Comparison of a small-scale 3D PCM thermal control model with a validated 2D PCM thermal control model, *Sol. Energy Mater. Sol. Cells* 90 (2006) 1961–1972, <https://doi.org/10.1016/j.solmat.2006.02.001>.
- [67] D. Pernsteiner, L. Kasper, A. Schirrer, R. Hofmann, S. Jakubek, Co-simulation methodology of a hybrid latent-heat thermal energy storage unit, *Appl. Therm. Eng.* 178 (2020) 115495, <https://doi.org/10.1016/j.applthermaleng.2020.115495>.
- [68] D. Pepper, J. Heinrich, The Finite Element Method: Basic Concepts and Applications. Series in Computational and Physical Processes in Mechanics and Thermal Sciences, CRC Press, 2005. URL <https://books.google.at/books?id=x01sBgAAQBAJ>. ISBN: 978-0203942352.
- [69] H.P. Langtangen, K.A. Mardal, R. Winther, Numerical methods for incompressible viscous flow, *Adv. Water Resour.* 25 (2002) 1125–1146, [https://doi.org/10.1016/S0309-1708\(02\)00052-0](https://doi.org/10.1016/S0309-1708(02)00052-0).
- [70] C. Gau, R. Viskanta, Melting and solidification of a pure metal on a vertical wall, *J. Heat Transfer* 108 (1986) 174–181, <https://doi.org/10.1115/1.3246884>.
- [71] A.D. Brent, V.R. Voller, K.J. Reid, Enthalpy-porosity technique for modeling convection-diffusion phase change: application to the melting of a pure metal, *Num. Heat Transfer* 13 (1988) 297–318, <https://doi.org/10.1080/10407788808913615>.
- [72] V. Kumar, F. Durst, S. Ray, Modeling moving-boundary problems of solidification and melting adopting an arbitrary Lagrangian-Eulerian approach, *Num. Heat Transfer, Part B: Fundament.* 49 (2006) 299–331, <https://doi.org/10.1080/10407790500379981>.
- [73] N. Hannoun, V. Alexiades, T.Z. Mai, Resolving the controversy over tin and gallium melting in a rectangular cavity heated from the side, *Num. Heat Transfer, Part B: Fundament.* 44 (2003) 253–276, <https://doi.org/10.1080/101080/713836378>.
- [74] K. Wittig, P.A. Nikrityuk, Three-dimensionality of fluid flow in the benchmark experiment for a pure metal melting on a vertical wall, *IOP Conf. Series: Mater. Sci. Eng.* 27 (2012) 012054, <https://doi.org/10.1088/1757-899x/27/1/012054>.
- [75] ANSYS Workbench, Release 16.0, 2016. ANSYS Meshing.
- [76] R. Courant, K. Friedrichs, H. Lewy, Über die partiellen Differenzgleichungen der mathematischen Physik, *Math. Ann.* 100 (1928) 32–74, <https://doi.org/10.1007/BF01448839>.
- [77] N. Madden, M. Stynes, A curious property of oscillatory fem solutions of one-dimensional convection-diffusion problems, *Appl. Mathe.* 2012 (2012) 188–196.
- [78] M. Liu, W. Saman, F. Bruno, Review on storage materials and thermal performance enhancement techniques for high temperature phase change thermal storage systems, *Renew. Sustain. Energy Rev.* 16 (2012) 2118–2132, <https://doi.org/10.1016/j.rser.2012.01.020>.
- [79] J. Vogel, M. Johnson, M. Eck, D. Laing, Numerical analysis of natural convection in a latent heat thermal energy storage system containing rectangular enclosures, 2014, URL <https://elib.dlr.de/113475/>.

- [80] H. Herr, Wärmelehre: technische Physik Band 3. Europa-Lehrmittel, 1994.
- [81] S. Dusek, R. Hofmann, S. Gruber, Design analysis of a hybrid storage concept combining Ruths steam storage and latent thermal energy storage, *Appl. Energy* 251 (2019) 113364, <https://doi.org/10.1016/j.apenergy.2019.113364>.
- [82] M. Medrano, M. Yilmaz, M. Nogués, I. Martorell, J. Roca, L.F. Cabeza, Experimental evaluation of commercial heat exchangers for use as pcm thermal storage systems, *Appl. Energy* 86 (2009) 2047–2055, <https://doi.org/10.1016/j.apenergy.2009.01.014>.
- [83] M. Longeon, A. Soupart, J.F. Fourmigué, A. Bruch, P. Marty, Experimental and numerical study of annular pcm storage in the presence of natural convection, *Appl. Energy* 112 (2013) 175–184, <https://doi.org/10.1016/j.apenergy.2013.06.007>.
- [84] B. Kamkari, H. Shokouhmand, Experimental investigation of phase change material melting in rectangular enclosures with horizontal partial fins, *Int. J. Heat Mass Transf.* 78 (2014) 839–851, <https://doi.org/10.1016/j.ijheatmasstransfer.2014.07.056>.
- [85] M. Kind, H. Martin, VDI-Wärmeatlas, 2013. doi:10.1007/978-3-642-19981-3.
- [86] V. Shatikian, G. Ziskind, R. Letan, Numerical investigation of a pcm-based heat sink with internal fins, *Int. J. Heat Mass Transf.* 48 (2005) 3689–3706, <https://doi.org/10.1016/j.ijheatmasstransfer.2004.10.042>.
- [87] C.W. Robak, T.L. Bergman, A. Faghri, Enhancement of latent heat energy storage using embedded heat pipes, *Int. J. Heat Mass Transf.* 54 (2011) 3476–3484, <https://doi.org/10.1016/j.ijheatmasstransfer.2011.03.038>.
- [88] D. Pernsteiner, A. Schirrer, L. Kasper, R. Hofmann, S. Jakubek, Data-based model reduction for phase change problems with convective heat transfer, *Appl. Therm. Eng.* 116228 (2020), <https://doi.org/10.1016/j.applthermaleng.2020.116228>.

Paper 2

Experimental characterization, parameter identification and numerical sensitivity analysis of a novel hybrid sensible/latent thermal energy storage prototype for industrial retrofit applications

published in Applied Energy in collaboration with Dominik Pernsteiner, Alexander Schirrer, Stefan Jakubek, and René Hofmann

After the hybrid RSS/LHTES retrofit concept was examined in multiple simulation studies, the project consortium I was part of initialized the construction of the first fully functional prototype of the hybrid TES. In this journal paper, I presented the first experimental investigation of the TES concept. It explains the considerations that shaped the final prototype construction starting from a very simplified concept and describes the full test rig set-up. The lab-scale RSS was retrofitted with eight, structurally identical, LHTES modules. A detailed analysis of the full storage, but also of the observed differences between the individual LHTES modules, was conducted. Furthermore, the paper provides a brief explanation of the applied simulation models and their validation. A sensitivity analysis via numerical simulation illustrates the influence of critical parameters on the hybrid TES performance in order to answer research question RQ 1.2 of this thesis. While budgetary restrictions ruled out further iterations of the prototype, the results provide essential insights for further hybrid TES development.

My contribution: Methodology, Validation, Software, Experimental and numerical investigation, Data Curation, Formal Analysis, Writing – Original Draft & Editing, Visualization

L. Kasper, D. Pernsteiner, A. Schirrer, S. Jakubek & R. Hofmann (2023a). “Experimental characterization, parameter identification and numerical sensitivity analysis of a novel hybrid sensible/latent thermal energy storage prototype for industrial retrofit applications”. In: Applied Energy 344, p. 121300. ISSN: 0306-2619. DOI: 10.1016/j.apenergy.2023.121300



Contents lists available at ScienceDirect

Applied Energy

journal homepage: www.elsevier.com/locate/apenergy

Experimental characterization, parameter identification and numerical sensitivity analysis of a novel hybrid sensible/latent thermal energy storage prototype for industrial retrofit applications

Lukas Kasper^{a,*}, Dominik Pernsteiner^b, Alexander Schirrer^b, Stefan Jakubek^b, René Hofmann^a

^a TU Wien, Institute of Energy Systems and Thermodynamics, Getreidemarkt 9/BA, 1060 Vienna, Austria

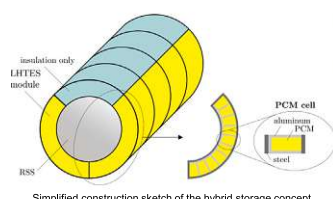
^b TU Wien, Institute of Mechanics and Mechatronics, Getreidemarkt 9/BA, 1060 Vienna, Austria

GRAPHICAL ABSTRACT

First-of-a-kind industrial steam storage retrofit with phase change material

First prototype of a novel hybrid thermal energy storage concept

- Combination of Ruths steam storage (RSS) and latent heat thermal energy storage (LHTES)
- Easy, reversible retrofit procedure to meet industrial requirements
- Economic option for increasing storage
- Could leverage the advantages of both storage types

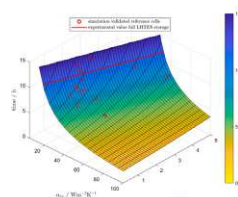


Experimental investigation of operational behaviour

- Real measurement results during operation in an industrial steel plant
- Storage operation between 150°C and 220°C
- Storage capacity increase by 30%
- Charging/discharging times of 10.4/8.6 h

Numerical modelling and detailed sensitivity analysis

- Heat transfer between RSS and LHTES is critical to performance
- Potential to reduce charging/discharging times 10-fold
- Flexible LHTES modules are proposed for future improvement of hybrid storage



ARTICLE INFO

Keywords:

Thermal energy storage
Phase change material
Experimental investigation
Parameter optimization
Sensitivity analysis

ABSTRACT

Hybrid design combinations of sensible and latent heat thermal energy storage (TES) leverage the advantages and reduce the disadvantages of both types. Thus, the range of application of said individual storage types is extended and crucial retrofit opportunities are enabled. Such hybrid TES concept consisting of a Ruths steam storage (RSS) and a surrounding layer of storage containers filled with an eutectic mixture of sodium nitrate (NaNO_3) and lithium nitrate (LiNO_3) as phase change material (PCM) was for the first time realized and investigated during operation in a steel production plant.

In this work, the hybrid TES prototype is characterized with the help of detailed modelling and real measurement results. Uncertain model parameters are identified via parameter optimization and the numerical models show satisfactory validation results. Additional 30% of thermal energy could be stored in the PCM containers retrofitted to the lab-scale RSS. Charging/discharging times and specific thermal power of the PCM containers were roughly measured as 8 h and 12 h and 560 kWm^{-3} – 802 kWm^{-3} , respectively, in the typical operation region. A sensitivity analysis of the performance indicators reveals potential but also engineering challenges for following generations of the hybrid TES concept. Compared to the achieved experimental results, charging/discharging power could be increased by up to 10 and 5 times, respectively, in the future by adequate measures to increase heat transfer between both storage types.

<https://doi.org/10.1016/j.apenergy.2023.121300>

Received 17 February 2023; Received in revised form 23 April 2023; Accepted 13 May 2023

Available online 26 May 2023

0306-2619/© 2023 The Author(s). Published by Elsevier Ltd. This is an open access article under the CC BY license (<http://creativecommons.org/licenses/by/4.0/>).

Nomenclature**Acronyms**

LHTES	Latent Heat Thermal Energy Storage
PCCs	Phase Change Composites
PCM	Phase Change Material
RMSE	Root Mean Square Error
RSS	Ruths Steam Storage

Indices

<i>alu</i>	aluminium
<i>i</i>	index in sum
<i>L</i>	liquid
<i>n</i>	number of simulation/ measurement values
<i>S</i>	solid
<i>stl</i>	steel
<i>in</i>	inner value
<i>lower</i>	lower sensor positions of Type A instrumentation
<i>out</i>	outer value
<i>ref</i>	reference
<i>upper</i>	upper sensor positions of Type A instrumentation

Parameters and Variables

α	heat transfer coefficient ($\text{W m}^{-2} \text{K}^{-1}$)
β	volumetric thermal expansion coefficient (K^{-1})
ΔH	enthalpy difference (J)
Δl_m	specific latent heat (kJ kg^{-1})
Δt	time step (s)
Δx_{PCM}	cavity PCM dimension in <i>x</i> direction (m)
Δy_{PCM}	cavity PCM dimension in <i>y</i> direction (m)
Δmass	mass difference (kg)
\dot{m}	mass flow (kg/s)
\dot{Q}	heat flux (W)
ϵ	mushy region temperature range (K)
\hat{T}	simulated temperature
\mathbf{f}	force density ($\text{kg m}^{-2} \text{s}^{-2}$)
\mathbf{g}	gravitational acceleration vector (m s^{-2})
\mathbf{q}	specific heat flux (W m^{-2})
\mathbf{u}	velocity vector (m s^{-1})
μ	dynamic viscosity (N s m^{-2})
ϕ	inclination angle
ρ	density (kg m^{-3})
ρ_0	constant density of PCM (kg m^{-3})
$\sigma()$	error band (standard deviation)
θ	uncertain parameters (optimization variable)
$\bar{\theta}$	solution of optimization problem
c	specific heat capacity ($\text{J kg}^{-1} \text{K}^{-1}$)
H	enthalpy (J)
h	specific enthalpy (J kg^{-1})
$J(\theta)$	objective function

k	thermal conductivity ($\text{W m}^{-1} \text{K}^{-1}$)
L_x, L_y	length of PCM segment in <i>x,y</i> direction (m)
p	absolute pressure (N m^{-2})
T	temperature ($^{\circ}\text{C}$)
t	time (s)
T_m	melting temperature ($^{\circ}\text{C}$)
u, v	velocity components in <i>x, y</i> direction (m s^{-1})
V	volume of RSS (m^3)
x, y	space coordinates (m)

Symbols

$D, \partial D$	spatial domain, boundary of spatial domain
∇	Nabla operator: $\nabla = (\partial/\partial x, \partial/\partial y)$

1. Introduction**1.1. Motivation**

Due to the substitution of fossil fuels with intermittent renewable energy sources, a substantial increase in energy storage capacity is needed worldwide over the next years [1]. In this context, thermal energy storage (TES) is in focus due to its ability to balance thermal energy supply with consumption, allowing to overcome the problem related to the intermittency of renewables, and increasing the efficiency and the flexibility of energy systems [2–4]. Hence, research on TES has experienced a rapid increase in terms of numbers of publications [5].

Despite considerable research effort in this field, integration of TES technology in industry is not straightforward, since short payback time and profitability are key criteria for investment decisions [6] and high initial capital cost is a major impediment [7–9]. Furthermore, due to their individual advantages and disadvantages, the applicability of storage technologies strongly depends on the process requirements and technical restrictions such as available conversion technologies and thermodynamic constraints [6]. Typically, process technologies and energy supply systems have long lifetimes of several years to decades [10]. However, process requirements change more frequently. Thus, retrofit approaches which feature small changes in the infrastructure of the energy system have special relevance for the current transition phase [11].

1.2. Background

Steam systems are a part of almost every major industrial process today [12]. Worldwide, steam systems account for approximately 30% of the energy used in manufacturing facilities [13], which in turn are accountable for nearly a third of the world's energy consumption [14]. Even small increases in efficiency of steam systems can thus account for considerable energy savings on a global scale. Here, TES integration and expansion is a viable solution to increase flexibility and efficiency of industrial plants [3,4,7,15] and is available for various temperature and pressure ranges.

* Corresponding author.

E-mail address: lukas.kasper@tuwien.ac.at (L. Kasper).

1.2.1. Ruths steam storage

The Ruths steam storage (RSS) is a well-known and widely applied sensible TES type in industrial steam systems [16–19]. The RSS is a pressure vessel containing a two-phase mixture of liquid water and steam, which is directly charged and discharged with steam [20]. Thus, the storage medium is equal to the heat transfer medium and no heat exchangers are required. During charging of the storage tank, the incoming steam partly condenses, which leads to an increase in the liquid filling level, pressure and temperature. During discharging, the saturated steam contained in the storage tank is extracted, causing a decrease of pressure, temperature and liquid filling level to maintain a thermodynamic equilibrium in the vessel [21,22].

The fast reaction time and high charging and discharging rates are considered as main advantages of the RSS [16,17]. However, steam pressure in an RSS drops during discharging. Options to avoid such pressure drop, which is disadvantageous for some applications, include the integration of an external flash evaporator and integration of phase change material (PCM) inside the storage vessel [16]. A further disadvantage of RSS is that its storage capacity is always determined by vessel volume and the allowed system pressure operation range. Thus, no capacity expansion is possible in the case of increased requirements during the storage life time. Furthermore, acquiring additional RSS units is rather expensive with the price being mainly driven by the pressure vessel costs at high temperatures [6]. This highlights the necessity for cost-efficient alternatives.

1.2.2. Latent heat thermal energy storage

Amongst all TES technologies, latent heat thermal energy storage (LHTES) are currently the most studied category in the literature [5]. LHTES primarily consist of a heat exchanger, which transfers energy between a heat transfer fluid and phase change material (PCM). PCM can store a large amount of energy during, typically liquid–solid, phase change within a small temperature range. This nearly isothermal charging/discharging process together with its high energy density compared to sensible TES is often considered as major advantage of LHTES over the latter [23]. However, while many materials have been considered and studied for use in LHTES, only few of them reached the stage of commercial application [24–28]. Underlying problems, which have not yet been fully overcome, include phase separation, subcooling, corrosion, long-term stability, and low heat conductivity [29]. The most critical disadvantage with regards to TES performance is the low thermal conductivity of most PCM [23]. In the scientific literature, various methods have been presented for increasing the heat transfer between the heat transfer medium and PCM [30]. Prominent strategies include adding fins or other extended surfaces [31–34], heat pipes [35], porous media [36], or nanoparticles [37,38] into PCM. Among various high-conductivity fillers, carbon-based porous materials, such as carbon/graphene based foam [39] and aerogel [40,41] carbon nanotube sponge [42] and expanded graphite [43] are frequently adopted to improve the thermal conductivity of PCMs by fabricating phase change composites (PCCs) [44]. For recent review articles on the topic of heat transfer enhancement for PCM containers, see, for example [45]. Furthermore, we refer to a comprehensive recent review on metal-, carbon-, and ceramic-based PCCs by Wu et al. [46]

1.2.3. Hybrid storage approaches

As mentioned above, each TES type exhibits advantages and disadvantages depending on the specific application [11]. This fact motivates the basic idea to combine both sensible and latent heat TES to leverage the advantages and reduce the disadvantages of both types.

Some combinations of sensible water storage with PCM have been proposed in literature. E.g., Abdelsalam et al. [47] and Zhao et al. [48] numerically investigated the integration of PCM modules inside a liquid water storage, showing promising increase in energy storage capacity and charging rates. Frazzica et al. [49] pursued a similar approach by testing macro-encapsulated PCMs added to water storage. Underwood

et al. [50] evaluated a hot water storage tank enhanced by PCM encapsulated in pipe coils and Cabeza et al. [51] experimentally tested the addition of PCM at the top of a stratified hot water storage. Zauner et al. [52] presented a hybrid sensible/latent heat storage system in the form of an inverted shell-and-tube configuration, where PCM was arranged in tubes, and thermal oil was used as sensible storage and as heat transfer medium.

Besides sensible water storage, often found in the building sector [49,53], also examples of hybrid steam/PCM storage, more relevant for industrial application, can be found in literature. The arrangement of pressure-resistant PCM capsules inside the RSS pressure vessel was mentioned by Steinmann & Eck [16], Buschle et al. [54] and Tamme et al. [55]. Another proposed option is to use a tube register surrounded by PCM to extend the RSS [54,55]. Buschle et al. [54] found that the tube register arranged outside the pressure vessel provides better results in terms of solidification time than the arrangement at the internal side of the pressure vessel.

A novel hybrid storage concept was proposed by Dusek & Hofmann [56,57] in 2018. Therein, PCM filled containers are placed at the shell surface of the RSS. The authors state that this configuration combines the high charging and discharging rates of the RSS and the high energy density of PCM. It is also possible to divide the outer PCM containers into several chambers, enabling the arrangement of PCM with different material properties [58]. Such mixture can lead to increased charging rate [59,60] in LHTES. Furthermore, the concept of Dusek & Hofmann [58] considers the integration of electrical heating elements or heat exchangers inside the PCM containers. The authors state that placing these inside the PCM instead of the RSS is advantageous, since pressure increase in the RSS is reduced and delayed. Such power-to-heat options are expected to become an increasingly relevant and cost-effective technology, especially at high temperature levels [61].

Niknam & Sciacovelli [62] presented the first holistic techno-economic investigation of the hybrid storage concept proposed by Dusek & Hofmann [56,57]. They provided calculation and comparison of total costs by including capital expenditures (CAPEX), annual fuel and non-fuel related operating costs and also taking technology lifetime into account. This investigation resulted in CAPEX of the hybrid storage system that are 5% less than the case with a conventional RSS and additional relative operational savings of about 5.5%, thus confirming the results of Hofmann et al. [63] that such hybrid storage can be advantageous and cost-effective. However, while their analysis is based on a dynamically modelled RSS/LHTES system, the modelling approach includes several simplifications. For example, the LHTES part is only modelled in one dimension, and, more critically, perfect heat transfer between both storage types is assumed.

1.3. Scope of this investigation

In this work, the novel hybrid sensible/latent TES prototype first proposed by Dusek and Hofmann [56,57] is experimentally investigated. In our previous work, a model of the hybrid storage was established and the RSS model was validated with data from an industrial plant [58]. Furthermore, a non-linear design optimization tool for such hybrid storage system was developed by Hofmann et al. [63] to enable cost-effective retrofitting of conventional RSS. A detailed simulation study of different hybrid storage PCM arrangements were compared and presented in Dusek et al. [64]. A detailed numerical simulation model of the PCM containers was established [65] and in-depth parameter studies on the influence of natural convection under inclination on optimal aluminium proportions and fin spacings were carried out [66]. In addition, we established a co-simulation methodology for the hybrid storage prototype [67], followed by work on data-based model reduction [68] and state estimation of nonlinear LHTES problems [69] to allow for optimal operational control of LHTES and hybrid sensible/latent TES storage.

To further assess this hybrid RSS/LHTES retrofit concept, the first-of-a-kind prototype was constructed and investigated during operation in a steel plant. In this work, the hybrid TES prototype is characterized with the help of real measurement results and detailed numerical simulations.

Based on the state of the art outlined above, the main contributions of this article are as follows:

- We conducted the first experimental characterization of a novel hybrid sensible/latent thermal energy storage prototype for industrial retrofit applications.
- We successfully validate developed numerical models of the hybrid storage and identify uncertain numerical model parameters via experimental data.
- We characterized key performance values of the novel hybrid storage such as retrofitted storage capacity, charging/discharging duration and power.
- We performed a sensitivity analysis of parameters critical to the hybrid storage performance, and reveal potential for future improvement.
- Our analysis presents essential guidelines for future development of hybrid storage applications.

1.4. Paper structure

After this introduction, this paper is organized as follows: Section 2 presents the experimental setup, numerical modelling and analysis methods used in this study. The results of experimental and numerical investigations are given in Section 3. In Section 4, the main findings are highlighted and critically assessed. Furthermore, specific suggestions for further research are emphasized.

2. Methods

In this chapter, the experimental setup, numerical modelling and analysis methods used in this study are presented.

2.1. Problem statement

In the proposed hybrid storage concept by Dusek & Hofmann [56, 57], introduced in Section 1.3, PCM filled containers are placed at the shell surface of an RSS. Fig. 1 illustrates a simplified construction sketch of a possible realization. However, to enable industrial exploitation, the actual design is bound to a number of thermodynamic, economic and safety requirements. In a recent review, Gasia et al. [70] established more than 25 requirements for both sensible and latent heat TES to handle in order to ensure optimal performance and further achieve widespread deployment. These can be grouped into chemical, kinetic, physical and thermal (from a material point of view) and environmental, economic and technological (from both material and system points of view) [70]. Naturally, optimization of all of these, partly opposing, aspects is impossible and trade-offs have to be tolerated. Our most important considerations are given in the following list.

- The LHTES retrofit should increase the effective thermal energy storage capacity while reducing investment costs compared to equivalent additional RSS capacity. This is only possible without interfering with existing steam infrastructure.
- Thermal heat transfer between RSS and LHTES should be optimized to maximize charging/discharging power and efficiency.
- Both material configuration and mechatronic setup should allow adequate control over the TES, to optimize its operation within the operating conditions.
- The retrofit construction must not permanently modify the RSS and must allow access to the pressure vessel's internal and external surface area under reasonable effort. This is necessary to allow for mandatory recurrent inspection at an interval of five to ten years.

- Material choice and construction design should ensure durability (i.e. no corrosion or deformation) and workplace safety (i.e. no toxicity, fire and explosion hazard).

When it came to the last item in the above list, i.e. ensuring durability and safety of the construction design, there were two main issues:

- Corrosion effects: It was found that corrosion occurs especially when in contact with water, e.g., humid air. Therefore, also the purity of the used PCM is of importance and direct contact of the PCM and the RSS pressure vessel was disregarded because of safety concerns.
- Thermal expansion: the thermal expansion of $\text{NaNO}_3\text{-LiNO}_3$ was determined in small-scale experiments and resulted in 14 to 17% between 25 and 220 °C, which would result in high stresses in a closed-container design.

While carefully assessing all technical decision criteria and also budgetary restrictions, we arrived at a first prototype design as described in Section 2.2.1. Detailed reasoning on the design choices for the here investigated prototype exceed the scope of this contribution and we refer to the project's public report for further information [71].

2.2. Experimental design and setup

Experimental investigations of the dynamic behaviour of the hybrid storage device were conducted at the steel production facility of voestalpine Stahl Donawitz GmbH, located in Leoben, Austria. The lab-scale storage tank, described in detail in Section 2.2.1, is charged with steam via the discharge pipe of one of the 80 m³ industrial size RSS vessels operated on site. Discharging takes place against ambient pressure.

2.2.1. The hybrid storage prototype

A fully functional lab-scale RSS was constructed to replicate the behaviour of a typical industrial-size RSS while reducing prototype cost to a minimum. It consists of a cylindrical pressure vessel with hemispherical sides. A steam lance with a series of injecting nozzles is located inside the base vessel body for charging. A typical steam collector is located on top of the base body for discharging. All relevant geometry parameters are given in Table 1.

Eight LHTES container modules, four on each side of the vessel, were constructed to mount onto the RSS. Fig. 1 shows a concept sketch of their positioning. During discharging, the top part of a horizontal steam storage vessel contains dry steam, which has a very poor heat transfer coefficient of $10 \text{ W m}^{-2} \text{ K}^{-1}$, which is 70 times smaller than that of liquid water. Hence no reasonable heat transfer rates between RSS and LHTES can be achieved [67]. Therefore, the modules of the hybrid storage are not forming a full half-circle (corresponding to maximum storage capacity), but instead only surround the vessel to an angle of 133.5° from the bottom, leaving the rest to be insulated. To find the most economically efficient share of LHTES module coverage, the combined behaviour of the hybrid system must be studied under operating conditions. For this purpose, we provided a co-simulation methodology in our previous work, see Pernsteiner et al. [67].

LHTES modules are made from stainless steel (1.4571) with a wall thickness of 3 mm. Inside, an aluminium fin structure is installed, orientated in the radial-axial plane of the RSS. The relevant geometry parameters are also given in Table 1. A concept was developed to exhaust any gases, that may escape the liquefied PCM, from the installation hall. It consists of a 32 mm reinforced polyurethane hose which connects two DN50 flanges from each of the 8 modules. The PCM modules were tightened to the RSS with metallic springs up to a pre-calculated permissible force. This should ensure direct contact between the RSS surface and the PCM modules and reduce separation occurring due to dissimilarity of the steels and construction imprecisions. Major

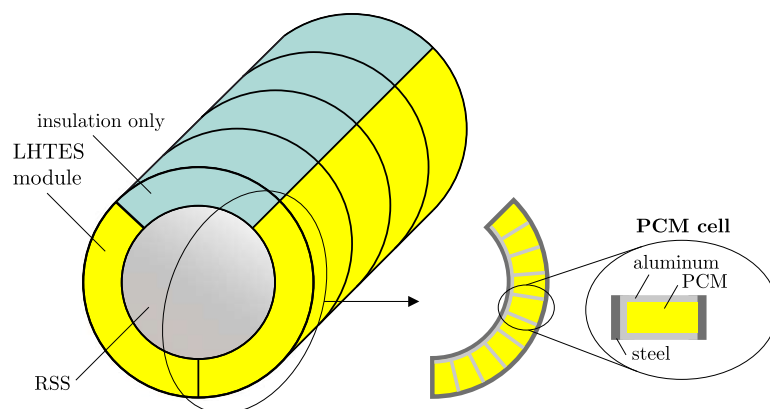


Fig. 1. Simplified construction sketch of the hybrid storage. PCM modules are attached to the cylindrical steam storage up to an angle of 133.5° from the bottom. The modules consist of a stainless steel shell and an aluminium fin structure in the radial-axial plane, thus forming multiple separated PCM cells. Note: sketch is not true to scale.

Table 1
Relevant geometry parameters of the hybrid storage prototype.

RSS pressure vessel	
Material	Steel (P235GH)
Outer diameter	711 mm
Wall thickness	12.5 mm
Cylindrical length	2319 mm
Dished ends wall thickness	15 mm
Dished ends height	186 mm
LHTES container modules	
Wall material	Stainless steel (1.4571)
PCM	LiNO ₃ -NaNO ₃
Width (outer dimension)	545 mm
Inner radius	355.5 mm
Height of PCM layer (radial to RSS)	30 mm
Wall thickness (lateral)	5 mm
Wall thickness (inner, outer, top, bottom)	3 mm
RSS angle covered	133.5°
Number of modules	8
PCM mass per module	19.52, 19.58, 19.83, 19.03, 19.00, 19.61, 19.74, 19.83 kg
Aluminium fins	
Fin material	Aluminium (AW-6060T66)
Fin number per module	85
Fin thickness	2 mm
Fin height	29.5 mm
Fin spacing	10 mm
Insulation	
Insulation material	Mineral wool
Thickness	100 mm

Table 2
Relevant material properties of LHTES prototype.

Property	PCM (LiNO ₃ -NaNO ₃)	Aluminium (AW-6060T66)	Steel (Stainless 1.4571)
density	$\frac{\rho}{\text{kg m}^{-3}}$ 2317 [72]	2700 [73]	8000 [74]
spec. heat capacity	$\frac{J}{(\text{kg K})^{-1}}$ 1350 (S) [72] 1720 (L) [72]	910 [73]	500 [74]
heat conductivity	$\frac{k}{\text{W}(\text{m K})^{-1}}$ 0.87 (S) [72] 0.575 (L) ^a	237 [73]	15 [74]
melting temperature	$\frac{T_m}{^\circ\text{C}}$ 192 ^b	-	-
mushy region temperature range	$\frac{\epsilon}{^\circ\text{C}}$ 0.4 ^b	-	-
spec. latent heat	$\frac{\Delta l_m}{\text{kJ kg}^{-1}}$ 309.1 ^b	-	-
thermal expansion coefficient	$\frac{\beta}{\text{K}^{-1}}$ 3.5 · 10 ^{-4c}	-	-
dynamic viscosity	$\frac{\mu}{\text{Ns m}^{-2}}$ 5.8 · 10 ^{-4c}	-	-

^aAverage value from literature [72] and [55].

^bValue from measurement at AIT Austrian Institute of Technology GmbH (accredited laboratory - EN ISO/IEC 17025) .

^cNo values available in the literature for LiNO₃-NaNO₃, value taken from [73] for KNO₃-NaNO₃ (similar PCM compound).

advantages of this concept are that no modification of the RSS is needed and other, possibly expensive, materials to increase heat transfer are spared.

The used PCM is an eutectic mixture of sodium nitrate (NaNO₃) and lithium nitrate (LiNO₃). The ratio is 15.938 kg NaNO₃ to 15.313 kg LiNO₃. The two compounds, each purchased with a specified purity of ≥ 99 %, were mixed in solid, powdery state and heated in batches to 350 °C. The relevant PCM material parameters are given in Table 2. The PCM modules were covered in heating mats controlled to 250 °C and filled with liquid PCM to a specified filling level. The resulting PCM mass per module was measured and ranged from 19.00 kg to 19.83 kg, as given in Table 1.

2.2.2. Sensor placement and measurement

The RSS is equipped with sensors for a pressure measurement, a temperature measurement and a differential pressure measurement of the liquid level in the vessel. The charging steam flow is defined by a

pressure measurement in the charging pipe and its specific enthalpy is determined assuming that the steam is saturated.

The PCM modules are instrumented with PT100 temperature sensors in two different arrangements (Type A and Type B). The first type of instrumentation (Type A) includes 36 sensors on different positions as it can be seen on the right side of Fig. 2. One module was instrumented according to Type A instrumentation while the second type of instrumentation (Type B) includes only two sensors. Fig. 2 presents the position of the individual modules on the pressure vessel. All sensors are placed as centrally as possible in the PCM layer. The sensor depth, i.e. the distance from the inner module wall on the RSS side measured in radial direction, is 15 mm for all sensors of the Type B instrumentation. The 36 sensors of the Type A instrumentation are arranged in 12 groups of 3 sensors. Each group includes sensor depths of 8 mm, 15 mm and 25 mm. The total depth of the PCM layer is 30 mm as summarized in Table 1.

The PT100 measurement sensors used have a class A measurement tolerance according to IEC 751 resp. EN 60751 which is defined by $\Delta T = 0 \pm (0.15^\circ\text{C} + 0.002 \cdot T)$ at a temperature T in the operation range $-200^\circ\text{C} \leq T \leq 600^\circ\text{C}$. All sensors were further tested with

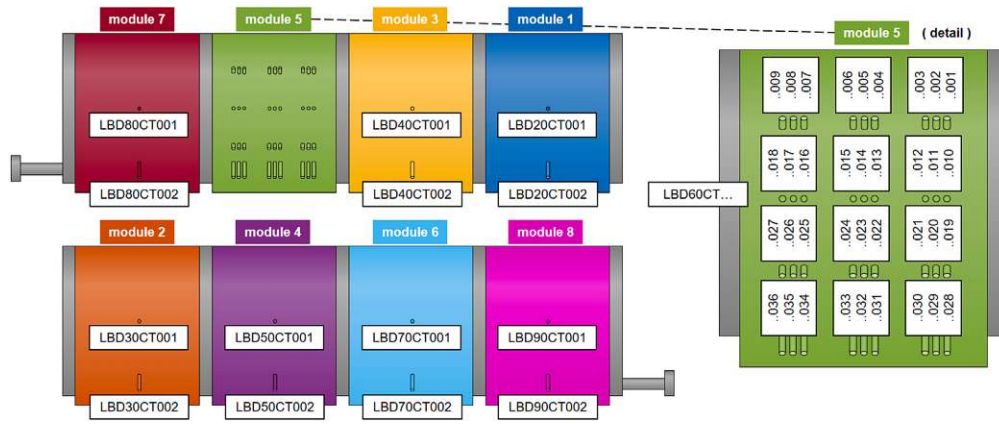


Fig. 2. Temperature measurement setup and sensor denotation in LHTES modules. On the left, the position of the individual modules on the two lateral sides of the pressure vessel is illustrated. On the right, a detailed sketch of the sensor arrangement of the Type A module is presented.

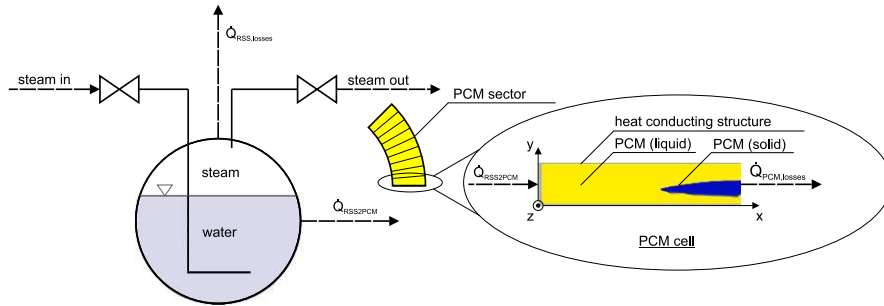


Fig. 3. Schematic illustration of heat flows during hybrid storage charging/discharging. Source: Reprinted from [67] with permission from Elsevier.

Die approbierte gedruckte Originalversion dieser Dissertation ist an der TU Wien Bibliothek verfügbar. The approved original version of this doctoral thesis is available in print at TU Wien Bibliothek.

the same calibration device and no significant deviations were found, i.e. deviations of well below 1.0 °C.

2.2.3. Control strategy

Charging/discharging of the hybrid storage is only possible via the RSS by injecting/extracting steam or by draining water via the corresponding loading, unloading and purge valves. The PCM attached to the walls of the RSS can be charged/discharged solely by the exchanged heat flows due to the temperature difference. Fig. 3 illustrates steam charging/discharging of the RSS and heat flows between RSS, the LHTES and the environment.

The loading and unloading valves become active when the differential pressure (setpoint to measurement value) exceeds 1.5 bar. Furthermore, only either the charging or discharging valve can be active, which means that simultaneous charging and discharging of the storage device is not possible. The purge valve is used to control the filling level of the RSS. When the measured filling level exceeds a certain threshold, the purge valve is activated and water is drained to ensure safe operation of the RSS.

Fig. 4 shows the full hybrid storage prototype setup in the experimental environment.

2.3. RSS modelling

To model an RSS, thermodynamic equilibrium is commonly assumed in literature, see, e.g. Steinmann & Eck [16]. Thereby, the two phases inside the storage vessel, namely water and steam, are considered always in saturated state with both phases at the same temperature. The implemented RSS model is adapted from the validated equilibrium model by Dusek & Hofmann [58].

2.3.1. Governing equations

The variables pressure and temperature, which are directly related in thermodynamic equilibrium, are not sufficient for a complete description of the system. Therefore, another variable is required to fully characterize the state of the system, for example, the specific enthalpy.

The energy and mass balances are expressed as combinations of the two phases (one-dimensional), treating the two phases together as a single fluid mixture. The corresponding governing equations are

$$m_{RSS} \frac{dh_{RSS}}{dt} = \dot{m}_{RSS,in}(h_{RSS,in} - h_{RSS}) + \quad (1)$$

$$\dot{m}_{RSS,out}(h_{RSS,out} - h_{RSS}) + \dot{Q}_{RSS} + V_{RSS} \frac{d\rho_{RSS}}{dt}, \text{ and}$$

$$V_{RSS} \frac{d\rho_{RSS}}{dt} = \dot{m}_{RSS,in} + \dot{m}_{RSS,out}. \quad (2)$$

The steam mass fraction and the corresponding mixing law are defined as

$$x_{RSS} = \frac{m_{RSS,s}}{m_{RSS,s} + m_{RSS,w}}, \text{ and} \quad (3)$$

$$h_{RSS} = x_{RSS}h_{RSS,s} + (1 - x_{RSS})h_{RSS,w}. \quad (4)$$

Therein, m_{RSS} , \dot{m}_{RSS} , h_{RSS} and ρ_{RSS} denote the mass, mass flow, specific enthalpy, and density of an equivalent water–steam mixture, respectively. The indices “w” and “s” stands for the water and steam fractions (liquid and vapour phase) and the index additions “in” and “out” denote stream quantities entering and leaving the RSS vessel, respectively. In the assumed saturated state, the pressure p_{RSS} is the same for both phases. The RSS model is considered as an aggregate domain where the balance equations are not further subdivided. The overall volume V_{RSS} is subject to the heat flow

$$\dot{Q}_{RSS} = \dot{Q}_{RSS2PCM} + \dot{Q}_{RSS,loss}, \quad (5)$$



(a) Lab-scale RSS device with LHTES container modules attached to the pressure vessel's surface. The modules are instrumented with PT100 temperature sensors. (b) Final experimental setup of the hybrid storage prototype, including heat insulation.

Fig. 4. Images of lab-scale hybrid storage prototype in the experimental environment. Photographs by courtesy of AIT Austrian Institute of Technology GmbH.

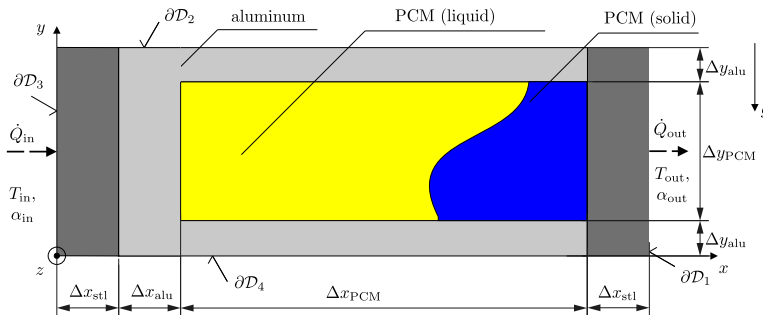


Fig. 5. PCM cell dimensions.

which includes heat losses to the environment $\dot{Q}_{RSS,loss}$ and the heat flow to the attached PCM modules $\dot{Q}_{RSS2PCM}$.

2.4. PCM module modelling

We developed a detailed multi-phase thermodynamic model including melting/solidification, heat conduction, and natural convection in two dimensions. The model was developed, successfully validated with experimental data and thoroughly documented in [65,66] and is briefly explained here.

2.4.1. Modelling domain

The PCM modules of the hybrid storage feature an aluminium fin structure orientated in the radial-axial plane of the RSS. Hence, modelling can be reduced to two dimensions when assuming that the depth of the enclosure in z -direction is large enough for wall boundary layer effects to be negligible [66]. Furthermore, an outer diameter of the RSS of 711 mm is considered large against the full enclosure width in y -direction of 36 mm, thus justifying a rectangular approximation of single fin segments. Fig. 5 illustrates the abstracted fin segment consisting of a rectangular aluminium enclosure filled with PCM. This segment is modelled in local coordinates (x, y) in the two-dimensional spatial domain D and its boundary ∂D .

2.4.2. Mathematical model

The governing equations within the given assumptions are the energy Eq. (6), continuity Eq. (7) and Navier–Stokes Eqs. (8) as follows:

$$\rho_{PCM} c \frac{\partial T}{\partial t} = k_{PCM} \nabla \cdot (\nabla T) - \rho_{PCM} c (\mathbf{u} \cdot \nabla) T \quad (6)$$

$$\nabla \cdot \mathbf{u} = 0 \quad (7)$$

$$\rho_{PCM} \frac{\partial \mathbf{u}}{\partial t} + \rho_{PCM} (\mathbf{u} \cdot \nabla) \mathbf{u} - \mu \nabla \cdot (\nabla \mathbf{u}) = \mathbf{f}(T) - \nabla p_{PCM} \quad (8)$$

Therein, the temperature field $T = T(x, y, t)$ is treated as dependent variable in the energy Eq. (6), and the velocity field $\mathbf{u} = [u, v]^T$ with spatial components $u(x, y, t)$ and $v(x, y, t)$ is treated as dependent variable in the Navier–Stokes Eq. (8). The variable p_{PCM} stands for the pressure in the PCM. The symbols ρ_{PCM} , k and μ denote the parameters density, heat conductivity and dynamic viscosity, respectively. Phase change is modelled via the apparent heat capacity method [75], hence the apparent heat capacity

$$c(T) = \begin{cases} c_S & \text{if: } T < T_m - \epsilon \\ \frac{\Delta l_m + c_S \cdot (T_m + \epsilon - T) + c_L \cdot (T - (T_m + \epsilon))}{2\epsilon} & \text{if: } T_m - \epsilon \leq T \leq T_m + \epsilon \\ c_L & \text{if: } T > T_m + \epsilon \end{cases} \quad (9)$$

accounts for the latent heat of melting/solidification Δl_m in a mushy region ϵ around the melting temperature T_m . The force density \mathbf{f} describes the buoyancy force

$$\mathbf{f} = \rho g \approx \rho_0 g (1 - \beta (T - T_{ref})) \quad (10)$$

which is calculated via the Boussinesq approximation as given in [76] by the volumetric thermal expansion coefficient β , the constant (reference) density ρ_0 , a reference temperature T_{ref} , and the gravitational standard acceleration vector g .

The time-dependent energy Eq. (6) is discretized using a standard Galerkin finite element approach with four-noded bilinear rectangular elements, and the incompressible Navier–Stokes Eqs. (7)–(8) are solved via finite differences. The obtained velocity field is applied in the next time step of the energy equation. For details, please refer to Kasper (2020) [65].

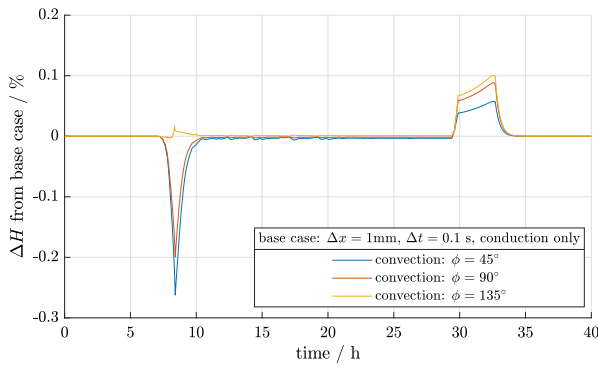


Fig. 6. Deviation of total enthalpy ΔH between simulations of base case (without convection) and including natural convection for different fin orientation angles ϕ of PCM cells under a typical operation scenario. We observed only minor deviations and thus considered only conductive heat transfer in the subsequent analysis.

The symmetry boundaries on the upper and lower side of the domain are treated as adiabatic:

$$q|\partial D_2, \partial D_4 = 0 \quad (11)$$

For the left and right boundaries, Robin boundary conditions,

$$q|\partial D_3 = \alpha_{in} \cdot (T(x, y, t) - T_{in}), \quad (12)$$

$$q|\partial D_1 = \alpha_{out} \cdot (T(x, y, t) - T_{out}), \quad (13)$$

are prescribed following Newton's law of cooling, where $\alpha_{in}, \alpha_{out}$ are the overall heat transfer coefficients, q is the specific heat flux across the boundary, and T_{in}, T_{out} present boundary temperatures at the left and right wall surfaces, respectively.

2.4.3. Influence of natural convection

Different fin orientation angles in the LHTES part of the hybrid storage correspond to the inclination of a single PCM cell, as illustrated in Fig. 1. In our studies, we defined the inclination angle ϕ to be 0° when parallel to the gravitational vector, i.e. facing downwards.

While it is often reported that natural convection is negligible during the discharge of LHTES (see, for example [77–79]), it can have significant influence on the charging behaviour [80]. We therefore studied the influence of natural convection on the charging and discharging behaviour of the abstracted single PCM cell for a typical reference operation case and the LHTES geometry and parameters of our prototype (see Fig. 6).

We obtained only slight deviations in total enthalpy and temperature distribution, hence charging/discharging behaviour, between cases modelled with convection at different angles ϕ and the reference case, where convection is neglected. Thus, subsequent analysis, validation and parameter identification was conducted considering only conductive heat transfer in the PCM domain.

2.4.4. Grid size and time step independence

The numerical accuracy implications of the element grid and time step sizes were carefully tested to keep the computational effort in reasonable limits. When natural convection is not considered in the model, a uniformly distributed finite element grid of 1440 elements, corresponding to an element size of $\Delta x = \Delta y = 0.5$ mm proved adequate, as well as a time step size of $\Delta t = 1.0$ s. Further information on grid and time step sensitivity can be found in Appendix A.

2.5. Parameter identification and optimization

Uncertain physical model parameters of the single PCM cell model presented in Section 2.4 were identified via the experimental temperature measurement data of the reference case given in Fig. 12 (exp-II).

The parameter identification procedure aims to find optimal values of the uncertain parameters θ that minimize an objective function $J(\theta)$. The objective function (15) is defined as the RMSE between simulated temperature $\hat{T}(\theta, t)$ and measured temperature $T(t)$ evaluated at n_t points in time.

The optimization problem

$$\tilde{\theta} := \arg \left(\min_{\theta} J(\theta) \right) \quad (14)$$

with

$$J(\theta) = \sqrt{\frac{1}{n_t} \sum_{i=1}^{n_t} \left(\hat{T}(t_i, \theta) - T(t_i) \right)^2} \quad (15)$$

is solved in MATLAB[®] using the Augmented Lagrangian Genetic Algorithm (ALGA) implemented in MATLAB[®]'s solver *ga* with the maximum number of iterations for the genetic algorithm to perform set to 100, yielding the optimal parameter values $\tilde{\theta}$.

The overall heat transfer coefficients α_{in} and α_{out} are considered the primary source of uncertainty in the PCM cell model, while most of the other parameters can be considered to be accurate. Hence, $\theta = \{\alpha_{in}, \alpha_{out}\}$ in the subsequent analysis in Section 3.

3. Results and discussion

3.1. RSS model validation

To validate the RSS model, experiments were conducted using the insulated RSS without the LHTES modules attached. The experiments include dynamic load ramps and closed-valve cool-down tests. The injected and extracted mass flows were determined by balancing calculation using measurements of filling level, total mass, and pressure difference as well as valve characteristics.

Detailed results of the RSS model validation are presented in Appendix B. The experiments provided satisfactory results for the RSS model.

The further experimental setup was designed in such a way that the influence of the LHTES modules on the RSS and the total storage capacity can be identified.

3.2. RSS characterization

Fig. 7 shows the pressure and enthalpy changes of the RSS during exemplary operating scenarios. In this state, no LHTES modules were attached to the RSS before insulation of the pressure vessel.

In the case illustrated in 7(a), the pressure setpoint was increased from 9 bar to 15 bar and after 30 min set to 10 bar. Charging/discharging is completed in roughly 10 min and the maximum feasible power due to enthalpy change is 283 kW. This corresponds to a specific volumetric power of 281 kW m⁻³. However, it should be noted that the feasible RSS power depends more on the available pressure of the charging steam source and the piping and valve sizes than on the vessel volume. Additionally, a limit on permissible pressure gradients due to safety and durability requirements could further limit the maximum power.

Fig. 7(b) illustrates a test of the full operating range of the RSS, i.e. charging to 23 bar and discharging to 7 bar. During the charging process, 165 MJ of energy were stored in the RSS and 228 MJ were discharged. For typical operating ranges, we characterized the constructed small-scale RSS with a storage capacity of 200 MJ. This corresponds to a volumetric energy density of 198 MJ m⁻³.

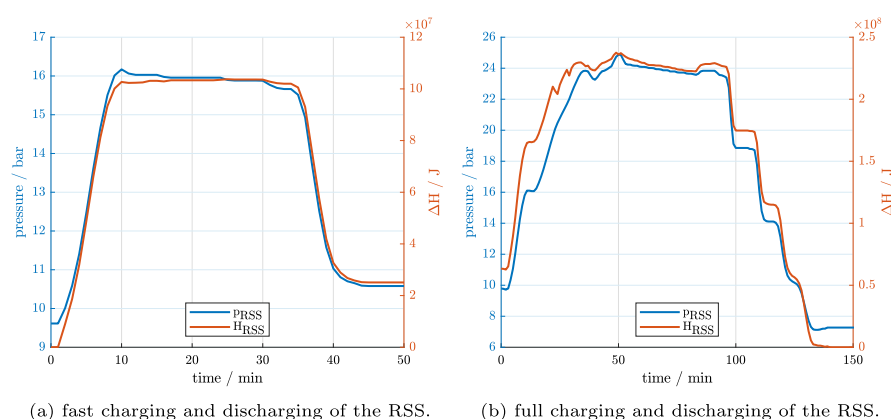


Fig. 7. RSS pressure and enthalpy during different operating scenarios without LHTES modules attached.

3.3. General LHTES container module behaviour

3.3.1. Comparison of equal modules

During the experimental investigations, we found significant differences in behaviour, i.e. temperature response, between the eight different modules. Fig. 8 illustrates all measurements of the Type B instrumentation (and corresponding values of the Type A instrumentation) for a 24 h charging scenario. The initial state was stationary and the RSS was held at a pressure of 7 bar, well below the PCM melting point. The RSS was then charged to a pressure of 21 bar, corresponding to a temperature of roughly 217 °C. This pressure was held for 24 h, whereafter it was reduced to a target value of 10 bar.

Comparison of the different LHTES modules in Fig. 8 shows qualitatively similar behaviour during charging and discharging, apart from sensor positions LBD20CT001, LBD80CT001, which show seemingly unphysical behaviour and where thus not considered in further analysis. In fact, the doubtful observation can be explained by a misplaced sensor rod, which did not reach the PCM domain but instead is assumed to record the temperature of the air surrounding the outer side of the adjoining PCM, hence the phase-transition like plateau, well below the actual melting point.

The “quasi-stationary” temperature measurements before the beginning of the charging process, after 24 h of charging and after 18 h hours of discharging show significant differences between modules, which naturally also correlates with charging/discharging power. This discrepancy could be explained by varying effective heat transfer coefficients between RSS and LHTES modules caused by the unequal fitting of the modules to the RSS shell. Since no additional layer to enhance heat transfer was added, the concept relies on the direct contact between the metal surfaces. Even small air gaps in between these surfaces can have immense impact on heat transfer since air features thermal insulating properties. This effect will be discussed in more detail in Section 4.

3.3.2. Comparison of vertical differences

No significant deviation between lower and upper LHTES modules could be obtained, compared to the deviation between different modules on the same horizontal level, see Fig. 8(c). While a tendency of higher measurement values for the upper sensor positions can be obtained, these prove to be on the borderline of significance, as can be seen from the standard deviation plotted in 8(c).

3.3.3. Detailed evaluation of single LHTES module

With the 36 sensors placed in the Type A instrumentation, as described in Section 2.2.2, detailed insight into the single LHTES module is possible (see Fig. 9).

Differences in measurements for different sensor depth proved to be marginal compared to overall variations, that is to say, we obtained a temperature decrease of around 2 °C between the inner most sensor and the outer most sensor, located 8 mm and 25 mm to the inner module wall, respectively. Between the sensors allocated horizontally the difference in the measured temperature is very low, as can be expected. However, differences between sensors allocated vertically are significantly higher though not consistently deviating along one direction along the vertical. This fact suggests uneven heat transfer between RSS and LHTES module, which could be caused by an air gap between these two TES parts.

In light of the results of module comparison presented in Sections 3.3.1 and 3.3.2, we note that the obtained result can by no means be generalized to other modules. Regardless, the insights can be useful for the general interpretation of results and evaluation of the prototype concept, discussed in more detail in Section 4.

3.3.4. Reproducibility of experiments

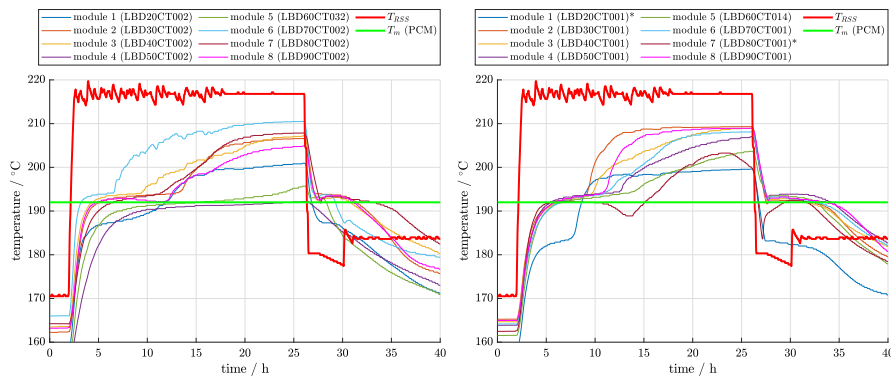
Naturally, experiment trajectories were repeated several times to ensure reproducibility of the results. Fig. 10 shows comparison between the experiment trajectory introduced in the beginning of this Section, denoted as *exp-I*, and a second run, where it was aimed to reach the same RSS conditions, denoted as *exp-II*, that took place three weeks later. Only minor deviations in temperature measurements can be observed that can be attributed to fluctuations in the RSS temperature trajectory. The experiments were thus considered to be reproducible and their results verifiable.

3.4. LHTES model validation and parameter optimization

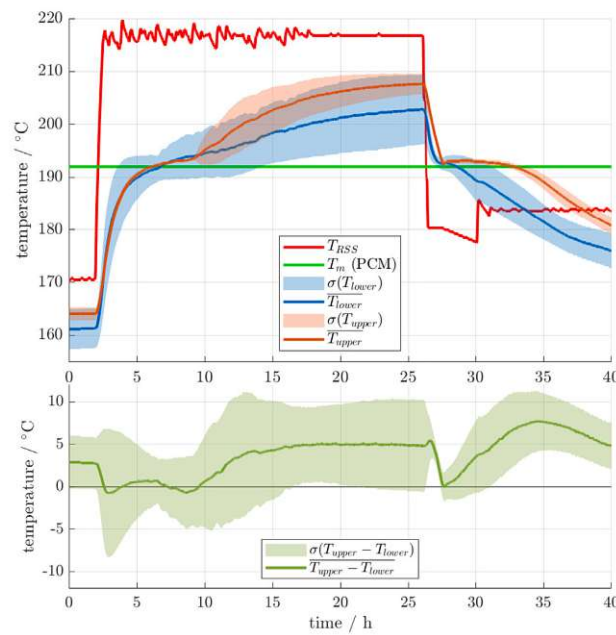
We used the measurement data from each of the 8 PCM container modules (see Section 2.2.2) to validate the single PCM cell model, outlined in Section 2.4. Uncertain physical model parameters were optimized to fit experimental results, as methodically presented in Section 2.5.

Fig. 11 shows the validation results for three representative sensor positions. Here, only α_{in} and α_{out} were considered as uncertain and optimized to fit the experimental temperature measurement. Table C.6 presents the obtained values as well as the resulting validation errors for the 8 LHTES modules and two sensor positions each.

Additionally, we aimed for improvement of the model fit by allowing the variation of the mushy region temperature range ϵ of the PCM and the specific heat capacities c of PCM and aluminium. The latter two variations did not lead to significant improvement of the results and were thus excluded from further analysis. While allowing larger values of ϵ led to slightly lower absolute root-mean-squared-errors



(a) Temperature measurement in RSS and lower sensor positions in LHTES modules. (b) Temperature measurement in RSS and upper sensor positions in LHTES modules.



(c) Mean values and corresponding standard deviation of lower T_{lower} and upper sensors T_{upper} for all eight modules respectively (upper figure) and mean value and corresponding standard deviation of the calculated difference between six of the eight sensor pairs ($T_{upper} - T_{lower}$).

*Note: modules 1 and 7 were removed from this evaluation, since their measurement values are not representative.

Fig. 8. Comparison of temperature measurement in all eight LHTES container modules during a 24h-charging scenario. We measured striking differences between modules, but only borderline significant deviations between lower and upper sensor positions.

(RMSE), the measurement results indicate a relatively small mushy region temperature range. Thus, also variation of ϵ was dismissed based on qualitative assessment.

With the help of the optimization of α_{in} and α_{out} , satisfactory validation results for used LHTES model were achieved for most sensor positions (e.g. LBD30CT001 in Fig. 11). Charging behaviour is reproduced very well except for minor temporal deviation. During discharging, larger discrepancies can be observed. We assume that further fit improvement is not possible with the presented single PCM cell model within the given framework of assumptions. Remaining deviations could be caused by global heat transfer effects, i.e. intra-cell heat transfer instead of inter-cell heat transfer and possibly disregarded physical effects like, for example, sub-cooling.

The results summarized in Table C.6 show large deviations between the identified values for the effective heat transfer coefficients of individual LHTES module sectors, in accordance with the results in Section 3.3. The RMSE values between simulated and observed temperature over the whole observation period ranged between 1.8 °C and 6 °C for all sensor positions.

3.5. Performance analysis of hybrid storage

Performance of the LHTES part of the hybrid storage is characterized by additional storage capacity as well as charging/discharging

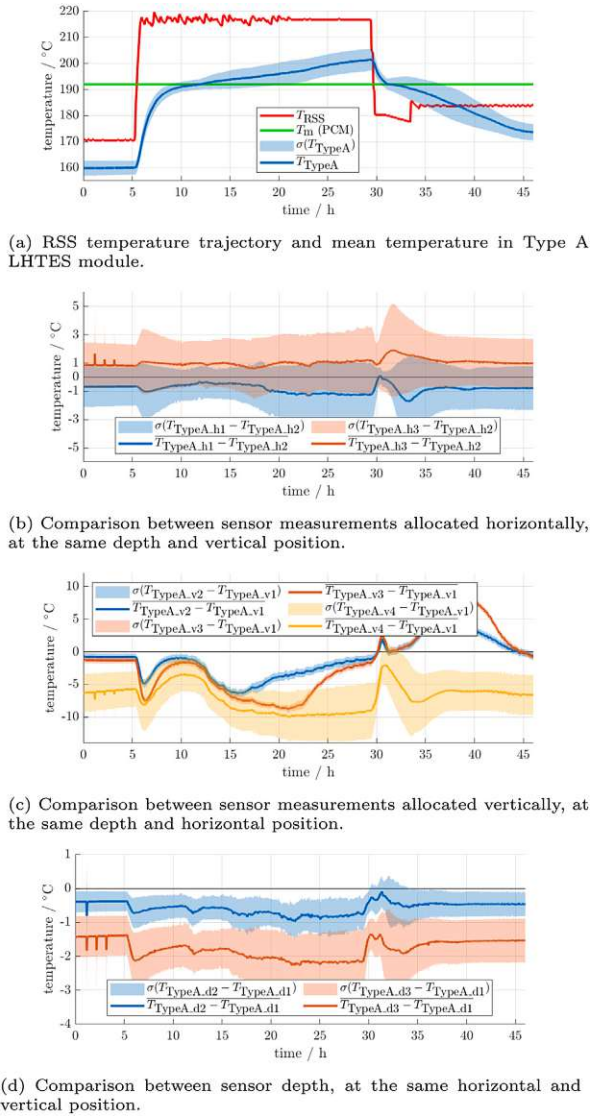


Fig. 9. Detailed analysis of single LHTES module of Type A instrumentation. Temperature measurement deviations between different sensor depths 9(d) and horizontal positions 9(b) behaved as expected and proved to be small, whereas significant deviations are observed between different vertical positions 9(c).

power and duration. The total enthalpy stored within the LHTES modules

$$H = \sum_{i=1}^{n=M} \left(\int_0^{T_i} m_{PCM,i} c_{PCM}(T) dT + m_{alu} c_{alu} T_i + m_{stl} c_{stl} T_i \right) \quad (16)$$

is approximated via $M = 16$ temperature measurement points T_i , two for each of the eight modules, replacing the measurement points LBD80CT001 and LBD20CT002, which are considered faulty, by surrogate values of LBD40CT001 and LBD40CT002, respectively. In Eq. (16), c_{alu} and c_{stl} are the specific heat capacities for aluminium and steel, and c_{PCM} is the apparent heat capacity as given in Eq. (9), containing the latent heat Δl_m and the sensible specific heat capacities c_s and c_l of the PCM in the solid and liquid region, respectively. The temperature of each measurement value is assumed constant for half of each LHTES module's mass.

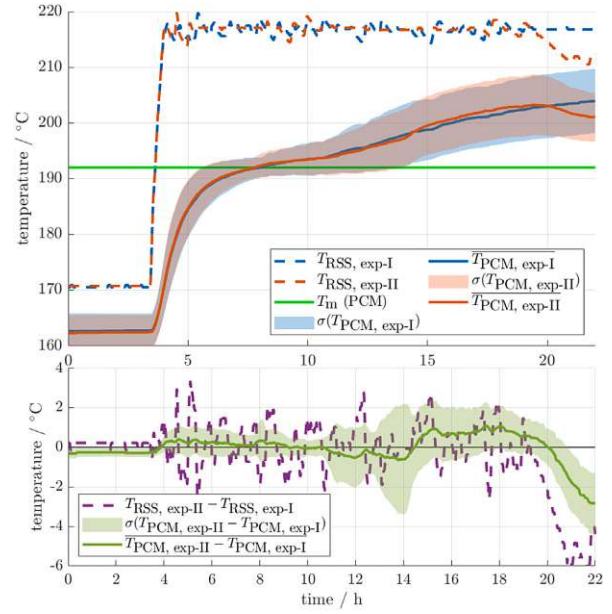


Fig. 10. Comparison of measurement results for two similar charging experiments. Only minor deviations were observed and the experiments were thus considered to be reproducible. *Note: modules 1 and 7 were removed from this evaluation, since their measurement values are not representative.

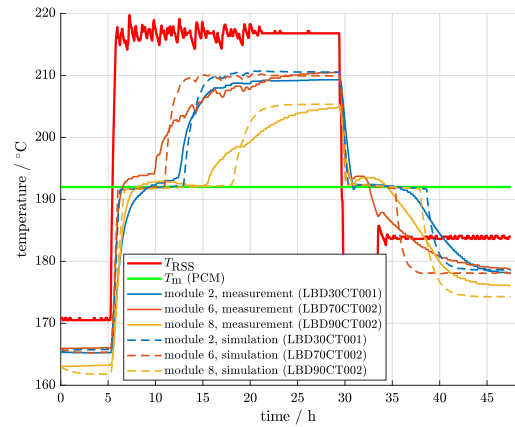


Fig. 11. Validation results of single PCM cell model for three representative sensor positions (LBD30CT001, LBD70CT002, LBD90CT002) and a 24h charging process. Experimental measurements are depicted as solid lines, simulation results are depicted as dashed lines. We obtained satisfactory validation results for most LHTES sensor positions. However, discrepancies are apparent during discharging.

Simulation values are calculated by scaling enthalpy values of the validated single PCM cell models (see, Section 3.4) according to the full LHTES module's mass.

3.5.1. Additional storage capacity by PCM containers

In order to obtain the usable additional storage capacity provided by the LHTES modules, a specific PCM activation test was carried out. In the first experiment (exp-I), the RSS was kept at a constant pressure of 7bar, corresponding to a temperature of roughly 170 °C, which is well below the PCM melting temperature. Thus, it is ensured that no PCM is activated, meaning latent enthalpy stored in the PCM. The RSS was then charged to a value of 21 bar, corresponding to a temperature of approximately 215 °C and immediately afterwards discharged to 7 bar.

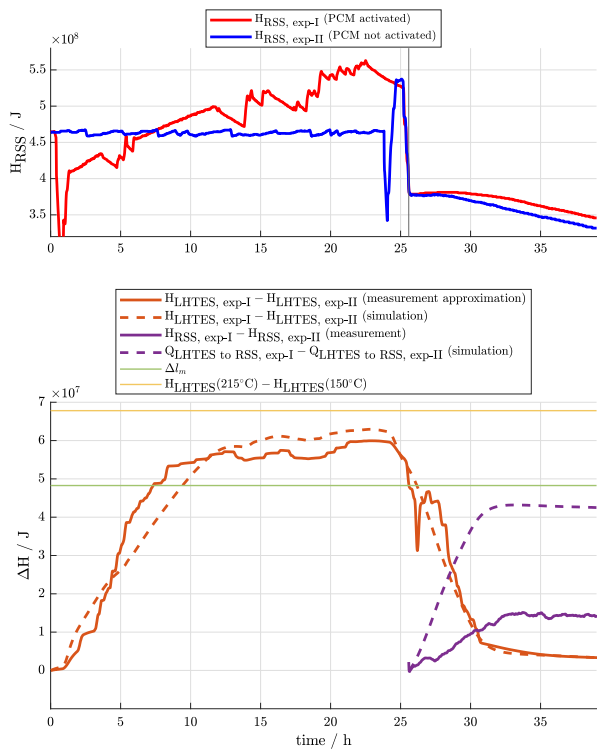


Fig. 12. PCM activation experiments: Enthalpy in the RSS for two different experiment trajectories is plotted in the upper subfigure. In the lower subfigure, additional enthalpy stored in LHTES (solid orange line) and recovered in the RSS during discharging (solid violet line) is plotted. Simulation results are depicted as dashed lines.

All valves of the RSS were then closed and temperature and pressure inside the RSS was monitored for another 24 h. In a second experiment (exp-II), the RSS was kept at a constant pressure of 21 bar for 24 h, thus ensuring that all PCM is fully activated, i.e. liquefied. All valves of the RSS were then closed as in exp-I.

Fig. 12 shows relative enthalpy values stored in the RSS for exp-I (red) and exp-II (blue) in the upper part of the figure and the RSS enthalpy difference between exp-I and exp-II in the lower part of the figure. An approximation of the enthalpy difference in the PCM is depicted in the orange line.

Since the approximation based on PCM temperature measurement points given in Eq. (16) is prone to a large error, additional data guidelines were added, indicating the total available latent enthalpy (green) and the total enthalpy difference between 215 °C and 150 °C LHTES module temperature (yellow). These values equal 48.3 MJ and 67.8 MJ, respectively. The approximate enthalpy stored in the LHTES part was 60 MJ. During discharging, the enthalpy difference in the RSS between activated and not activated PCM reached a maximum value of 15.1 MJ after 8.5 h of discharging. We can deduce from this experiment that approximately 26% of the stored enthalpy in the LHTES could be recovered in the RSS during a discharging period of 8.5 h. The 60 MJ of achieved storage capacity corresponds to a volumetric energy density of 437 MJ m⁻³. Note that this value differs from the volumetric phase change enthalpy of the pure PCM compound, valued at 716 MJ m⁻³, since the LHTES' full module volume and temperature operating range is considered. The LHTES storage capacity amounts to 30% of the RSS storage capacity valued at 200 MJ in Section 3.2 and the LHTES features 221% of the RSS' energy density. The total energy density of the hybrid storage amounts to 227 MJ m⁻³.

Agreement of the simulation values with the experimental observations (see Fig. 12) are considered satisfactory.

Table 3

Mean LHTES power values and duration for the period until 90% of the maximum experimental charging/discharging enthalpy was reached.

		duration	mean power	mean specific power
		h	W	W m ⁻³
Charging	(experimental)	11.88	7.69 · 10 ⁴	5.60 · 10 ⁵
	(simulation)	10.45	8.78 · 10 ⁴	6.40 · 10 ⁵
Discharging	(experimental)	7.85	-1.10 · 10 ⁵	-8.02 · 10 ⁵
	(simulation)	8.65	-1.01 · 10 ⁵	-7.36 · 10 ⁵

3.5.2. Charging/discharging power characterization

Power values estimated by experimental temperature measurements are prone to strong fluctuations, caused by RSS pressure measurement fluctuations and the nature of enthalpy estimation. Therefore, we introduced a mean power value, which is calculated for the duration until 90% of the maximum experimental charging/discharging enthalpy was reached. Hence, quantitative comparison of both charging/discharging power and duration is enabled between experimental observations and different simulation scenarios. For the evaluation presented here and illustrated in Fig. 13, typical operation scenarios were assumed, as already introduced in Section 3.5.1. During charging, the RSS' target pressure was set to 21 bar, corresponding to a temperature of roughly 217 °C. During discharging, the RSS' target pressure was set to 10 bar, corresponding to a temperature of roughly 184 °C.

The results for the obtained mean LHTES power values are given in Table 3. Fig. 13 shows the charging and discharging power characterization of the LHTES part of the hybrid storage via both power estimated by experimental measurements and power deduced from multiple single PCM cell simulations.

We observed good agreement between the simulated and measured values for mean power and charging/discharging duration. The charging duration is slightly underestimated by the simulation, while discharging duration is slightly overestimated compared to the experimental values. Discharging is faster than charging for this trajectory, i.e. the absolute value of discharging power is higher than the charging power, since undesired heat losses of the LHTES accelerate the discharging process.

Table 4 presents mean LHTES power values and charging duration for simulations with different reference cells scaled to the full LHTES storage mass. The rather low LHTES power rates and long time periods are a result of low heat transfer values (see Table C.6) between the RSS and the LHTES in this first hybrid storage prototype, and, relative to that, high heat losses to the environment. While we expected that heat transfer between the RSS and the LHTES part of the hybrid storage prototype is very critical to overall performance, it proved to be even more difficult to manage than initially expected. This fact is also reflected in the surprisingly strong deviating temporal behaviour between the eight LHTES modules, which are identical in construction, as presented in Section 3.3.

3.6. Sensitivity analysis of key process parameters

With the help of the validated single PCM cell models, we carried out a sensitivity analysis on the influence of the critical process parameters α_{in} and α_{out} on the key process parameters charging/discharging duration and power (see Fig. 14). The large dependency of the boundary heat transfer coefficients on the charging duration is apparent.

To put the measurement results into perspective, we consider the "theoretical" optimum values for the heat transfer coefficients assuming direct contact, i.e. perfect heat transfer between solid construction elements. We assume a heat transfer coefficient from liquid water inside the RSS to its steel shell of 700 W m⁻² K⁻¹ as given in [64,81], perfect heat transfer between the RSS' steel shell and the PCM containers' steel shell and heat conduction in the PCM container's steel walls according to the material properties and geometry values given in Tables 1 and 2, respectively. Furthermore, we assume a typical heat conductivity

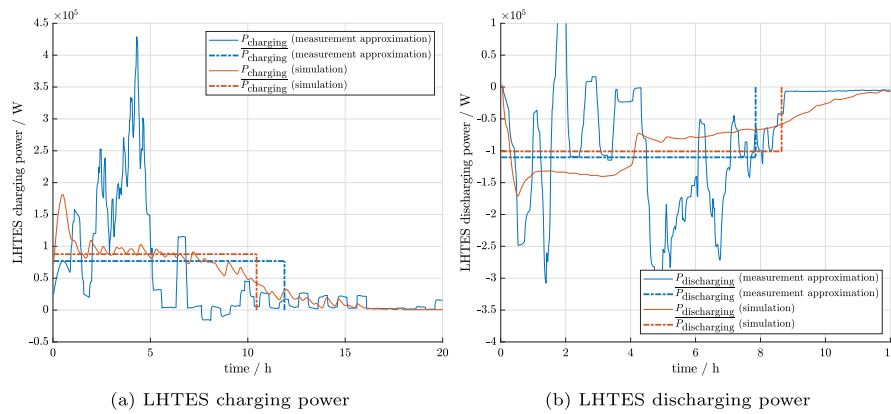


Fig. 13. Charging and discharging power characterization of the LHTES part of the hybrid storage. Experimental values (blue) are calculated via the enthalpy estimated by Eq. (16). Simulation values are calculated via the validated LHTES module parameters. Dashed-dotted lines represent the mean power values for the duration until 90% of the maximum experimental charging/discharging enthalpy was reached.

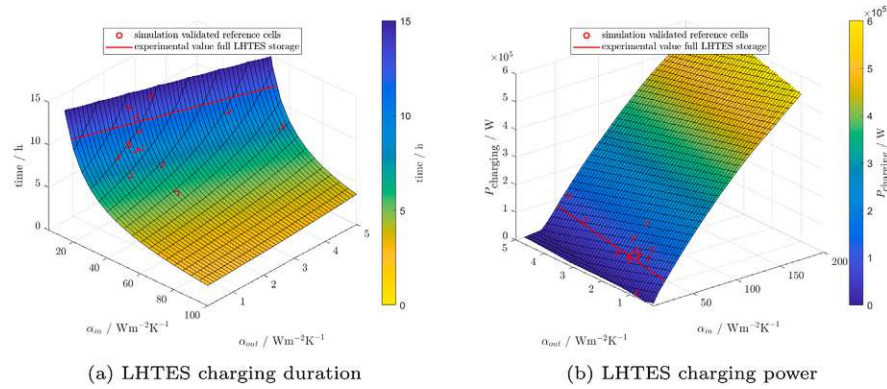


Fig. 14. LHTES charging duration and power for varying values of the critical heat transfer coefficients α_{in} and α_{out} . Simulation values of the validated reference cells scaled to the full LHTES mass are illustrated as red circles. The experimental measurement value of the full LHTES storage is given as red isoline.

Table 4
Mean LHTES power values and duration for the period until 90% of the maximum experimental charging/discharging enthalpy was reached for simulation of different reference cells. The power values were scaled to the full LHTES storage mass.

Sensor identifier	charging duration h	mean power W	mean specific power Wm^{-3}
LBD20CT001	7.70	$1.19 \cdot 10^5$	$8.67 \cdot 10^5$
LBD30CT001	7.73	$1.26 \cdot 10^5$	$9.15 \cdot 10^5$
LBD40CT001	9.01	$1.02 \cdot 10^5$	$7.40 \cdot 10^5$
LBD50CT001	7.67	$1.19 \cdot 10^5$	$8.71 \cdot 10^5$
LBD60CT014	13.47	$6.79 \cdot 10^4$	$4.95 \cdot 10^5$
LBD70CT001	10.02	$9.13 \cdot 10^4$	$6.66 \cdot 10^5$
LBD80CT001 ^a	13.50	$6.78 \cdot 10^4$	$4.94 \cdot 10^5$
LBD90CT001	8.92	$1.03 \cdot 10^5$	$7.48 \cdot 10^5$
LBD20CT002 ^a	10.12	$9.05 \cdot 10^4$	$6.59 \cdot 10^5$
LBD30CT002	10.68	$8.57 \cdot 10^4$	$6.24 \cdot 10^5$
LBD40CT002	9.05	$1.01 \cdot 10^5$	$7.38 \cdot 10^5$
LBD50CT002	38% ^b	$2.45 \cdot 10^4$	$1.79 \cdot 10^5$
LBD60CT032	14.57	$6.28 \cdot 10^4$	$4.58 \cdot 10^5$
LBD70CT002	5.38	$1.70 \cdot 10^5$	$1.24 \cdot 10^6$
LBD80CT002	9.65	$9.49 \cdot 10^4$	$6.91 \cdot 10^5$
LBD90CT002	11.85	$7.72 \cdot 10^4$	$5.63 \cdot 10^5$

^aMeasurements not representative due to experimental errors, see Section 3.3.1.
^bOnly 38% of charging capacity reached.

$597.49 Wm^{-2}K^{-1}$ for the maximum, i.e. best possible, value of α_{in} and $0.41 Wm^{-2}K^{-1}$ for the minimum, i.e. best possible, value of α_{out} .

While the assumption of perfect contact between the RSS' and the PCM containers' steel shell delivers "theoretical" benchmarks for fast charging/discharging and large power values, these are unlikely to be reached. Hence, we consider another scenario (scenario 4 in Table 5) where heat transfer enhancement via a small layer of heat conductivity paste between the two storage types is achieved. Assuming that this layer is 5 mm wide and filled with typical high temperature heat conductivity paste with a heat conductivity value of $3 WmK^{-1}$, we arrive at an overall heat transfer coefficient of α_{in} and $299.37 Wm^{-2}K^{-1}$.

Table 5 lists the resulting charging/discharging duration and mean power of these scenarios together with simulation values of the actual LHTES prototype and the best achieved LHTES values. These results show that charging/discharging times can be reduced by up to 10 times and specific power could be increased by up to 10 and 5 times, respectively compared to the achieved values. Therefore, feasible ways to enhance heat transfer between the RSS' steel shell and the LHTES containers' steel shell, i.e. α_{in} have to be found.

The hybrid storage prototype construction, as presented in Section 2.2.1, relies on direct contact between the two storage types, i.e. between two metallic surfaces of cylindrical shape. With the heat conductivity of still air being as low as $0.038 WmK^{-1}$, small gaps of around 1 mm width lead to a crucial drop in overall heat transfer. Fig. 15 illustrates the dependency of the overall heat transfer coefficient α_{in} on the width of a gap between the RSS' steel shell and the LHTES containers' shell.

value for compressed mineral wool of $0.045 WmK^{-1}$ for the 100 mm insulation layer and a heat transfer coefficient of $5 Wm^{-2}K^{-1}$ from this insulation layer to the environment. These assumptions correspond to scenario 3 in Table 5. Under these assumptions, we arrive at

Table 5

Calculation of mean LHTES power values and duration, for the period until 90% of the maximum experimental charging/discharging enthalpy was reached, for different scenarios. Scenario 1 corresponds to the mean value of validated LHTES modules of the built prototype, as given in Table 3. Scenario 2 corresponds to the best validated LHTES module (based on sensor LBD70CT002) scaled to the full prototype mass. Scenario 3 assumes perfect heat transfer conditions. Scenario 4 considers a design iteration with, again, perfect heat transfer conditions but a layer of heat conductivity paste between RSS and LHTES modules.

scenario	α_{in} $Wm^{-2}K^{-1}$	α_{out} $Wm^{-2}K^{-1}$	duration h	mean power W	mean specific power Wm^{-3}
1 (charging)	–	–	11.88	$7.69 \cdot 10^4$	$5.60 \cdot 10^5$
1 (discharging)	–	–	7.85	$-1.10 \cdot 10^5$	$-8.02 \cdot 10^5$
2 (charging)	29.61	1.42	5.38	$1.70 \cdot 10^5$	$1.24 \cdot 10^6$
2 (discharging)	–	–	5.50	$-1.58 \cdot 10^5$	$-1.15 \cdot 10^6$
3 (charging)	597.49	0.41	0.77	$1.24 \cdot 10^6$	$9.04 \cdot 10^6$
3 (discharging)	–	–	1.28	$-6.93 \cdot 10^5$	$-5.05 \cdot 10^6$
4 (charging)	299.37	0.41	1.08	$8.60 \cdot 10^5$	$6.27 \cdot 10^6$
4 (discharging)	–	–	1.87	$-4.72 \cdot 10^5$	$-3.44 \cdot 10^6$

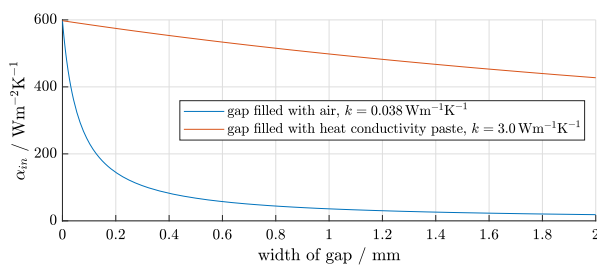


Fig. 15. Theoretic dependency of the overall heat transfer coefficient α_m on the width of an assumed gap between the RSS steel shell and the attached LHTES module, filled with still air (blue line) and filled with heat conductivity paste (orange line).

It should be noted that more research on the technical feasibility of the proposed application of heat conductivity paste (scenario 4) is necessary. While some suppliers offer non-hardening high-temperature compounds (e.g., silicon-based pastes such as Omegatherm 201 or Silicon Solutions SS-240), compound integrity under cycling operation must be tested. Furthermore, economic viability of the holistic concept (see, e.g., Niknam & Sciacovelli [62]) could be strongly influenced by the costs of such modification.

4. Conclusion

4.1. Summary of results

We presented the first-of-a-kind functional lab-scale prototype of the novel hybrid RSS/LHTES storage concept presented by Dusek & Hofmann [56,57]. While previous investigations focused on numerical characterization and techno-economic assessments, we delivered the first technically feasible construction and experimental investigation of such hybrid storage. The RSS could be retrofitted with additional 60 MJ storage capacity by means of LHTES modules. This corresponds to a storage capacity increase of 30% compared to the lab-scale RSS unit, which features a capacity of 200 MJ in the typical operating range. The retrofitted LHTES features a volumetric energy density of $437 MJ m^{-3}$, which is 221% of the RSS' energy density. The total energy density of the hybrid storage amounts to $227 MJ m^{-3}$.

Charging/discharging times and specific thermal power of the LHTES modules were roughly measured as 8 h/ 12 h and $560 Wk m^{-3}$ / $-802 kW m^{-3}$, respectively, in the typical operation region. During the PCM activation experiments, approximately 26% of the stored enthalpy in the LHTES could be retrieved back to the RSS.

Numerical models for both RSS and LHTES part of the hybrid storage were validated with satisfactory results. Via parameter optimization, the effective heat transfer coefficients α_{in} and α_{out} were identified individually for different LHTES module sectors. The RMSE

values between simulated and observed temperature over the whole observation period ranged between $1.8^\circ C$ and $6^\circ C$ for all sensor positions. Qualitatively, charging behaviour of the LHTES is reproduced very well except for minor temporal deviations while larger discrepancies in the discharging behaviour can be observed.

With the help of our validated thermal model, a sensitivity analysis of the key process parameters on the hybrid storage performance was carried out. The results show that specific charging/discharging power could be increased by up to 10 and 5 times compared to the achieved values with realistic re-adjustment of heat transfer between RSS and LHTES part, e.g., by using a layer of high temperature heat conductivity paste or similar concepts.

4.2. Outlook on future research and development

The hybrid storage prototype realized in this experimental investigation is very promising for industrial application due to its easy retrofit procedure. However, the investigations have shown that heat transfer between RSS and LHTES must be improved further to increase charging/discharging power and heat recovery. In the developed construction concept, direct contact between the RSS and the LHTES containers is essential for efficient storage operation. Fixed, permanent mounting to the RSS shell was disregarded due to technical and safety restrictions given in detail in Section 2.1. Unfortunately, the metallic springs, intended to ensure a tight fit of LHTES containers to the RSS surface, proved inadequate.

Future iterations of this hybrid storage could include high-temperature heat-conducting paste, thermal oil or other heat transfer compounds between the two storage parts in order to eliminate the possibility of air gaps. Such re-adjustments were not considered in the present study for the sake of simplicity, due to safety concerns, and because of limited resources to invest in both costly material and time to investigate additional safety issues introduced with such compounds.

A fundamentally different approach of flexible LHTES container designs mounted on the RSS should also be considered and re-evaluated. For example, construction by means of injection molding or additive manufacturing could provide essential advantages compared to the solid steel body construction in the present prototype. Such a container design could, as the presented prototype, maintain high safety requirements and technical constraints of operating a steam vessel. The use of flexible elastomer-based encapsulations of PCM, e.g., as developed by Yu et al. [82] or Li et al. [83], to allow for thermal expansion could provide essential benefits, if heat conductivity of the encapsulation material is sufficiently high. Wu et al. [84] developed polymer and graphite based highly thermally conductive, form-stable, flexible and leakage-proof phase change composites that are also promising for application in the TES use case targeted in our work. However, most research focuses on micro-scale encapsulation of PCM and temperature ranges below pressurized steam applications. The combined properties of flexibility, high heat conductivity and thermal stability [85] for macro-scale encapsulation have not been optimized for widespread

use, yet. Furthermore, more research on the interaction of the combined setup under operating conditions is necessary to optimize hybrid storage performance.

Our experimental analysis of this first-of-a-kind hybrid RSS/LHTES storage presents guidelines for future development of hybrid storage applications. Ultimately, future retrofit hybrid thermal energy storage concepts should become efficient, economically viable and accepted in industry and thus a key part to overcome the ever-increasing problem of mismatch between energy supply and demand.

CRediT authorship contribution statement

Lukas Kasper: Data curation, Formal analysis, Investigation, Methodology, Software, Validation, Visualization, Writing – original draft, Writing – review & editing. **Dominik Pernsteiner:** Investigation, Methodology, Software, Writing – review & editing. **Alexander Schirrer:** Conceptualization, Formal analysis, Investigation, Methodology, Writing – review & editing. **Stefan Jakubek:** Conceptualization, Funding acquisition, Supervision. **René Hofmann:** Conceptualization, Funding acquisition, Methodology, Supervision, Writing – review & editing.

Declaration of competing interest

The authors declare that they have no known competing financial interests or personal relationships that could have appeared to influence the work reported in this paper.

Data availability

Data will be made available on request.

Acknowledgements

This work was funded through the research project HySTEPS as part of the Austrian Climate and Energy Fund's initiative Energy Model Region 2nd call (KLIEN/FFG project number 868842). We are grateful for the fruitful collaboration with our project partners AIT Austrian Institute of Technology GmbH, Edtmayer Systemtechnik GmbH and voestalpine Stahl Donawitz GmbH.

This work is also connected to the patent application EP 3 260 803 A1 by R. Hofmann, C. Zauner, S. Dusek, and F. Hengstberger [86]. Furthermore, the authors acknowledge TU Wien Bibliothek for financial support through its Open Access Funding programme.

Appendix A. Grid and time step size sensitivity of numerical PCM model

As presented in Section 2.4.4, a uniformly distributed finite element grid of 1440 elements, corresponding to an element size of $\Delta x = \Delta y = 0.5$ mm, and a time step size of $\Delta t = 1.0$ s proved adequate for the numerical PCM simulations in this work.

For sensitivity analysis of grid and time step size, a typical simulation case, representative for the results in this paper, was chosen. The grid size sensitivity is illustrated for a reference simulation case in Fig. A.1. The time step size sensitivity is illustrated in Fig. A.2. Comparison was made by means of total enthalpy deviation to a base case, since this metric is of major importance to the numerical studies in this paper. Both figures show fast convergence and indicate that further refinement of the chosen values has no significant impact on the simulation results.

Appendix B. Validation of RSS model

Here, more details on the RSS model validation presented in Section 3.1 can be found. Fig. B.3 presents the most characteristic values for the RSS model validation in six subfigures for a given pressure setpoint trajectory.

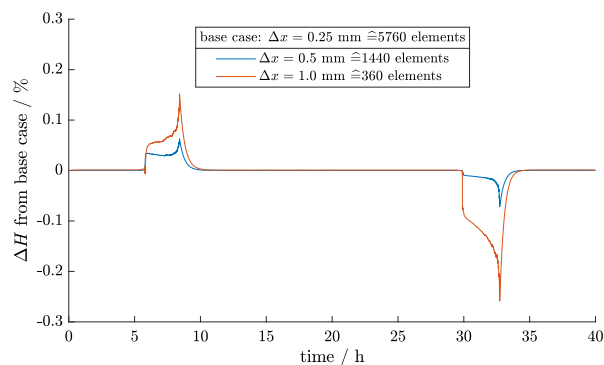


Fig. A.1. Grid size sensitivity of reference case, carried out with a time step size $\Delta t = 0.1$ s.

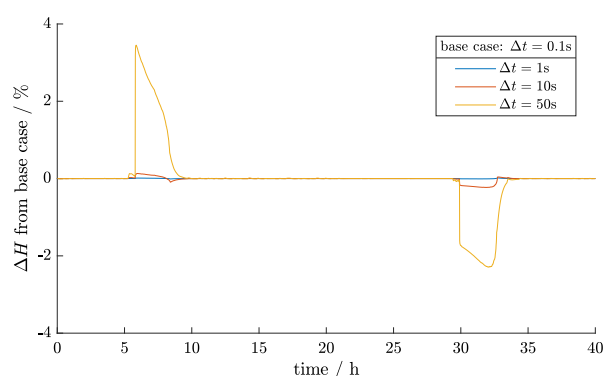


Fig. A.2. Time step sensitivity of reference case, carried out with a grid size of 5760 elements, corresponding to an element size of $\Delta x = \Delta y = 0.25$ mm.

Table C.6

Validation results of single PCM cell model for different sensor positions for the reference case given in Fig. 11. The uncertain physical parameters α_{in} and α_{out} (column two and three) were optimized to fit the measurement data. Column four and five present the obtained absolute RMSE and maximal error, respectively, between the measured and simulated temperature trajectory in the observed period.

Sensor identifier	α_{in} Wm ⁻² K ⁻¹	α_{out} Wm ⁻² K ⁻¹	RMSE K	max. error K
LBD20CT001	45.70	3.79	4.0	10.4
LBD30CT001	30.28	1.72	1.8	6.4
LBD40CT001	33.27	1.65	3.1	5.2
LBD50CT001	8.15	0.83	2.2	7.6
LBD60CT014	48.76	5.02	5.1	14.3
LBD70CT001	51.49	1.81	2.6	6.0
LBD80CT001 ^a	30.16	1.40	3.4	10.9
LBD90CT001	28.4	1.73	2.3	6.8
LBD20CT002 ^a	59.11	4.77	5.7	19.5
LBD30CT002	35.80	1.15	2.1	10.9
LBD40CT002	32.33	1.50	3.3	9.7
LBD50CT002	40.42	1.91	6.0	13.4
LBD60CT032	26.24	1.63	2.8	8.9
LBD70CT002	29.61	1.42	3.1	10.7
LBD80CT002	29.34	2.16	3.6	8.8
LBD90CT002	29.72	1.08	2.1	10.4

^aMeasurements not representative due to experimental errors, see Section 3.3.1.

Appendix C. Detailed results of single PCM cell model validation

Table C.6 presents the obtained values as well as the resulting validation errors for the 8 LHTES modules and two sensor positions each.

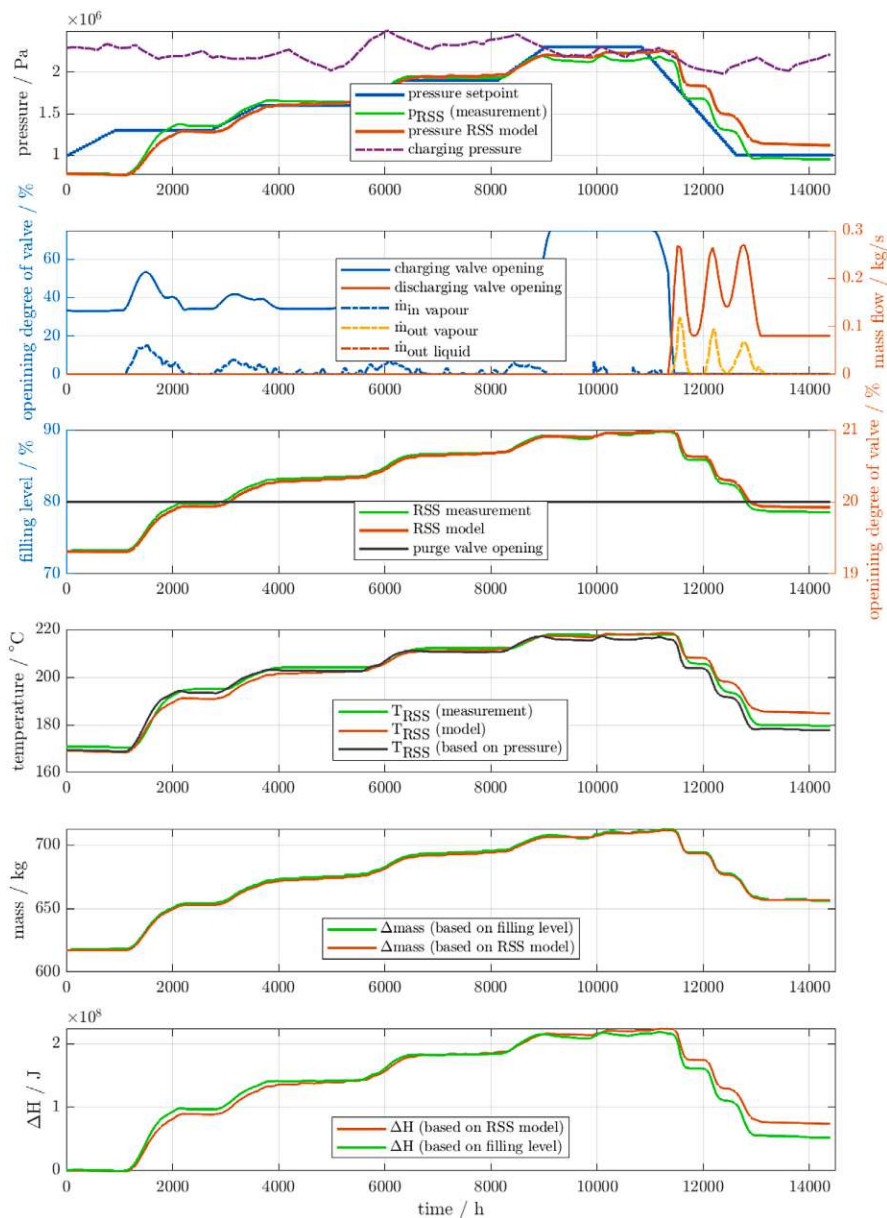


Fig. B.3. RSS measurement values and model outputs for a given pressure setpoint trajectory.

References

- [1] Leonard MD, Michaelides EE, Michaelides DN. Energy storage needs for the substitution of fossil fuel power plants with renewables. *Renew Energy* 2020;145:951–62. <http://dx.doi.org/10.1016/j.renene.2019.06.066>.
- [2] Cabeza LF. 2 - Advances in thermal energy storage systems: methods and applications. In: Cabeza LF, editor. *Advances in thermal energy storage systems (Second Edition)*. Woodhead Publishing Series in Energy, second ed.. Woodhead Publishing; 2021, p. 37–54. <http://dx.doi.org/10.1016/B978-0-12-819885-8.00002-4>.
- [3] Arce P, Medrano M, Gil A, Oró E, Cabeza LF. Overview of thermal energy storage (TES) potential energy savings and climate change mitigation in Spain and Europe. *Appl Energy* 2011;88(8):2764–74. <http://dx.doi.org/10.1016/j.apenergy.2011.01.067>.
- [4] Borri E, Zsembinszki G, Cabeza LF. Recent developments of thermal energy storage applications in the built environment: A bibliometric analysis and systematic review. *Appl Therm Eng* 2021;189:116666. <http://dx.doi.org/10.1016/j.applthermaleng.2021.116666>.
- [5] Cabeza LF, de Gracia A, Zsembinszki G, Borri E. Perspectives on thermal energy storage research. *Energy* 2021;231:120943. <http://dx.doi.org/10.1016/j.energy.2021.120943>.
- [6] Beck A, Sevault A, Drexler-Schmid G, Schöny M, Kauko H. Optimal Selection of Thermal Energy Storage Technology for Fossil-Free Steam Production in the Processing Industry. *Appl Sci* 2021;11(3). <http://dx.doi.org/10.3390/app11031063>.
- [7] Alva G, Lin Y, Fang G. An overview of thermal energy storage systems. *Energy* 2018;144:341–78. <http://dx.doi.org/10.1016/j.energy.2017.12.037>.
- [8] Therkelsen P, McKane A. Implementation and rejection of industrial steam system energy efficiency measures. *Energy Policy* 2013;57:318–28. <http://dx.doi.org/10.1016/j.enpol.2013.02.003>.
- [9] Rathgeber C, Lävemann E, Hauer A. Economic top-down evaluation of the costs of energy storages—A simple economic truth in two equations. *J Energy Storage* 2015;2:43–6. <http://dx.doi.org/10.1016/j.est.2015.06.001>.
- [10] Halmschlager D, Beck A, Knöttner S, Koller M, Hofmann R. Combined optimization for retrofitting of heat recovery and thermal energy supply in industrial systems. *Appl Energy* 2022;305:117820. <http://dx.doi.org/10.1016/j.apenergy.2021.117820>.

- [11] Gibb D, Johnson M, Gasia JRJ, Cabeza LF, Seitz A. Process integration of thermal energy storage systems – Evaluation methodology and case studies. *Appl Energy* 2018;230:750–60. <http://dx.doi.org/10.1016/j.apenergy.2018.09.001>.
- [12] Einstein D, Worrell E, Khrushch M. Steam systems in industry: Energy use and energy efficiency improvement potentials. Lawrence Berkeley National Laboratory 2001. Retrieved from <https://escholarship.org/uc/item/3m1781f1>.
- [13] Yang M, Dixon RK. Investing in efficient industrial boiler systems in China and Vietnam. *Energy Policy* 2012;40:432–7. <http://dx.doi.org/10.1016/j.enpol.2011.10.030>, Strategic Choices for Renewable Energy Investment.
- [14] IEA. Tracking industrial energy efficiency and CO2 emissions. (OECD) Organisation for Economic Co-operation and Development; 2007. ISBN: 978-92-64-03016-9.
- [15] González-Gómez P, Laporte-Azcué M, Fernández-Torrijos M, Santana D. Hybrid storage solution steam-accumulator combined to concrete-block to save energy during startups of combined cycles. *Energy Convers Manage* 2022;253:115168. <http://dx.doi.org/10.1016/j.enconman.2021.115168>.
- [16] Steinmann W-D, Eck M. Buffer storage for direct steam generation. *Sol Energy* 2006;80(10):1277–82. <http://dx.doi.org/10.1016/j.solener.2005.05.013>, Solar Power and Chemical Energy Systems (SolarPACES'04).
- [17] González-Roubaud E, Pérez-Osorio D, Prieto C. Review of commercial thermal energy storage in concentrated solar power plants: Steam vs. molten salts. *Renew Sustain Energy Rev* 2017;80:133–48. <http://dx.doi.org/10.1016/j.rser.2017.05.084>.
- [18] Biglia A, Comba L, Fabrizio E, Gay P, Ricauda Aimonino D. Steam batch thermal processes in unsteady state conditions: Modelling and application to a case study in the food industry. *Appl Therm Eng* 2017;118:638–51. <http://dx.doi.org/10.1016/j.applthermaleng.2017.03.004>.
- [19] Kuravi S, Trahan J, Goswami DY, Rahman MM, Stefanakos EK. Thermal energy storage technologies and systems for concentrating solar power plants. *Prog Energy Combust Sci* 2013;39(4):285–319. <http://dx.doi.org/10.1016/j.peccs.2013.02.001>.
- [20] Goldstern W. Steam storage installations: construction, design, and operation of industrial heat accumulators, vol. 4. Pergamon; 1970.
- [21] Stevanovic VD, Maslovaric B, Prica S. Dynamics of steam accumulation. *Appl Therm Eng* 2012;37:73–9. <http://dx.doi.org/10.1016/j.applthermaleng.2012.01.007>.
- [22] Biglia A, Comba L, Fabrizio E, Gay P, Ricauda Aimonino D. Steam batch thermal processes in unsteady state conditions: Modelling and application to a case study in the food industry. *Appl Therm Eng* 2017;118. <http://dx.doi.org/10.1016/j.applthermaleng.2017.03.004>.
- [23] Ibrahim NI, Al-Sulaiman FA, Rahman S, Yilbas BS, Sahin AZ. Heat transfer enhancement of phase change materials for thermal energy storage applications: A critical review. *Renew Sustain Energy Rev* 2017;74:26–50. <http://dx.doi.org/10.1016/j.rser.2017.01.169>.
- [24] Mehling H, Cabeza LF. Heat and cold storage with PCM. Springer Berlin Heidelberg; 2008. <http://dx.doi.org/10.1007/978-3-540-68557-9>.
- [25] Dincer I, Rosen M. Thermal energy storage: systems and applications. John Wiley & Sons; 2002. URL <https://books.google.at/books?id=EsfcWESIX40C>.
- [26] Bista S, Hosseini SE, Owens E, Phillips G. Performance improvement and energy consumption reduction in refrigeration systems using phase change material (PCM). *Appl Therm Eng* 2018;142:723–35. <http://dx.doi.org/10.1016/j.applthermaleng.2018.07.068>.
- [27] Zalba B, Marin JM, Cabeza LF, Mehling H. Review on thermal energy storage with phase change: materials, heat transfer analysis and applications. *Appl Therm Eng* 2003;23(3):251–83. [http://dx.doi.org/10.1016/S1359-4311\(02\)00192-8](http://dx.doi.org/10.1016/S1359-4311(02)00192-8).
- [28] Nguyen T-T, Martin V, Malmquist A, Silva CA. A review on technology maturity of small scale energy storage technologies. In: Goodfield D, editor. *Renew Energy Environ Sustain* 2017;2:36. <http://dx.doi.org/10.1051/rees/2017039>.
- [29] Cabeza LF, Martorell I, Miró L, Fernández AI, Barreneche C, Cabeza LF, Fernández AI, Barreneche C. 1 - Introduction to thermal energy storage systems. In: Cabeza LF, editor. *Advances in thermal energy storage systems* (Second Edition). Woodhead Publishing Series in Energy, second ed.. Woodhead Publishing; 2021, p. 1–33. <http://dx.doi.org/10.1016/B978-0-12-819885-8.00001-2>.
- [30] Merlin K, Delaunay D, Soto J, Traonvouez L. Heat transfer enhancement in latent heat thermal storage systems: Comparative study of different solutions and thermal contact investigation between the exchanger and the PCM. *Appl Energy* 2016;166:107–16. <http://dx.doi.org/10.1016/j.apenergy.2016.01.012>.
- [31] Yang X, Lu Z, Bai Q, Zhang Q, Jin L, Yan J. Thermal performance of a shell-and-tube latent heat thermal energy storage unit: Role of annular fins. *Appl Energy* 2017;202:558–70. <http://dx.doi.org/10.1016/j.apenergy.2017.05.007>.
- [32] Eslamnezhad H, Rahimi AB. Enhance heat transfer for phase-change materials in triple tube heat exchanger with selected arrangements of fins. *Appl Therm Eng* 2017;113:813–21. <http://dx.doi.org/10.1016/j.applthermaleng.2016.11.067>.
- [33] Augspurger M, Choi K, Udaykumar H. Optimizing fin design for a PCM-based thermal storage device using dynamic Kriging. *Int J Heat Mass Transfer* 2018;121:290–308. <http://dx.doi.org/10.1016/j.ijheatmasstransfer.2017.12.143>.
- [34] Muhammad M, Badr O. Performance of a finned, latent-heat storage system for high temperature applications. *Appl Therm Eng* 2017;116:799–810. <http://dx.doi.org/10.1016/j.applthermaleng.2017.02.006>.
- [35] Motahar S, Khodabandeh R. Experimental study on the melting and solidification of a phase change material enhanced by heat pipe. *Int Commun Heat Mass Transfer* 2016;73:1–6. <http://dx.doi.org/10.1016/j.icheatmasstransfer.2016.02.012>.
- [36] Mesalhy O, Lafdi K, Elgafy A, Bowman K. Numerical study for enhancing the thermal conductivity of phase change material (PCM) storage using high thermal conductivity porous matrix. *Energy Convers Manage* 2005;46(6):847–67. <http://dx.doi.org/10.1016/j.enconman.2004.06.010>.
- [37] Motahar S, Nikkam N, Alemrajabi AA, Khodabandeh R, Toprak MS, Muhammed M. A novel phase change material containing mesoporous silica nanoparticles for thermal storage: A study on thermal conductivity and viscosity. *Int Commun Heat Mass Transfer* 2014;56:114–20. <http://dx.doi.org/10.1016/j.icheatmasstransfer.2014.06.005>.
- [38] Khodadadi J, Hosseinzadeh S. Nanoparticle-enhanced phase change materials (NEPCM) with great potential for improved thermal energy storage. *Int Commun Heat Mass Transfer* 2007;34(5):534–43. <http://dx.doi.org/10.1016/j.icheatmasstransfer.2007.02.005>.
- [39] Yang J, Qi G-Q, Bao R-Y, Yi K, Li M, Peng L, Cai Z, Yang M-B, Wei D, Yang W. Hybridizing graphene aerogel into three-dimensional graphene foam for high-performance composite phase change materials. *Energy Storage Mater* 2018;13:88–95. <http://dx.doi.org/10.1016/j.ensm.2017.12.028>.
- [40] Huang X, Xia W, Zou R. Nanoconfinement of phase change materials within carbon aerogels: phase transition behaviours and photo-to-thermal energy storage. *J Mater Chem A* 2014;2:19963–8. <http://dx.doi.org/10.1039/C4TA04605F>.
- [41] Min P, Liu J, Li X, An F, Liu P, Shen Y, Koratkar N, Yu Z-Z. Thermally Conductive Phase Change Composites Featuring Anisotropic Graphene Aerogels for Real-Time and Fast-Charging Solar-Thermal Energy Conversion. *Adv Funct Mater* 2018;28(51):1805365. <http://dx.doi.org/10.1002/adfm.201805365>.
- [42] Aftab W, Mahmood A, Guo W, Yousaf M, Tabassum H, Huang X, Liang Z, Cao A, Zou R. Polyurethane-based flexible and conductive phase change composites for energy conversion and storage. *Energy Storage Mater* 2019;20:401–9. <http://dx.doi.org/10.1016/j.ensm.2018.10.014>.
- [43] Wu S, Li T, Tong Z, Chao J, Zhai T, Xu J, Yan T, Wu M, Xu Z, Bao H, Deng T, Wang R. High-Performance Thermally Conductive Phase Change Composites by Large-Size Oriented Graphite Sheets for Scalable Thermal Energy Harvesting. *Adv Mater* 2019;31(49):1905099. <http://dx.doi.org/10.1002/adma.201905099>.
- [44] Wu M, Li T, Wang P, Wu S, Wang R, Lin J. Dual-Encapsulated Highly Conductive and Liquid-Free Phase Change Composites Enabled by Polyurethane/Graphite Nanoplatelets Hybrid Networks for Efficient Energy Storage and Thermal Management. *Small* 2022;18(9):2105647. <http://dx.doi.org/10.1002/sml.202105647>.
- [45] Zayed ME, Zhao J, Li W, Elsheikh AH, Elbanna AM, Jing L, Geweda A. Recent progress in phase change materials storage containers: Geometries, design considerations and heat transfer improvement methods. *J Energy Storage* 2020;30:101341. <http://dx.doi.org/10.1016/j.est.2020.101341>.
- [46] Wu M, Wu S, Cai Y, Wang R, Li T. Form-stable phase change composites: Preparation, performance, and applications for thermal energy conversion, storage and management. *Energy Storage Mater* 2021;42:380–417. <http://dx.doi.org/10.1016/j.ensm.2021.07.019>.
- [47] Abdelsalam M, Sarafraz P, Cotton J, Lightstone M. Heat transfer characteristics of a hybrid thermal energy storage tank with Phase Change Materials (PCMs) during indirect charging using isothermal coil heat exchanger. *Sol Energy* 2017;157:462–76. <http://dx.doi.org/10.1016/j.solener.2017.08.043>.
- [48] Zhao J, Ji Y, Yuan Y, Zhang Z, Lu J. Energy-Saving Analysis of Solar Heating System with PCM Storage Tank. *Energies* 2018;11(1). <http://dx.doi.org/10.3390/en11010237>.
- [49] Frazzica A, Manzan M, Sapienza A, Freni A, Toniato G, Restuccia G. Experimental testing of a hybrid sensible-latent heat storage system for domestic hot water applications. *Appl Energy* 2016;183:1157–67. <http://dx.doi.org/10.1016/j.apenergy.2016.09.076>.
- [50] Underwood C, Shepherd T, Bull S, Joyce S. Hybrid thermal storage using coil-encapsulated phase change materials. *Energy Build* 2018;159:357–69. <http://dx.doi.org/10.1016/j.enbuild.2017.10.095>.
- [51] Cabeza LF, nez MI, Solé C, Roca J, Nogués M. Experimentation with a water tank including a PCM module. *Sol Energy Mater Sol Cells* 2006;90(9):1273–82. <http://dx.doi.org/10.1016/j.solmat.2005.08.002>.
- [52] Zauner C, Hengstberger F, Mörzinger B, Hofmann R, Walter H. Experimental characterization and simulation of a hybrid sensible-latent heat storage. *Appl Energy* 2017;189:506–19. <http://dx.doi.org/10.1016/j.apenergy.2016.12.079>.
- [53] Tatsidjoudoung P, Le Pierrès N, Luo L. A review of potential materials for thermal energy storage in building applications. *Renew Sustain Energy Rev* 2013;18:327–49. <http://dx.doi.org/10.1016/j.rser.2012.10.025>.
- [54] Buschle J, Steinmann W-D, Tamme R. Latent heat storage for process heat applications. In: 10th International conference on thermal energy storage ECOSTOCK 2006, vol. 31. 2006, p. 1–8. URL <https://elib.dlr.de/55379/>.
- [55] Tamme R, Bauer T, Buschle J, Laing D, Müller-Steinhagen H, Steinmann W-D. Latent heat storage above 120°C for applications in the industrial process heat sector and solar power generation. *Int J Energy Res* 2008;32(3):264–71. <http://dx.doi.org/10.1002/er.1346>.

- [56] Dusek S, Hofmann R. A hybrid energy storage concept for future application in industrial processes. *Therm Sci* 2018;22:2235–42. <http://dx.doi.org/10.2298/TSCI171230270D>.
- [57] Dusek S, Hofmann R. A Hybrid Storage Concept for Improving Classical Ruth's Type Steam Accumulators. In: *Proceedings of the 12th SDEWES Conference, Dubrovnic, Croatia. 2017*, p. 4–8.
- [58] Dusek S, Hofmann R. Modeling of a Hybrid Steam Storage and Validation with an Industrial Ruths Steam Storage Line. *Energies* 2019;12(6). <http://dx.doi.org/10.3390/en12061014>.
- [59] Fang M, Chen G. Effects of different multiple PCMs on the performance of a latent thermal energy storage system. *Appl Therm Eng* 2007;27(5):994–1000. <http://dx.doi.org/10.1016/j.applthermaleng.2006.08.001>.
- [60] Li W, Zhang Y, Zhang X, Zhao J. Studies on performance enhancement of heat storage system with multiple phase change materials. *J Energy Storage* 2021;103585. <http://dx.doi.org/10.1016/j.est.2021.103585>.
- [61] Nepustil U, Laing-Nepustil D, Lodemann D, Sivabalan R, Hausmann V. High Temperature Latent Heat Storage with Direct Electrical Charging – Second Generation Design. *Energy Procedia* 2016;99:314–20. <http://dx.doi.org/10.1016/j.egypro.2016.10.121>, 10th International Renewable Energy Storage Conference, IRES 2016, 15–17 March 2016, Düsseldorf, Germany.
- [62] Niknam PH, Sciacovelli A. Hybrid PCM-steam thermal energy storage for industrial processes – Link between thermal phenomena and techno-economic performance through dynamic modelling. *Appl Energy* 2023;331:120358. <http://dx.doi.org/10.1016/j.apenergy.2022.120358>.
- [63] Hofmann R, Dusek S, Gruber S, Drexler-Schmid G. Design Optimization of a Hybrid Steam-PCM Thermal Energy Storage for Industrial Applications. *Energies* 2019;12(5). <http://dx.doi.org/10.3390/en12050898>.
- [64] Dusek S, Hofmann R, Gruber S. Design analysis of a hybrid storage concept combining Ruths steam storage and latent thermal energy storage. *Appl Energy* 2019;251:113364. <http://dx.doi.org/10.1016/j.apenergy.2019.113364>.
- [65] Kasper L. Modeling of the phase change material of a hybrid storage using the finite element method. TU Wien Academic Press; 2020. <http://dx.doi.org/10.34727/2020/isbn.978-3-85448-037-2>.
- [66] Kasper L, Pernsteiner D, Koller M, Schirrer A, Jakubek S, Hofmann R. Numerical studies on the influence of natural convection under inclination on optimal aluminium proportions and fin spacings in a rectangular aluminium finned latent-heat thermal energy storage. *Appl Therm Eng* 2021;190:116448. <http://dx.doi.org/10.1016/j.applthermaleng.2020.116448>.
- [67] Pernsteiner D, Kasper L, Schirrer A, Hofmann R, Jakubek S. Co-simulation methodology of a hybrid latent-heat thermal energy storage unit. *Appl Therm Eng* 2020;178:115495. <http://dx.doi.org/10.1016/j.applthermaleng.2020.115495>.
- [68] Pernsteiner D, Schirrer A, Kasper L, Hofmann R, Jakubek S. Data-based model reduction for phase change problems with convective heat transfer. *Appl Therm Eng* 2021;184:116228. <http://dx.doi.org/10.1016/j.applthermaleng.2020.116228>.
- [69] Pernsteiner D, Schirrer A, Kasper L, Hofmann R, Jakubek S. State estimation concept for a nonlinear melting/solidification problem of a latent heat thermal energy storage. *Comput Chem Eng* 2021;153:107444. <http://dx.doi.org/10.1016/j.compchemeng.2021.107444>.
- [70] Gasia J, Miró L, Cabeza LF. Review on system and materials requirements for high temperature thermal energy storage. Part 1: General requirements. *Renew Sustain Energy Rev* 2017;75:1320–38. <http://dx.doi.org/10.1016/j.rser.2016.11.119>.
- [71] HyStEPs | NEFI URL <https://www.nefi.at/en/project/hysteps>.
- [72] Pereira da Cunha J, Eames P. Thermal energy storage for low and medium temperature applications using phase change materials – A review. *Appl Energy* 2016;177:227–38. <http://dx.doi.org/10.1016/j.apenergy.2016.05.097>.
- [73] Vogel J, Felbinger J, Johnson M. Natural convection in high temperature flat plate latent heat thermal energy storage systems. *Appl Energy* 2016;184:184–96. <http://dx.doi.org/10.1016/j.apenergy.2016.10.001>.
- [74] thyssenkrupp: Stainless Steel datasheets . Retrieved from <https://www.thyssenkrupp-materials.co.uk/stainless-steel-316ti-14571.html>.
- [75] Tenchev R, Mackenzie J, Scanlon T, Stickland M. Finite element moving mesh analysis of phase change problems with natural convection. *Int J Heat Fluid Flow* 2005;26(4):597–612. <http://dx.doi.org/10.1016/j.ijheatfluidflow.2005.03.003>, CHT'04.
- [76] Huang M, Eames P, Norton B. Comparison of a small-scale 3D PCM thermal control model with a validated 2D PCM thermal control model. *Sol Energy Mater Sol Cells* 2006;90(13):1961–72. <http://dx.doi.org/10.1016/j.solmat.2006.02.001>.
- [77] Medrano M, Yilmaz M, Nogués M, Martorell I, Roca J, Cabeza LF. Experimental evaluation of commercial heat exchangers for use as PCM thermal storage systems. *Appl Energy* 2009;86(10):2047–55. <http://dx.doi.org/10.1016/j.apenergy.2009.01.014>.
- [78] Seddegh S, Wang X, Henderson AD. A comparative study of thermal behaviour of a horizontal and vertical shell-and-tube energy storage using phase change materials. *Appl Therm Eng* 2016;93:348–58. <http://dx.doi.org/10.1016/j.applthermaleng.2015.09.107>.
- [79] Longeon M, Soupert A, Fourmigué J-F, Bruch A, Marty P. Experimental and numerical study of annular PCM storage in the presence of natural convection. *Appl Energy* 2013;112:175–84. <http://dx.doi.org/10.1016/j.apenergy.2013.06.007>.
- [80] Mostafavi Tehrani SS, Diarce G, Taylor RA. The error of neglecting natural convection in high temperature vertical shell-and-tube latent heat thermal energy storage systems. *Sol Energy* 2018;174:489–501. <http://dx.doi.org/10.1016/j.solener.2018.09.048>.
- [81] Herr H. *Wärmelehre: Technische Physik Band 3. Europa-Lehrmittel; 1994*.
- [82] Yu D-H, He Z-Z. Shape-remodeled macrocapsule of phase change materials for thermal energy storage and thermal management. *Appl Energy* 2019;247:503–16. <http://dx.doi.org/10.1016/j.apenergy.2019.04.072>.
- [83] Li W-W, Cheng W-L, Xie B, Liu N, Zhang L-S. Thermal sensitive flexible phase change materials with high thermal conductivity for thermal energy storage. *Energy Convers Manage* 2017;149:1–12. <http://dx.doi.org/10.1016/j.enconman.2017.07.019>.
- [84] Wu S, Li T, Wu M, Xu J, Hu Y, Chao J, Yan T, Wang R. Highly thermally conductive and flexible phase change composites enabled by polymer/graphite nanoplatelet-based dual networks for efficient thermal management. *J Mater Chem A* 2020;8:20011–20. <http://dx.doi.org/10.1039/D0TA05904H>.
- [85] Jacob R, Bruno F. Review on shell materials used in the encapsulation of phase change materials for high temperature thermal energy storage. *Renew Sustain Energy Rev* 2015;48:79–87. <http://dx.doi.org/10.1016/j.rser.2015.03.038>.
- [86] Hofmann R, Zauner C, Dusek S, Hengsbarger F. DAMPFSPEICHER EU Patent 3 260 803 A1. 2017, URL <https://patents.google.com/patent/EP3260803A1>.

Paper 3

Digitalization possibilities and the potential of the Digital Twin for steam supply systems

published in vgb energy journal (formerly VGB PowerTech Journal) in collaboration with Thomas Bacher, Felix Birkelbach, and René Hofmann

This journal paper presents a literature review and analysis of possibilities offered by digitalization and I4.0 for energy systems, hence tackling research question *RQ 2.1*. The application focus was on steam supply systems, i.e., steam boilers and storage at industrial sites and power plants. The paper first presents a definition and history of the topics of digitalization and I4.0, since there are often misconceptions. Furthermore, it explains the most relevant enabling technologies of I4.0 and introduces the idea of the DT as one of the most promising technologies for the digital future in I4.0. A basic DT modeling framework consisting of five dimensions is reviewed: (1) The physical entity, (2) the virtual entity, (3) the data- and (4) service dimension, and (5) the connection between the other parts. The conceptual application of this theoretical framework for the DT of a steam generator is presented. Recommendations for approaching each DT dimension are given. Finally, use cases are presented to demonstrate where DT implementation can create major benefits in the operation and maintenance of steam supply systems. For example, proactive control as the evolution of predictive control is introduced and soft sensors are highlighted as a more than useful addition to conventional measurement technology. The analysis and concepts established in this paper laid the foundation for my later work in Paper 4 and Paper 5, where a functioning DT platform was developed and tested in operation.

My contribution: Conceptualization, Investigation, Resources, Writing – Original Draft & Editing, Visualization

L. Kasper, T. Bacher, F. Birkelbach & R. Hofmann (2020). "Digitalization possibilities and the potential of the Digital Twin for steam supply systems". In: VGB PowerTech 11/2020, pp. 45–52.

URL: <https://www.vgb.org/vgbmultimedia/PT202011HOFMANN-p-16462.pdf>

Digitalization possibilities and the potential of the Digital Twin for steam supply systems

Lukas Kasper, Thomas Bacher, Felix Birkelbach and René Hofmann

Kurzfassung

Möglichkeiten der Digitalisierung und das Potenzial des Digital Twin für Dampfversorgungssysteme

Digitalisierung führt zu einer weiteren Revolution industrieller Prozesse und eröffnet völlig neue Anwendungsmöglichkeiten. Die Zukunftsvisionen von Industry4.0 und Energy4.0, wie sie in dieser Arbeit zusammengefasst sind, zeichnen ein Bild beispielloser Vernetzung von Gegenständen und Dienstleistungen im Internet of Things. Sie versprechen einen noch nie dagewesenen Grad an Vernetzung, Flexibilisierung und Automatisierung von Produkten und Systemen, sowie enorme Potenziale zur Senkung von Kosten und Energieverbrauch sowie zur Steigerung der Nachhaltigkeit.

Als Auszug aus dem VGB-Forschungsprojekt DigiSteam, werden in diesem Beitrag die vielversprechendsten Möglichkeiten der Digitalisierung evaluiert und der Zusammenhang mit dem Konzept von Referenzarchitekturen, wie RAMI4.0, mit Fokus auf den Dampferzeugungssektor untersucht. Unter Anwendung der hier thematisierten theoretischen Grundlagen wird eine Adaption eines fünfdimensionalen Modells für einen Digitalen Zwilling von einem Dampferzeuger präsentiert, bestehend aus physikalischem Dampferzeuger, Kommunikationsmodell, virtuellem Dampferzeuger, Datenmodell und Servicemodell. Ein ganzheitliches Prognose- und System Health Management werden illustriert und Anwendungsfälle zeigen, dass die Systemüberwachung, -vorhersage und -optimierung stark verbessert werden kann.

Digitalization is more and more becoming part of industrial processes and opens up completely new application areas. The visions of Industry4.0 and Energy4.0, as summarized in this article, both paint a picture of an unprecedented level of interconnectedness of devices and smart services in the Internet of Things. Systems and products will be created that have a high degree of networking, flexibility and automation. Because of these features, they have a huge potential for reducing cost, energy consumption and for improving economic sustainability.

In this article, as an excerpt from the VGB research project DigiSteam, the most promising possibilities offered by digitalization are evaluated with special focus on the steam supply sector. The connection with the concept of reference architectures, such as RAMI4.0, is discussed and the Digital Twin is introduced. Based on these theoretical fundamentals, an adaption of a five-dimensional Digital Twin model to a steam generator is presented. It consists of physical steam generator, communication model, virtual steam generator, data model and service model. A holistic Boiler Prognostics and System Health Management is outlined and with use cases, it is shown that system monitoring, prediction and optimization can be greatly improved by employing this Digital Twin.

1. Introduction

We are currently in the middle of what is often referred to as the fourth industrial revolution or Industry4.0 (I4.0). Driven by the rapid development of Information and Communication Technologies (ICT), the integration of digital technologies is advancing rapidly in every industry sector, not least the energy sector. For the energy industry, new and more advanced technologies are becoming available that will heavily affect energy generation, transmission, distribution, storage, and even its consumption. These new technologies come at just the right time because they provide the tools to cope with the challenges that have emerged through the energy

transition: changes in the regulatory framework, such as the liberalization of the energy market, and the increase of renewable and decentral energy generation. But these new technologies are not only a way to cope with challenges ahead, they also have great potential for increasing energy efficiency, reducing cost and even to generate completely new business models [1-3]. While some researchers warn that digitalization could increase energy consumption due to subsequent rebound effects and economic growth [4, 5], most researchers and organizations agree on the huge potential for reducing energy consumption and for increasing economic sustainability [2, 6-8]. In this way, digitalization can contribute immensely to meeting the increasingly stringent CO₂ reduction targets [2]. Just like any other revolution, I4.0 and the energy transition may be a threat or an opportunity. One way or the other: digitalization will heavily affect the energy sector and business actors have to carefully navigate this transition [8-10].

Within the energy sector, steam supply systems are of major importance. The growing demand for power plants and power generation processes has been fueling the demand for steam boiler systems substantially [11]. Digitalization technologies might be the key to unlock untapped optimization potential in steam supply systems, by supporting the optimal integration of technologies and utilization of infrastructure. For this reason, the VGB Research Foundation (https://www.vgb.org/en/vgb_research.html) has commissioned two parallel research projects in 2019 to take a close look at digitalization in the energy sector. DigiPoll@Energy [12] was conducted at the University of Duisburg-Essen (UDE). They assessed the current situation in industry regarding digitalization in the energy sector and expectations of industry leaders. DigiSteam [13] was carried out at TU Wien with the goal to identify opportunities through digitalization in the energy sector, especially in the field of steam supply systems. In that project, digitalization methods and their expected effect were assessed, and reference architectures, such

Authors

Dipl.-Ing. Lukas Kasper
 Dipl.-Ing. Thomas Bacher
 Dipl.-Ing. Dr. techn. Felix Birkelbach
 Univ. Prof. Dipl.-Ing. Dr. techn.
 René Hofmann
 Technische Universität Wien
 Institut für Energietechnik und
 Thermodynamik
 Forschungsbereich Industrielle
 Energiesysteme
 Vienna, Austria

as the Reference Architecture Model 4.0 (RAMI4.0), were evaluated. The Digital Twin (DT) was identified as one of the most promising digitalization applications to date. In this article, we present the most relevant results of the project *DigiSteam* and highlight our main findings.

2. Digitalization and Industry4.0

The aim of this section is to present a definition of and a broad overview on digitalization and digital technologies, as well as a discussion of the terms *Industry4.0* (I4.0) and *Energy4.0* (E4.0). Furthermore, reference architecture models are evaluated which provide the basis for successful implementation of I4.0 concepts.

The term *digitization* generally refers to the conversion of analogue data into a digital form. For the term *digitalization*, on the other hand, there is neither a universal definition nor is it used consistently. From a socio-economic perspective, the aim of digitalization is not only to convert analogue to digital signals but also to create value using digital content [14]. Digitalization also describes the connection between business processes, creation of efficient interfaces, and integrated data exchange and management [15]. In the context of industrialization, digitalization describes the transition to new, disruptive business cases driven by evolving Information and Communication Technologies (ICT), the automation and flexibilization of business operation and the interconnection of information, things and operatives [10]. Business models are already changing to take into account the increasing share of digital technologies as smart services [16]. In the present article, digitalization is seen in the context of industrialization. In our understanding, it refers to a more fundamental change than just digitizing existing processes or work products. To emphasize this fundamental change, the term *digital transformation* is also often used, especially if the change is happening on multiple levels, including the process level, organization level, business domain level and society level [9].

The term *Industry4.0* (I4.0) was first introduced in Germany in 2011, referring to the Fourth Industrial Revolution. In that sense, it is essentially equivalent to the definition of the digital transformation given in the previous paragraph. Just as with digitalization, there exists no universal definition of this term. However, I4.0 can be characterized in the following way [17]:

- The dynamic connection of internal and external data sources and
- the automated analysis and processing of thereby generated information
- for demand-driven preparation or control of processes,
- located at different points in the value chain of an industrial company,

- to make them faster, cheaper, customer-oriented, more efficient, resource-saving and flexible.

In analogy to I4.0, E4.0 characterizes the transition to energy systems of the fourth generation. These energy systems will be based on renewable, volatile energy carriers, a high amount of flexibilization, and interconnection between different industry sectors. Furthermore, they feature extensive application of digital technologies. The declared goal of E4.0 is to exploit efficiency- and flexibilization-potentials in processes to optimize the conversion, distribution and consumption of energy [18].

2.1 Digital (Enabling) Technologies of I4.0

Digitalization and consequently I4.0 are driven by recent developments within the area of digital base technologies. These technologies are also often referred to as (*key*) *enabling technologies*. Typical examples include next-generation sensors, Big Data, Machine Learning (ML), Artificial Intelligence (AI), the Internet of Things (IoT), Smart Services, Mechatronics and Advanced Robotics, Cloud Computing, Cyber Physical Systems (CPS), Additive Manufacturing, Digital Twins (DT), and Machine-to-Machine (M2M) communication [2]. Enabling technologies can both be implemented in new plants and retrofitted to existing plants. Out of the large number of key enabling technologies, we are going to focus on the four most relevant and address them in more detail: IoT, CPS, Big Data and AI or ML.

The backbone of every digital application in I4.0 is a (global) networking infrastructure. This role can be assumed by the IoT, which is defined as an interconnected world, where electronic sensors, actuators, and other digital devices are networked and connected with the purpose of collecting and exchanging data [19]. Other definitions also include features such as self-configuring capabilities, interoperable communication protocols and virtual personalities of “things” in the definition of IoT (Internet of Things European Research Cluster (IERC), Brussels: <http://www.internet-of-things-research.eu>; Internet of Things European Research Cluster (IERC), Brussels: <http://www.internet-of-things-research.eu>). Especially in the energy sector, an IoT based online monitoring system has a big potential, as has been demonstrated, for example, in a steel casting production line [19]. Most importantly, the IoT also satisfies elementary demands for the implementation of a DT [20].

The IoT also enables the creation of CPS, which connect the virtual space with the physical reality and integrates computing, communication and storage capabilities. A CPS works in real-time and it is reliable, secure, stable and efficient [21]. The core concepts of a CPS are computation, com-

munication, and control. The goal is to achieve collaborative and real-time interaction between the real world and the digital world through feedback loops and the interaction between computational processes and physical processes [21]. The bidirectional connection between the real and the digital world also provides the foundation for a DT [22], as will be explained in more detail later.

Big Data describes ways of leveraging data rather than the data itself. It is maybe the most prominent enabling technology of all. It has even been claimed that “the world’s most valuable resource is no longer oil, but data”. Big data is usually defined by the five Vs: Volume, Velocity, Variety, Veracity and Value [23, 24]. *Big Data analytics* refer to techniques used to examine and process Big Data in a way that hidden underlying patterns are revealed, relationships are identified, and new insights concerning the application under investigation are generated [23]. The term Big Data is also interpreted as the ability to quickly acquire hidden value and information from heterogeneous and large amount of data [25]. Without doubt, there are numerous possibilities for leveraging Big Data, not least in the energy sector, where direct measurement of key process variables is extremely difficult, nearly impossible or simply unreliable [26-28]. Here, Big Data can help to monitor these key processes with higher accuracy. In this context it is often also referred to as Smart Data [29].

Automated methods to extract information from Big Data are ML or AI, among others. Often used synonymously, ML can be seen as a subset of AI that focuses on training a machine on how to learn [3]. ML technologies are related to pattern recognition and statistical inference. A ML model is capable of learning to improve the performance of a task, based on its own previous experience. While ML rather aims the creation of knowledge from experience (historic data), AI can more generally be defined as the attempt to create a human-like, cognitive intelligence with the ability to learn and to solve problems on its own [30]. AI and related technologies can enhance resource efficiency in industrial processes, which is a crucial factor for a successful realization of I4.0 [31]. Although AI and ML approaches are rather new and not yet mature, many industrial applications already exist. A review of such applications in the Austrian energy industry is given in the White Paper “Digitalization in Industry - an Austrian Perspective” [3].

2.2 Implementation Concepts and Reference Architectures

The realization of I4.0 and E4.0 is a complex design task, because the gradual integration of new technology in this complex overall framework must be seen in a holistic context. This requires intensive cooper-

ation between experts of different disciplines such as electrical engineering, mechanical engineering and information technology (IT). Reference architectures provide common and consistent definitions of the system of interest, its compositions, and design patterns. Additionally, they provide a common terminology to discuss the specification of implementations [32].

In 2012, the Smart Grid Coordination Group published the Smart Grid Architecture Model (SGAM) [33], with the aim to establish a reference designation system to describe business cases as well as smart grid technical use cases. While SGAM was designed with the electrical energy sector in mind, the Reference Architecture Model 4.0 (RAMI4.0), a similar but more universal model was defined and presented by *Plattform Industrie 4.0* (<https://www.plattform-i40.de>) in 2015 [34]. To achieve a common understanding of standards, tasks and use cases, three different aspects (dimensions) are combined in the RAMI4.0, as depicted in Figure 1. RAMI4.0 expands the hierarchy levels of IEC 62264, by Product and Connected World, defines six layers for an IT representation of an *Industry4.0* component, and considers the life cycle of products/systems according to IEC 62890 (<http://i40.semantic-interoperability.org/>). For a detailed description of the RAMI4.0, see, for example, [34, 35].

RAMI4.0 allows for step-by-step migration of technology from the present industrial stage into the world of I4.0 [36], by breaking down tasks and workflows into manageable pieces [3]. The three dimensions support new technologies, applications and use cases in industry. Smart Services and their functional enhancements in the energy sector can easily be extended and used by a variety of other applications at different layers of the RAMI4.0 [37]. Furthermore, current and future standards and services can be located in RAMI4.0 to identify overlapping as well as missing standardization efforts.

Based on expert interviews in a recent study [38], the main fields for future potential in the energy sector were identified: (1) increasing transparency in the energy system, (2) flexibility in energy supply and (3) increase of energy efficiency [38]. According to that study, RAMI4.0 and SGAM can help to keep track of the complex design task of realizing E4.0 and focus on appropriate norms and standards. However, some pitfalls of RAMI4.0 were determined when applying it to an industrial reference use case [39]. It is clear that a more dynamic framework will be necessary to exploit the main fields for future potential during operation of energy systems.

3. The Digital Twin

Prominent concepts like *Industry4.0* (I4.0) or *Energy4.0* (E4.0) evoke a vision of the future industry and energy system, where enabling technologies are used extensively. They promise an unprecedented degree of networking, system flexibility and automation. The key is the consequent integration of the real/physical world with the virtual/digital world. While RAMI4.0 is a useful tool to identify areas where deeper integration is necessary, it cannot be used to do the actual integration. For this task, the Digital Twin (DT), as a high-fidelity digital mirror of its physical counterpart, is a promising concept to reach this convergence of the physical with the digital world. For this reason, the DT is considered a key technology for implementing the digital future in I4.0 and E4.0 [40, 41].

3.1 Review and Definition

The idea of the DT originates from an earlier concept of a physical twin, which was introduced by the American space agency NASA during the Apollo space program while testing operations on a replica on earth. Only in 2012 the concept was picked up again by NASA and continued under the name Digital Twin [42]. Since then, an al-

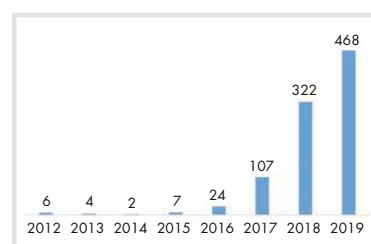


Fig. 2. Scientific Publications on DT from 2012 to 2019 (for more details, refer to the project report *DigiSteam* [13]).

most exponential increase in the number of scientific publications on DT has been recorded, as an extensive literature review [13] shows (see Figure 2).

In NASA's definition, the DT is a multiphysics, scalable and probabilistic image (simulation model) of a physical object or system that is used to map certain aspects of the real object, taking into account historical and real-time sensor data. However, there remains some controversy about the exact definition of the DT. There is a wide consensus, that also the bidirectional data exchange between physical and digital object in real time is a prerequisite for a DT [43].

After the DT concept was adopted by NASA (<https://www.nasa.gov>) in 2012, research and development on the DT was mainly driven forward in the field of aviation [44]. In recent years, the DT has found its way into more and more industry sectors, such as automotive, oil & gas and healthcare & medicine [45]. In 2018, DT was listed on top of the „Gartner-Hype-Cycle“ (<https://www.gartner.com>), and the time in which DT is used as an applied concept within companies, has been put at 5 to 10 years.

With the rapid growth of the Internet of Things (IoT) and other Information and Communication Technologies (ICT), a large number of application possibilities, such as energy optimization, performance tuning, predictive maintenance and product optimization have been suggested. However, in order to make the most of these individual, already existing possibilities, a holistic approach is required. Here, the excellent scalability of the DT offers many benefits over the entire life cycle of an asset [46].

Despite the large number of promising approaches proposed in literature, a general lack of in-depth research on DT modeling is evident. Additionally, modeling methods for DTs are very heterogeneous, sometimes even inconsistent. In a recent literature review, the lack of a uniform modeling method was found to be very critical [47]. Thus, while DT implementations are considered to have huge potential, there is an urgent need to standardize interfaces and communication protocols, as well as a need for uniform DT modeling approaches to enable its practical introduction into industrial energy systems.

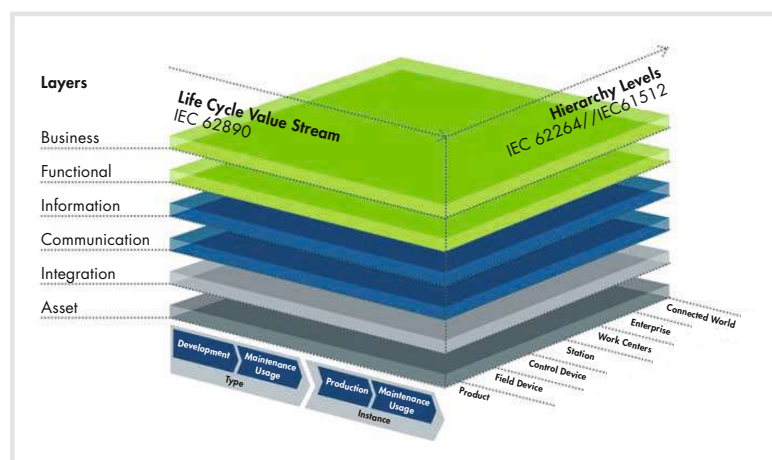


Fig. 1. RAMI4.0 [© Plattform Industrie 4.0, reproduced with permission].

3.2 Modelling Framework

To unify modeling of DTs, modeling frameworks have been introduced. An early DT modeling framework is the one by Grieves [48]. It is characterized by a three-dimensional approach (3D-DT), where the DT is described by the following three dimensions:

- The physical unit, i.e. the physical object or system, in the real world,
- the digital unit or system in the virtual world, also called virtual entity, and
- the connection between physical and digital entities through data and information.

This framework is very similar to the definition of a CPS (see Section). However, these dimensions do not present the extent to which new types of services are made available in this concept. Furthermore, data and information only act as connection between the real and virtual world. How this data is processed and the extent to which information can be retrieved from it is not made explicit. The rapid development of enabling technologies, omnipresent availability of data, and the need for services are the main reasons, why an extension of Grieves' 3D-DT framework was necessary [48, 49]. In order to prevent the pitfalls of unspecified data processing and restricted usability/serVICation, the model was extended by the following two dimensions by Tao et al. [50] to arrive at the 5D-DT:

- The data model, in which data from all sources is collected, managed and processed into usable information.
- The service model contains services resulting from the functionality of the DT and makes them available to the user of the DT.

With the help of the bidirectional connection and closed loop between physical and virtual space in the 5D-DT modeling approach, all components can be optimized and a significant increase in the physical object's performance can be achieved through the implemented services. The 5D-DT approach has recently been praised for its usefulness and generality in a number of contributions [20, 49-53]. In these publications, a wide range of use cases has been demonstrated and evaluated as well.

4. The Digital Twin of a Steam Generator

In this section, a digitalization concept based on a DT tailored to steam generation applications is presented. Applying the theoretical fundamentals and basic definitions that were assessed in the project *DigiSteam* [13] and outlined in the sections above, a five-dimensional DT-Model (5D-DTM) for a steam generator is outlined and discussed. A steam generator, as one of the most important thermal energy supply systems, is directly affected by the paradigm shift in

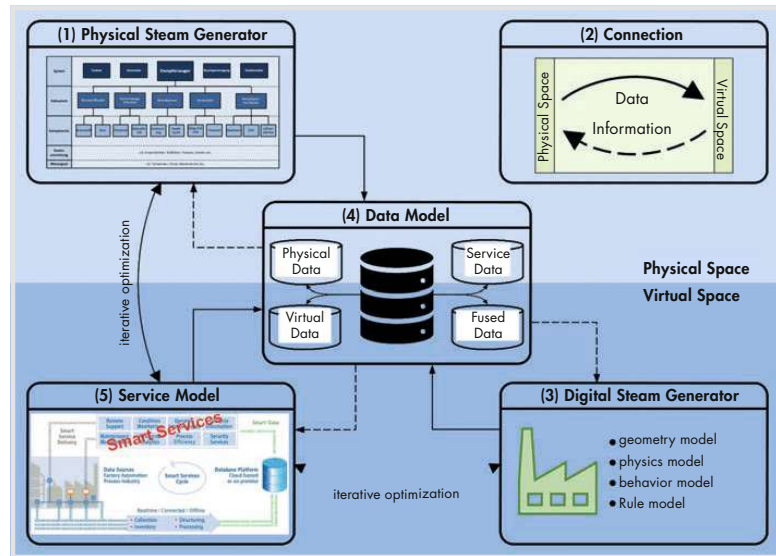


Fig. 3. 5D-DT model of a Steam Generator, adapted from [50]. The Physical Steam Generator (1) in the physical space is linked via the Connection dimension (2) to the virtual space, which consists of the Digital Steam Generator (3), i.e. virtual entity, the Data model (4) and the Service model (5).

Industry4.0 and *Energy4.0*. Steam generators will have to work in increasingly dynamic settings, which frequently leads to off-design conditions. For system operators, increasingly frequent load changes pose a great challenge to retain the economic operation of their systems [54]. Therefore, these difficult conditions are ideally suited to illustrate the advantages of a DT.

To illustrate the value creation by employing a Digital twin, a Smart Service system based on the 5D-DT concept is outlined: a holistic Boiler Prognostics and System Health Management (Boiler-PHM). It is shown that the system monitoring, prediction and optimization can be greatly improved. Figure 3 illustrates the 5D-DTM, based on the approach first presented by Tao et al. [50]. The DT consists of:

- Physical steam generator (i.e. physical entity)
- Connection between the respective dimensions (i.e. communication model)
- Digital steam generator (i.e. virtual entity)
- Data model
- Service model

Each aspect of modelling this 5D-DT is discussed in the following subsections. In Section 4.6 a demonstrative use cases and an economic evaluation is presented. A more in-depth treatment of this topic can be found in the final report of the *DigiSteam* project [13].

4.1 Physical entity

The physical entity consists of all functional subsystems and any physical sensor/actuator technology that is built into the steam supply system.

4.2 Communication model

The communication model in a 5D-DT fulfills the basic task of establishing connections between all other parts of the model, most importantly between the real and virtual space. It is only through this bidirectional communication infrastructure that the 5D-DT has the ability to access data from the physical entity and process it digitally to obtain relevant information. Essential characteristics of the communication model are real-time capability, integration of heterogeneous end-devices, scalability and security [55].

Exemplary communication infrastructures for I4.0 and Digital Twins based on IoT technology are given in [56, 57]. The use of open communications standards for industrial automation, notably OPC Unified Architecture (OPC UA) are highly encouraged in literature. OPC UA also provides the basis for further information modeling in the data model.

4.3 Virtual entity

The virtual entity of the DT is a high-fidelity representation of the physical entity. The virtual entity reproduces the geometry, physical properties, behaviours and rules of the physical entity in the virtual world [50]. The coupling of these four sub model classes is used to form a complete mirror image of the physical entity. In addition to this division in sub model classes, a modular modelling approach can be applied to reduce complexity of the virtual representation and increase the flexibility and scalability of the virtual entity. An example for such a modular design would be a hierarchical structure consisting of the system level, sub-system level, component level,

auxiliary equipment and signal (sensor) level.

The geometric model of a virtual entity is commonly modelled based on 3D Computer-aided Design (CAD) models. Even though no functional properties or restrictions are stored in the geometric model, it serves as foundation for the physical, the behaviour and the rule model of the steam generator. These, in turn, serve to represent physical processes, state-specific behavioural patterns and the control behaviour of the entire steam generator system. These models combined must be able to represent all possible influencing variables and their interactions as well as the control behaviour of the system.

Three categories of simulation models can be distinguished [58]:

- White-box models use a well-known physical relationship in mathematical form to describe a certain behavior.
- Black-box models, also known as (purely) data-driven models, are built on data only, without exploiting any physical knowledge.
- Grey-box models combine physical knowledge and empirical data, which often yields excellent results in practice [3, 58].

Typically, a combination of these simulation model categories is used with higher-level optimization models to create the functionality of the virtual entity.

4.4 Data model

In the data model, also known as information model or knowledge representation, static data for the description of different attributes of the physical entity is provided and dynamic status and operational data is processed. The heterogeneity of DT data, which is caused by the combination of different data sources working on different timelines, poses a big challenge for DT operation. Furthermore, a DT must be capable of extracting specific domain knowledge from experts or from existing data and making it accessible [59]. Therefore, DT need interpretable reliable data in standardized machine-readable formats [60]. With the help of the data model, anything from plain sensors to complex plants can be described in a semantically meaningful way [61].

To fully exploit the potentials of CPS, IoT and DT, proper data models should be employed, such as ontologies [62, 63]. Ontologies are explicit, semantic and formal representations of the relationships between concepts, data and entities in a domain [22]. They are the core semantic technology that provide intelligence embedded in the smart CPS [10] and can facilitate the integration of large amounts of data from various sources [64].

4.5 Service model

Digital transformation is driving I4.0 towards a service-oriented Product-Service-

System. As a consequence, services in general and especially services related to physical products play an increasingly important role [65]. Users of the DT come from various industries with different technical requirements. This poses a challenge for the effective interaction between the DT and users/stakeholders. To solve the problem of interoperability and to enable innovative business models, the functions of the DT can be encapsulated into standardized services with user-friendly interfaces for easy and on-demand usage [49].

The service model includes services for physical and virtual entity. It optimizes the operation of the physical entity, and ensures the high fidelity of the virtual entity through automatic parameter adaptation during run-time. In general, services can be grouped into four basic types:

- Functional service: these define core business operations
- Enterprise service: these implement the functionality defined by the functional services
- Application service: these are confined to specific application content
- Infrastructure service: implements non-functional tasks such as authentication, auditing, security, and logging

More in-depth reviews of services and application scenarios can be found in [22, 66, 67]. Smart service architectures should provide interoperability by acting as foundation for data integration and data exchange between various applications as part of the DT functionality. Smart service architectures were, for example, proposed by the German electrical and electronic manufacturers association (ZVEI) [68] and in [37]. Therefore, the use of an ontology-based smart service architecture is highly encouraged for complex physical systems such as a steam generator.

4.6 Use Cases and Economic Evaluation

The DT can create value in all stages of the steam generator's live cycle: starting in the design phase, during product manufacturing and also in the operation and maintenance (o&m) phase [53]. A detailed discussion of many use cases can be found in the *DigiSteam* report [13]. In this article, we focus on value creation in the o&m phase, because it plays a particularly important role for steam generators.

Steam generators are designed to maintain a functional and efficient state over long periods of time with as little downtime as possible. To minimize downtime, monitoring and control strategies are applied. With conventional strategies data is collected and then evaluated by a team of engineers or a simple decision component to operate the system and draw conclusions on its current state. The system undergoes maintenance in regular intervals or whenever a

part breaks. This approach can be labelled "offline monitoring and reactive control" (0). More advanced evolutionary stages of control concepts can be grouped, in ascending order of complexity, into online control (1), or condition monitoring, predictive maintenance (2) and proactive control (3) [69, 70].

To improve the operating performance of steam boilers, there already are a range of digital technologies available, that can readily be applied. Essential improvements that can be achieved by additional monitoring include the reduction of flue gas flows, reduction of pollutants, improvement of the ash quality, increase of the overall efficiency, reduction of corrosion [71]. In the context of digitalization and DT, so-called soft sensors or data-driven or virtual sensors are increasingly being considered. In contrast to conventional control methods, the usage of soft sensors has, for example, proven to lead to significant reductions in temperature and pressure fluctuations during operation [72]. In addition, soft sensors evidently provide high-quality quantification of synthesis gas calorific value. With currently available hardware sensors, this would not be possible at reasonable cost [26, 56].

Predictive maintenance is a procedure that improves the maintenance planning of systems in such a way that the current and predictive future system status can be included in the planning of maintenance measures and thus, downtime due to system failures is reduced. As a simple example, by consistent automated implementation of the RIMAP method (Risk Based Inspection and Maintenance Procedures for European Industry) [73], risk-based decision-making is achieved. Another example of a significant increase in productivity through a predictive maintenance strategy is presented in [74]. In this study, the dynamics of boiler efficiency and the expectations regarding heat demand are solved in an optimization model via dynamic programming, based on empirical operating data. It has been shown that the total operating costs of a steam generator in the observation period can be reduced by at least 8%, compared to periodic maintenance (e.g. yearly) [74].

The most extensive and complex concept of monitoring and control that has been proposed is proactive operation control. The goal is to achieve an optimization of the overall system by considering all relevant aspects of the system. For this purpose, soft sensors and information of the predictive maintenance strategy are included in a holistic control strategy. The benefit of such a combined approach has been shown for fouling control [75-77], where big improvements could be achieved by taking maintenance information into account in the optimization and control strategy.

So where does the DT come in? The DT provides a platform for integrating all

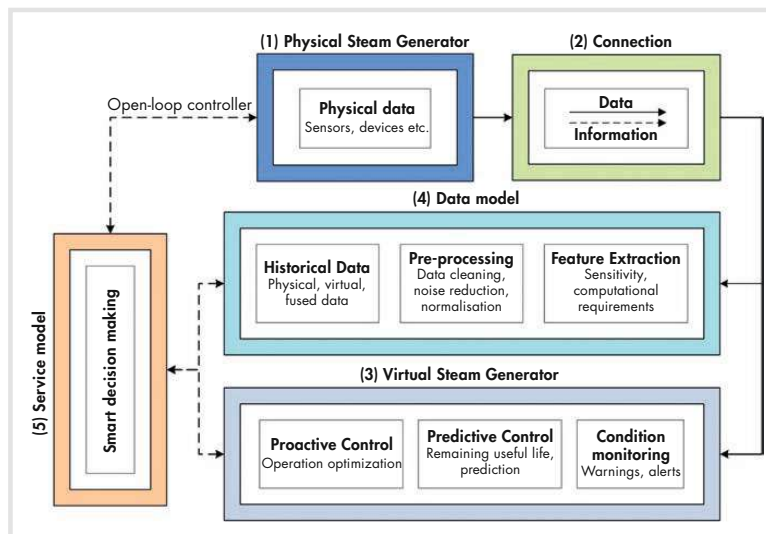


Fig. 4. Boiler System Health Management scheme according to [78] in the 5D-DT framework.

these smart services (soft sensors, predictive maintenance, proactive control), allowing them to communicate and giving them access to a shared data (knowledge) base. It allows the predictive maintenance service to access data from a soft sensor. It facilitates the information flow from the predictive maintenance service to the operation planning service, so that the next maintenance interval can be incorporated in the planning. The result is a holistic Boiler Prognostics and System Health Management, which has been adapted from [78]. Figure 4 illustrated this process in the 5D-DT framework.

This use case shows that even if many individual digitalization methods are already implemented in steam generators, they are not working at their full potential because they are isolated solutions, more often than not. With the help of the 5D-DT approach, these isolated solutions can be integrated into one single framework that allows all the components to communicate. This is made possible by setting up a central data management in the data model. By using extensive knowledge representation in the data model, the data is given meaning (Smart Data) and smart services can be extracted.

Another great advantage of the 5D-DT approach is that it can be built step by step, adding new services as needed. Starting from a very basic DT, the functionality can be extended continuously. The result is a comprehensive, holistic model that makes the DT more and more intelligent and creates value by a combination of smart services.

Conclusion and Outlook

The digital transformation and *Industry4.0* (I4.0) will have immense impact on the energy sector, including steam supply sys-

tems. It provides an opportunity for reducing cost and energy consumption and for improving economic sustainability. As novel digitalization methods are reaching a level of maturity that makes them ready for industrial implementation, opportunities but also challenges emerge. One big challenge is ensuring interoperability between services and the need to connect different systems and devices into a central knowledge base. These challenges were also highlighted in the recent survey and analysis in *DigiPoll@Energy* [12].

The reference model RAMI4.0 can aid the stepwise implementation of enabling digitalization technologies and, in this way, lead the way to I4.0 and E4.0. To make the most of opportunities offered by I4.0 and E4.0, the Digital Twin (DT) was identified as key application in the design, operation and maintenance phase. For the implementation of a DT standardized interfaces and data modelling via ontologies are the central part. During the ongoing digital transformation, RAMI4.0 can support the implementation of dynamic frameworks such as the presented 5D-DT of a steam generator.

DTs enable the horizontal integration of otherwise stand-alone digital services such as condition monitoring, predictive maintenance and operational optimization, to name just a few. The DT serves as a platform for these services that gives them access to a common knowledge base (Smart Data and models) and bi-directional communication with the real asset. It is considered a key technology to maximize the added value from enabling technologies and achieve a combined optimum of transparency, flexibility, economic sustainability and efficiency in energy systems.

Even though the benefits of advanced digitalization technologies like the DT in the steam supply sector are evident, they have

not yet been implemented in industry. For this reason, interdisciplinary collaboration between scientists and industry is necessary to transfer these new technologies into practice and keep the competitive edge.

Acknowledgement

This article has received funding from the VGB research foundation as research project 429 – *DigiSteam* (“Identification of digitalization possibilities in the energy sector especially in the field of steam supply systems”).

Abbreviations and Acronyms

DT	Digital Twin
ICT	Information and Communication Technologies
I4.0	Industry4.0
E4.0	Energy4.0
RAMI4.0	Reference Architecture Model 4.0
ML	Machine Learning
AI	Artificial Intelligence
IoT	Internet of Things
CPS	Cyber Physical System
M2M	Machine-to-Machine communication
IT	Information Technology
SGAM	Smart Grid Architecture Model
3D-DT	three dimensional Digital Twin
5D-DT	five dimensional Digital Twin
PHM	Prognostics and System Health Management
OPC UA	OPC Unified Architecture
RUL	Remaining Useful Lifetime
RIMAP	Risk Based Inspection and Maintenance Procedures
o&m	operation and maintenance phase

References

- [1] Loock, M. (2020). *Unlocking the value of digitalization for the European energy transition: A typology of innovative business models*. Energy Research & Social Science, 69, 101740. <https://doi.org/10.1016/j.erss.2020.101740>.
- [2] Branca, T.A., Fornai, B., Colla, V., Murri, M.M., Streppa, E., & Schröder, A.J. (2020). *The Challenge of Digitalization in the Steel Sector*. Metals, 10, 288. <https://doi.org/10.3390/met10020288>.
- [3] Hofmann, R., Halmeschlager, V., Leitner, B., Pernsteiner, D., Prendl, L., Sejkora, C., Steindl, G., & Traupmann, A. (2020a). *Digitalization in Industry – An Austrian Perspective*. Whitepaper: Bericht für Klima- und Energiefond. 122 p. <https://sic.tuwien.ac.at/fileadmin/t/sic/Dokumente/White-Paper-Digitalization-in-Industry.pdf>.
- [4] Lange, S., Pohl, J., & Santarius, T. (2020). *Digitalization and energy consumption. Does ICT reduce energy demand? Ecological Economics*, 176, 106760. <https://doi.org/10.1016/j.ecolecon.2020.106760>.
- [5] Hilty, L., & Bieser, J. (2017). *Opportunities and Risks of Digitalization for Climate Protection in Switzerland*: University of Zurich. <https://doi.org/10.5167/uzh-141128>.

- [6] Kiel, D., Müller, J., Arnold, C., & Voigt, K.-I. (2017). *Sustainable Value Creation: Benefits and Challenges of Industry 4.0*. International Journal of Innovation Management, 21, 1740015. <https://doi.org/10.1142/S1363919617400151>.
- [7] Beier, G., Niehoff, S., Ziems, T., & Xue, B. (2017). *Sustainability aspects of a digitalized industry – A comparative study from China and Germany*. International Journal of Precision Engineering and Manufacturing-Green Technology, 4, 227-234. <https://doi.org/10.1007/s40684-017-0028-8>.
- [8] Irlbeck, M. (2017). *Digitalisierung und Energie 4.0 – Wie schaffen wir die digitale Energiewende?* In Doleski, O.D. (Ed.), Herausforderung Utility 4.0: Wie sich die Energiewirtschaft im Zeitalter der Digitalisierung verändert (pp. 135-148): Springer Fachmedien Wiesbaden. https://doi.org/10.1007/978-3-658-15737-1_8.
- [9] Parviainen, P., Tihinen, M., Kääriäinen, J., & Teppola, S. (2017). *Tackling the digitalization challenge: How to benefit from digitalization in practice*. International journal of information systems and project management, 5, 63-77. <https://doi.org/10.12821/ijispm050104>.
- [10] Hanschke, I. (2018). *Digitalisierung und Industrie 4.0 – einfach und effektiv systematisch und lean die digitale Transformation meistern: Digitalisierung und Industrie 4.0 – einfach & effektiv*. München: München Hanser.
- [11] Zion Market Research (Upcoming). *Steam Boiler System Market: Global Industry Analysis, Size, Share, Growth, Trends, and Forecast, 2018-2026*. <https://www.zionmarketresearch.com/report/steam-boiler-system-market>. Accessed 21.10.2020.
- [12] Weigel, P., & Görner, K. (2020). *DigiPoll@Energy 2020 – Ergebnisbericht Digitalisierung im Energiesektor – Status-quo, Ausblick und Handlungsbedarf*: University of Duisburg-Essen, VGB research project P428. Available at: https://www.vgb.org/fue_projekt428.html.
- [13] Hofmann, R., Kasper, L., Bacher, T., & Birkelbach, F. (2020b). *DIGI STEAM – Digitalization in the energy sector: Identification of digitalization possibilities in the energy sector especially in the field of steam supply systems*: TU Wien, VGB research project P429. Available at: https://www.vgb.org/fue_projekt429.html.
- [14] Kemmerich, M., & Storch, H. (2016). *Process heat recovery and digitalisation in sulphuric acid plants*. Procedia Engineering, 138, 220-230. <https://doi.org/10.1016/j.proeng.2016.02.079>.
- [15] Bogner, E., Voelklein, T., Schroedel, O., & Franke, J. (2016). *Study Based Analysis on the Current Digitalization Degree in the Manufacturing Industry in Germany*. Procedia CIRP, 57, 14-19. <https://doi.org/10.1016/j.procir.2016.11.004>.
- [16] Zheng, P., Wang, Z., Chen, C.-H., & Pheng Khoo, L. (2019). *A survey of smart product-service systems: Key aspects, challenges and future perspectives*. Advanced Engineering Informatics, 42, 100973. <https://doi.org/10.1016/j.aei.2019.100973>.
- [17] Manzei, C., Schlepuner, L., & Heinze, R. (2016). *Industrie 4.0 im internationalen Kontext Kernkonzepte, Ergebnisse, Trends: Industrie 4.0 im internationalen Kontext Kernkonzepte, Ergebnisse, Trends*: VDE Verlag GmbH Beuth.
- [18] Rehtanz, C. (2015). *Energie 4.0 – Die Zukunft des elektrischen Energiesystems durch Digitalisierung*. Informatik-Spektrum, 38, 16-21. <https://doi.org/10.1007/s00287-014-0855-8>.
- [19] Zhang, F., Liu, M., Zhou, Z., & Shen, W. (2016). *An IoT-Based Online Monitoring System for Continuous Steel Casting*. IEEE Internet of Things Journal, 3, 1355-1363. <https://doi.org/10.1109/JIOT.2016.2600630>.
- [20] Cheng, J., Zhang, H., Tao, F., & Juang, C.-F. (2020). *DT-II: Digital twin enhanced Industrial Internet reference framework towards smart manufacturing*. Robotics and Computer-Integrated Manufacturing, 62, 101881. <https://doi.org/10.1016/j.rcim.2019.101881>.
- [21] Cheng, G., Liu, L., Qiang, X. & Liu, Y. (2016). *Industry 4.0 Development and Application of Intelligent Manufacturing*. In 2016 International Conference on Information System and Artificial Intelligence (ISAI) (pp. 407-410). <https://doi.org/10.1109/ISAI.2016.0092>.
- [22] Negri, E., Fumagalli, L., & Macchi, M. (2017). *A Review of the Roles of Digital Twin in CPS-based Production Systems*. Procedia Manufacturing, 11, 939-948. <https://doi.org/10.1016/j.promfg.2017.07.198>.
- [23] Iqbal, R., Doctor, F., More, B., Mahmud, S., & Yousuf, U. (2017). *Big Data analytics and Computational Intelligence for Cyber-Physical Systems: Recent trends and state of the art applications*. Future Generation Computer Systems. <https://doi.org/10.1016/j.future.2017.10.021>.
- [24] Chang, V. (2015). *Towards a Big Data system disaster recovery in a Private Cloud*. Ad Hoc Networks, 35, 65-82. <https://doi.org/10.1016/j.adhoc.2015.07.012>.
- [25] Qi, Q., & Tao, F. (2018). *Digital Twin and Big Data Towards Smart Manufacturing and Industry 4.0: 360 Degree Comparison*. Ieee Access, 6, 35853593. <https://doi.org/10.1109/ACCESS.2018.2793265>.
- [26] Kabugo, J.C., Jämsä-Jounela, S.-L., Schiemann, R., & Binder, C. (2020). *Industry 4.0 based process data analytics platform: A waste-to-energy plant case study*. International Journal of Electrical Power & Energy Systems, 115, 105508. <https://doi.org/10.1016/j.ijepes.2019.105508>.
- [27] Shang, C., Yang, F., Huang, D., & Lyu, W. (2014). *Data-driven soft sensor development based on deep learning technique*. Journal of Process Control, 24, 223-233. <https://doi.org/10.1016/j.jprocont.2014.01.012>.
- [28] Liu, Y., Fan, Y., & Chen, J. (2017). *Flame Images for Oxygen Content Prediction of Combustion Systems Using DBN*. Energy & Fuels, 31, 8776-8783. <https://doi.org/10.1021/acs.energyfuels.7b00576>.
- [29] Boschert, S., & Rosen, R. (2016). *Digital Twin-The Simulation Aspect*. In Hehenberger, P. & Bradley, D. (Eds.), Mechatronic Futures: Challenges and Solutions for Mechatronic Systems and their Designers (pp. 59-74). Cham: Springer International Publishing. https://doi.org/10.1007/978-3-319-32156-1_5.
- [30] Fraunhofer-Gesellschaft (2018): *Maschinelles Lernen. Eine Analyse zu Kompetenzen, Forschung und Anwendung (2020)*. <http://publica.fraunhofer.de/dokumente/N-497408.html>.
- [31] Kagermann, H., Wahlster, W., & Helbig, J. (2013). *Securing the future of German manufacturing industry*. Recommendations for implementing the strategic initiative INDUSTRIE, 4, 14.
- [32] Iordache, O. (2017). *Implementing Polytope Projects for Smart Systems*. Studies in Systems, Decision and Control, v.92. Cham: Springer International Publishing. <https://doi.org/10.1007/978-3-319-52551-8>.
- [33] CEN-CENELEC-ETSI Smart Grid Coordination Group (2012). *Smart Grid Reference Architecture*. https://ec.europa.eu/energy/sites/ener/files/documents/xpert_group1_reference_architecture.pdf.
- [34] Adolphs, P., Bedenbender, H., Dirzuz, D., Ehlich, M., Eppe, U., & Hankel, M. et al. (2015). *Reference architecture model industrie 4.0 (rami4.0)*. ZVEI and VDI, Status report.
- [35] Döbrich, U., Hankel, M., Heidel, R., Hoffmeister, M., & e. V. D. I. N. (2017). *Basiswissen RAMI 4.0 Referenzarchitekturmodell und Industrie 4.0-Komponente Industrie 4.0*. Berlin, GERMANY: Beuth Verlag.
- [36] Pauker, F. (2019). *OPC UA Information Model Design OPC UA Informationsmodellierung für Cyber-Physical Production Systems*. OPC UA Information Model Design – Information Modelling for Cyber-Physical Production Systems. Wien: Wien.
- [37] Steindl, G., Heinzl, B., & Kastner, W. (2019a). *A Novel Ontology-Based Smart Service Architecture for Data-Driven Model Development: in eKNOW 2019 – The Eleventh International Conference on Information, Process, and Knowledge Management, 26-27*.
- [38] Scharl, S., & Praktijnjo, A. (2019). *The Role of a Digital Industry 4.0 in a Renewable Energy System*. International Journal of Energy Research, 43, 3891-3904. <https://doi.org/10.1002/er.4462>.
- [39] Frysak, J., Kaar, C., & Stary, C. (2018 - 2018). *Benefits and pitfalls applying RAMI4.0*. In 2018 IEEE Industrial Cyber-Physical Systems (ICPS) (pp. 32-37): IEEE. <https://doi.org/10.1109/IC-PHYS.2018.8387633>.
- [40] Kuhn, T. (2017). *Digitaler Zwilling*. Informatik-Spektrum, 40, 440-444. <https://doi.org/10.1007/s00287-017-1061-2>.
- [41] Kamel, E., & Memari, A.M. (2019). *Review of BIM's application in energy simulation: Tools, issues, and solutions*. Automation in Construction, 97, 164-180. <https://doi.org/10.1016/j.autcon.2018.11.008>.
- [42] Glaessgen, E.H., & Stargel, D.S. (2012). *The digital twin paradigm for future NASA and U.S. air force vehicles*. In Astronautics (Ed.). <https://doi.org/10.2514/6.2012-1818>.
- [43] Kritzinger, W., Karner, M., Traar, G., Henjes, J., & Sihn, W. (2018). *Digital Twin in manufacturing: A categorical literature review and classification*. IFAC-PapersOnLine, 51, 1016-1022. <https://doi.org/10.1016/j.ifacol.2018.08.474>.
- [44] Tuegel, E.J., Ingraffea, A.R., Eason, T.G., & Spottswood, S.M. (2011). *Reengineering Aircraft Structural Life Prediction Using a Digital Twin*. International Journal of Aerospace Engineering, 2011, 1-14. <https://doi.org/10.1155/2011/154798>.
- [45] Tao, F., Zhang, M., & Nee, A. Y. C. (2019a). *Digital Twin Driven Smart Manufacturing:*

- Academic Press. <https://doi.org/10.1016/C2018-0-02206-9>.
- [46] Modoni, G.E., Caldarella, E.G., Sacco, M., & Terkaj, W. (2019). *Synchronizing physical and digital factory: benefits and technical challenges*. *Procedia CIRP*, 79, 472-477. <https://doi.org/10.1016/j.procir.2019.02.125>.
- [47] Tao, F., Zhan, H., Liu, A., & Nee, A.Y.C. (2019b). *Digital Twin in Industry: State-of-the-Art*. *Ieee Transactions on Industrial Informatics*, 15, 2405-2415. <https://doi.org/10.1109/tii.2018.2873186>.
- [48] Grieves, M. (2014). *Digital twin: Manufacturing excellence through virtual factory replication*. White paper, 1-7.
- [49] Tao, F., Zhang, M., & Nee, A.Y.C. (2019c). *Chapter 3 – Five-Dimension Digital Twin Modeling and Its Key Technologies*. In Tao, F., Zhang, M. & Nee, A.Y.C. (Eds.), *Digital Twin Driven Smart Manufacturing* (pp. 63-81). Academic Press. <https://doi.org/10.1016/B978-0-12-817630-6.00003-5>.
- [50] Tao, F., Zhang, M., Liu, Y., & Nee, A.Y.C. (2018). *Digital twin driven prognostics and health management for complex equipment*. *CIRP Annals*, 67, 169-172. <https://doi.org/10.1016/j.cirp.2018.04.055>.
- [51] Tao, F., & Zhang, M. (2017). *Digital Twin Shop-Floor: A New Shop-Floor Paradigm Towards Smart Manufacturing*. *Ieee Access*, 5, 20418-20427. <https://doi.org/10.1109/access.2017.2756069>.
- [52] Josifovska, K., Yigitbas, E., & Engels, G. (2019). *Reference Framework for Digital Twins within Cyber-Physical Systems*. In (pp. 25-31): Institute of Electrical and Electronics Engineers Inc. <https://doi.org/10.1109/SEsCPS.2019.00012>.
- [53] Duan, B., Umeda, K., Hwang, W., Hu, C., Gao, W., & Xu, C., et al. (Eds.) (2020). *Study on the application of digital twin technology in complex electronic equipment*: 7th Asia International Symposium on Mechatronics, AISM 2019, 589: Springer Verlag.
- [54] Wittenburg, R., Hübel, M., Prause, H., Gierow, C., Reißig, M., & Hassel, E. (2019). *Effects of rising dynamic requirements on the lifetime consumption of a combined cycle gas turbine power plant*. *Energy Procedia*, 158, 5717-5723. <https://doi.org/10.1016/j.egypro.2019.01.562>.
- [55] Yun, S., Park, J.H., & Kim, W.T. (2017). *Data-centric middleware based digital twin platform for dependable cyber-physical systems*. In S. Information (Ed.) (pp. 922-926): IEEE Computer Society. <https://doi.org/10.1109/ICUFN.2017.7993933>.
- [56] Kabugo, J.C., Jämsä-Jounela, S., Schiemann, R., & Binder, C. (2019). *Process Monitoring Platform based on Industry 4.0 tools: a waste-to-energy plant case study*. In (pp. 264-269). <https://doi.org/10.1109/SYSTOL.2019.8864766>.
- [57] Souza, V., Cruz, R., Silva, W., Lins, S., & Lucena, V. (2019). *A Digital Twin Architecture Based on the Industrial Internet of Things Technologies*. In 2019 IEEE International Conference on Consumer Electronics (ICCE 2019): Las Vegas, Nevada, USA, 11-13 January 2019 (pp. 1-2). Piscataway, NJ: IEEE. <https://doi.org/10.1109/ICCE.2019.8662081>.
- [58] Hofmann, R., Halmeschlager, V., Koller, M., Scharinger-Urschitz, G., Birkelbach, F., & Walter, H. (2019). *Comparison of a physical and a data-driven model of a Packed Bed Regenerator for industrial applications*. *Journal of Energy Storage*, 23, 558-578. <https://doi.org/10.1016/j.est.2019.04.015>.
- [59] Qi, Q., Tao, F., Hu, T., Anwer, N., Liu, A., & Wei, Y. et al. (2019). *Enabling technologies and tools for digital twin*. *Journal of Manufacturing Systems*. <https://doi.org/10.1016/j.jmsy.2019.10.001>.
- [60] Andryushkevich, S.K., Kovalyov, S.P., & Nefedov, E. (2019-2019). *Composition and Application of Power System Digital Twins Based on Ontological Modeling*. In 2019 IEEE 17th International Conference on Industrial Informatics (INDIN) (pp. 1536-1542): IEEE. <https://doi.org/10.1109/INDIN41052.2019.8972267>.
- [61] Steindl, G., Frühwirth, T., & Kastner, W. (2019b). *Ontology-Based OPC UA Data Access via Custom Property Functions*. In (pp. 95-101). <https://doi.org/10.1109/ETFA.2019.8869436>.
- [62] Negri, E., Fumagalli, L., Garetti, M., & Tanca, L. (2016). *Requirements and languages for the semantic representation of manufacturing systems*. *Computers in Industry*, 81, 55-66. <https://doi.org/10.1016/j.compind.2015.10.009>.
- [63] Garetti, M., Fumagalli, L., & Negri, E. (2015). *Role of Ontologies for CPS Implementation in Manufacturing*. *Management and Production Engineering Review*, 6, 26-32. <https://doi.org/10.1515/mper-2015-0033>.
- [64] Borgo, S. (2014). *An ontological approach for reliable data integration in the industrial domain*. *Computers in Industry*, 65, 1242-1252. <https://doi.org/10.1016/j.compind.2013.12.010>.
- [65] Tao, F., & Qi, Q. (2019). *New IT Driven Service-Oriented Smart Manufacturing: Framework and Characteristics*. *IEEE Transactions on Systems, Man, and Cybernetics: Systems*, 49, 81-91. <https://doi.org/10.1109/TSMC.2017.2723764>.
- [66] Jones, D., Snider, C., Nassehi, A., Yon, J., & Hicks, B. (2020). *Characterising the Digital Twin: A systematic literature review*. *CIRP Journal of Manufacturing Science and Technology*, 29, 36-52. <https://doi.org/10.1016/j.cirpj.2020.02.002>.
- [67] Padovano, A., Longo, F., Nicoletti, L., & Mirabelli, G. (2018). *A Digital Twin based Service Oriented Application for a 4.0 Knowledge Navigation in the Smart Factory*. *IFAC-PapersOnLine*, 51, 631-636. <https://doi.org/10.1016/j.ifacol.2018.08.389>.
- [68] Koschnick, G. (2020). *Industrie 4.0: Smart Services*. *ZVEI – Zentralverband Elektrotechnik- und Elektronikindustrie e.V.*, Frankfurt am Main.
- [69] Bauer, T., Antonino, P.O., & Kuhn, T. (2019). *Towards Architecting Digital Twin-Permeated Systems*. In (pp. 66-69). <https://doi.org/10.1109/SESOS/WDES.2019.00018>.
- [70] Yao, X., Zhou, J., Zhang, C., & Liu, M. (2017). *Proactive manufacturing-a big-data driven emerging manufacturing paradigm*. *Computer Integrated Manufacturing Systems*, 23, 172-185.
- [71] Beckmann, M., & Rostkowski, S. (2010). *Optimierung von Biomasse- und Abfallverbrennungsanlagen durch Monitoring*. In Thomé-Kozmiensky, K.J. & Beckmann, M. (Eds.), *Energie aus Abfall – Band 7* (pp. 3-18). Neuruppin: TK Verlag Karl Thomé-Kozmiensky.
- [72] Kortela, J., & Jämsä-Jounela, S.L. (2012). *Fuel-quality soft sensor using the dynamic superheater model for control strategy improvement of the BioPower 5 CHP plant*. *International Journal of Electrical Power & Energy Systems*, 42, 38-48. <https://doi.org/10.1016/j.ijepes.2012.03.001>.
- [73] VGB Richtlinie: 3. Auflage, 2019, VGB-S-506-R-00;2012-03.DE. (3.Auflage 2019): VGB Powertech.
- [74] Macek, K., Endel, P., Cauchi, N., & Abate, A. (2017). *Long-term predictive maintenance: A study of optimal cleaning of biomass boilers*. *Energy and Buildings*, 150, 111-117. <https://doi.org/10.1016/j.enbuild.2017.05.055>.
- [75] Pattanayak, L., Ayyagari, S.P.K., & Sahu, J. N. (2015). *Optimization of sootblowing frequency to improve boiler performance and reduce combustion pollution*. *Clean Technologies and Environmental Policy*, 17, 1897-1906. <https://doi.org/10.1007/s10098-015-0906-0>.
- [76] Romeo, L.M., & Garetta, R. (2009). *Fouling control in biomass boilers*. *Biomass and Bioenergy*, 33, 854-861. <https://doi.org/10.1016/j.biombioe.2009.01.008>.
- [77] Tang, S.-Z., Li, M.-J., Wang, F.-L., He, Y.-L., & Tao, W.-Q. (2020). *Fouling potential prediction and multi-objective optimization of a flue gas heat exchanger using neural networks and genetic algorithms*. *International Journal of Heat and Mass Transfer*, 152, 119488. <https://doi.org/10.1016/j.ijheatmasstransfer.2020.119488>.
- [78] Khan, S., & Yairi, T. (2018). *A review on the application of deep learning in system health management*. *Mechanical Systems and Signal Processing*, 107, 241-265. <https://doi.org/10.1016/j.ymssp.2017.11.024>.



Paper 4

Toward a Practical Digital Twin Platform Tailored to the Requirements of Industrial Energy Systems

published in Applied Sciences in collaboration with Felix Birkelbach, Paul Schwarzmayr, Gernot Steindl, Daniel Ramsauer, and René Hofmann

This journal paper investigated research question *RQ 2.2*. Based on a detailed literature review, the most crucial barriers impeding DT development in the energy sector were assessed and the requirements for DT implementation in industrial energy systems were identified. Furthermore, the paper reviewed common DT architectures and standardization aspects. Equipped with this knowledge, a DT platform tailored to the identified requirements was developed. The five-dimensional modeling concept was used as a fundamental pattern and the data architecture of the platform is aligned with the generic DT architecture developed in co-author publication D. To facilitate the implementation of the platform, particular implementation issues were addressed, and universal, yet specific, approaches for resolving these issues were proposed. The goal of this work was to pave the way for easy but standardized DT implementation in the energy sector with efficient encapsulation of DT service engineering for domain experts. The DT platform was later instantiated for a TES and equipped with various services, see Paper F and Paper 5. Furthermore, since its publication, the DT platform also found application in Hydropower (see, Tubeuf et al. 2023).


My contribution: Conceptualization, Methodology, Investigation, Formal Analysis, Writing – Original Draft & Editing, Visualization

L. Kasper, F. Birkelbach, P. Schwarzmayr, G. Steindl, D. Ramsauer & R. Hofmann (2022). "Toward a Practical Digital Twin Platform Tailored to the Requirements of Industrial Energy Systems". In: Applied Sciences 12.14. Section "Energy Science and Technology". Special Issue "Industry 4.0 Technologies Supporting the Energy Transition". ISSN: 2076-3417.

DOI: 10.3390/app12146981

Article

Toward a Practical Digital Twin Platform Tailored to the Requirements of Industrial Energy Systems

Lukas Kasper ^{1,*} , Felix Birkelbach ¹ , Paul Schwarzmayr ¹ , Gernot Steindl ² , Daniel Ramsauer ² 
and René Hofmann ¹ 

¹ Institute of Energy Systems and Thermodynamics, TU Wien, Getreidemarkt 9/BA/E302, A-1060 Vienna, Austria; felix.birkelbach@tuwien.ac.at (F.B.); paul.schwarzmayr@tuwien.ac.at (P.S.); rene.hofmann@tuwien.ac.at (R.H.)

² Institute of Computer Engineering, TU Wien, Treitlstrasse 3, A-1040 Vienna, Austria; gernot.steindl@tuwien.ac.at (G.S.); daniel.ramsauer@tuwien.ac.at (D.R.)

* Correspondence: lukas.kasper@tuwien.ac.at; Tel.: +43-1-58801-302319

Abstract: Digitalization and concepts such as digital twins (DT) are expected to have huge potential to improve efficiency in industry, in particular, in the energy sector. Although the number and maturity of DT concepts is increasing, there is still no standardized framework available for the implementation of DTs for industrial energy systems (IES). On the one hand, most proposals focus on the conceptual side of components and leave most implementation details unaddressed. Specific implementations, on the other hand, rarely follow recognized reference architectures and standards. Furthermore, most related work on DTs is done in manufacturing, which differs from DTs in energy systems in various aspects, regarding, for example, multiple time-scales, strong nonlinearities and uncertainties. In the present work, we identify the most important requirements for DTs of IES. We propose a DT platform based on the five-dimensional DT modeling concept with a low level of abstraction that is tailored to the identified requirements. We address current technical implementation barriers and provide practical solutions for them. Our work should pave the way to standardized DT platforms and the efficient encapsulation of DT service engineering by domain experts. Thus, DTs could be easy to implement in various IES-related use cases, host any desired models and services, and help get the most out of the individual applications. This ultimately helps bridge the interdisciplinary gap between the latest research on DTs in the domain of computer science and industrial automation and the actual implementation and value creation in the traditional energy sector.

Keywords: industrial energy systems; integrated energy systems; digital twin platform; digital twin requirements; service engineering; service-oriented architecture



Citation: Kasper, L.; Birkelbach, F.; Schwarzmayr, P.; Steindl, G.; Ramsauer, D.; Hofmann, R. Toward a Practical Digital Twin Platform Tailored to the Requirements of Industrial Energy Systems. *Appl. Sci.* **2022**, *12*, 6981. <https://doi.org/10.3390/app12146981>

Academic Editors: Stefano Rinaldi, Marco Pasetti and Beatrice Marchi

Received: 12 June 2022

Accepted: 8 July 2022

Published: 10 July 2022

Publisher's Note: MDPI stays neutral with regard to jurisdictional claims in published maps and institutional affiliations.



Copyright: © 2022 by the authors. Licensee MDPI, Basel, Switzerland. This article is an open access article distributed under the terms and conditions of the Creative Commons Attribution (CC BY) license (<https://creativecommons.org/licenses/by/4.0/>).

1. Introduction

The mitigation of climate change and environmental damage due to industrial activity are regarded as some of the most pressing issues that society faces today [1]. Consequently, decarbonization and sustainable production are high-priority goals that also have huge implications for the present and the future of energy systems. There are two concurrent transformations with the common goal to make energy systems more efficient: the shift toward integrated energy systems and digitalization. Both of these transitions can mutually benefit from each other [2] since they share essential characteristics, both being highly influenced by technological innovations [3].

The key characteristics of integrated energy systems are that they utilize a high share of energy produced by intermittent renewable sources, high energy-efficient systems, and strong integration of electricity, gas, heating/cooling, mobility systems, and markets to maximize the synergies among new technical solutions [4]. The transition toward integrated energy systems is also eminent within industrial energy systems (IES), where renewable energy sources are gradually replacing fossil sources in an attempt to reduce greenhouse

gas emissions. Although this transition is supported by policies [5], implementation and even more so the operation of such systems confronts us with serious challenges. The interconnection between different sectors and stakeholders, diversity of demands and technology, numerous sources of uncertainty and large scales to consider require novel approaches from various disciplines.

The digitalization of IES is driven by the rapid development of information and communication technologies. This paradigm shift is often referred to as the fourth industrial revolution or Industry 4.0 [6]. While there is justified concern that digitalization could increase energy consumption due to subsequent rebound effects and economic growth [7], there is undoubtedly an immense potential for digitalization and Industry 4.0 to reduce energy consumption and increase economic sustainability [8]. To realize this potential, various applications based on novel digital technologies have been proposed such as forecasting, demand response, operational and design optimization, fault prediction and predictive maintenance, to name just a few. However, today, all these digital applications are usually considered individually. By integrating these solutions into a collaborative platform, their impact could be even more significant.

To realize the visions of Industry 4.0 and smart, sustainable integrated energy systems, the digital twin (DT) is considered one of the most promising concepts [9]. DTs are the key enabler for integrating the solutions mentioned in the previous paragraph [10]. DTs in the energy sector can thus fundamentally change the way IES operate, minimize energy consumption and increase the integration of renewable energy sources [11].

However, the concepts and capabilities of DTs are not yet clearly defined and still vigorously debated in contemporary scientific literature. So far, a unified DT platform has not been established but is considered to be direly needed [9]. Furthermore, most work on DTs has focused on the manufacturing domain [12,13], which differs from the domain of energy systems in various aspects.

Tao et al. [9] state that the history of DTs is rather brief and that the concept was first introduced as early as 2003 by Grieves in the context of product lifecycle management [14]. The first actual definition of a DT was given by NASA in 2012 [15]. To date, various definitions have arisen and are still the subject of discussion in the literature [16]. Negri et al. [17] and Liu et al. [18] even presented tables of 16 and 21 separate definitions of the DT, which they found in the literature. The basic characteristics given by NASA [15] are still aligned with the refined definition given by Negri et al. [17] and reported by Cimino et al. [16] and Kritzing et al. [19]: *“The DT consists of a virtual representation of a production system that is able to run on different simulation disciplines that is characterized by the synchronization between the virtual and real system, thanks to sensed data and connected smart devices, mathematical models and real time data elaboration”*. Most definitions, such as this one, are tailored to *production systems*, which hints at the origin of DTs in the manufacturing domain. For a more general understanding, we can break down the definition to the term physical object [20] or physical entity [21]. Josifovska et al. [21] define a physical entity as an abstraction of a “thing” persisting in the real world which has to be mirrored or twinned in the virtual world. In this framing, the definition by Negri et al. [17] is suited for industrial energy systems, where the physical entity of a considered DT can be a single process unit or even part of that unit but also a whole energy system including boundary conditions (e.g., external energy supply systems/grids). Therefore, this is the definition that we adhere to. It is important to note the difference in the level of data integration between mere digital models of a physical entity and a full DT, which was most prominently discussed by Kritzing et al. [19]. While DTs are using digital models to dynamically simulate the physical entity and thus can build on the same principles, their key feature is bidirectional automated data exchange, i.e., synchronization with the real world. This is where the technical complexity of DT modeling arises. Hence, DT frameworks and practical platforms are needed to allow for the strict synchronization of digital models with their physical entities and to enable additional functionalities compared to a mere model.

Although the number and maturity of DT concepts is increasing, there is still no uniform platform available for the practical implementation of a DT [18]. Most proposals focus on the conceptual side, maintaining a high level of abstraction and leaving important implementation details unaddressed [22]. Concrete DT implementations, on the other hand, are mostly realized with a specific application in mind without any architectural template [21] or only offer a limited set of services [16], hence not reaching the full potential. Thus, there is still a significant gap in DT research regarding how to offer a higher number of services in the same environment to support complex decision making [16]. Missing architectural guidelines result in application-specific solutions which are barely reusable, hence increasing development time and maintenance costs [22].

After its origin in the aerospace industry [15,23], the DT was widely announced following Grieves' Whitepaper [14] in 2014 [24]. Only then did the DT topic find its way into other sectors, such as automotive, oil and gas [25], and healthcare and medicine [26] and was driven forward massively in (discrete) manufacturing, which is apparent by the distribution of DT applications analyzed in Jones et al. [12], Negri et al. [17], and also Melesse et al. [13]. In recent years, the DT was also explored in the context of chemical process engineering [27] and the food industry [28]. In the domain of energy systems, DTs are notably represented in the domain of electric power systems [29] and especially in the context of smart grids [30] and battery management [31]. Other examples include DTs for decision making in energy system design [32] and, during operation, the application of DTs for wind turbines [33] and for scheduling [34] and state estimation [35], to name just a few. Only recently, the transfer of the DT concept to thermal IES has begun [36,37]. For a complete overview of existing DT research and industrial application, we refer interested readers to the current literature review by Liu et al. [18].

1.1. Scope of This Paper

Even though both industry and academia ascribe huge potential to DTs in IES, their use in this domain is lagging behind other sectors, most notably the manufacturing sector [12], which differs from DT research in energy systems in various aspects. A relatively low number of papers can be found in the literature addressing DTs in the energy domain [38]. In a current literature review by Kaiblinger et al. [39], only 5 % of evaluated DT case studies could be attributed to the energy domain, which is inline with the findings of Yu et al. [11] and Sleiti et al. [37]. Regarding application scenarios, DTs are mostly represented in the area of prognostics and health management, while Tao et al. [9] found that the areas of DTs in dispatching optimization and operational control are currently underexplored but very promising.

Based on the past evolution and current difficulties in DT development outlined above, we focused our research on a tangible implementation of a DT platform for IES. In this paper, we

- identify the most important requirements on DT of IES,
- propose a DT platform tailored to these requirements in line with current standardization developments,
- address essential architecture and implementation challenges,
- solve technical implementation barriers by providing practical solutions, and,
- highlight the advantages of service engineering on this DT platform.

Ultimately, our work aims to bridge the gap between the latest research on DTs in the domain of computer science and practical deployment in the energy sector. The proposed DT platform should pave the way to standardized DT implementations with service encapsulation and thus efficient DT service engineering. In this way, DTs will be easy to implement in various cases related to energy systems and be capable of hosting various complex models and services fulfilling different application purposes.

1.2. Paper Structure

After this introduction into the topic, we elaborate on specific features and requirements of energy systems and the need for an appropriate DT platform in Section 2. We also compare the most relevant DT concepts and architectures. We will show that none of the existing implementations is a good match for IES but that the five-dimensional (5D) DT concept is feasible despite its high level of abstraction. In Section 3, we propose concrete solutions to fill in the blanks in the 5D-DT concept and overcome implementation barriers, thus creating a practical DT platform. We highlight the capabilities and benefits and critically discuss the proposed DT platform with regard to the specific requirements of IES as well as emphasizing the potential of service engineering in Section 4.

2. State of the Art

Considering that the typical claim of DT platforms is that they are universal, i.e., that they are not just applicable for the specific system that they were developed for, but that they are transferable to any physical entity, the scarce use of DTs in the energy domain compared to the manufacturing domain appears unjustified. This disparity cannot be explained by the DT's historical evolution alone. There must also be a number of distinct differences that distinguish manufacturing and energy systems. We thus argue that the unique requirements of energy systems have to be considered for the successful development of a DT platform.

2.1. Characteristics of Industrial Energy Systems

As a typical use case for a DT platform in this domain, we consider an exemplary industrial energy system, as illustrated in Figure 1. It is composed of a conventional combined heat and power unit, electrically powered heating units and internal renewables based on photovoltaics for electric and thermal energy supply. A number of production processes typically account for electric and thermal energy demand. Heat exchanger networks and heat pumps are used for waste heat recovery. Electrical and thermal energy storage components are employed to provide additional flexibility and improve the energy efficiency enhancement of the IES. Furthermore, the IES is not isolated but instead coupled with both the electricity grid and a district heating/cooling network.

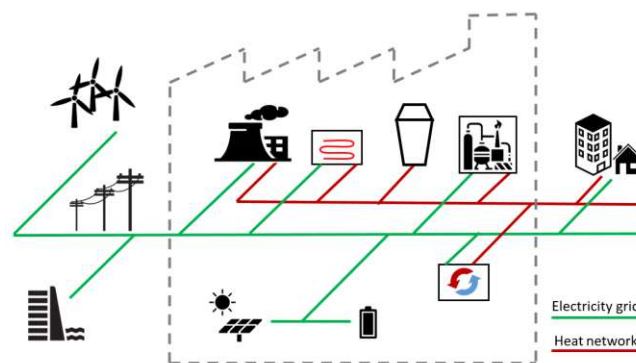


Figure 1. Sketch of the target use case: a typical industrial energy system.

Such an IES is a complex integrated energy system that has a number of characteristics that set it apart from typical manufacturing systems:

- Many sources of uncertainty such as weather influences, prices on the energy market and stochastic processes within the system itself make the optimal operation of an IES challenging.
- Energy system units feature complex thermophysical behaviors, hence leading to strong nonlinearities in mathematical model descriptions.

- Energy systems are often vast and distributed systems with specialized equipment.
- Power plants as well as industrial and urban energy systems have very long lifetimes or are even continuously refurbished instead of being rebuilt. Thus, “off the shelf” solutions have a limited field of applications.
- Energy systems are very dynamic systems with a broad range of operational time scales.
- Some process quantities cannot be measured directly, e.g., due to high temperatures or abrasive conditions.
- System properties change over time, e.g., the efficiency of a unit can change due to wear, while the mechanical resistance of a system can degrade due to fatigue.
- Energy systems consist of continuous processes as opposed to processes with discrete units in manufacturing; hence, scalar and vector fields instead of single values are used to describe the system.
- Given their critical nature within the power grid infrastructure, cyber attacks targeting IES have potential for disastrous consequences.

All of these aspects more or less differentiate from manufacturing systems and can be considered specific features of IES, thus contributing to the fact that DTs are underdeveloped in the energy sector. We deduce that these characteristics explain why DT frameworks that have been applied successfully in the manufacturing domain have not been extensively transferred to the energy domain yet. One way or another, if DTs are to be widely deployed in the energy sector, these specific properties must be properly considered.

2.2. Digitalization Developments and Opportunities in Industrial Energy Systems

Technical developments such as Internet of Things (IoT) technologies and the growing data acquisition in energy systems have resulted in new challenges and opportunities for energy systems [40]. Digital innovations have the potential to trigger significant changes in the energy sector in the near future [41]. For example, the increasing maturity of machine learning approaches enables applications to improve the accuracy of demand, generation, and price forecasting [40]. Various other solutions have been proposed, such as intelligent energy management [42], demand response [43], operational optimization [44] and design optimization [45], fault prediction [46] as well as preventive and predictive maintenance for energy efficiency [47] and to extend the lifespan of machinery [48]. In the area of battery management, IoT and data science technologies enable numerous solutions to optimize battery manufacturing, operation and re-utilization [49].

Existing DT concepts and implementations in the energy sector aim to provide at least one specific solution. In a recent study by Wang et al. [50], targeting energy neighborhood applications emphasized the use of DT in energy storage use cases, which are equally important in IES. The estimation of stage of charge and aging state of storage devices as well as the cloud-based interconnection of multiple units to enhance computational abilities and overall operation management were highlighted. A recent summary of the modest amount of DT development in the area of power generation was given by Sleiti et al. [37], including electricity generation, power distribution, the renewable and nuclear power industry, and the energy vehicle and storage sector. They concluded that while the energy industry is actively pursuing the tremendous opportunities of DT, most articles did not include details on the comprehensiveness of their DTs or details on the used models and enabling technologies. Furthermore, the scope of implementations is mostly very limited to specific applications scenarios.

Weigel et al. [41] provided a structured overview of digital applications in the German energy sector, and Ardebili et al. [51] listed the most frequent application scenarios for DTs in smart energy systems based on a systematic literature review. Furthermore, Yu et al. [11] recently derived a structured list of DT applications in the process and energy industry from the literature. Grouped into three lifecycle phases, these included [11]: virtual testing [52] and design optimization [53] in the Designing phase, process optimization [54], prediction [55], monitoring [56] and training [57] as well as production control [58] in the processing phase

and fault detection and diagnosis [59] in the service phase. Based on these studies, we deduced a list of application categories which we consider most relevant for industrial energy systems from a technical perspective (see Table 1).

Table 1. Most relevant technical categories of digital applications considered for value creation during operation of industrial energy systems. For an in-depth review, we refer to [11,41,51].

ID	Application
A1	Condition monitoring
A2	Anomaly/deviation detection
A3	Fault classification and analysis
A4	Predictive maintenance
A5	Forecasting
A6	Operational optimization

The condition monitoring (A1) of physical components by analyzing measurement data is crucial to guarantee the optimal and safe operation of energy systems [33]. Furthermore, condition monitoring via models and “soft sensors” can facilitate this process, especially in harsh environments and for quantities that cannot be directly measured. On top of monitoring, anomaly or deviation detection (A2) aims to detect deviations between the expected and observed behavior of physical components, which is often via the use of simulation models. The application of fault classification (A3) is typically designated to identify the type and cause of detected anomalies or errors and sometimes also to predict future fault scenarios. Predictive maintenance (A4) aims to predict and extend the remaining useful lifetime of machinery to determine an optimal maintenance schedule. Forecasting (A5) of energy demand, prices and environmental conditions becomes increasingly relevant and also more feasible by using historical and external data and advanced analytic methods. The operational optimization (A6) and control of IES generally aims to decide on optimal operating points and scheduling in order to minimize energy consumption or overall costs. We consider the leveraging and marketing of demand flexibility also within this category, although it is sometimes known as demand-side management, since it is generally based on very similar methods and merely considers different operational variables, constraints and external information sources.

Weigel et al. [41] derived the benefits of such digital applications from the literature, which were allocated into six clusters: (1) system stability, (2) environmental protection, (3) energy demand reduction, (4) revenue increase, (5) cost reduction and (6) customer expectations. These benefits are based on the potential of individual applications, i.e., to automate and improve efficiency in processes and optimize the operation and maintenance of systems but also on digitalization’s potential to create interacting networks, increase transparency and improve convenience [41]. While some of these categories clearly show some correlation with each other, cost reduction is inherently covered in all of them. Yu et al. [11] evaluated the main driving benefits for DT adoption in the energy sector from the literature as energy efficiency, profit, decarbonization, throughput, quality and safety.

To enable individual digital applications and thus leverage the benefits ascribed to them, various methodical approaches were already successfully developed. However, although many of these solutions have been deployed in all energy value stream steps, the value stream itself has remained mostly unchanged [60]. A major problem today is that all these solutions are usually considered individually. By integrating them into a collaborative platform, their impact could be much more significant, and future development and software maintenance effort could be reduced. The DT is considered as such a platform that can host a large number of services in a single environment [16]. These services can either provide specific application purposes on their own [61] or can be loosely coupled with other small software services to build service-oriented applications [22]. This microservice architectural style gains increasing popularity in software development due to its improved scalability and maintainability [62].

The most common services and features of DTs in general have been reviewed by a number of researchers. Tao et al. [61] listed nine main services of DTs in the production sector, while Cimino et al. [16] grouped these in six categories; however, these are specifically tailored to manufacturing systems. Ardebili et al. [51] list the most frequent goals and applications for DTs in the energy sector, and Steindl et al. [63] identified six groups of functional services: simulation services, monitoring services, diagnosis services, prediction services, control services, and reconfiguration services.

2.3. Barriers Impeding Digital Twin Implementation

The distinct features of IES, which we outlined in Section 2.1, present challenges for the implementation of DTs in these systems in addition to general technical barriers. The fact that DTs are relatively scarcely addressed in the literature relating to the energy domain both gives evidence to such challenges and reinforces the underdevelopment of DTs for IES. In that regard, we see the energy domain at a similar stage as the process industry, where similar difficulties led to the fact that little research on DTs has been conducted [64]. This fact is supported by the review from Yu et al. [11], where only 50 papers were retrieved for process or energy DT within a thousand research papers on DTs in general since 2010. Perno et al. [65] recently presented a systematic review of barriers for DT implementation in the process industry. Such barriers are equally present in the energy domain. A summary of the most crucial barriers impeding DT development from a technical perspective is given in Table 2.

Table 2. Most crucial technical barriers impeding DT implementation. We endorse and apply the categories established by Perno et al. [65] for the process industry and provide a summary of topics causing difficulty in the energy domain.

ID	Barrier Category	Challenges
B1	System integration issues	Lack of system integration; Interoperability issues; Legacy systems
B2	Security issues	Data protection; Real-time communication; Robustness
B3	Performance issues	Prediction accuracy; Data volume; Scalability; Flexibility; Standardization
B4	Organizational issues	Fragmented data management; Data availability; Technology investment decisions
B5	Data quality issues	Data validity; Lack of methodologies and tools; Low DT maturity
B6	Environmental issues	Software decisions; High-fidelity modelling; Multi-disciplinarity; Heterogeneity

System integration issues (B1) include interoperability issues and often problems with legacy systems. Fuller et al. [66] stated that such DT challenges fall into the area of IoT and IIoT. DT implementations should thus not only feature a standardized architecture but also a certain flexibility to retrofit existing infrastructure. This is especially critical for IES that feature very long lifetimes.

Security issues (B2) are a barrier that is not necessarily crucial during DT development but during DT deployment. The key enabling technologies for DT must follow the current practices and updates in security and privacy regulations to resolve this barrier [66].

Performance issues (B3) cannot be solved alone by large computational capacities but include aspects of standardization and scalability. Standardization will facilitate the interoperability of new and existing supporting software [37]. Only when standardization is achieved can DT really thrive in the energy sector due to the easy exchange of information and models.

Data quality issues (B5) include the lack of methodologies, low data validity or low DT maturity that results, e.g., in information resulting from DT models that are untrustworthy or incomprehensible. This is crucial in IES, where many sources of uncertainty complicate operation.

Organizational issues (B4) and environmental issues (B6) feature multidisciplinary problems that also needs to be tackled from the area of business management, impeding the fast development of DTs.

Yu et al. [11] stated that DT development in the energy sector is inherently multidisciplinary, including fields such as chemical, mechanical, electrical, civil, software engineering and data science. Additionally, DT operation should ideally be unclosed to non-technical staff and business managers. Thus, further non-technical challenges arise that have to be countervailed by a convenient DT architecture.

For more details on barriers and possible enablers in current DT research, we refer to the reviews of Perno et al. [64,65], Yu et al. [11] and Fuller et al. [66].

2.4. Requirements on Digital Twins in the Energy Sector

Since most DT implementations are realized following a specific goal without any architectural template [21], it is impossible to overcome the implementation barriers given in Section 2.3 in a standardized manner. However, a DT that is tailored to the specific characteristics of IES (i.e., one that meets their requirements) could be an enabler to integrate digital applications on a single platform and thus make IES significantly more efficient. While having mainly different scopes of applications in mind than the energy sector, some researchers directed their research on establishing common focus points in DT development and servitization. Furthermore, they listed requirements they deemed as necessary DT capabilities. These requirements are summarized in the following paragraph and critically reviewed to provide a foundation for our assessment in regard to IES.

Boje et al. [67] highlighted requirements on DTs in the construction sector. Demands for smart factory systems were established in Ref. [68]. Moyné et al. [69] studied DT definitions in manufacturing and clustered them into requirements (1) derived from the literature, (2) derived from DTs in use today, and (3) applications in the near future. Weskamp et al. [70] formulated requirements for the architecture of a knowledge exploration platform of industrial data for integration into digital services. Steindl et al. specified functional and non-functional requirements for a DT service framework derived in a literature review [22] and clustered these requirements based on three RAMI 4.0 layers (information, functional and business). Negri et al. [71] collected requirements for ontological modeling in industrial applications. Tao et al. [72] proposed eight rules for DT modeling, which are, in their original short denomination, (1) data and knowledge based, (2) modularization, (3) light weight, (4) hierarchy, (5) standardization, (6) servitization, (7) openness and scalability, and (8) robustness. Neto et al. [73] summarized and identified four features of digital twins based on the literature, including digital modeling, analytical support, timeliness update and control. Sleiti et al. [37] stated seven requirements for their DT architecture for power plants.

Based on this literature about DT requirements and considering the specific characteristics of IES and technical barriers impeding the DT development outlined in this subsection, we established a set of key requirements for DTs in the energy domain. These requirements are listed in Table 3 together with references that provided motivation for them.

Requirements R1 and R3 express the need for bidirectional automated information exchange between physical and virtual entities, which is considered the most distinctive feature of a DT [19]. Especially for highly dynamic systems, the DT must be capable of informing and warning human operators (R2).

Both requirements R5 and R7 address the issue that the DT must not only provide recommendations for action but to trigger these actions, hence optimizing the operation of IES.

Since IES and their corresponding DTs should be in operation for very long time-spans, IES are continuously evolving; i.e., components are added and environment variables change. Therefore, DTs should be modular (R4), scalable (R6) and build on standardized technologies (R12), thus facilitating the maintenance and continuous development of the DT platform.

Especially in IES, parameters of physical units can change significantly, e.g., due to degradation in harsh conditions. Hence, the DT must be robust in that it can automatically

adapt to behavioral changes (R9). This reinforces also requirement R10, which is a typical DT requirement also in other domains.

Table 3. Requirements of DT platforms for application in IES. The requirements are specified together with an identifier for later reference and with literature sources that provided motivation for them.

ID	Requirement	Source
R1	The DT must be able to observe the physical world in real time via the use of sensors.	[61,67]
R2	The DT must be able to monitor, inform and issue warnings on relevant physical alterations.	[37,67]
R3	The DT must be able to actuate physical components.	[67]
R4	The DT should be designed in a modular fashion.	[61,69,72]
R5	The DT must be able to make decisions and trigger actions on the virtual entity.	[67]
R6	The DT should be open, re-usable, and scalable.	[61,69]
R7	The DT must be able to optimize operation of the physical entity.	[61,67]
R8	The DT must provide interfaces for seamless user interaction.	[70,74]
R9	The DT must be robust and able to provide automatic model adaptation, i.e., for simulating the physical entity.	[69,72]
R10	The DT must be able to predict the behavior of the physical entity based on simulations and sensing.	[61,67,69]
R11	The DT should be able to accommodate simulation models for various applications and in arbitrary fidelity.	[61,67]
R12	The DT should build on standardized technologies and use available metadata, hence facilitating model integration, information exchange and maintenance.	[70,72]
R13	The DT must be able to process heterogeneous data from different sources.	[37,61]
R14	The DT should be able to store data with context information and exchange information in a semantically meaningful way.	[61,69,70]
R15	The DT must allow for safe and secure operation of the physical entity.	[75]

The need for the accommodation of various types of simulation models (R11) is particularly important in IES, where models of both varying fidelity and different physical considerations are applied, e.g., heat transfer, fluid dynamics, mechanical stress and chemical kinetics.

The need for heterogeneous data processing (R13) is crucial in IES, since specific tasks may require data from multiple simulation models, different legacy measurement devices and also input data streams with respect to the surrounding integrated energy system.

Dynamic processes in IES can be very complex, and operation experience is still indispensable. Hence, storing data with context information and exchanging information in a semantically meaningful way (R14) makes a DT a much more powerful tool.

Last but not least, both plant safety procedures and cyber-security concerns should be addressed (R15) in a way that the DT must not impede the safe operation of the physical entity and, ideally, increase the overall security of the energy system.

Even though this list could be extended even further, it should cover the most relevant requirements and provide a solid foundation for evaluating a proper DT platform in the energy domain. Other researchers argued that a DT must deliver quantifiable metrics and ultimately add value in its application area [69]. However, while we share this opinion for DTs in general, we see this not as a necessary consideration for the technical implementation of a DT platform. In addition, lifecycle aspects are often raised. While we do not assign a high value to this topic with regard to IES, we argue that basic requirements for the lifecycle aspect in DTs are already covered by various functional requirements in our list (e.g., R6). For more detailed necessities, e.g., on information technology (IT) infrastructure, service- and model management, we refer to the particular literature presented above, i.e., the work of Weskamp et al. [70], Steindl et al. [22] and Negri et al. [71].

2.5. Digital Twin Architectures

A number of research articles have addressed DT concepts, architectures and platforms in varying levels of abstraction in recent years. Cimino et al. [16] and Semerano et al. [76] broach the issue of DT architectures as part of their respective review papers. However, we could only ascribe four references [51,63,77,78] to the energy domain. While it is

considered an urgent necessity to define standardized DT frameworks, no consensus has been reached [9] yet. This is even more critical for DTs in the energy domain.

In this subsection, concepts and architectures for DTs and related work for cyber-physical systems (CPS) are reviewed and then discussed with regard to their viability for DTs of IES.

2.5.1. Existing Digital Twin Concepts, Architectures and Platforms

The first DT concept was published by Grieves [14] in 2014, defining the three basic aspects of (i) the physical space, (ii) the virtual space and (iii) the connection between them to exchange data and information. These three main dimensions are found in most other concepts and architectures. Concurrently, they are often organized into physical (i), computing (ii) and network layers (iii) [67,76]. Grieves' three-dimensional approach is very minimalistic, and consequently, many extensions have been proposed in recent years to reflect the growing complexity of DT concepts.

Tao et al. [79] argued that Grieves' three dimensions do not indicate the extent to which services and features can be provided, and also, the extent to which information can be retrieved and data can be processed is not explicitly presented. These shortcomings in combination with the rapid development of enabling technologies, omnipresent availability of data, and the need for services led Tao et al. [24,80] to propose a 5D-DT concept, adding (iv) DT data and (v) DT services to the three dimensions proposed by Grieves [14]. In the 5D-DT concept, especially the service dimension is emphasized as an important part. The functionality of the DT is encapsulated into standardized services with user-friendly interfaces for easy and on-demand usage.

Stark et al. [81] propose a "DT 8-dimension model" to provide a template for planning DTs; however, they admit that further research is needed toward a reference model for the implementation of a DT.

Wang et al. [31] presented DT models and a four-layer networked architecture of cloud-side-end collaboration for battery management systems. This architecture contains four layers from the perspective of hardware functionality, namely "edge computing layer", "data access layer", "data storage and analysis layer" and "data-based application layer".

Sleiti et al. [37] proposed a five-component DT architecture for robust power plant operation, consisting of (1) a physics-based dynamic system model, (2) an anomaly detection model, (3) a sensor database, (4) a digital thread model and (5) localized in-depth simulations. While this architecture is specific regarding purpose and possible modeling techniques for physical components, the authors circumvent the important topics of data storage and processing and connections within the DT. Furthermore, no standardization aspects are considered to ensure the scalability and openness of the architecture.

In [21], a "Reference Framework for Digital Twins" is presented that specifies the structure and interrelations of the main DT building blocks, which were identified based on a literature review. Interestingly, the blocks are almost identical to the dimension in the 5D-DT concept by Tao et al. [72,80] except for the notable absence of an equivalent to the connection dimension.

The concept for a "Cognitive Twin Toolbox" was presented in [82] with a special focus on the process industry. The toolbox is organized into the five layers, which again have some similarity to the 5D-DT [72]. The "Data Ingestion and Preparation Layer" and the "Service Management Layer" are of a similar design as the data and service dimension in the 5D-DT. The "Model Management Layer" serves a similar function as the virtual entity. Additionally, the toolbox also has a "Twin Management Layer", to handle synchronization of the DT structure, and a "User Interaction Layer". Just like the "Reference Framework for Digital Twins", the "Cognitive Twin Toolbox" has no explicit connection layer.

The three main building parts of a DT presented by Grieves [14] align with the definition of CPS, which is a concept that is very prominent in the industrial production domain. Various papers in the manufacturing field mention the use of the DT to simulate a CPS [17]. Therefore, some researchers see a DT as merely the digital model inside a CPS [10],

and this conversely implies that a DT is the prerequisite for a CPS [12]. Zheng et al. [83] state that the DT in the broad sense belongs to the CPS but has a higher fidelity and focuses more on data and models with ultra-high-fidelity simulations. Either way, DTs and CPSs are undoubtedly very similar, and thus, CPS architectures are also highly relevant for DT implementations.

The prominent five-layer architecture (5C architecture) for CPSs proposed by Lee et al. [84] consists of the five pyramid-like layers “Smart Connection Level”, “Data-to-Information Conversion Level”, “Cyber Level”, “Cognition Level”, and “Configuration Level”, in order from bottom to top, bearing similarity with the 5D-DT architecture by Tao et al. [72,80]. The 5C architecture aims to guide the development and deployment of CPSs in manufacturing even though it cannot be considered to be a mature DT platform.

In Ref. [85], an “Intelligent Digital Twin” architecture for implementation in CPSs was proposed. In the “Cyber Layer”, a synchronization interface is introduced besides a data acquisition interface to keep simulation models of the DT consistent with the physical entity. Furthermore, a co-simulation interface is described as a component of the architecture to facilitate interaction between simulation models and to enable communication with other DTs. While focus of this architecture lies on automated synchronization and inseparability, the dimension of services seems underdeveloped, since the “DT” is only regarded as a virtual replication of physical functionalities in that article.

2.5.2. Standardization Aspects

We see that the available reference architectures for DTs and related concepts such as CPSs use either structured elements (e.g., building blocks, components, dimensions) or some kind of layers (also interfaces) to structure functionality and reduce complexity for DT implementation. These basic DT parts often have the same function even though they have different names, which impedes direct comparison. In an attempt to bring order to this topic, several standardization efforts have been made.

The Asset Administration Shell (AAS) was introduced in the context of the Industry 4.0 initiative as a standardized digital representation of an asset [86,87]. The AAS is used to uniquely identify assets, describe their functionality over the whole lifecycle and enable the communication among assets within a single factory and between companies. The AAS is still being developed, and the integration of models into the AAS is due to be added soon [88]. However, it is not in the scope of the AAS to provide simulations [20], hence missing basic requirements for a DT. For this reason, the AAS can rather be seen as the first step to a standardized DT solution providing the basic DT functionalities of resource description, discovery and access.

The ongoing standardization initiatives by the International Organization for Standardization (ISO) under the code ISO 23247 and title “Automation systems and integration—Digital twin framework for manufacturing” are also noteworthy as are the DT implementations that are built on these [89] as well as other standards relating to the scope of DTs, such as ISO 22989 and ISO 10303. However, both the transferability of such standards to the energy sector and ultimately the acceptance of the norms are not foreseeable yet.

In an attempt to establish a common view and terminology, the Reference Architecture Model Industry 4.0 (RAMI 4.0) was introduced in the context of Industry 4.0 [90]. RAMI 4.0 is a guidance framework for implementing Industry 4.0 aspects and developing a common understanding of standards, tasks and use cases. Thus, RAMI 4.0 provides a very useful system for localizing the parts of a DT.

To connect RAMI 4.0 with DT concepts, the Generic Digital Twin Architecture (GDTA) was proposed by Steindl et al. [63]. In it, the 5D-DT concept [72] was used as a basic conceptual model and aligned with the six interoperability layers of RAMI 4.0 (Business, Functional, Information, Communication, Integration and Asset Level [63]) in an attempt to achieve a consistent naming and understanding of the layers. The GDTA targets the “instance-phase” of the RAMI 4.0 lifecycle, i.e., the operational phase as opposed to the “type” or engineering phase. A DT can be located at various hierarchy levels within

RAMI 4.0, depending on the physical entity for which it is designed for, potentially covering all levels [63]. Defined data models within the AAS can be semantically lifted to a knowledge representation based on Resource Description Framework (RDF) [91], enabling the representation of the AAS inside the shared knowledge base of a GDTA-based DT.

2.5.3. Summary and Discussion

In Table 4, a summary of the concepts, architectures and frameworks presented in the preceding paragraphs is given. The table was adapted and extended from our previous work [63]. It also gives a classification of the architectures based on their level of abstraction ranging from “high” (more general concept) to “low” (concrete framework, targeting implementation details).

Table 4. Overview of concepts, architectures and frameworks for DTs. Adapted and extended from Steindl et al. [63].

Name	Target Domain	Structure	Main Parts	Level of Abstraction
3D-DT [14]	Lifecycle management	component-based	3 components	high
5D-DT [72]	Manufacturing	component-based	5 components	high
5C Architecture [84]	CPSs in manufacturing	layer-based	5 layers	high
Intelligent DT [85]	Production systems	component-based	4 interfaces and 9 components	low
Ref. Framework for DT [21]	CPSs in general	component-based	4 main components	low
“4S” architecture [31]	Battery management	layer-based	4 layers	low
COGNITWIN [82]	Process industry	components and layers	5 layers and 19 components	low
Conceptual DT model [92]	CPS in general	layer-based	6 layers	medium
ASS [86,87]	Manufacturing	only meta-model	ongoing work	-
The Twinning process [12]	DT characterization	only synchronization model	sequential processes	high
Data-driven reference architecture for DT [93]	Various industries	layer-based	6 layers and several components	high
Digital Twin 8-dimension model [81]	Smart manufacturing	component based	8 components	high
Application framework of DT [83]	Lifecycle management	modules and layers	3 components and 1 layer	high
The Interactive Digital Twin [32]	Decision making in energy system design	only design model	sequential processes	low
GDTA [63]	Industrial Energy Systems	components, layers and services	6 layers	medium
Robust DT for power plants [37]	Power plants	component-based	5 components	medium

While abstract DT concepts are very useful for the initial development of the DT platform for a particular use case, they mostly do not indicate how to implement a DT. The propositions at a low level of abstraction that we found in our literature search either do not meet energy system specific requirements or lack the perspective of standardization.

Aligning solutions with the architectural guidelines of the GDTA outlined above facilitates technology-independent implementations of DTs, thus ensuring reusability ultimately reducing development expenses. However, services are still considered in an abstract way in the GDTA, and appropriate implementation technologies have to be chosen. The prominent 5D-DT concept is being simple to understand in theory while keeping implementation details vague.

We conclude that a more tangible DT platform, addressing the requirements for the domain of IES, can significantly facilitate DT implementation. Therefore, we propose a DT platform in Section 3 based on the previous work on the 5D-DT concept [80] and the GDTA [63]. The 5D-DT concept allows to conceptualize a specific DT based on five main dimensions, which are found in the majority of existing literature concepts. The GDTA, being also based on the 5D-DT concept, aims structuring its essential components and functionality and helps to classify, combine, and re-use already existing frameworks and technologies based on its alignment with RAMI 4.0.

3. The Digital Twin Platform

Taking the 5D-DT concept as a fundamental pattern, we developed a DT platform that is tailored to the specific requirements of IES (see Section 2).

The architecture of the developed DT platform is presented in Figure 2. The connection dimension is at the center of our platform, which highlights its function as the central communication hub. All parts of the DT can communicate via a message broker. The physical entity (left-most box in Figure 2) is connected to the virtual space via the supervisory control and data acquisition (SCADA) system. New data points are sent to the message broker, and control signals are received. The virtual entity (right-most box in Figure 2) is connected via the model management layer. Via this model management layer, models are made available to the other parts of the DT. Each model is associated with an identifier and models can be added, updated and fetched. The data dimension (box at the bottom center of Figure 2) provides a uniform interface and semantic structuring to the various data sources in the DT. Queries are received from the message broker, processed, and the result is returned via the broker to the requesting client. In the service dimension (top center in Figure 2), each service can connect directly to the message broker. Services can send requests for models to the virtual entity and send data queries to the data dimension. The coordination of the various services and the realization of complex sequences is realized by the service orchestrator.

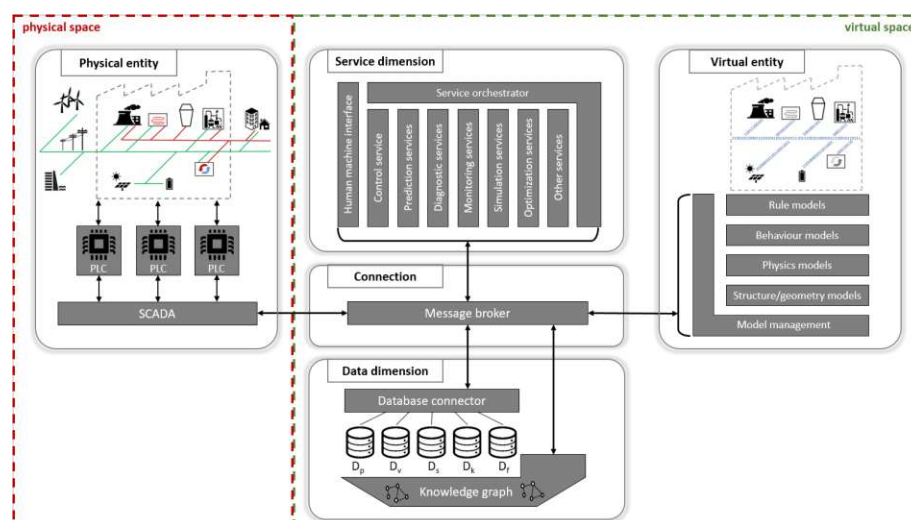


Figure 2. Illustration of the DT platform for an IES inspired by the five-dimensional 5D-DT concept and the GDTA.

In the following subsections, we address the particular implementation issues of each dimension of the DT and propose universal, yet concrete, approaches for resolving these issues. As a use case, we consider a generic IES comprised of typical components, as illustrated in Figure 1.

3.1. Connection Dimension

The main task of the connection dimension is to enable the communication between all parts of the DT. The goal of our DT platform is to provide powerful yet versatile standards, which can be used easily, while allowing the implementation of more efficient alternatives for applications with special requirements. Implementing various communication channels between the parts of the DT would result in an unnecessarily complicated architecture. Instead, the main communication channel should be designed so that it is interoperable with all parts of the DT.

There are numerous choices for appropriate communication technology, such as Message Queuing Telemetry Transport (MQTT), Advanced Message Queuing Protocol (AMQP), Constrained Application Protocol (CoAP), Hyper Text Transport Protocol (HTTP) or Open Platform Communications Unified Architecture (OPC UA) [94], to name just a few. The choice is often application-specific and depends on reliability, speed and resource constraints, amongst other things. For a review on messaging technologies for IoT systems, see, for example, the work of Naik [95] and Profanter et al. [96]. To enable event-driven asynchronous communication between all dimensions, a publish–subscribe message queue in form of a message broker is the most viable solution [97].

We thus chose MQTT as the default communication protocol of our DT platform. Human et al. [94] demonstrated the effective use of MQTT for DTs of complex systems. It is appropriate because of its versatile topic-based publish/subscribe functionality, lightweight messages and low bandwidth requirements, which allows 1:n as well as n:1 communication [22]. It is well established in IoT [96] and can be utilized by clients based on the Internet Protocol Suite TCP/IP; hence, it is also compatible with heterogeneous hardware components of the physical entity. Furthermore, it features three levels of Quality of Service (QoS) for reliable message delivery and an adequacy for large networks [94].

Each of the other four dimensions of the DT is connected to the MQTT message broker in the connection dimension as a client and can publish and subscribe to different topics. These topics are defined and managed by the MQTT message broker. The broker is responsible for receiving all messages, filtering the messages, determining who subscribed to which topic, and sending the messages to those subscribed clients. On an even more abstract level, all parts of the DT can be considered some kind of service, and the whole DT can be modeled in analogy to a microservice framework (see, e.g., [22]). By applying a message broker in this way, the connection dimension turns into a central communication hub, as it is shown in Figure 2.

With regard to the practical implementation of the DT platform, we propose Eclipse Mosquitto (<https://mosquitto.org/>, accessed on 10 June 2022) as an MQTT message broker. The lightweight architecture allows for deploying on different devices and does support various authentication and encryption protocols, such as username/password authentication, and certificate-based encryption. Depending on the application which aims to connect to the broker, various MQTT client libraries are available that support the used MQTT version 3.1.1 (OASIS Standard. Available online: <http://docs.oasis-open.org/mqtt/mqtt/v3.1.1/os/mqtt-v3.1.1-os.html>, accessed on 10 June 2022).

Figure 3 illustrates an exemplary request–response message pattern in our DT platform and the message topics involved. The function of the service orchestrator is explained in detail in Section 3.5.

Each client publishing to the broker has to follow an MQTT topic naming convention depending on the type of message. This ensures that published messages have a defined payload allowing subscribed clients to process received messages accordingly. However, the DT platform does not require a request/response message pattern, which is not supported by MQTT out of the box, as it follows the publish/subscribe pattern. Therefore, considerations on how to implement such a request/response message mechanism had to be made, which include two implementation possibilities: (1) one MQTT topic for request and response messages or (2) one MQTT topic for a request message and one MQTT topic for the correlated response message. The first approach requires to define the type of message within the payload alongside a unique identifier to correlate messages. Alternatively, the unique identifier could be appended to the MQTT topic for reducing the payload, but this would require parsing the MQTT topic for retrieving the identifier. Thus, we opted for the second approach, which defines the type of the message by the MQTT topic; hence, only the unique identifier has to be appended to the payload. An application would then need to parse the topic for getting the type of message and the identifier for message correlation. This approach allows exchanging messages while still enabling the use of arbitrary payloads.

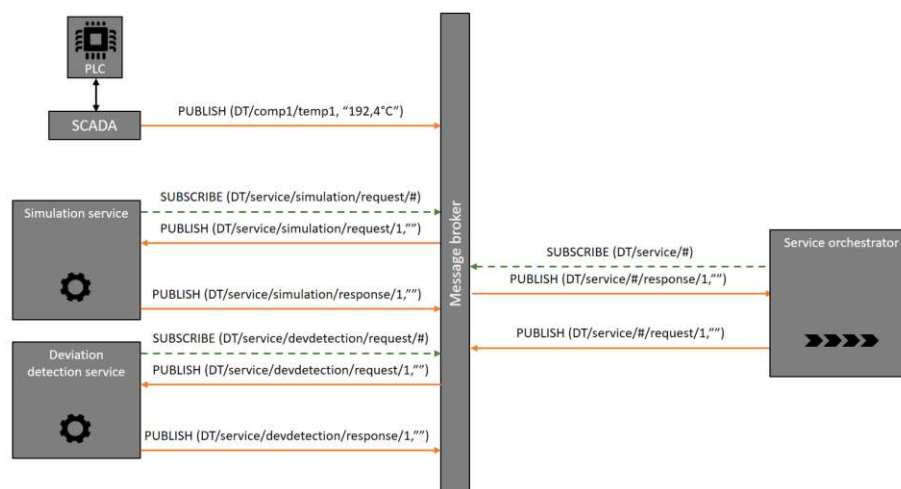


Figure 3. Exemplary request–response message pattern in the DT platform. Services subscribe to their respective request–topics and thereby receive messages published by the service orchestrator, e.g., to start operating. When a service instance has completed a run, it publishes to its response topic, which is monitored by the service orchestrator via subscription. Note: The function of the service orchestrator is explained in detail in Section 3.5. Character # denotes a multi-level wildcard, hence receives all messages of a topic that begins with the pattern before the wildcard character, and "" contains message payloads.

3.2. Physical Entity

The key for realizing a DT is to enable a tight integration of physical and virtual space. To that end, a lot of information has to be exchanged with the physical entity. Data have to be recorded by sensors, and control signals have to be fed back to the actuators in the energy system. However, most DT applications do not mention the connection of the DT environment to the control system [16]. Hence, this critical implementation barrier needs to be dissolved.

In a typical DT deployment scenario for IES, it can be assumed that there is already a pre-existing system for at least basic interfacing of the physical entity in place. Various measurement values are typically connected via a programmable logic controller (PLC) to a state-of-the-art SCADA system. Our DT platform builds upon on such SCADA systems; hence, we locate them inside the physical entity dimension (see Figure 2). Such SCADA systems (or merely PLCs) can then be interfaced to the DT via standard industrial IoT protocols. In case of our DT platform, this is MQTT.

This tight integration would also allow realizing certain control tasks in the DT. The advantage is obvious: on the DT, the controller has access to more detailed models and more computation power. However, other factors that need to be taken into account are hard real-time and dependability requirements, which cannot be guaranteed for communication via the used network transmission protocols. For this reason, high-speed control tasks and plant safety measures should not be executed within the DT, but they always run on the PLC directly.

For our DT implementation, XAMControl (<https://en.evon-automation.com/>, accessed on 10 June 2022) was used as the SCADA platform, which allows to define, visualize, program and configure PLCs. In order to integrate this system into the proposed architecture, a prototype version of the server software enables publishing and receiving messages to and from the MQTT broker. These messages can then be processed by any interested application by subscribing to the relevant MQTT topic.

3.3. Virtual Entity

One of the key features of a DT is that its virtual entity represents the state of the physical entity at all times. This requires that models or the model parameters are adapted to changes in the physical entity. An adaptation of the models in the virtual entity will, for example, be required when degradation changes the process performance, when parts have been replaced or refurbished in a maintenance intervention, or when new components were installed for modernization of the IES. The job of the DT is to keep track of these changes and manage the different versions of each model/parameter set.

In our platform, this requirement is fulfilled by the model management in the virtual entity. It essentially runs a database of all available model instances and stores information on each model in a local knowledge graph. Information includes (amongst other factors) the URI (Uniform Resource Identifier), scope, inputs, outputs, validity ranges, accuracy and time of validity. The model management runs an MQTT endpoint over which models can be queried and afterwards processed. The models can thus be provided for specific services.

Our DT platform allows for model integration developed in different environments. Thus, also different types of models, for example, physical, data-driven or hybrid models, with varying fidelity, can be applied for designated tasks within the DT. For details on modeling enabling technologies for DTs, see, for example [98].

Accessing the metadata of model instances and storing them within an ontology requires standardized interfaces. Functional Mock-up Interfaces (FMIs) (<https://fmi-standard.org/>, accessed on 10 June 2022) are an established standard to create relevant model instances and their input and output parameters (connections). This allows storing a model instance as a single file via corresponding Functional Mock-up Units (FMUs). By including a metadata file, which contains descriptions of the connection types, these two files provides all necessary information to describe the virtual entity.

Figure 4 illustrates how services can access virtual entity models within the DT platform. The platform contains a model management service written in Python (<https://www.python.org/>, accessed on 10 June 2022), which processes these files and provides access to the FMU model via the File Transfer Protocol (FTP). In order to select a specific model, any service connected to the MQTT broker is able to query all provided models of the model management service via an MQTT request and subsequently can access them via FTP. The reason for using FTP in contrast to provide the FMU file via MQTT lies within the nature of MQTT, which is not designed for exchanging binary files, hence the choice of using the much more suitable File Transfer Protocol.

3.4. Data Dimension

Generally, the data dimension holds information about five data categories according to Tao et al. [72,80] and as illustrated in Figure 2. In addition to sensor data from the physical entity (D_p), model and simulation data from the virtual entity (D_v), and data from the Service dimension (D_s), it contains semantic data about the system and all the relationships within the DT, i.e., domain knowledge (D_k), and fused data (D_f) of D_p , D_v , D_s and D_k .

However, the data dimension must not only store these data but also provide semantics to it. Therefore, in our DT platform, we use a so-called knowledge graph, which is a knowledge-based system, consisting of an ontology and a built-in reasoner that is capable of acquiring and integrating external information sources [99]. This knowledge graph consists of several ontologies that hold information about plant equipment, topology, instrumentation, etc. The runtime data from the IES, which is usually stored in relational databases, is integrated into the knowledge graph via ontology-based data access (OBDA). By defining mappings between the relational database structure and the ontologies, the implicit knowledge about the data models is made explicit. Thus, the knowledge graph acts as a semantic abstraction layer [100] where data can stay in the original local database, e.g., within an SQL database of the SCADA system. Data are only loaded when accessed,

which also enhances performance [101]. For more detailed information about the data access, we refer to our previous work in references [22,63].

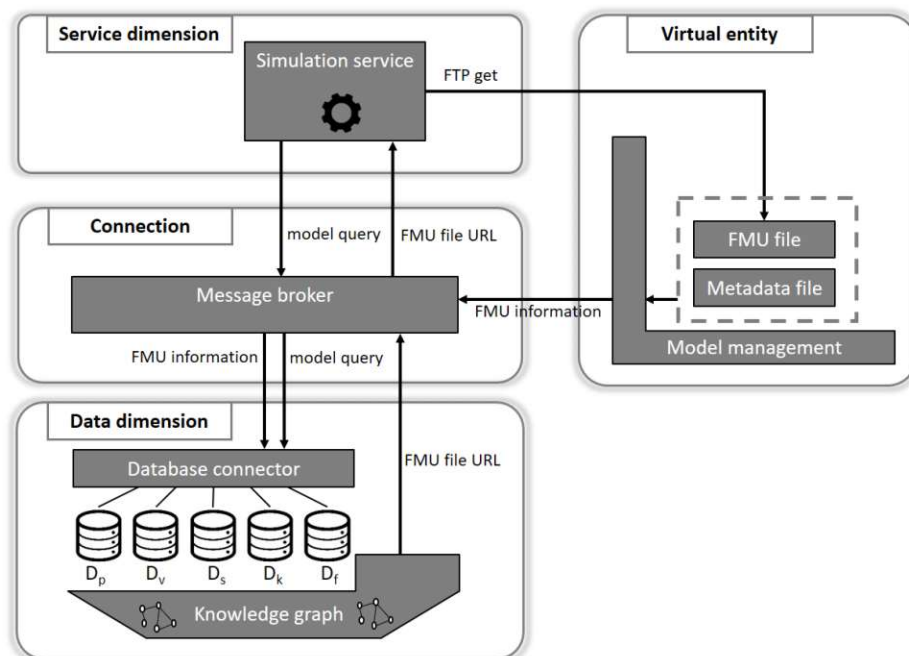


Figure 4. An exemplary service (simulation service from Figure 3) queries for a specific model instance within the virtual entity of the DT platform. The knowledge graph provides its access point via the FMU’s file URL, and the service can fetch the FMU file via the FTP get command.

As a crucial methodical foundation, domain-specific ontologies have to be applied for IES. However, knowledge engineers do not need to build ontologies from scratch, but they can use and integrate existing standards that were developed in collaborative efforts among industry and academia and be conveniently created via open source tools (e.g., [102]). For our DT platform for IES, relevant ontologies include PETIont (Plant, Equipment, Topology and Instrumentation Ontology) [103], Sensor, Observation, Sample, and Actuator (SOSA) ontology [104], PQOnt (Electrical Power Quality Ontology) [105], OntoPowSys (Power System Ontology) [106], OpenEnergy [107], OntoCAPE (Ontology for Computer-aided Process Engineering) [108], and OntoEIP (Ontology for Eco-Industrial Park) [109]. Furthermore, for including information on services and virtual entity models in the knowledge graph, existing semantic web ontologies such as OWL-S (Web Ontology Language for Service) [110] and OWL-Time (Web Ontology Language of Temporal Concepts) [111], extended with Quality of Service (QoS), are considered as foundation. Domain ontologies, e.g., FMUont (Functional Mock-up Ontology) [112] and ML-Schema [113] for simulation services, are built on top, inheriting all classes and properties of the base service ontology [63]. The creation of a single generic ontology for IES is beyond the scope of this contribution. However, it has already been successfully demonstrated, e.g., by Ocker et al. [114], that the highly reusable terminological components of such ontologies can be (semi-)automatically merged to fit the requirements of specific applications.

For the practical use of the ontology, hence instancing the concepts of it and creating the relations between them, a triplestore provides the means to store the ontology similar to a database. A semantic triple consists of three entities, namely subject, predicate and object, and represents a relation between them. This way, knowledge can be structured in a machine-readable and standardized way. For the implementation, the RDF framework RDF4J (<https://rdf4j.org/>, accessed on 10 June 2022) is used, which supports a variety

of established ontology file formats and provides a SPARQL endpoint to access data. For ontology-based data access, Ontop (<https://github.com/ontop/ontop>, accessed on 10 June 2022) enables connecting a SQL database into the knowledge graph, which means that data remain in the data source without being moved. A wrapper service, which translates MQTT requests to SPARQL queries (database connector in Figure 2), enables the integration into the DT platform. Listing 1 shows how to formulate a SPARQL query to receive the values from a sensor (FBR-TE-1A1) between two timestamps. Such a query can be automatically submitted, e.g., from the deviation detection service mentioned in Figure 3.

For connecting other databases to the DT platform, one requirement is that it supports MQTT, which is, for instance, fulfilled by InfluxDB (<https://www.influxdata.com/>, accessed on 10 June 2022).

Listing 1. Exemplary SPARQL query, requesting measurement values from a sensor (FBR-TE-1A1) between two timestamps from the DT's knowledge graph.

```

1 PREFIX rdf: <http://www.w3.org/1999/02/22-rdf-syntax-ns#>
2 PREFIX rdfs: <http://www.w3.org/2000/01/rdf-schema#>
3 PREFIX sosa: <http://www.w3.org/ns/sosa/>
4 PREFIX : <http://tuwien.ac.at/dt>
5
6 SELECT * WHERE {
7   :FBR-TE-1A1 sosa:madeObservation ?obs.
8
9   ?obs sosa:resultTime ?time;
10      sosa:hasSimpleResult ?result.
11   FILTER( ?time > "2022-04-02T08:00:00"^^xsd:dateTime &&
12           ?time < "2022-04-02T09:00:00"^^xsd:dateTime)
13 }ORDER BY (?time)

```

3.5. Service Dimension

The service dimension in our DT platform is realized according to the microservice framework by Steindl et al. [22], which is aligned with the GDTA and the RAMI 4.0 IT layers. A key advantage of this framework is that small services can be realized and developed independently. To compose and deploy services, choreography or orchestration can be used [22]. Compared to the sometimes advantageous decentralized choreography approach, our platform builds on service orchestration, leading to an integrated service logic and a potentially less laborious development [115]. To realize and manage complex processes and computations, multiple services can be linked in workflows. Workflows can be defined in a graphical language, such as BPMN (Business Process Model and Notation) and executed via a workflow engine, which is located in the Service Orchestration (see Figure 2). For the inter-service communication, again, the central MQTT message broker is used. Once deployed, the services can be containerized for the sake of reliability. Each service holds its relevant data in its own local database or triplestore and can add relevant information to the shared knowledge graph in the data dimension via a federated SPARQL query engine. For details, we refer to the work of Steindl et al. [22] and the corresponding source code [116].

The services within our service dimension are grouped in accordance with the GDTA [63]. We consider different forms of control, prediction, diagnostic, monitoring and simulation services to be implemented in our platform as well as potential non-categorized services relevant for DTs of IES. Services that require models can fetch the up-to-date model instances from the virtual entity via the MQTT message broker. Additionally, we consider the human-machine interface (HMI) as an important service in this dimension, since humans have to be informed about the current state of the physical entity as well as the DT itself to interact with it. This is possible via the platform's workflow engine. Different HMIs for the sole purpose of physical entity monitoring located in the SCADA system are also viable.

As indicated by Figure 3, the DT platform uses a BPMN workflow engine as a service orchestrator, namely Zeebe (<https://github.com/camunda-cloud/zeebe>, accessed on 10 June 2022). It allows loading BPMN files and enriching them with metadata necessary for

the connection to MQTT. In particular, these enriched BPMN files cover MQTT request and response topics. Figure 5 illustrates a simple exemplary workflow, which incorporates application category A2, respectively, deviation detection, of Section 2.2. This workflow is either triggered by a timer, i.e., in a predefined interval, or manually by the request of a user or another service. The activities in this workflow (“Simulation (virtual entity)” and “Deviation detection”) describe the services which the workflow engine will call on their corresponding MQTT request topic, as seen in Figure 3. In case of the “Deviation detected” activity, this send activity will trigger another workflow, which handles the classification of the deviation for further processing, e.g., to detect possible faults. The intermediate message events (“Simulation results received” and “Deviation detection results”) indicate that the workflow has to wait at these events until the services successfully complete their processing and return a result on the respective MQTT response topic. Other application categories can be modeled and integrated in a similar way.

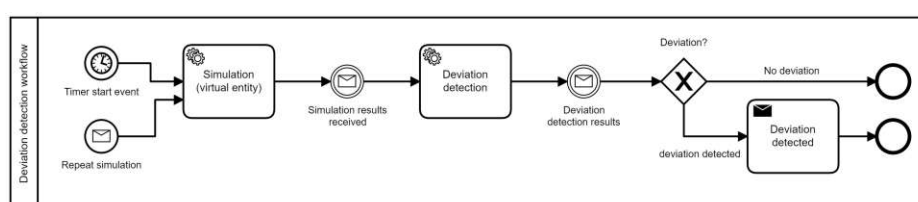


Figure 5. BPMN representation of an exemplary workflow for the application deviation detection. Services communicate via their corresponding MQTT request and response topics, as illustrated in Figure 3. The simulation service can query and fetch virtual entity models via information from the data dimension (see Figure 4).

The proposed architecture of the service dimension aims to be very flexible, which includes allowing the deployment on various machines. For this, the containerization framework Docker (<https://www.docker.com/>, accessed on 10 June 2022) allows running services in so-called containers, which include all necessary libraries the services require. Therefore, no additional software besides Docker has to be installed on the host machine. However, as the DT platform already covers multiple services, it would be cumbersome to start every single container with the correct parameterization manually. In order to automate this process, Docker Compose (<https://docs.docker.com/compose/>, accessed on 10 June 2022) enables defining a single file in which multiple containers and their configuration are specified. This allows starting the DT platform based on a single file.

4. Discussion

In the following, we discuss and evaluate our proposed DT platform by aligning it with the requirements identified in Section 2, addressing the benefits of the platform and discussing the potential of service engineering.

4.1. Alignment with the Requirements on Industrial Energy Systems

We developed the DT platform with a special focus on IES that has some unique features, resulting in specialized requirements, as emphasized in Section 2. In Table 5, we summarize how these requirements are met by our DT platform.

Some important requirements for DTs of IES are fulfilled via adequate use of the physical entity in our platform, such as R1 and R3, which are achieved by the efficient use of typical infrastructure such as SCADA/PLC systems and interconnection with the DT via a reliable message broker. Real-time observation (R1) is realized via PLCs connected to the SCADA system, which itself can publish values via the message broker. Actuation of the physical components (R3) can also be triggered by services within the DT via the message broker.

The connection within the DT is a crucial part of the whole platform. Using a message broker with event-based messaging supports the fulfillment of several requirements (R4, R5, R6, R7, R8, and R14).

The microservice architectural style of the platform supports the modularity (R4), scalability and maintainability (R6). Models can be defined via FMI and all services are containerized, facilitating maintainability and transferability. Complex processes can be realized via multiple interlinked DT services assembled to workflows. Defining, maintaining and adapting workflows within the DT is conveniently achieved via BPMN. This was highlighted in Section 3.5 via an exemplary workflow within the DT platform.

Table 5. Alignment of the identified requirements (see Table 3) supported by implementation aspects of the proposed DT platform. The requirements are listed along with their given IDs, an abbreviation of their description in Table 3, and structured via localization within the five dimensions (5D-DT) of the DT platform for IES.

ID	Requirement (Abbreviation)	5D-DT	DT Platform for IES
R1	Real-time observation	Physical entity	SCADA/PLC system
R2	Reaction on physical alterations	Service dimension	Various orchestrated services + HMI
R3	Physical entity actuation	Physical entity	SCADA/PLC system
R4	Modularity	Connection dimension	Microservice architecture + message broker integration
R5	Decision capability	Service dimension	Service orchestration
R6	Scalability	Service dimension	Microservice architecture + containerization
R7	Optimization capability	Service dimension	Optimization services
R8	User interaction	Service dimension	HMI + workflow engine
R9	Robust modelling	Virtual entity	Model management
R10	Prediction capability	Virtual entity	Simulation and Prediction services
R11	Model versatility	Virtual entity	Model management + Service encapsulation
R12	Standardized foundation	Data dimension	Alignment with RAMI 4.0 based on existing ontologies
R13	Heterogeneous data processing	Data dimension	Federated knowledge graph
R14	Semantic interoperability	Data dimension	Federated knowledge graph + message broker
R15	Secure operation	Physical entity	SCADA/PLC system

The DT is able to optimize operation of the physical entity (R7) via specific target applications (see also Table 1) that can be conveniently incorporated in the DT platform via workflows and by the use of specialized (micro)services. Optimized operation schedules are executed on the physical entity via control services.

User interaction (R8) is primarily localized within the service dimension, but different interfacing possibilities are feasible. For the sole observation of physical entity state variables, existing interfaces within legacy SCADA systems and also the use of such systems in a greenfield approach are encouraged. Observation of the DT and access to it is conveniently realized via the BPMN workflow engine as a service orchestrator. An HMI is already covered in typical software packages, such as for example Zeebe, in our implementation. Additional specific HMIs, e.g., for virtual entity services, could be realized accordingly. The DT is thus able to monitor, inform and issue warnings on relevant physical alterations (R2). Decision frameworks can be integrated via workflows and trigger corresponding actions on the virtual entity (R5) via the message broker.

Our virtual entity implementation accounts for robust and adaptive modeling (R9), extensive simulation and prediction capabilities (R10) and model versatility (R11). These properties are enabled by providing standardized interfaces and model management as presented in Section 3.3 and Figure 4 as well as the possibility to host models developed in different environments and varying fidelity.

Our implementation of the data dimension (see Section 3.4) with a federated knowledge graph facilitates heterogeneous data processing (R13) and provides semantic interoperability (R14). It holds information about plant equipment, topology, instrumentation, etc. in a machine-readable and standardized format and integrates runtime data via OBDA. The implementation with the RDF framework provides means to semantically access data via SPARQL endpoints. A wrapper service, which translates MQTT requests to SPARQL queries, enables information exchange within the DT. Standardization technologies and metadata (R12) are applied throughout our DT platform, e.g., by the use of established protocols such as MQTT and standards such as FMI for virtual model description. However, these requirements are especially crucial in the data dimension. Therein, domain-specific standardized ontologies are a crucial methodical foundation, fulfilling this requirement. Existing IES ontologies, as introduced in Section 3.4, can be (semi-)automatically merged to fit the demands of specific DT services, exploiting their highly reusable terminological components. AAS or ISO frameworks, as introduced in Section 2.5.2, can be conveniently incorporated in the data dimension of the platform to ensure conformance in case these are established as recognized standards. The knowledge graph in the data dimension of the DT platform provides a single access point to acquire and integrate external information sources, e.g., metadata, further aiding the scalability of the DT (R6). Furthermore, the whole DT platform builds on the GDTA [63] and RAMI 4.0, hence aiding the re-use of existing frameworks and technologies.

Security requirements (R15) are only inherently covered in our DT platform. We argue that cyber-security mechanisms should be contained in the applied fundamental technologies and further investigated in the pertinent literature. As outlined in Section 3.2, plant safety measures and critical high-performance control loops should be implemented on the PLC/SCADA system. However, specialized services could be integrated to automatically reconfigure and compile these control mechanisms on the PLC if, for example, the plant topology changes.

Even if the message broker is designed to be the only means of communication between the parts of the DT, there might be situations where direct communication is a more suitable option. For example, if a specific service within the DT needs to access a large data set in one of the relational databases, MQTT's maximum message size might be a limiting factor. In such a case, the service could request information about the location of the data set from the knowledge graph and then send a query directly to the database endpoint. The access to FMU files within the virtual entity via FTP or SFTP, as presented in Section 3.3, is another example.

Furthermore, service management is currently completed by hand and still has to be established if a DT should feature automated service deployment. Therefore, several (micro)services, e.g., for service discovery and access, still have to be implemented.

4.2. Digital Twin Platform Benefits

Our contribution aims to overcome the technical implementation barriers relevant for energy systems summarized in Table 2 and to enable different value-creating applications (see Table 1) in the same platform. Via the simple exemplary workflow for a deviation detection application, given in Figure 5, and considering typical use cases, it is possible to assess the attributes of our platform that aim to maximize the benefits of individual applications.

We have to stress here that the final benefits such as energy demand reduction, revenue increase and cost reduction that are expected from DT (see Section 2.2) are only provided via the respective applications integrated as services. However, we consider the detailed discussion of individual services to be out of scope of this contribution and refer to specialized literature instead. Nonetheless, via this evaluation, the platform's qualitative benefits are clearly evident.

Instead of having one monolithic application that takes care of all aspects of fault detection starting from the data cleansing, deviation detection, and fault classification to

decision making and also scheduling maintenance actions, the process can be split into microservices that are coordinated by the service orchestrator in the DT platform. For the deviation detection workflow itself, nothing changes, but it enables it to integrate it more tightly with other DT services. For example, if a deviation is detected by the deviation detection service (see Figure 5), a message can trigger a workflow for fault classification in order to check if the deviation is caused by a fault or due to a normal drift in the system's behavior. In case of the latter, this information can then be used to trigger a model adaption workflow. For a more in-depth discussion of a semantic microservice framework, we refer to Steindl et al. [22], where automatic sensor data evaluation serves as a proof of concept.

To react to new data points within the IES, a dedicated topic for each sensor value is set up on the message broker. Any service that needs to react to new data points subscribes to the respective topics. Whenever a new data point is available, the SCADA system publishes a message on the corresponding topic, and the message broker will deliver the new data points to all services that require this data point. Through the publish/subscribe function of the message broker, neither the SCADA system nor the services need to have any information about each other aside from the name of the topic where data points are transferred.

The ability of the DT to adapt to changes of the plant is enabled by the separation of models and the services that use these models. If a continuous drift in the system's behavior was detected via fault classification, models within the virtual entity can be automatically replaced or updated, e.g., via data-driven modeling and validation services, to fit the altered behavior. When a simulation service starts, it fetches the newest validated model instance from the virtual entity.

Figure 6 illustrates how the presented DT platform leverages the integration of digital applications to offer associated benefits. In addition to the easy integration, operation and maintainability of applications, another important aspect is that synergies between these individual solutions can be conveniently exploited. Naturally, applications such as condition monitoring and deviation detection can provide basic unidirectional information for subsequent fault classification and analysis. However, also, back-feeding information between applications can provide additional benefits. For example, a schedule derived from operational optimization can be used for estimations within predictive maintenance applications. Conversely, the latter can determine operational constraints for operational optimization services. This is not possible without sufficient information management. The architectural design of our platform, i.e., the division into the five DT dimensions with the message broker as the central communication hub and a microservice framework for managing inter-service workflows, facilitates interconnection between different applications and the access of distributed data sources. As presented in Section 2.2, these digital applications integrated in a DT platform provide benefits such as system stability, environmental protection, energy demand reduction, revenue increase or cost reduction.

4.3. The Potential of Service Engineering

While the energy industry strives to implement DTs as soon as possible to leverage its potential benefits, one of the biggest current obstacles remains to be that in-depth knowledge from various domains is required. Within the energy sector, most technical contributors have a background in electrical, chemical, mechanical, thermal or operations engineering, due to the fact that IES to date have been very complex systems requiring profound expertise in these fields to manage and develop. Industry 4.0, and with it concepts such as the DT, set a paradigm shift in motion, introducing more and more novel technology from information and communications technology to this sector. While energy domain experts struggle to understand modern IoT methods and what the implications for their work are, computer scientists typically do not fully comprehend the intricacies of IES and the challenges of operating them. The DT platform provides a common understanding of operational DTs, and it also defines clear interfaces to separate the work of the engineers

and the computer scientists. In this way, everyone can focus on their strengths while still working efficiently on the big picture: the DT.

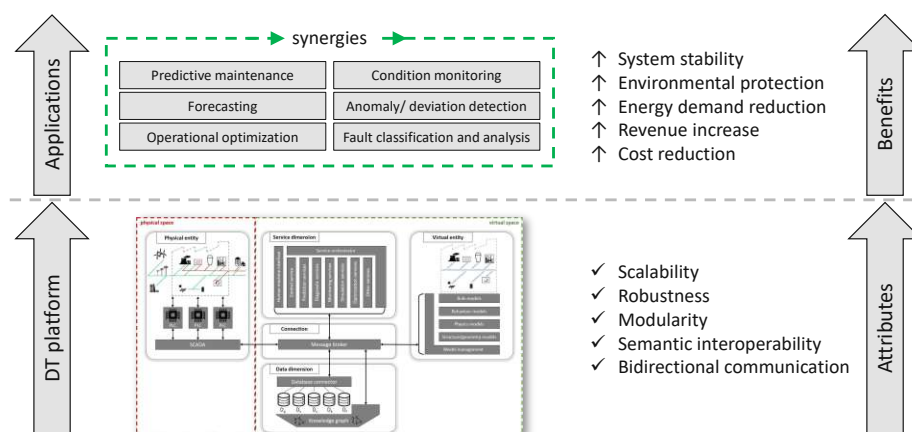


Figure 6. Illustration of DT platform benefits. By fulfilling IES-related requirements, hence realizing attributes such as scalability, robustness, modularity and semantic interoperability, the integration, operation and maintainability of applications as given in Table 1 are facilitated. These applications are leveraged, individually and by using synergies between them, to obtain benefits for the IES.

The engineering of complex IES-related models and services will still rely on expertise and profound experience with the respective assets in the years to come. However, these services can be encapsulated in standardized form in the DT platform. Deployment is facilitated by providing an appropriate IT infrastructure, making information from both physical and virtual entities easily accessible. Thus, on one hand, IES experts who develop new services and models have clear interfaces within the DT platform. Therefore, they can concentrate on application-related domain problems instead of deployment and connection within the DT.

On the other hand, computer scientists can focus on the infrastructure to provide an open, scalable, reliable, and secure DT platform solution by converging the operation technology and IT world. In this context, interoperability is key for integrating third-party systems and providing openness to enable new business opportunities. Therefore, interoperability must be established on a technical, syntactical, semantical, and operational level.

We presume that on the technical side, interdisciplinary work in DT development between computer scientists and energy system experts will have some distinct focus points. We see such a major overlap in the area of knowledge representation, i.e., the development of ontologies or knowledge graphs for IES. Methodologies such as METHONTOLOGY [117] structure and guide the work to build ontologies, but they also rely on the knowledge of domain experts.

5. Conclusions

In this paper, we identified special requirements on digital twins (DT) in industrial energy systems (IES) that set IES apart from other domains, where DTs are already established. On this foundation, we developed a DT platform that is tailored to the requirements of IES. Our DT platform is based on the five-dimensional DT (5D-DT) concept and provides solutions to various implementation issues that are not addressed in the 5D-DT concept. It also complies with the Generic Digital Twin Architecture (GDTA), hence facilitating alignment with existing technology and standardization.

The DT platform should prove a practical tool for interdisciplinary teams that aim to implement a DT for IES. The platform is designed to provide clear interfaces that allow domain experts to develop their services without in-depth knowledge about IT

implementation aspects. Through the efficient service encapsulation of the proposed DT platform, energy domain experts can focus their work on engineering services, virtual entity models and ultimately the optimal operation of IES. At the same time, computer scientists can leverage their expertise on the scalability, reliability and security of the DT platform and on establishing interoperability on a technical, syntactical, semantical, and operational level.

The main benefit of the DT platform for the operation of IES will be that individual digitalization solutions such as predictive maintenance, deviation detection, fault classification, and operational optimization, which are typically developed and deployed as standalone solutions today, can be more tightly integrated, and synergies can be exploited. The DT platform provides the basis for the standardized implementation of complex digital applications that make the operation of IES more efficient and thus get us one step closer to the paradigm of integrated, decarbonized energy systems with sustainable production.

Author Contributions: Conceptualization, L.K., F.B., P.S., G.S. and R.H.; methodology, L.K., G.S. and D.R.; formal analysis, L.K., F.B. and R.H.; investigation, L.K.; writing—original draft preparation, L.K., F.B. and P.S.; contribution to contents, review and editing, G.S., D.R. and R.H.; visualization, L.K.; supervision, R.H. All authors have read and agreed to the published version of the manuscript.

Funding: The authors acknowledge funding support of this work through the research project *5DIndustrialTwin* as part of the Austrian Climate and Energy Fund's initiative Energieforschung (e!MISSION) 6th call (KLIEN/FFG project number 881140).

Acknowledgments: The authors acknowledge TU Wien Bibliothek for financial support through its Open Access Funding Programme.

Conflicts of Interest: The authors declare that they have no known competing financial interest or personal relationships that could have appeared to influence the work reported in this paper.

Abbreviations

The following abbreviations are used in this manuscript:

DT	Digital Twin
CPS	Cyber-Physical System
5D-DT	Five-Dimensional Digital Twin
SCADA	Supervisory Control and Data Acquisition
IES	Industrial Energy System
PLC	Programmable Logic Controller
GDTA	Generic Digital Twin Architecture
AAS	Asset Administration Shell
RAMI 4.0	Reference Architecture Model Industry 4.0
HMI	Human–Machine Interface
MQTT	Message Queuing Telemetry Transport
OBDA	Ontology-Based Data Access
OPC UA	Open Platform Communications Unified Architecture
RDF	Resource Description Framework
SQL	Structured Query Language
SPARQL	SPARQL Protocol and RDF Query Language
HTTP	Hypertext Transfer Protocol
IIoT	Industrial Internet of Things
IoT	Internet of Things
IT	Information Technology
QoS	Quality of Service
TCP/IP	Transmission Control Protocol/Internet Protocol
FMI	Functional Mock-up Interface
FMU	Functional Mock-up Unit
FTP	File Transfer Protocol
BPMN	Business Process Model and Notation

References

1. Gibb, D.; Johnson, M.; Romání, J.; Gasia, J.; Cabeza, L.F.; Seitz, A. Process integration of thermal energy storage systems—Evaluation methodology and case studies. *Appl. Energy* **2018**, *230*, 750–760. [[CrossRef](#)]
2. Nagasawa, T.; Pillay, C.; Beier, G.; Fritzsche, K.; Pougel, F.; Takama, T.; The, K.; Bobashev, I. *Accelerating Clean Energy Through Industry 4.0: Manufacturing the Next Revolution: A Report of the United Nations Industrial Development Organization, Vienna, Austria*; United Nations Industrial Development Organization: Vienna, Austria, 2017.
3. Bonilla, S.; Silva, H.; Da Terra Silva, M.; Franco Gonçalves, R.; Sacomano, J. Industry 4.0 and Sustainability Implications: A Scenario-Based Analysis of the Impacts and Challenges. *Sustainability* **2018**, *10*, 3740. [[CrossRef](#)]
4. Commission, E.; Centre, J.R.; Kavvadias, K.; Jiménez Navarro, J.; Thomassen, G. *Decarbonising the EU Heating Sector: Integration of the Power and Heating Sector*; Publications Office: Luxembourg, 2019. [[CrossRef](#)]
5. Mendes, G.; Ioakimidis, C.; Ferrão, P. On the planning and analysis of Integrated Community Energy Systems: A review and survey of available tools. *Renew. Sustain. Energy Rev.* **2011**, *15*, 4836–4854. . [[CrossRef](#)]
6. Parida, V.; Sjödin, D.; Reim, W. Reviewing literature on digitalization, business model innovation, and sustainable industry: Past achievements and future promises. *Sustainability* **2019**, *11*, 391. [[CrossRef](#)]
7. Lange, S.; Pohl, J.; Santarius, T. Digitalization and energy consumption. Does ICT reduce energy demand? *Ecol. Econ.* **2020**, *176*, 106760. [[CrossRef](#)]
8. Kiel, D.; Müller, J.; Arnold, C.; Voigt, K.I. Sustainable Value Creation: Benefits and Challenges of Industry 4.0. *Int. J. Innov. Manag.* **2017**, *21*, 1740015. [[CrossRef](#)]
9. Tao, F.; Zhang, H.; Liu, A.; Nee, A.Y.C. Digital Twin in Industry: State-of-the-Art. *IEEE Trans. Ind. Inform.* **2019**, *15*, 2405–2415. [[CrossRef](#)]
10. Lu, Y.; Liu, C.; Wang, K.I.K.; Huang, H.; Xu, X. Digital Twin-driven smart manufacturing: Connotation, reference model, applications and research issues. *Robot. Comput.-Integr. Manuf.* **2020**, *61*, 101837. [[CrossRef](#)]
11. Yu, W.; Patros, P.; Young, B.; Klinac, E.; Walmsley, T.G. Energy digital twin technology for industrial energy management: Classification, challenges and future. *Renew. Sustain. Energy Rev.* **2022**, *161*, 112407. [[CrossRef](#)]
12. Jones, D.; Snider, C.; Nassehi, A.; Yon, J.; Hicks, B. Characterising the Digital Twin: A systematic literature review. *CIRP J. Manuf. Sci. Technol.* **2020**, *29*, 36–52. [[CrossRef](#)]
13. Melesse, T.Y.; Pasquale, V.D.; Riemma, S. Digital Twin Models in Industrial Operations: A Systematic Literature Review. *Proced. Manuf.* **2020**, *42*, 267–272. [[CrossRef](#)]
14. Grieves, M. *Digital Twin: Manufacturing Excellence through Virtual Factory Replication*; White Paper; Florida Institute of Technology: Melbourne, FL, USA, 2014; pp. 1–7.
15. Glaessgen, E.; Stargel, D. The Digital Twin Paradigm for Future NASA and U.S. Air Force Vehicle. In Proceedings of the 53rd AIAA/ASME/ASCE/AHS/ASC Structures, Structural Dynamics and Materials Conference, Honolulu, HI, USA, 23–25 April 2012; pp. 1–14. . [[CrossRef](#)]
16. Cimino, C.; Negri, E.; Fumagalli, L. Review of digital twin applications in manufacturing. *Comput. Ind.* **2019**, *113*, 103130. [[CrossRef](#)]
17. Negri, E.; Fumagalli, L.; Macchi, M. A Review of the Roles of Digital Twin in CPS-based Production Systems. *Proced. Manuf.* **2017**, *11*, 939–948. [[CrossRef](#)]
18. Liu, M.; Fang, S.; Dong, H.; Xu, C. Review of digital twin about concepts, technologies, and industrial applications. *J. Manuf. Syst.* **2021**, *58*, 346–361. [[CrossRef](#)]
19. Kritzinger, W.; Karner, M.; Traar, G.; Henjes, J.; Sihn, W. Digital Twin in manufacturing: A categorical literature review and classification. *IFAC-PapersOnLine* **2018**, *51*, 1016–1022. [[CrossRef](#)]
20. Wagner, C.; Grothoff, J.; Epple, U.; Drath, R.; Malakuti, S.; Grüner, S.; Hoffmeister, M.; Zimmermann, P. The role of the Industry 4.0 asset administration shell and the digital twin during the life cycle of a plant. In Proceedings of the IEEE International Conference on Emerging Technologies and Factory Automation, ETFA, Torino, Italy, 4–7 September 2018; pp. 1–8. [[CrossRef](#)]
21. Josifovska, K.; Yigitbas, E.; Engels, G. Reference Framework for Digital Twins within Cyber-Physical Systems. In Proceedings of the 2019 IEEE/ACM 5th International Workshop on Software Engineering for Smart Cyber-Physical Systems (SEsCPS), Montreal, QC, Canada, 28 May 2019; Institute of Electrical and Electronics Engineers Inc.: Piscataway, NJ, USA, 2019; pp. 25–31. [[CrossRef](#)]
22. Steindl, G.; Kastner, W. Semantic Microservice Framework for Digital Twins. *Appl. Sci.* **2021**, *11*, 5633. [[CrossRef](#)]
23. Tuegel, E.J.; Ingrassia, A.R.; Eason, T.G.; Spottswood, S.M. Reengineering Aircraft Structural Life Prediction Using a Digital Twin. *Int. J. Aerosp. Eng.* **2011**, *2011*, 1–14. [[CrossRef](#)]
24. Tao, F.; Zhang, M.; Nee, A.Y.C. *Digital Twin Driven Smart Manufacturing*; Academic Press: Cambridge, MA, USA, 2019. [[CrossRef](#)]
25. Wanasinghe, T.R.; Wroblewski, L.; Petersen, B.K.; Gosine, R.G.; James, L.A.; De Silva, O.; Mann, G.K.I.; Warrrian, P.J. Digital Twin for the Oil and Gas Industry: Overview, Research Trends, Opportunities, and Challenges. *IEEE Access* **2020**, *8*, 104175–104197. [[CrossRef](#)]
26. Bruynseels, K.; Santoni de Sio, F.; van den Hoven, J. Digital Twins in Health Care: Ethical Implications of an Emerging Engineering Paradigm. *Front. Genet.* **2018**, *9*, 31. [[CrossRef](#)]
27. He, R.; Chen, G.; Dong, C.; Sun, S.; Shen, X. Data-driven digital twin technology for optimized control in process systems. *ISA Trans.* **2019**, *95*, 221–234. [[CrossRef](#)]

28. Bottani, E.; Vignali, G.; Carlo Tancredi, G.P. A digital twin model of a pasteurization system for food beverages: tools and architecture. In Proceedings of the 2020 IEEE International Conference on Engineering, Technology and Innovation (ICE/ITMC), Cardiff, UK, 15–17 June 2020; pp. 1–8. [CrossRef]
29. Brosinsky, C.; Westermann, D.; Krebs, R. Recent and prospective developments in power system control centers: Adapting the digital twin technology for application in power system control centers. In Proceedings of the 2018 IEEE International Energy Conference (ENERGYCON), Limassol, Cyprus, 3–7 June 2018; pp. 1–6. [CrossRef]
30. O'Dwyer, E.; Pan, I.; Charlesworth, R.; Butler, S.; Shah, N. Integration of an energy management tool and digital twin for coordination and control of multi-vector smart energy systems. *Sustain. Cities Soc.* **2020**, *62*, 102412. [CrossRef]
31. Wang, Y.; Xu, R.; Zhou, C.; Kang, X.; Chen, Z. Digital twin and cloud-side-end collaboration for intelligent battery management system. *J. Manuf. Syst.* **2022**, *62*, 124–134. [CrossRef]
32. Granacher, J.; Nguyen, T.V.; Castro-Amoedo, R.; Maréchal, F. Overcoming decision paralysis—A digital twin for decision making in energy system design. *Appl. Energy* **2022**, *306*, 117954. [CrossRef]
33. Olatunji, O.O.; Adedeji, P.A.; Madushele, N.; Jen, T.C. Overview of Digital Twin Technology in Wind Turbine Fault Diagnosis and Condition Monitoring. In Proceedings of the 2021 IEEE 12th International Conference on Mechanical and Intelligent Manufacturing Technologies (ICMIMT), Cape Town, South Africa, 13–15 May 2021; pp. 201–207. [CrossRef]
34. You, M.; Wang, Q.; Sun, H.; Castro, I.; Jiang, J. Digital twins based day-ahead integrated energy system scheduling under load and renewable energy uncertainties. *Appl. Energy* **2022**, *305*, 117899. [CrossRef]
35. Darbali-Zamora, R.; Johnson, J.; Summers, A.; Jones, C.B.; Hansen, C.; Showalter, C. State Estimation-Based Distributed Energy Resource Optimization for Distribution Voltage Regulation in Telemetry-Sparse Environments Using a Real-Time Digital Twin. *Energies* **2021**, *14*, 774. [CrossRef]
36. Kohne, T.; Burkhardt, M.; Theisinger, L.; Weigold, M. Technical and digital twin concept of an industrial heat transfer station for low exergy waste heat. *Proced. CIRP* **2021**, *104*, 223–228. [CrossRef]
37. Sleiti, A.K.; Kapat, J.S.; Vesely, L. Digital twin in energy industry: Proposed robust digital twin for power plant and other complex capital-intensive large engineering systems. *Energy Rep.* **2022**, *8*, 3704–3726. [CrossRef]
38. Cioara, T.; Anghel, I.; Antal, M.; Salomie, I.; Antal, C.; Ioan, A.G. An Overview of Digital Twins Application Domains in Smart Energy Grid. To Be Submitted to an IEEE Conference. 2021. Available online: <https://arxiv.org/abs/2104.07904> (accessed on 10 June 2022).
39. Kaiblinger, A.; Woschank, M. State of the Art and Future Directions of Digital Twins for Production Logistics: A Systematic Literature Review. *Appl. Sci.* **2022**, *12*, 669. [CrossRef]
40. Mosavi, A.; Salimi, M.; Faizollahzadeh Ardabili, S.; Rabczuk, T.; Shamshirband, S.; Varkonyi-Koczy, A.R. State of the Art of Machine Learning Models in Energy Systems, a Systematic Review. *Energies* **2019**, *12*, 1301. [CrossRef]
41. Weigel, P.; Fishedick, M. Review and Categorization of Digital Applications in the Energy Sector. *Appl. Sci.* **2019**, *9*, 5350. [CrossRef]
42. Brosinsky, C.; Krebs, R.; Westermann, D. Embedded Digital Twins in future energy management systems: Paving the way for automated grid control. *Automatisierungstechnik* **2020**, *68*, 750–764. [CrossRef]
43. Stanelyte, D.; Radziukyniene, N.; Radziukynas, V. Overview of Demand-Response Services: A Review. *Energies* **2022**, *15*, 1659. [CrossRef]
44. Wang, X.; Palazoglu, A.; El-Farra, N.H. Operational optimization and demand response of hybrid renewable energy systems. *Appl. Energy* **2015**, *143*, 324–335. [CrossRef]
45. Halmschlager, D.; Beck, A.; Knöttner, S.; Koller, M.; Hofmann, R. Combined optimization for retrofitting of heat recovery and thermal energy supply in industrial systems. *Appl. Energy* **2022**, *305*, 117820. [CrossRef]
46. Tzani, N.; Andriopoulos, N.; Magklaras, A.; Mylonas, E.; Birbas, M.; Birbas, A. A Hybrid Cyber Physical Digital Twin Approach for Smart Grid Fault Prediction. In Proceedings of the 2020 IEEE Conference on Industrial Cyberphysical Systems (ICPS), Tampere, Finland, 10–12 June 2020; Volume 1, pp. 393–397. [CrossRef]
47. Macek, K.; Endel, P.; Cauchi, N.; Abate, A. Long-term predictive maintenance: A study of optimal cleaning of biomass boilers. *Energy Build.* **2017**, *150*, 111–117. [CrossRef]
48. Fox, H.; Pillai, A.C.; Friedrich, D.; Collu, M.; Dawood, T.; Johanning, L. A Review of Predictive and Prescriptive Offshore Wind Farm Operation and Maintenance. *Energies* **2022**, *15*, 504. [CrossRef]
49. Liu, K.; Wang, Y.; Lai, X. *Data Science-Based Full-Lifespan Management of Lithium-Ion Battery: Manufacturing, Operation and Reutilization*; Springer: Berlin/Heidelberg, Germany, 2022. [CrossRef]
50. Wang, Y.; Kang, X.; Chen, Z. A Survey of Digital Twin Techniques in Smart Manufacturing and Management of Energy Applications. *Green Energy Intell. Transp.* **2022**, 100014. [CrossRef]
51. Ardebili, A.A.; Longo, A.; Ficarella, A. Digital Twin (DT) in Smart Energy Systems—Systematic Literature Review of DT as a growing solution for Energy Internet of the Things (EIoT). *E3S Web Conf.* **2021**, *312*, 09002. [CrossRef]
52. Zhang, H.; Liu, Q.; Chen, X.; Zhang, D.; Leng, J. A Digital Twin-Based Approach for Designing and Multi-Objective Optimization of Hollow Glass Production Line. *IEEE Access* **2017**, *5*, 26901–26911. [CrossRef]
53. Zečević, N. Energy intensification of steam methane reformer furnace in ammonia production by application of digital twin concept. *Int. J. Sustain. Energy* **2022**, *41*, 12–28. [CrossRef]

54. Min, Q.; Lu, Y.; Liu, Z.; Su, C.; Wang, B. Machine Learning based Digital Twin Framework for Production Optimization in Petrochemical Industry. *Int. J. Inf. Manag.* **2019**, *49*, 502–519. [[CrossRef](#)]
55. Prawiranto, K.; Carmeliet, J.; Defraeye, T. Physics-Based Digital Twin Identifies Trade-Offs Between Drying Time, Fruit Quality, and Energy Use for Solar Drying. *Front. Sustain. Food Syst.* **2021**, *4*, 606845. [[CrossRef](#)]
56. Yu, J.; Liu, P.; Li, Z. Hybrid modelling and digital twin development of a steam turbine control stage for online performance monitoring. *Renew. Sustain. Energy Rev.* **2020**, *133*, 110077. [[CrossRef](#)]
57. Developing a Digital Twin: The Roadmap for Oil and Gas Optimization. In Proceedings of the SPE Offshore Europe Conference and Exhibition, Aberdeen, UK, 3–6 September 2019; Volume Day 1 Tue. [[CrossRef](#)]
58. Zabala, L.; Febres, J.; Sterling, R.; López, S.; Keane, M. Virtual testbed for model predictive control development in district cooling systems. *Renew. Sustain. Energy Rev.* **2020**, *129*, 109920. [[CrossRef](#)]
59. Abdrakhmanova, K.N.; Fedosov, A.V.; Idrisova, K.R.; Abdrakhmanov, N.K.; Valeeva, R.R. Review of modern software complexes and digital twin concept for forecasting emergency situations in oil and gas industry. *IOP Conf. Ser. Mater. Sci. Eng.* **2020**, *862*, 032078. [[CrossRef](#)]
60. Weigel, P.; Fishedick, M.; Viebahn, P. Holistic Evaluation of Digital Applications in the Energy Sector—Evaluation Framework Development and Application to the Use Case Smart Meter Roll-Out. *Sustainability* **2021**, *13*, 6834. [[CrossRef](#)]
61. Tao, F.; Cheng, J.; Qi, Q.; Zhang, M.; Zhang, H.; Sui, F. Digital twin-driven product design, manufacturing and service with big data. *Int. J. Adv. Manuf. Technol.* **2018**, *94*, 3563–3576. [[CrossRef](#)]
62. De Lauretis, L. From Monolithic Architecture to Microservices Architecture. In Proceedings of the 2019 IEEE International Symposium on Software Reliability Engineering Workshops (ISSREW), Berlin, Germany, 28–31 October 2019; pp. 93–96. [[CrossRef](#)]
63. Steindl, G.; Stagl, M.; Kasper, L.; Kastner, W.; Hofmann, R. Generic Digital Twin Architecture for Industrial Energy Systems. *Appl. Sci.* **2020**, *10*, 8903. [[CrossRef](#)]
64. Perno, M.; Hvam, L.; Haug, A. Implementation of digital twins in the process industry: A systematic literature review of enablers and barriers. *Comput. Ind.* **2022**, *134*, 103558. [[CrossRef](#)]
65. Perno, M.; Hvam, L.; Haug, A. Enablers and Barriers to the Implementation of Digital Twins in the Process Industry: A Systematic Literature Review. In Proceedings of the 2020 IEEE International Conference on Industrial Engineering and Engineering Management (IEEM), Singapore, 14–17 September 2020; pp. 959–964. [[CrossRef](#)]
66. Fuller, A.; Fan, Z.; Day, C.; Barlow, C. Digital Twin: Enabling Technologies, Challenges and Open Research. *IEEE Access* **2020**, *8*, 108952–108971. [[CrossRef](#)]
67. Boje, C.; Guerriero, A.; Kubicki, S.; Rezzgui, Y. Towards a semantic Construction Digital Twin: Directions for future research. *Autom. Constr.* **2020**, *114*, 103179. [[CrossRef](#)]
68. Mabkhot, M.M.; Al-Ahmari, A.M.; Salah, B.; Alkhalefah, H. Requirements of the Smart Factory System: A Survey and Perspective. *Machines* **2018**, *6*, 23. [[CrossRef](#)]
69. Moyné, J.; Qamsane, Y.; Balta, E.C.; Kovalenko, I.; Faris, J.; Barton, K.; Tilbury, D.M. A Requirements Driven Digital Twin Framework: Specification and Opportunities. *IEEE Access* **2020**, *8*, 107781–107801. [[CrossRef](#)]
70. Weskamp, J.N.; Ghosh Chowdhury, A.; Pethig, F.; Wisniewski, L. Architecture for Knowledge Exploration of Industrial Data for Integration into Digital Services. In Proceedings of the 2020 IEEE Conference on Industrial Cyberphysical Systems (ICPS), Tampere, Finland, 10–12 June 2020; Volume 1, pp. 98–104. [[CrossRef](#)]
71. Negri, E.; Fumagalli, L.; Garetti, M.; Tanca, L. Requirements and languages for the semantic representation of manufacturing systems. *Comput. Ind.* **2016**, *81*, 55–66. [[CrossRef](#)]
72. Tao, F.; Zhang, M.; Nee, A.Y.C. Chapter 3—Five-Dimension Digital Twin Modeling and Its Key Technologies. In *Digital Twin Driven Smart Manufacturing*; Tao, F., Zhang, M., Nee, A.Y.C., Eds.; Academic Press: Cambridge, MA, USA, 2019; pp. 63–81. [[CrossRef](#)]
73. Assad Neto, A.; Ribeiro da Silva, E.; Deschamps, F.; Pinheiro de Lima, E. Digital twins in manufacturing: An assessment of key features. *Proced. CIRP* **2021**, *97*, 178–183. [[CrossRef](#)]
74. Gorecky, D.; Schmitt, M.; Loskyll, M.; Zühlke, D. Human-machine-interaction in the industry 4.0 era. In Proceedings of the 2014 12th IEEE International Conference on Industrial Informatics (INDIN), Porto Alegre, Brazil, 27–30 July 2014; pp. 289–294. [[CrossRef](#)]
75. Gehrman, C.; Gunnarsson, M. A Digital Twin Based Industrial Automation and Control System Security Architecture. *IEEE Trans. Ind. Inform.* **2020**, *16*, 669–680. [[CrossRef](#)]
76. Semeraro, C.; Lezoche, M.; Panetto, H.; Dassisti, M. Digital twin paradigm: A systematic literature review. *Comput. Ind.* **2021**, *130*, 103469. [[CrossRef](#)]
77. Massel, L.V.; Massel, A.G. Development Of Digital Twins And Digital Shadows of Energy Objects And Systems Using Scientific Tools For Energy Research. *E3S Web Conf.* **2020**, *209*, 2019. [[CrossRef](#)]
78. Kohne, T.; Theisinger, L.; Scherff, J.; Weigold, M. Data and optimization model of an industrial heat transfer station to increase energy flexibility. *Energy Inform.* **2021**, *4*, 1–17. [[CrossRef](#)]
79. Tao, F.; Zhang, M. Digital Twin Shop-Floor: A New Shop-Floor Paradigm Towards Smart Manufacturing. *IEEE Access* **2017**, *5*, 20418–20427. [[CrossRef](#)]
80. Tao, F.; Zhang, M.; Liu, Y.; Nee, A. Digital twin driven prognostics and health management for complex equipment. *CIRP Ann.* **2018**, *67*, 169–172. [[CrossRef](#)]

81. Stark, R.; Damerou, T. Digital Twin. In *CIRP Encyclopedia of Production Engineering*; Springer: Berlin/Heidelberg, Germany, 2019; pp. 1–8. [\[CrossRef\]](#)
82. Abburu, S.; Berre, A.J.; Jacoby, M.; Roman, D.; Stojanovic, L.; Stojanovic, N. COGNITWIN—Hybrid and Cognitive Digital Twins for the Process Industry. In Proceedings of the 2020 IEEE International Conference on Engineering, Technology and Innovation (ICE/ITMC), Cardiff, UK, 15–17 June 2020; pp. 1–8. [\[CrossRef\]](#)
83. Zheng, Y.; Yang, S.; Cheng, H. An application framework of digital twin and its case study. *J. Ambient. Intell. Humaniz. Comput.* **2019**, *10*, 1141–1153. [\[CrossRef\]](#)
84. Lee, J.; Bagheri, B.; Kao, H.A. A Cyber-Physical Systems architecture for Industry 4.0-based manufacturing systems. *Manuf. Lett.* **2015**, *3*, 18–23. [\[CrossRef\]](#)
85. Talkhestani, B.A.; Jung, T.; Lindemann, B.; Sahlab, N.; Jazdi, N.; Schloegl, W.; Weyrich, M. An architecture of an Intelligent Digital Twin in a Cyber-Physical Production System. *Automatisierungstechnik* **2019**, *67*, 762–782. [\[CrossRef\]](#)
86. Bader, S.; Barnstedt, E.; Bedenbender, H.; Billmann, M.; Boss, B.; Braunmandl, A.; Clauer, E.; Deppe, T.; Diedrich, C.; Flubacher, B.; et al. *Details of the Asset Administration Shell. Part 1—The Exchange of Information between Partners in the Value Chain of Industrie 4.0 (Version 2.0)*; Federal Ministry for Economic Affairs and Energy: Berlin, Germany, 2019.
87. Bader, S.; Berres, B.; Boss, B.; Gatterburg, A.; Hoffmeister, M.; Kogan, Y.; Köpke, A.; Lieske, M.; Miny, T.; Neidig, J.; et al. *Details of the Asset Administration Shell. Part 2—Interoperability at Runtime—Exchanging Information via Application Programming Interfaces*; Federal Ministry for Economic Affairs and Energy: Berlin, Germany, 2020.
88. Bouter, C.; Pourjafarian, M.; Simar, L.; Wilterdink, R. Towards a Comprehensive Methodology for Modelling Submodels in the Industry 4.0 Asset Administration Shell. In Proceedings of the 2021 IEEE 23rd Conference on Business Informatics (CBI), Bolzano, Italy, 1–3 September 2021; Volume 2, pp. 10–19. [\[CrossRef\]](#)
89. Jacoby, M.; Volz, F.; Weißenbacher, C.; Stojanovic, L.; Usländer, T. An approach for Industrie 4.0-compliant and data-sovereign Digital Twins: Realization of the Industrie 4.0 Asset Administration Shell with a data-sovereignty extension. *Automatisierungstechnik* **2021**, *69*, 1051–1061. [\[CrossRef\]](#)
90. Adolphs, P.; Bedenbender, H.; Dirzus, D.; Martin, E. *Reference Architecture Model Industrie 4.0 (RAMI4.0)*; Technical Report July; VDI/VDE: Gesellschaft, Germany, 2015.
91. Bader, S.R.; Maleshkova, M. The Semantic Asset Administration Shell. In Proceedings of the Semantic Systems. The Power of AI and Knowledge Graphs, Karlsruhe, Germany, 9–12 September 2019; Acosta, M., Cudré-Mauroux, P., Maleshkova, M., Pellegrini, T., Sack, H., Sure-Vetter, Y., Eds.; Springer International Publishing: Cham, Switzerland, 2019; pp. 159–174. [\[CrossRef\]](#)
92. Al-Ali, A.R.; Gupta, R.; Zaman Batool, T.; Landolsi, T.; Aloul, F.; Al Nabulsi, A. Digital Twin Conceptual Model within the Context of Internet of Things. *Future Internet* **2020**, *12*, 163. [\[CrossRef\]](#)
93. Rathore, M.M.; Shah, S.A.; Shukla, D.; Bentafat, E.; Bakiras, S. The Role of AI, Machine Learning, and Big Data in Digital Twinning: A Systematic Literature Review, Challenges, and Opportunities. *IEEE Access* **2021**, *9*, 32030–32052. [\[CrossRef\]](#)
94. Human, C.; Basson, A.H.; Kruger, K. Digital Twin Data Pipeline Using MQTT in SLADTA. In Proceedings of the International Workshop on Service Orientation in Holonic and Multi-Agent Manufacturing, Paris, France, 1–2 October 2020; Springer: Berlin/Heidelberg, Germany, 2020; pp. 111–122. [\[CrossRef\]](#)
95. Naik, N. Choice of effective messaging protocols for IoT systems: MQTT, CoAP, AMQP and HTTP. In Proceedings of the 2017 IEEE International Systems Engineering Symposium (ISSE), Vienna, Austria, 11–13 October 2017; pp. 1–7. [\[CrossRef\]](#)
96. Profanter, S.; Tekat, A.; Dorofeev, K.; Rickert, M.; Knoll, A. OPC UA versus ROS, DDS, and MQTT: Performance Evaluation of Industry 4.0 Protocols. In Proceedings of the 2019 IEEE International Conference on Industrial Technology (ICIT), Melbourne, Australia, 13–15 February 2019; pp. 955–962. [\[CrossRef\]](#)
97. Data Flow and Communication Framework Supporting Digital Twin for Geometry Assurance, Volume 2: Advanced Manufacturing. In Proceedings of the ASME International Mechanical Engineering Congress and Exposition, Tampa, FL, USA, 3–9 November 2017. [\[CrossRef\]](#)
98. Qi, Q.; Tao, F.; Hu, T.; Anwer, N.; Liu, A.; Wei, Y.; Wang, L.; Nee, A. Enabling technologies and tools for digital twin. *J. Manuf. Syst.* **2021**, *58*, 3–21. [\[CrossRef\]](#)
99. Ehrlinger, L.; Wöß, W. Towards a Definition of Knowledge Graphs. *SEMANTiCS Posters Demos SuCCESS* **2016**, *48*, 2.
100. Schachinger, D.; Kastner, W.; Gaida, S. Ontology-based abstraction layer for smart grid interaction in building energy management systems. In Proceedings of the 2016 IEEE International Energy Conference (ENERGYCON), Leuven, Belgium, 4–8 April 2016; pp. 1–6. [\[CrossRef\]](#)
101. Steindl, G.; Kastner, W. Query Performance Evaluation of Sensor Data Integration Methods for Knowledge Graphs. In Proceedings of the 2019 Big Data, Knowledge and Control Systems Engineering (BdKCSE), Sofia, Bulgaria, 21–22 November 2019; pp. 1–8. [\[CrossRef\]](#)
102. Frühwirth, T.; Kastner, W.; Krammer, L. A methodology for creating reusable ontologies. In Proceedings of the 2018 IEEE Industrial Cyber-Physical Systems (ICPS), Saint Petersburg, Russia, 15–18 May 2018; pp. 65–70. [\[CrossRef\]](#)
103. Steindl, G.; Kastner, W. Ontology-Based Model Identification of Industrial Energy Systems. In Proceedings of the 2020 IEEE 29th International Symposium on Industrial Electronics (ISIE), Delft, The Netherlands, 17–19 June 2020; pp. 1217–1223. [\[CrossRef\]](#)
104. Janowicz, K.; Haller, A.; Cox, S.J.; Le Phuoc, D.; Lefrançois, M. SOSA: A lightweight ontology for sensors, observations, samples, and actuators. *J. Web Semant.* **2019**, *56*, 1–10. [\[CrossRef\]](#)

105. Küçük, D.; Salor, Ö.; Inan, T.; Çadırcı, I.; Ermiş, M. PQONT: A domain ontology for electrical power quality. *Adv. Eng. Inform.* **2010**, *24*, 84–95. [[CrossRef](#)]
106. Devanand, A.; Karmakar, G.; Krdzavac, N.; Rigo-Mariani, R.; Foo Eddy, Y.; Karimi, I.A.; Kraft, M. OntoPowSys: A power system ontology for cross domain interactions in an eco industrial park. *Energy AI* **2020**, *1*, 100008. [[CrossRef](#)]
107. Booshehri, M.; Emele, L.; Flügel, S.; Förster, H.; Frey, J.; Frey, U.; Glauer, M.; Hastings, J.; Hofmann, C.; Hoyer-Klick, C.; et al. Introducing the Open Energy Ontology: Enhancing data interpretation and interfacing in energy systems analysis. *Energy AI* **2021**, *5*, 100074. [[CrossRef](#)]
108. Morbach, J.; Wiesner, A.; Marquardt, W. OntoCAPE—A (re)usable ontology for computer-aided process engineering. *Comput. Chem. Eng.* **2009**, *33*, 1546–1556. [[CrossRef](#)]
109. Devanand, A.; Zhou, L.; Karimi, I.A.; Kraft, M. An Ontology Based Cyber-infrastructure for the Development of Smart Eco Industrial Parks. In Proceedings of the 13th International Symposium on Process Systems Engineering (PSE 2018), San Diego, CA, USA, 1–5 July 2018; Eden, M.R., Ierapetritou, M.G., Towler, G.P., Eds.; Elsevier: Amsterdam, The Netherlands, 2018; Volume 44, pp. 2047–2052. [[CrossRef](#)]
110. Martin, D.; Burstein, M.; Hobbs, J.; Lassila, O.; McDermott, D.; McIlraith, S.; Narayanan, S.; Paolucci, M.; Parsia, B.; Payne, T.; et al. OWL-S: Semantic markup for web services. *W3C Memb. Submiss.* **2004**, *22*. Available online: <https://www.w3.org/Submission/OWL-S/> (accessed on 10 June 2022).
111. Hobbs, J.; Little, C. Time Ontology in OWL. W3C Candidate Recommendation. *World Wide Web Consort.* **2020**, *27*, 3–36.
112. Mitterhofer, M.; Schneider, G.F.; Stratbücker, S.; Sedlbauer, K. An FMI-enabled methodology for modular building performance simulation based on Semantic Web Technologies. *Build. Environ.* **2017**, *125*, 49–59. [[CrossRef](#)]
113. Publio, G.C.; Esteves, D.; Ławrynowicz, A.; Panov, P.; Soldatova, L.; Soru, T.; Vanschoren, J.; Zafar, H. ML-Schema: Exposing the Semantics of Machine Learning with Schemas and Ontologies. *arXiv* **2018**, arXiv:1807.05351.
114. Ocker, F.; Vogel-Heuser, B.; Paredis, C.J. A framework for merging ontologies in the context of smart factories. *Comput. Ind.* **2022**, *135*, 103571. [[CrossRef](#)]
115. Richardson, C. *Microservices Patterns: With Examples in Java*; Manning: Hong Kong, China, 2018.
116. Steindl, G. Digital Twin Service Framework. 2021. Available online: <https://github.com/Smart-Industrial-Concept/DigitalTwinServiceFramework> (accessed on 25 January 2022).
117. Fernández-López, M.; Gómez-Pérez, A.; Juristo, N. METHONTOLOGY: From Ontological Art Towards Ontological Engineering. In Proceedings of the Ontological Engineering AAAI-97 Spring Symposium Series, Stanford, CA, USA, 24–26 March 1997; American Association for Artificial Intelligence: Menlo Park, CA, USA, 1997; pp. 24–26. Available online: <http://oa.upm.es/5484> (accessed on 10 June 2022).

Paper 5


A digital twin-based adaptive optimization approach applied to waste heat recovery in green steel production: Development and experimental investigation

submitted for publication¹ to Applied Energy in collaboration with Paul Schwarzmayr, Felix Birkelbach, Florian Javernik, Michael Schwaiger, and René Hofmann

This paper presents the implementation and evaluation of several micro-services on the DT platform, introduced in Paper 4, that automate MILP model updating and optimization. The use case is a waste heat recovery process in steel production. The hot off-gas from an electric arc furnace (EAF) is used for steam generation, which is needed for further metal processing, district heating, and electricity production. To balance the batch-wise operation of the EAF and the ramping restrictions of the steam generator, a PBTES is used. However, due to the high dust load of the EAF off-gas, the pressure drop in the PBTES systems increases gradually and the TES charging/discharging power decreases. This energy system was virtually modeled in a MILP-based UC problem. The PBTES test rig in our lab constitutes the physical entity of the instantiated DT. The detailed set-up of the test rig and the specific implementation of my DT platform (Paper 4) was presented in co-author publication F. The metrics of the behavior of our PBTES test rig were scaled up to this virtual energy system and controlled by DT services. Vice versa, the MILP optimization model provided the schedule for the test rig operation. Thus, the DT approaches could be tested in actual operation, featuring bidirectional real-time communication. The developed DT micro-services and workflows, presented in this paper, guarantee that (1) deviations between virtual entity models and physical entity behavior are detected, (2) the models are automatically updated, and (3) subsequently linearized to suit the MILP approach and (4) used for live operational optimization. This paper contributed to the answer to research question *RQ 2* in that benefits of the DT approach compared to state-of-the-art MILP optimization could be experimentally evaluated.

My contribution: Conceptualization, Methodology, Software, Formal analysis, Experimental investigation, Data curation, Writing – original draft, review & editing, Visualization.

L. Kasper, P. Schwarzmayr, F. Birkelbach, F. Javernik, M. Schwaiger & R. Hofmann (2023b). “A digital twin-based adaptive optimization approach applied to waste heat recovery in green steel production: Development and experimental investigation”. In: Applied Energy. Submitted for publication on 2023-06-30.

¹This paper was submitted for publication to the journal Applied Energy on 2023-06-30. The submitted manuscript is included on the next pages. You can check for updates at the author’s ORCID:  <https://orcid.org/0000-0001-9474-3021>

A digital twin-based adaptive optimization approach applied to waste heat recovery in green steel production: Development and experimental investigation

Lukas Kasper^{a,*}, Paul Schwarzmayr^a, Felix Birkelbach^a, Florian Javernik^b, Michael Schwaiger^b, René Hofmann^a

^aTU Wien, Institute of Energy Systems and Thermodynamics, Getreidemarkt 9/BA, 1060 Vienna, Austria
^bvoestalpine Stahl Donawitz GmbH, Kerpelystraße 199, 8700 Leoben, Austria

Abstract

Renewable-dominated power grids will require industry to run their processes in accordance with the availability of energy. Therefore, industrial energy systems must increase flexibility and energy efficiency of operation. At the same time, digitalization provides new solutions to leverage the untapped optimization potential to address these challenges. Mathematical optimization methods such as mixed-integer linear programming (MILP) are widely used to predict optimal operation plans for industrial systems. MILP models are difficult to adapt, but the viability of the predicted plans relies on accurate underlying models of the actual behavior. New automation paradigms, such as the digital twin (DT), can overcome these current drawbacks.

In this work, we present the implementation and experimental evaluation of several micro-services on a standardized five-dimensional DT platform that automate MILP model adaption and operation optimization. These micro-services guarantee that, (1) deviations between the physical entity and its virtual entity models are detected, (2) the models are adapted accordingly, (3) subsequently linearized to suit the MILP approach and (4) used for live operational optimization. The developed services and DT workflows that orchestrate them were experimentally tested with a packed bed thermal energy storage test rig that acts as a physical entity. A waste heat recovery use case in steel production is used as the evaluation scenario. Using the DT platform and the developed services, energy recovery can be improved and revenue generated by waste heat utilization can be increased compared to a state-of-the-art optimization approach.

Keywords: Thermal energy storage, Digital twin (DT), Mixed integer linear programming (MILP), Iron and Steel industry, Waste heat recovery, Operation optimization

1. Introduction

1.1. Motivation

Heat generation in the industry sector accounts for roughly 20% of global anthropogenic CO₂ emissions [1]. This ratio increases to over 40% of total emissions [2] when also emissions related to the industry's electricity demand are allocated to it. Tremendous efforts are made to reduce these emissions and thus mitigate environmental impact.

A major lever for this is reducing primary energy consumption through energy efficiency measures. Waste heat recovery, e.g., by using thermal energy storage (TES) for decoupling energy supply and demand, is considered a key aspect [3]. Yet, Martin & Chiu [4] found that the industry still restrains from TES application due to (1) economic feasibility, and (2) increased complexity to processes, hence increased operational risk. Thus, optimal utilization of TES potential is required, and, therefore, modeling and optimization of energy systems is crucial. However, this remains a challenging task, especially due to highly individualized components that feature a long usage lifetime operated under

*Corresponding author

Email address: lukas.kasper@tuwien.ac.at (Lukas Kasper)

harsh conditions and thus changing properties and behavior.

1.2. Background

1.2.1. Operational optimization of energy systems

Optimal control of industrial energy system operation is typically realized via at least two automated control layers [5]. Basic process control, via, e.g., proportional–integral–derivative (PID) controllers, is applied for the low-level realization of system states and must account for fast dynamics and possible disturbances [6]. On a higher level, typically unit commitment (UC) problems are solved to decide on the economically timed operation of energy supply, storage, and consumption for a prediction horizon of hours to months. We refer to this higher level of economic process control as operational optimization.

The UC problem, originating in electric power system research [7], has also been widely applied to thermal processes [8], where it is also often referred to as energy management problem [9, 10]. Various methods have been proposed to solve the UC problem, such as, for example, heuristic priority listing, dynamic programming, Lagrangian relaxation, simulated annealing, fuzzy logic, artificial neural networks, genetic algorithms, and linear and mixed-integer linear programming (MILP) [5]. Moser et al. [9] state that modern energy management is most commonly based on MILP. A MILP problem is a mathematical optimization problem featuring a linear objective function and linear inequality constraints on the variables, which can be either continuous or integer-valued. The main benefit of MILP is the existence of powerful solvers, which can solve even large optimization problems in a reasonable time and are accessible from almost any programming language [9]. Furthermore, MILP avoids the risk of terminating at non-global minima, associated with non-linear optimization [11]. The problem of highly nonlinear dependencies has been partly solved by numerous piecewise linear approximations applicable to energy system components that have been proposed in recent years (see, e.g., [12, 13, 14]).

Despite the successful demonstration of MILP implementations for various applications, a major handicap is that the outcome of optimization heavily relies on the accuracy of the underlying models. Especially for energy system components, where, for example, dust and fouling lead to continuously

changing component behavior, adaptive modeling and optimization would provide huge benefits for their operation. This is where digital twin (DT) technology could be a practical enabler [15].

1.2.2. Digital twin technology in the energy sector

The DT concept has received increasing attention over the last few years [16]. While there exist many different definitions [17, 18] and industrial application scenarios [19], one of the key pillars of DT technology is keeping digital representations of real-world plants in sync with their physical counterparts [20, 21]. In contrast to a simple virtual representation (i.e., a model), a DT features automated bidirectional information and data exchange between the real and virtual systems [20].

These characteristics make a DT perfectly suited to meet the challenge of adaptive operation optimization of industrial energy systems introduced above. According to a recent review by Yu et al. [16], DT technology could fundamentally change the way industrial energy systems operate. The promise of DTs is to increase automation and deliver more intelligent and efficient operation.

However, Sleiti et al. [22] found that DT research related to the energy sector is still in its infancy stage. Most crucially, the majority of proposed DT in the energy domain lack automated bidirectional connectivity between virtual and physical entity [16]. Yu et al. [16] concluded that adaptive DT technology for real-world behavior changes is a critical future research direction.

1.3. Scope of this work

Based on the state of the art, outlined above, the necessity for adaptive modeling methodologies is clear. These are especially valuable for the operational optimization of industrial energy systems due to the huge potential for reducing energy demand and CO₂ emissions.

Therefore, in this work, we

- present a DT-based approach to achieve adaptive TES modeling and MILP-based optimization for this use case,
- establish the set of DT services necessary to provide these automated adaptation capabilities,
- introduce a use case of TES integration in steel production that requires real-time adaptive optimization for energy-efficient operation, and,

- test and validate the developed approach in live operation on a packed bed TES test rig, emulating the use case.

1.4. Paper structure

After this introduction, this paper is organized as follows: Section 2 introduces the industrial use case in steel production, which provides means of evaluation of this work, and explains the necessity for the developed DT methodology in this use case. Section 3 briefly explains the DT platform that provides the foundation for this work, the TES test rig it is applied to, and a state-of-the-art UC problem of the use case, modeled via MILP. The novel DT-based methodology is presented in Section 4 and the experimental results of its application are given in Section 5. After this, Section 6 gives a brief conclusion of this work and an outlook on further research.

2. Use case and problem statement

2.1. Industrial energy system use case

The considered use case in this paper is a steel production process and the subsequent off-gas heat recovery. The iron and steel industry accounts for approximately 8% of annual global anthropogenic CO₂ emissions [23]. These emissions must be reduced drastically to realize the current 1.5 °C goal defined in the Paris Agreement. That is, despite the International Energy Agency’s predicted growing steel demand from around 1.9 billion tons in 2019 to over 2.5 billion tons in 2050 [24]. Therefore, breakthrough decarbonization technologies, such as electric arc furnaces (EAF) are essential [25]. However, still roughly a third of the total energy input is leaving the EAF via the sensible heat of the off-gas [26, 27]. Therefore, there is immense potential for energy recovery [28]. Given the substantial costs associated with implementing new low-emission strategies, a viable approach for operators of steel plants to significantly progress towards eco-friendly steel production is by installing heat recovery systems [27]. For an overview of waste heat recovery in the iron and steel industry, we refer to a recent analysis of Inayat [29].

The Austrian company *voestalpine Stahl Donawitz GmbH* recently announced the construction approval of a new EAF at their site in Leoben, Austria, as part of their “greentec steel” transformation path [30].

The company’s goal is a reduction of 30 % of the current CO₂ emissions from 2027 onward, and CO₂-neutral steel production by 2050. The first transformation step sees one of the two current steel routes, with a blast furnace and an LD converter each, replaced by an EAF. In this paper, we therefore consider the heat recovery process of the EAF route individually, albeit it will be connected to the existing industrial energy system at the site. This corresponds to the current medium-term adaption plans.

In the considered energy system use case, illustrated in Figure 1, the thermal energy of the hot off-gas of the EAF is recovered in a waste heat boiler. A similar system, specifically designed for steam generation of EAF off-gas, was designed by Steinparzer et al. [31] as a five-pass system including radiation passes, evaporation panels, evaporation bundles, and an economizer for preheating feed-water. We will reduce this system to its basic purpose from here on and simply call it steam generator (SG). The generated steam is valuable for multiple purposes. Firstly, a large amount of saturated steam is needed for further metal processing at the site. Secondly, lower-temperature heat can be decoupled from the steam system to provide facility heating on-site and district heating for the adjoining city. Thirdly, saturated steam can be superheated in the existing SG and fed into a turbine to produce electricity. Since the EAF operates as a batch process, its hot off-gas flow features not only high volatility but also periods of disruption [32, 31]. The SG, on the other hand, must adhere to power ramping constraints and should ideally never be shut down completely. Subjecting a SG to overly fluctuating input power can lead to excessive material stresses due to pressure and temperature gradients, and a wide range of other potentially life-limiting factors within the system [33]. Steinparzer et al. [31] and Keplinger et al. [27] argue that this challenge should be solved by integrating a TES between the EAF and the SG. During off-gas peaks, the TES can be charged, and during EAF downtimes or periods of lower heat flow occur, e.g., during initial raw material heating, the TES can be discharged to provide steady input power to the SG. Manente et al. [34] recently presented a procedure to identify the best TES option for the heat recovery of discontinuous flue gas in steel production for steam generation. They found that a packed bed thermal energy storage (PBTES) using rocks as a storage medium is the optimal choice from a

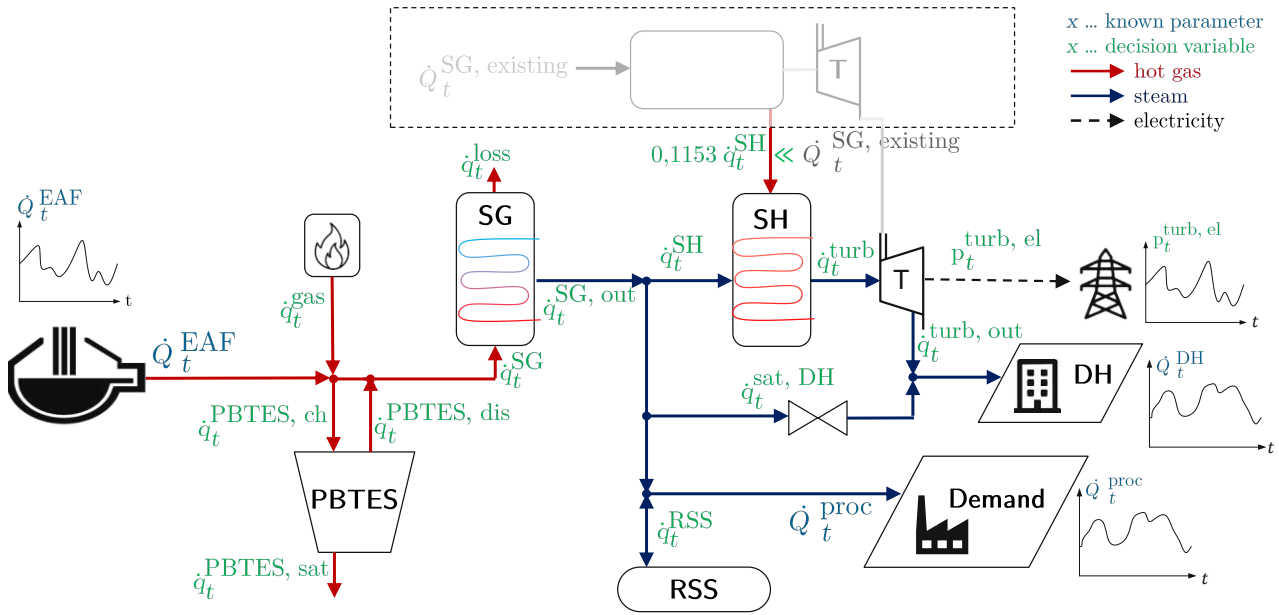


Figure 1: Sketch of the industrial use case that is modeled as a virtual energy system in this work

techno-economic perspective. Thus, in our use case a PBTES is considered to smoothen the volatile EAF off-gas flow, hence accommodating the load requirements of the SG. Comprehensive reviews on this type of TES technology can be found in the work of Gautam et al. [35, 36] and Xie et al. [37].

Another major challenge for EAF heat recovery systems are the high gas velocities in the inlet duct and the high dust load of the EAF exhaust gases [31]. Bause et al. [38] states a typical iron oxide dust concentration in EAF off-gas of 20 g/Nm^3 . Put another way, about 15 to 25 kg of dust per ton of produced steel accumulates [39]. Typically, this is why a drop-out box is arranged after the inlet duct of the hot gas line, which separates the coarse dust particles by gravitation [40, 28]. However, the majority of the EAF dust consists of particles below a size of $20 \mu\text{m}$ [39]. This raises the question of how the dust-laden exhaust gas used as heat transfer fluid (HTF) will affect the PBTES performance. Investigations are currently underway to quantify this behavior [41], but it can be expected that the small particles accumulate in the packed bed of the PBTES [42]. It is well known that dust deposits increase the air pressure drop across a packed bed [43, 44]. Thus, we deduce that the available PBTES charging/discharging power rates will gradually decrease based on the dust-induced pressure drop and a maximum air fan power at the end of the hot gas duct. This is a major effect besides, e.g., the

degrading heat capacity of PBTES storage media [45]. These degradation effects not only lead to design challenges for the heat recovery system but also call for intelligent operation approaches that consider the reduced PBTES power.

2.2. Problem statement

Our goal is to provide accurate operational scheduling of the heat recovery system in the presented industrial use case. The state-of-the-art approach for such economic operation problems is MILP [46, 9]. However, the changing physical behavior of system components is a challenge to optimal operation. This is where DT technology can make a great impact. As explained in Section 1, one of the main features of a DT should be to synchronize the models of its physical counterpart according to current behavior. Leveraging a DT for adaptive MILP modeling can therefore solve a major operational problem in the considered use case. A DT platform for industrial energy systems provides a foundation for this, see Section 1.2.2. This platform, however, needs to be equipped with appropriate functionality encapsulated in DT services.

To the best of our knowledge, there is no literature available on the topic of achieving this automated adaptivity using a DT. Therefore, we continue our previous work on DT technology for industrial energy systems and determine which services are needed for fulfilling the use case and

how they are composed. We further elaborate on the data transfer within the DT platform and the necessary workflow connectivity between the services. We present proof of the feasibility of the presented approach via experimental investigation on a PBTES test rig.

3. Material and Methods

3.1. Digital twin platform

The foundation of our DT approach is the DT platform developed in previous work, building on the Generic Digital Twin Architecture (GDTA) [47]. The DT platform was introduced by Kasper et al. [48]. Furthermore, Schwarzmayr et al. [49] presented the instantiation of the DT platform on the PBTES test rig, introduced in Section 3.2.

The instantiated DT platform is illustrated in Figure 2. It follows the basic five-dimensional DT concept introduced by Tao et al. [50]. Accordingly, it consists of (1) the physical entity, (2) the virtual entity, (3) the connection dimension, (4) the data dimension, and (5) the service dimension. The physical entity is connected to the virtual space via programmable logic controllers (PLC)s and the supervisory control and data acquisition (SCADA) system. New data points are sent to the message broker (connection dimension) and control signals are received. The virtual entity should be able to accurately represent the behavior and properties of the physical entity. This can be fulfilled by various types of virtual models. The data dimension provides semantic structuring of all data in the DT platform and a central access point for decentralized data storage. At the core of it is a knowledge graph (see, e.g., [51]), consisting of several ontologies and a built-in reasoner. We applied the Ontop framework [52] for this. With our implementation of the data dimension, it is possible to query and receive any information within the scope of the DT from a single endpoint using SPARQL Protocol and RDF Query Language (SPARQL). The aim of the service dimension is to encapsulate various functionalities of the DT into micro-services that provide user-friendly interfaces and allow easy on-demand use and adaptation. The timely and sequential coordination of various service instances is realized with a service orchestrator. We use a workflow engine, based on Business Process Model and Notation (BPMN) workflows for this.

For more details on the DT platform, we must refer to our previous publications [48, 49].

3.2. Packed bed thermal energy storage test rig

A lab-scale test rig of a PBTES is used for experimental evaluations in this work. The test rig, situated at the laboratory of TU Wien, consists of a vertically standing steel vessel that is filled with slag as storage material. The slag, a by-product from the iron and steel industry, is chosen as storage material because of its thermo-physical properties and low costs. It consists of irregularly shaped porous rocks which leads to an enhanced heat transfer between storage material and HTF and results in an even and homogeneous perfusion of the packed bed. To minimize heat losses to the surrounding the storage vessel and all piping is insulated with multiple layers of ceramic wool, rock wool and aluminum sheeting. For charging and discharging, the test rig can be supplied with air from an air supply unit (ASU). Air temperatures from 20 °C to 400 °C and a mass flow of 100 kg h⁻¹ to 400 kg h⁻¹ are available. To measure the current state of the storage, the test rig is equipped with multiple temperature and differential pressure sensors. Detailed descriptions of the test rig, its instrumentation, and the properties of the used materials can be found in the studies of Schwarzmayr et al. [49, 53]. Figure 3 shows the PBTES test rig with and without insulation as well as a photograph of the storage material.

To charge the test rig, the ASU provides hot air that enters the storage from the top, passes through the packed bed, thereby delivering heat to the storage material, and exits the storage at the bottom. To recover the heat stored in the TES, the ASU provides cold air that passes through the packed bed in the opposite direction and is thereby heated. Due to physical restrictions of the ASU, a 15 minute downtime between charging and discharging periods has to be maintained. These downtimes are necessary to preheat/precool the ASU so that it can deliver the HTF temperatures that are required for charging and discharging the storage. In reality, the HTF used to charge the TES will be accompanied by a significant amount of metal-oxide dust. As explained in Section 2, this will lead to a gradual degradation of the thermal performance of the PBTES. To simulate this effect of gradual degradation of the thermal performance in the laboratory setup, the HTF mass flow that is requested from the ASU is scaled with a factor that is smaller than one and gradually decreases over time.

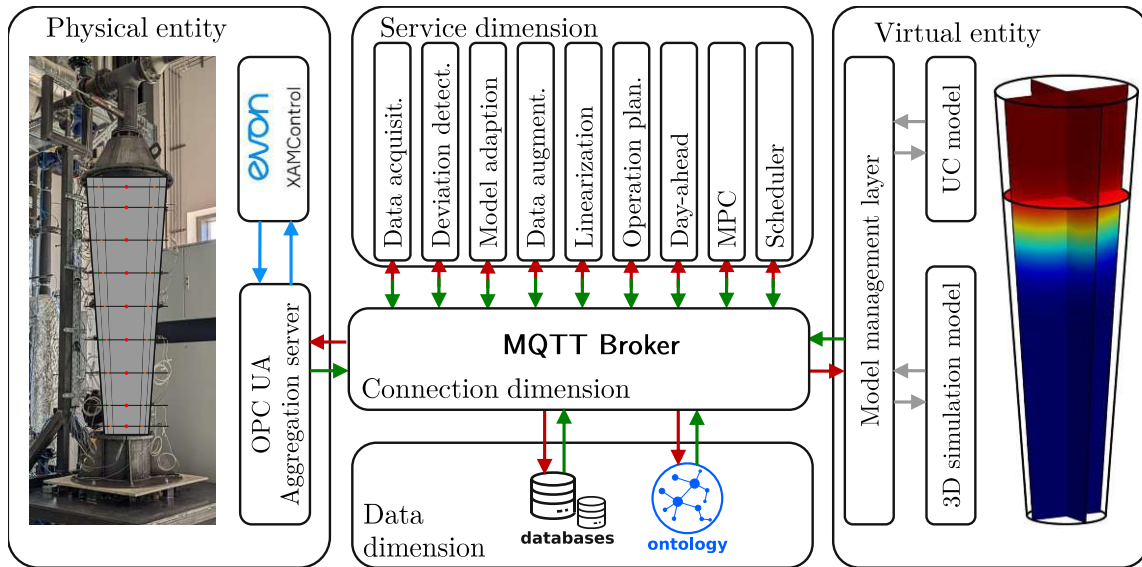


Figure 2: Five-dimensional DT platform implemented for the PBTES test rig. Adapted from the author's previous publication [49].

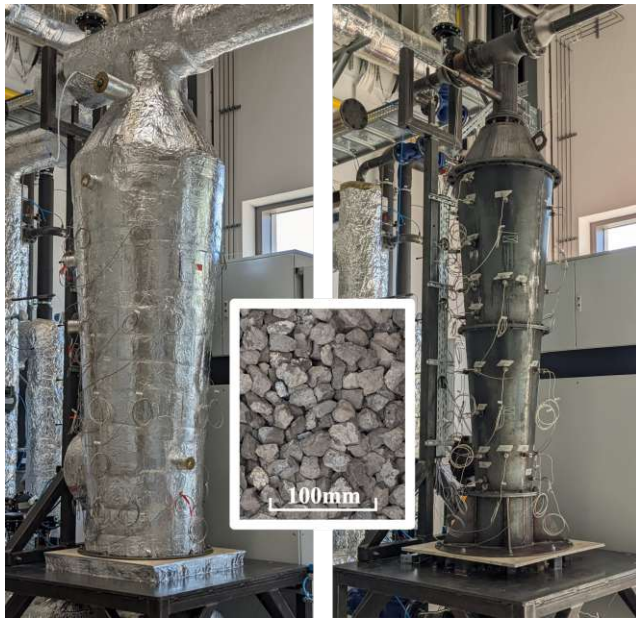


Figure 3: Test rig of a PBTES at the laboratory of TU Wien: with thermal insulation (left), storage material (center), without thermal insulation (right). Reprinted from [53] with permission from Elsevier.

3.2.1. Packed bed thermal energy storage operating behaviour

The PBTES' charging and discharging power depend on the temperature spread of the in- and out-flowing HTF. This temperature spread decreases towards the end of a cycle, hence thermal power is decreasing. During charging, we speak of saturation of the out-flowing HTF, and these saturation losses must be taken into account in operation in addition to the decreasing charging power. Furthermore, Koller et al. [14] showed that under dynamic operation, the PBTES power is not only dependent on the current SOC but also on the SOC at the end of the previous charging or discharging phase. To model partial cycle operation, also the initial SOC at the end of the previous charging or discharging phase must be taken into account. This behavior is illustrated in Figure 4.

3.3. Unit commitment model for the virtual energy system

The waste heat recovery use case, illustrated in Figure 1, is modeled via MILP. Here, the basic assumptions and fundamental modeling approaches are presented. In the remainder of this paper, we refer to this virtually modeled industrial use case as the virtual energy system (VES). In this paper, we consider the design of the VES as fixed. The design is not optimized but reasonable parameters

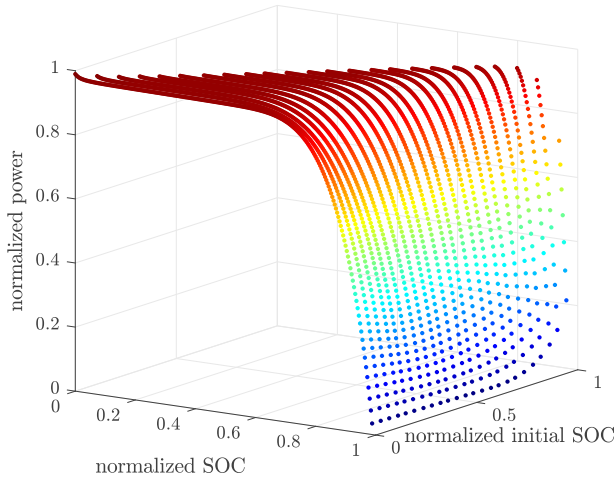


Figure 4: Dependency of the maximum charging power of a PBTES on the current SOC and the initial SOC at the last operation switch. The maximum discharging power features an equivalent but inverse dependency on the SOC.

were chosen, which are given in Appendix B. The evaluation input data is given in Appendix A.

The VES is modeled in a unit commitment (UC) formulation within a finite number n of discrete time steps $t \in \mathcal{T} = \{t_1, \dots, t_n\}$ at an equidistant time step width Δt . Energy flows in the VES are reduced to heat flows, i.e., neglecting temperature levels. This is a common approach in UC problems of industrial energy systems (see, e.g., [54, 55]), where temperature levels are considered at lower hierarchy control layers. Therefore, each unit $u \in \mathcal{U}$ is modeled via its thermal power $\dot{q}_t^u \in \mathbb{R}$ as decision variable in each time step. In this paper, decision variables are distinguished by lowercase writing and parameters are written in uppercase.

3.3.1. Basic unit power constraints

Some units are modeled with maximum ramping rates, hence their power is constrained between their minimum and maximum power ($\dot{Q}_{\min}^u, \dot{Q}_{\max}^u$) by

$$x_t^u \dot{Q}_{\min}^u \leq \dot{q}_t^u \leq x_t^u \dot{Q}_{\max}^u \quad \forall t \in \mathcal{T}, \quad (1)$$

with the binary decision variable $x_t^u \in \{0, 1\}$ denoting the on/off state of the unit u at a timestep t .

The ramping constraints are then given as

$$\begin{aligned} -\Delta \dot{Q}_{\text{ramp}}^u + (x_t^u - x_{t-1}^u) \left(\frac{\dot{Q}_{\min}^u}{\Delta t} - \Delta \dot{Q}_{\text{ramp}}^u \right) & \leq \frac{\dot{q}_t^u - \dot{q}_{t-1}^u}{\Delta t} \leq \\ -\Delta \dot{Q}_{\text{ramp}}^u + (x_t^u - x_{t-1}^u) \left(\frac{\dot{Q}_{\max}^u}{\Delta t} - \Delta \dot{Q}_{\text{ramp}}^u \right) & \quad \forall t \in \mathcal{T}, \quad (2) \end{aligned}$$

with, in this case, direction-independent maximum ramping rates $\Delta \dot{Q}_{\text{ramp}}^u$. Note, that the initial states $x_{t=0}^u$ and $\dot{q}_{t=0}^u$ must be provided.

For units featuring no ramping constraints and no minimal partial load (i.e. $\dot{Q}_{\min}^u = 0$), Equations (1)-(2) can be reduced to

$$\dot{Q}_{\min}^u \leq \dot{q}_t^u \leq \dot{Q}_{\max}^u \quad \forall t \in \mathcal{T}. \quad (3)$$

3.3.2. Storage formulation

The two TES units in this use case are modeled via a basic storage formulation, constraining the charging/discharging power rate \dot{q}_t^{TES} via

$$-\dot{Q}_{\max}^{\text{TES}} \leq \dot{q}_t^{\text{TES}} \leq \dot{Q}_{\max}^{\text{TES}} \quad \forall t \in \mathcal{T} \quad (4)$$

to a maximum available charging/discharging power rate $\dot{Q}_{\max}^{\text{TES}}$. Their state of charge (SOC) s_t^{TES} is constrained via

$$0 \leq s_t^{\text{TES}} \leq S_{\max}^{\text{TES}} \quad \forall t \in \mathcal{T} \quad (5)$$

to the TES unit's capacity S_{\max}^{TES} . The SOC changes are modeled neglecting conversion efficiencies which are assumed near one, but considering a thermal loss factor γ^{TES} . The factor expresses the ratio of the current SOC that dissipates through thermal losses during the time Δt . This results in the following set of equations:

$$s_{t+1}^{\text{TES}} = s_t^{\text{TES}} (1 - \gamma^{\text{TES}} \Delta t) - \dot{q}_t^{\text{TES}} \Delta t \quad \forall t \in \mathcal{T} \quad (6)$$

Note that the TES power rate is defined as negative when the storage is charged and that the final SOC $s_{t_{n+1}}^{\text{TES}}$ must be defined appropriately, so as not to discharge the storage completely at the end of the prediction horizon. The initial SOC value $s_{t_1}^{\text{TES}}$ is always set to the current SOC of the TES.

3.3.3. Packed bed thermal energy storage modeling

For the PBTES test rig, the basic storage constraints are extended with a formulation developed

by Koller et al. [14] to account for the nonlinear charging/discharging power rate dependency on the SOC, and for saturation losses during the charging process.

The charging/discharging power rate \dot{q}_t^{TES} of the PBTES, constrained by the basic formulation (see Section 3.3.2), is split into charging power $\dot{q}_t^{\text{PBTES, ch}}$ and discharging power $\dot{q}_t^{\text{PBTES, dis}}$, i.e.,

$$\dot{q}_t^{\text{TES}} = \dot{q}_t^{\text{PBTES, dis}} - \dot{q}_t^{\text{PBTES, ch}} \quad \forall t \in \mathcal{T}. \quad (7)$$

The binary variables $z_t^{\text{PBTES, ch}}, z_t^{\text{PBTES, dis}} \in \{0, 1\}$ are defined to take the value 1, if the PBTES is in charging or discharging state, respectively. Since our PBTES test rig features a minimum charging/discharging power $\dot{Q}_{\min}^{\text{PBTES}}$ due to limitations of the air supply unit, we introduced the minimum partial load constraints

$$\begin{aligned} z_t^{\text{PBTES, ch}} \dot{Q}_{\min}^{\text{PBTES}} &\leq \dot{q}_t^{\text{PBTES, ch}} \\ &\leq z_t^{\text{PBTES, ch}} \dot{Q}_{\max}^{\text{PBTES}} \quad \forall t \in \mathcal{T}, \end{aligned} \quad (8)$$

$$\begin{aligned} z_t^{\text{PBTES, dis}} \dot{Q}_{\min}^{\text{PBTES}} &\leq \dot{q}_t^{\text{PBTES, dis}} \\ &\leq z_t^{\text{PBTES, dis}} \dot{Q}_{\max}^{\text{PBTES}} \quad \forall t \in \mathcal{T}. \end{aligned} \quad (9)$$

In case the TES unit features a continuous power range, the left-hand side inequalities in equations (8) and (9) can be skipped.

The charging power is then constrained by

$$\begin{aligned} \dot{q}_t^{\text{PBTES, ch}} &\leq f^{\text{ch}} \left(\frac{s_t^{\text{TES}} + s_k^{\text{TES}}}{2}, h_t^{\text{ch}}, z_t^{\text{PBTES, ch}} \right) \\ &\forall t \in \mathcal{T}, k = \min\{t+1, t_n\}, \end{aligned} \quad (10)$$

and the discharging power is constrained analogously with f^{dis} . Here, f^{ch} and f^{dis} are linear functions of the stated decision variables. The auxiliary variables h_t^{ch} and h_t^{dis} represent the SOC at the end of the previous charging/discharging switch. For details on this formulation, which we consider too comprehensive to recapitulate, as well as for the constraints on the auxiliary variables $h_t^{\text{ch}}, h_t^{\text{dis}}$, we refer to Koller et al. [14].

The UC problem is further extended by the saturation losses $\dot{q}_t^{\text{PBTES, sat}}$, which are constrained by

$$\begin{aligned} \dot{q}_t^{\text{PBTES, sat}} &\geq f^{\text{sat}} \left(\dot{q}_t^{\text{PBTES, ch}}, z_t^{\text{PBTES, ch}}, T_t^{\text{spread}} \right) \\ &\forall t \in \mathcal{T}, \end{aligned} \quad (11)$$

with the linear function f^{sat} of the given decision variables. Here, T_t^{spread} denotes the temperature

spread at the PBTES outlet that can be constrained with the same linearized formulation as given in f^{ch} , albeit weighted to the maximum temperature spread instead of the maximum charging power. For details, we again refer to the original publication: [14]. To account for the limit in the total heat flow introduced to the PBTES during charging, we constrain $\dot{q}_t^{\text{PBTES, ch}}$ and $\dot{q}_t^{\text{PBTES, sat}}$ to the maximum available charging power of the PBTES:

$$\begin{aligned} 0 &\leq \dot{q}_t^{\text{PBTES, ch}} + \dot{q}_t^{\text{PBTES, sat}} \\ &\leq z_t^{\text{PBTES, ch}} \dot{Q}_{\max}^{\text{PBTES}} \quad \forall t \in \mathcal{T}. \end{aligned} \quad (12)$$

In contrast to Koller et al. [14], we do not implement the formulation for a minimum temperature requirement of gas stream mixing after the PBTES for the sake of simplicity of the UC model. However, this implementation would be straightforward.

3.3.4. Minimum downtime

The operation of our PBTES test rig must abide by a minimal downtime of 15 minutes between switches from charging to discharging and vice versa. This is due to limitations in the air supply unit, as presented in Section 3.2. Whenever the PBTES switches to idle mode, a bypass mode is activated to pre-heat or cool the air supply unit. To account for the downtime requirement in the operation schedule, a standard minimal downtime formulation is added to the UC problem, see, e.g., [56].

3.3.5. Energy balances

On the hot gas side, illustrated on the left side of Figure 1, the energy balance constraint

$$\begin{aligned} \dot{Q}_t^{\text{EAF}} + \dot{q}_t^{\text{gas}} &= \dot{q}_t^{\text{PBTES, ch}} + \dot{q}_t^{\text{PBTES, sat}} \\ -\dot{q}_t^{\text{PBTES, dis}} + \dot{q}_t^{\text{SG}} + \dot{q}_t^{\text{loss}} &\forall t \in \mathcal{T}, \end{aligned} \quad (13)$$

with $\dot{q}_t^{\text{loss}} \geq 0$ links the supply units with the PBTES and the SG. While the EAF waste heat flow \dot{Q}_t^{EAF} is fixed, a conventional gas burner with thermal power \dot{q}_t^{gas} provides flexibility on the hot gas side.

The SG is modeled to produce saturated steam $\dot{q}_t^{\text{SG, out}}$ with a constant efficiency, i.e.,

$$\dot{q}_t^{\text{SG}} = \frac{\dot{q}_t^{\text{SG, out}}}{\eta_{\text{SG}}} \quad \forall t \in \mathcal{T}. \quad (14)$$

A part of the saturated steam \dot{q}_t^{SH} can be further superheated in an existing waste heat boiler on-site

to provide superheated steam at 25 bar_a. For this, the energy balance

$$\dot{q}_t^{\text{turb}} = \dot{q}_t^{\text{SH}} \cdot 1.1153 \quad \forall t \in \mathcal{T} \quad (15)$$

holds¹.

The turbine considered in our use case is an existing extraction condensation steam turbine. A part of the steam supplied to the turbine can be extracted at low pressure to satisfy heat demands, while the rest can be used for electricity generation through steam expansion. The extraction ratio can be varied, therefore the heat and electricity generation is decoupled [57]. Thus, the energy balance between the turbine input thermal power \dot{q}_t^{turb} and the extracted heat $\dot{q}_t^{\text{turb, out}}$ and produced electricity $p_t^{\text{turb, el}}$ is modeled via the typical formulation [58]

$$\dot{q}_t^{\text{turb}} = \frac{\dot{q}_t^{\text{turb, out}}}{\eta_{\text{turb, out}}} + \frac{p_t^{\text{turb, el}}}{\eta_{\text{turb, el}}} \quad \forall t \in \mathcal{T}. \quad (16)$$

In case the electric turbine power was already committed on the market, it is fixed via

$$p_t^{\text{turb, el}} = P_t^{\text{el, fixed}} \quad \forall \{t \mid t \in T, j \in \mathcal{J} : t = j\}, \quad (17)$$

where \mathcal{J} is the set of time steps for which a fixed electric power $P_j^{\text{el, fixed}}$ is given.

Within the saturated steam system, the energy balance constraint

$$\dot{q}_t^{\text{SG, out}} - \dot{q}_t^{\text{SH}} + \dot{q}_t^{\text{RSS}} = \dot{Q}_t^{\text{proc}} + \dot{q}_t^{\text{sat, DH}} \quad \forall t \in \mathcal{T} \quad (18)$$

holds, with the RSS storage power \dot{q}_t^{RSS} , the fixed saturated steam demand for further production \dot{Q}_t^{proc} , and a proportion $\dot{q}_t^{\text{sat, DH}} (\geq 0)$ that can be used for additional district heating. Here, the district heating demand \dot{Q}_t^{DH} is considered as a limit rather than a hard constraint, hence:

$$\dot{q}_t^{\text{sat, DH}} - \dot{q}_t^{\text{turb, out}} \leq \dot{Q}_t^{\text{DH}} \quad \forall t \in \mathcal{T} \quad (19)$$

Furthermore,

$$\dot{q}_t^{\text{SG, out}} - \dot{q}_t^{\text{SH}} \geq 0 \quad \forall t \in \mathcal{T} \quad (20)$$

ensures that no lower-pressure steam discharged from the RSS is considered to be fed back to the high-pressure system.

¹A ratio of 0.1153 of the saturated steam enthalpy is additionally supplied by the existing waste heat boiler superheater. This is considered small. The ratio is given by the enthalpy difference between saturated steam at 25 bar_a and superheated steam at 25 bar_a at 100 K above the saturation point.

3.3.6. Objective function

The goal of the MILP UC problem of this use case is the maximization of the objective function

$$J_{\text{UC}} = \sum_{t \in \mathcal{T}} \left(C_t^{\text{el}} \cdot p_t^{\text{turb}} + C^{\text{DH}} \cdot \left(\dot{q}_t^{\text{sat, DH}} + \dot{q}_t^{\text{turb, out}} \right) - C^{\text{gas}} \cdot \frac{\dot{q}_t^{\text{gas}}}{\eta_{\text{gas}}} - c_t^{\text{slack}} \right), \quad (21)$$

which consists of the reward from electricity and district heating sales less the costs for the auxiliary gas burner. Additionally, a slack variable c_t^{slack} is added for the implementation of additional operational penalties. In this use case, the soft constraints

$$c_t^{\text{slack}} \geq A^{\text{slack}} (S_{\text{crit}}^{\text{TES}} - s_t^{\text{TES}}) \quad (22)$$

$$0 \leq c_t^{\text{slack}} \quad (23)$$

is added to penalize the violation of a critical RSS storage level.

3.4. Simulation of the virtual energy system

In our experimental operation, only the PBTES is physically operated, while the rest of the VES needs to be simulated. The PBTES power values during real operation can never exactly match the operation plan resulting from the MILP UC problem. Combining the actual PBTES power values with the VES operation plan of the remaining (virtual) components during the same time period would conflict with the energy balances given in Section 3.3.5. Thus, we emulate a low-level control procedure, to comply with the energy balances in the resulting simulated VES operation.

This low-level control procedure is based on the same MILP constraints as the UC problem given in Section 3.3 with the PBTES power values fixed to those that were experimentally realized. However, the objective (see, Equation (21)) is in this case not cost-efficient operation, but compliance with the previously predicted economic operation plan. Thus, the objective function consists of deviation terms of the planned power of VES units (gas burner, SG, RSS, and turbine) in the form of fixed parameters and the to-be-determined power of these units as variables. The individual deviation terms are weighted appropriately. The minimization of this objective returns a “simulated” VES schedule that complies with the energy balances while maintaining cost-efficient trajectories.

This “simulation” procedure of the VES replicates the low-level control of units according to the operation schedule in a real energy system. The procedure was included as a preliminary step linked to and executed before the MPC service is called. This service will be introduced in Section 4.1.7. When called, the described MILP UC problem is solved only for the current historic time period, which was not fixed via simulation yet.

The realized power values as well as the storage capacity of the PBTES test rig are scaled up in the VES by a constant factor. Equally, the results of the VES MILP UC problem are scaled down before scheduling power values on the test rig. This factor is 3000 and resulted from the test-rigs physical and operational constraints and a rough PBTES scaling in the use case.

4. Implementation

The five-dimensional DT platform first presented in [48] and briefly introduced in this paper in Section 3.1, was equipped with additional functionality in the form of micro-services and workflows to solve the problem statement given in Section 2.2.

All services were implemented in MATLAB[®] and/or Python language and virtualized in encapsulated containers via Docker [59]. For the services solving the MILP UC problem, the parser YALMIP [60] was used and GUROBI[®] 10.0.0 was used as a solver.

4.1. Digital twin micro-services

Services contain the main functionality within the DT platform, tailored to use-case-related objectives. Building on previous work, we developed additional micro-services. Seven services are fully functional while two services are currently only implemented as a mock-up. In the following section, the function of each service and the methods implemented therein are briefly explained.

4.1.1. Data acquisition service

While the SCADA system, considered as part of the physical entity [48], acts as the primary layer of data collection, the data acquisition service fulfills the purpose of data correction, enrichment, and storage.

In our implementation, this service calculates power rates of the charged and discharged HTF of

the test rig and estimates the SOC of the PBTES as

$$SOC_i = \frac{\sum_{k=1}^9 E_{i,k} - E_{SOC=0}}{E_{SOC=1} - E_{SOC=0}}, \quad (24)$$

where $E_{SOC=1}$ is the energy stored in a fully charged storage (constant charging temperature), $E_{SOC=0}$ is the energy of a fully discharged storage (constant discharging temperature) and $\sum_{k=1}^9 E_{i,k}$ is the currently stored energy which is calculated as

$$E_{i,k} = m_k c T_{i,k}. \quad (25)$$

The index k in Equations (24) and (25) represents the nine vertical volume sections in which the storage volume is discretized according to temperature sensor positions. The energy $E_{i,k}$ of the volume section k is calculated as the product of the mass of storage material m_k , the specific heat capacity of the storage material c and the measured value of the temperature sensor $T_{i,k}$ located in this section.

Furthermore, the data acquisition service processes the operating states of the air supply unit and stores this information in an SQL database. Thus, services such as MPC and operation planning service can fetch initial states as well as information on remaining downtime or last switches (important for initializing the auxiliary variables of the SOC, h_t^{ch} and h_t^{dis} , see Section 3.3.3).

4.1.2. Deviation detection service

The deviation detection service is currently implemented as a mock-up on our DT platform. Methods for robust detection of deviations are in the development phase (see, [49]). The service’s purpose is to detect any deviations between the observed behavior of the physical component and the models of its virtual entity. It has to detect deviations and, if they are considered significant, assess whether the cause is physical entity faults or virtual model drifts. Of course, also the classification of physical faults should be considered. For more complex procedures, a more separated functionality encapsulation could be helpful.

4.1.3. Model adaption service

The model adaption service is mainly based on experimental live data and a finite volume simulation model of the PBTES test rig. The finite volume simulation model was developed and validated by Schwarzmayr et al. [61] to be used as the

virtual entity in a DT framework. The model adaption service takes temperature measurements from the PBTES test rig as initial values and a set of parameters

$$\theta = \{k_b, k_t, k_{lat}, \lambda_{pb}, k_{pb}, \eta^+, \eta^-\} \quad (26)$$

to predict/reconstruct the thermal behavior of the test rig for a given schedule. The set of parameters θ includes several heat transfer coefficients that describe the heat losses to the surrounding (k_b, k_t, k_{lat}), the effective thermal conductivity of the packed bed λ_{pb} , the heat transfer coefficient between HTF and storage material k_{pb} as well as thermal efficiencies η^+ and η^- for the charging and discharging process which are the most important for the evaluations in this study. These two efficiencies are defined as

$$\eta = \frac{\dot{Q}_{htf}}{\dot{Q}_{pb}} \quad (27)$$

where \dot{Q}_{htf} is the thermal power rate that is expected to be delivered by the ASU and \dot{Q}_{pb} is the actual power rate provided by the ASU. For a PBTES with a clean packed bed and no gradual degradation of the thermal performance, these two power rates are the same (neglecting heat losses) and the efficiency η is at a constant value of 1 for both charging and discharging. As the behavior of the physical entity does not change over time, this finite volume model with a static set of parameters will be able to predict the behavior of the physical entity with high accuracy.

However, in case the thermal behavior of the physical entity gradually degrades over time (as is the case in this study) the set of parameters θ needs to be constantly updated in order to fit the behavior of the finite volume model to the behavior of the physical entity. To do so, the model adaption service takes experimental data from the test rig for the last 12 hours of operation and uses the finite volume model to reconstruct the experimentally measured behavior of the physical entity. To find the optimal set of parameters $\tilde{\theta}$ we solve the nonlinear optimization problem

$$\tilde{\theta} := \arg \left(\min_{\theta} J(\theta) \right) \quad (28)$$

with the objective function

$$J(\theta) = \sqrt{\frac{1}{n} \sum_{i=1}^n \left(w_T e_{T,i}^2 + w_{SOC} e_{SOC,i}^2 \right)} \quad (29)$$

where $e_{T,i}$ is the error between measured and reconstructed temperatures in the packed bed and $e_{SOC,i}$ is the error between the measured and the reconstructed state of charge (SOC) of the TES. w_T and w_{SOC} are empirically determined weights that adjust the order of magnitudes of e_T and e_{SOC} . The optimization problem defined in Equation (28) is solved with MATLAB[®]'s nonlinear solver *fmincon*. The optimal set of parameters $\tilde{\theta}$ found by the solver together with its time range of validity is stored in the DT's data dimension where it can be accessed by the other services of the DT.

4.1.4. Data augmentation service

The data augmentation service is triggered whenever a virtual entity model was adapted by the model adaption service and acts as a preliminary step before the linearization service (see, Section 4.1.5). Since it would be unreliable to fit a piecewise-linearized model based on a small amount of historic data, we chose the approach to simulate the whole SOC operating range with the maximum mass flow of the PBTES with the current accurate finite volume model fetched from the virtual entity.

The service first simulates a complete cycle of the PBTES, i.e., charging from SOC = 0 until SOC = 1 is reached with the maximum available power, and equally for discharging. It then loops through an equally grided time array of the initial cycle, simulating charging/discharging starting at different SOC levels until the final SOC is reached. This approach provides a high-resolution data set of the PBTES behavior for subsequent linearization.

4.1.5. Linearization service

This service automates the fitting of MILP-suitable piecewise-linear models of nonlinear operational behavior of system components. The service is triggered when new data from the data augmentation service (see, Section 4.1.4) is available and provides a current accurate model for the operation planning service and MPC service. In our implementation, the nonlinear dependency of the maximum PBTES charging/discharging power (see eq. (10)), as well as the dependency of the saturation losses on the state of charge (see eq. (11)), is linearized. The approach is based on the model formulation presented by Koller et al. [14]. We implemented a novel algorithm developed by Birkelbach [62] that provides robust fitting with hyperplanes in one or two convex regions. While Koller et al. manually fitted the linearization on the dataset, our

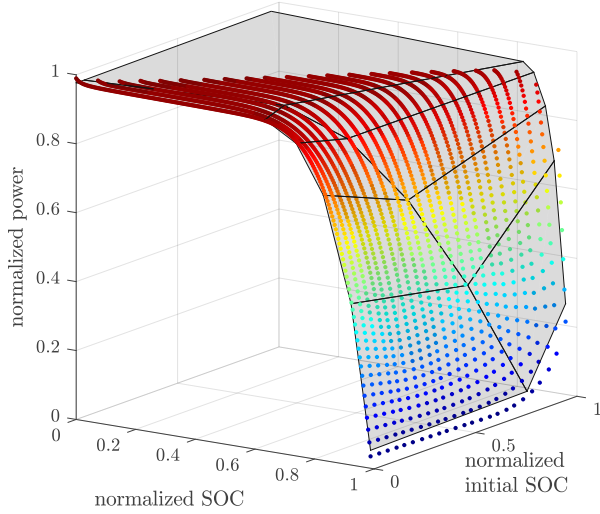


Figure 5: Typical approximation of the nonlinear dependency of the maximum charging power of the PBTES (Figure 4) by linear hyperplanes in two convex regions.

linearization service can automatically choose the separation of the two convex regions and approximate them with hyperplanes. The hyperplane parameters are then converted to MILP constraints. Furthermore, the service performs a basic feasibility check in the operating region to guarantee that no infeasibility issues in the subsequent application of the models arise. Figure 5 illustrates an exemplary linearization run of this service for the maximum PBTES charging power.

4.1.6. Operation planning service

The operational optimization of the physical system is split into two parts: A higher-hierarchy operation planning service that provides an optimal operation plan on a multi-day time horizon, and a lower-hierarchy MPC service that provides fast optimal control of the VES. Both services build on the same MILP model formulation given in Section 3.3, but differ in the length of the forecast horizon and additional boundary conditions. Such hierarchical energy management or also multi-layer optimization was proposed by multiple authors in recent years (see, for example, Fuhrmann et al. [63], Valibeygi et al. [64] or Polimeni et al. [65]).

In our implementation, the operation planning service is triggered every 6 hours and optimizes the operational schedule for the next 48 hours. The PBTES SOC after the final time step is constrained to $s_{t_{n+1}}^{\text{TES}} = 0.5 \cdot S_{\text{max}}^{\text{TES}}$. Furthermore, s_t^{TES} is soft-constrained to a critical value $S_{\text{crit}}^{\text{TES}} = 0.3 \cdot S_{\text{max}}^{\text{TES}}$

via Equation (22). This is a typical safety requirement for the operating plan.

Each UC run requires the current states of both the VES and the physical entity as initial values. To obtain the initial values, the service can query the data dimension of the DT platform via OBDA (see Section 3.1) and receive either the values themselves or the address to obtain them.

4.1.7. MPC service

As outlined above, the MPC service is configured to operate at a higher frequency than the operation planning service to provide optimal control of the VES. In our implementation, the MPC service is triggered every 5 minutes and optimizes the operational schedule for the next 12 hours. The PBTES SOC after the final time step $s_{t_{n+1}}^{\text{TES}}$ is constrained to the corresponding SOC from the operation planning service schedule at the time of t_{n+1} . This assures compliance with the long-term plan of the operation planning service. No other final constraints are set for the other components of the VES since their dynamic is considered to be relatively fast. The SOC of the steam storage s_t^{RSS} is soft-constrained to a critical value $S_{\text{crit}}^{\text{RSS}} = 0.2 \cdot S_{\text{max}}^{\text{RSS}}$, i.e. to a slightly lower value than the operation planning service since the MPC service has a shorter frequency of recurrence. Other than the here-stated constraints, the MILP UC problem is equal to that of the operation planning service. The initial values are fetched equivalently to the operation planning service, see Section 4.1.6.

4.1.8. Day-ahead service

The implemented service follows a very simple procedure. It is called every day at 12:00 local time by a corresponding workflow. When called, the service fetches the last known VES schedule predicted by the operation planning service and fixes the electric turbine power, resulting from this schedule, for the 24 hours of the next day. The fixed electric power in the database $P_j^{\text{el, fixed}}$ is then treated via Equation (17) in the UC problem. This simulates the typical procedure of electricity procurement and marketing of industrial companies, i.e. sending the forecast to the energy supplier and thus committing the plant to this load profile [66]. This DT service could be extended to also fulfill the automated load profile transmission to the energy supplier when applied in industrial applications.

4.1.9. Scheduler service

The scheduler service is responsible for sending the current set points of the optimized operation schedule to the SCADA system. It fetches the latest result schedule of the MPC service and searches for the values at the last time step before the current time. Power values are converted to an enthalpy difference based on the HTF mass flow and the temperature between the PBTES outlet and a fixed charging temperature. The corresponding values are then written to the OPC UA server of the SCADA system which directly controls the physical entity. This was implemented via Python OPC UA in this service. The OPC UA information model can be mapped once to an ontology in the DT platform's data dimension. After this, the node IDs of the respective control variables can be retrieved from the data dimension with a simple SPARQL query. This was demonstrated by Steindl et al. [67] and allows for a very flexible and scalable software implementation.

4.2. Digital twin workflows

As explained in Section 3.1, the runtime management of the DT services and the interaction between them is orchestrated by a workflow engine. Figure 6 shows the implemented workflows and their communication with the ontology as a BPMN representation.

The right box in Figure 6 represents the ontology, which is not part of BPMN but is included to highlight critical interaction between the individual services and the ontology. The solid arrows define the workflows, and the dashed arrows are visualizing the information flow between services and the ontology.

5. Results

5.1. Experimental procedure

The use case presented in Section 2 provided the means for experimental testing of the developed DT services and workflows for adaptive operation optimization. One week of typical operation of the industrial energy system, illustrated in Figure 1, was assumed. The evaluation data is given in Appendix B. As explained in Section 3.4, the power and SOC values of the PBTES test rig are scaled by a constant factor to the MILP UC problem, and vice versa. We considered the fixed temperatures of

200 °C and 50 °C for charging and discharging, respectively. The scheduler service (see Section 4.1.9) calculates the mass flow necessary for a requested power value based on the temperature difference. These values are then controlled in the SCADA system via PID controllers. To simulate the continuous degradation of the PBTES in our lab, we introduced an artificial error. This error reduces the requested power value, hence the mass flow, by an increasing factor. The factor increases linearly from 0 at the start of the experiment to 0.6 after 7 days of operation. The artificial error was added to the scheduler service but not specified anywhere else within the DT platform.

5.2. Model adaption results

As discussed in Section 4.1.3, the model adaption service reacts to deviations between the physical entity's behavior and the virtual entity's behavior by adjusting a set of parameters θ . Based on the artificial error that reduced the mass flow provided by the ASU, we expect the two parameters η^+ and η^- , which are part of θ , to gradually decrease over time. In Figure 7, this expected behavior of a perfectly working model adaption service is plotted as a black solid line. At this point, it should be mentioned that in reality, the model adaption service will always lag behind this black line because the adaption procedure can only be done with historical data. This behavior can be observed in Figure 7 in the blue and orange dots. These dots represent the values of η^+ and η^- that were fitted by the model adaption service on each execution. Although the model adaption is slightly lagging behind, it still detects the degradation of the thermal performance of the TES with acceptable accuracy. This information can be used by the other micro-services of the DT to improve the quality and accuracy of their output.

5.3. Virtual energy system results

The successful model adaption during our experimental operation provides the basis for the efficient operation of the VES over long periods. Figure 8 illustrates the predicted and achieved revenue during one week of VES operation. Here, the predicted revenue at a specific time corresponds to the mean revenue prediction by the MPC service that was made 12h before for its prediction horizon. The given achieved revenue is the moving average over the same 12h window resulting from the actual

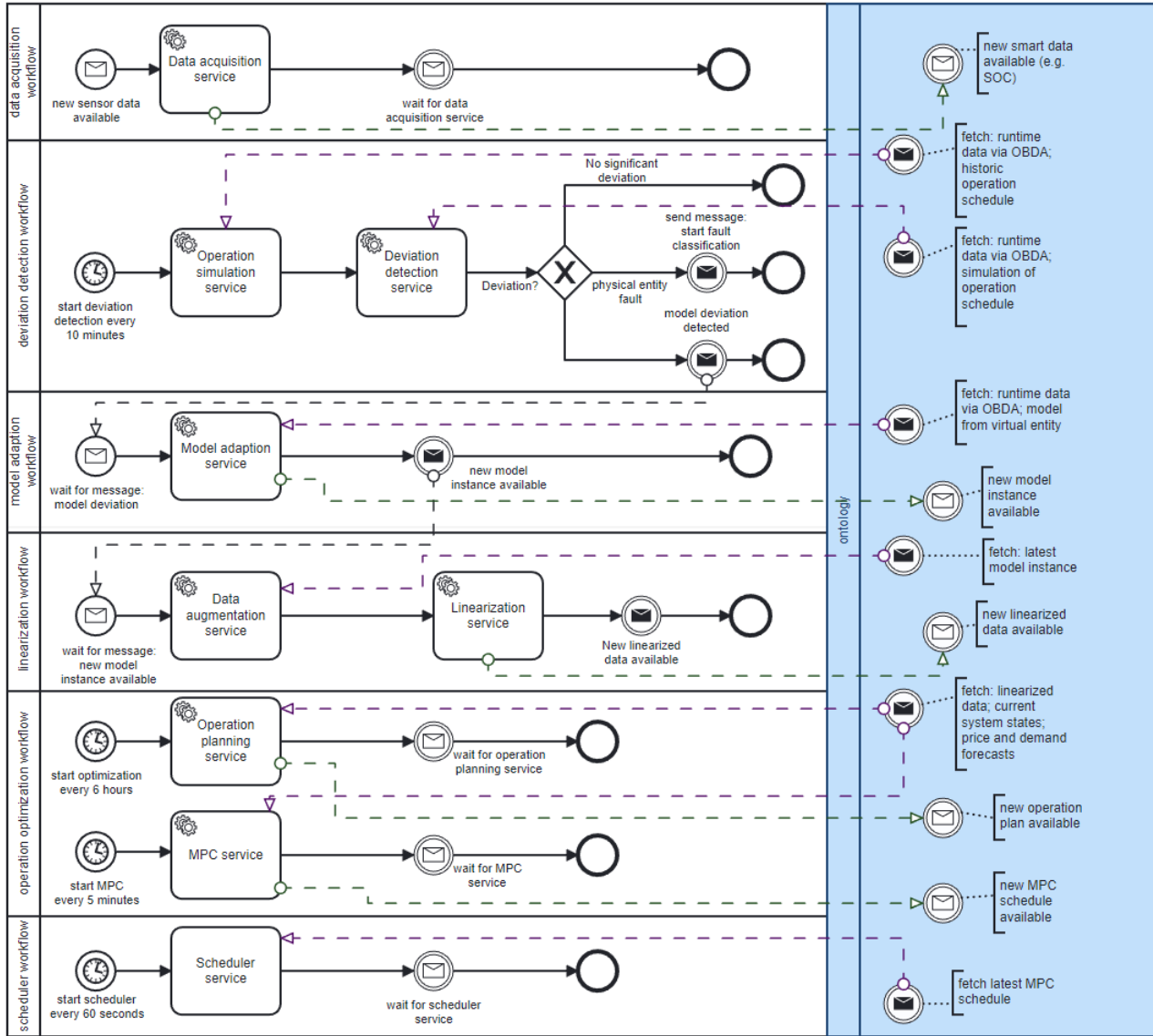


Figure 6: BPMN diagram of the workflows orchestrated in the DT. The accentuated right-hand box visualizes the communication of individual services with the ontology of the DT platform.

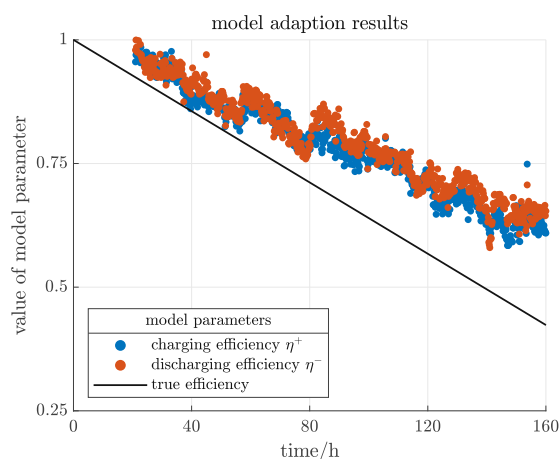


Figure 7: Evaluation results of the model adaption service.

VES simulation according to the PBTES test rig operation, as explained in Section 3.4. The VES operation is visualized in detail for an exemplary time period in Figure C.4 in Appendix C.

It is visible that the prediction error remains in a typical magnitude of 10 to 20% during the operation period, despite the degradation of the PBTES power. The decreasing absolute value of the VES revenue toward the end of the week cannot be directly ascribed to the reduced PBTES capabilities, but is mostly influenced by varying electricity prices and heat demands.

Further reduction of the prediction error is possible by the improvement of the experimental control. For example, we observed some delays in controlling the ASU of the test rig. A refined interval of the scheduler service could guarantee exact value setting according to the operation schedule. Furthermore, PID control of the HTF temperature entering the PBTES under varying mass flow is not trivial due to thermal inertia and leads to further fluctuations.

Despite the described options for further improvement, our experimental tests provided a successful proof of concept for the DT-based MILP model adaption. The automated adaption of the PBTES MILP model in the MPC and operation planning service ensured that efficient operational planning is not impaired.

6. Conclusion and outlook

In this paper, an approach for automated adaptive modeling and operation optimization for industrial energy systems is presented. System com-

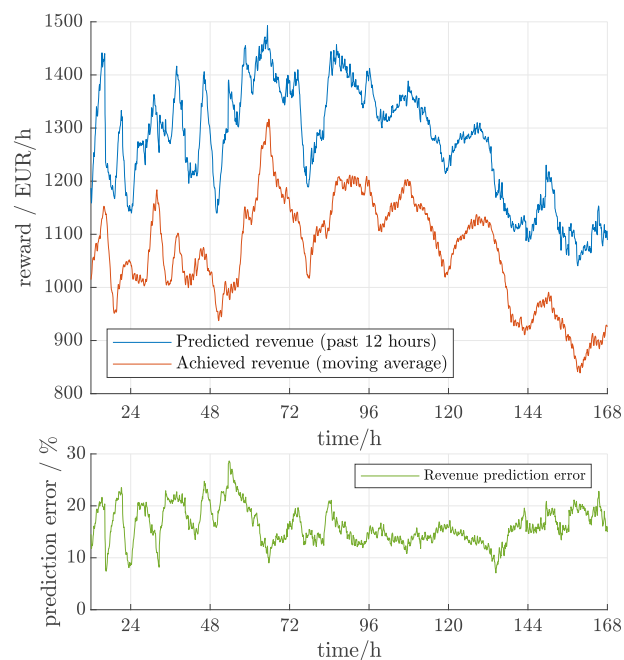


Figure 8: Results of one week VES operation. Upper figure: Predicted average revenue of the MPC service for the past 12h prediction horizon (blue) and 12h-moving average of the achieved revenue after PBTES operation and VES simulation (red). Lower figure: Deviation between predicted and achieved revenue.

ponents in the energy-intensive industry, such as the iron and steel sector, are exposed to harsh conditions, hence their performance tends to deteriorate. For effective operation planning, adaptive modeling is key. To address this challenge, we established a transferable and scalable methodology for this aim, based on innovative and promising digital twin (DT) technology. The foundation of this approach builds upon our previously developed five-dimensional DT platform. Several new DT micro-services, which encapsulate distinct functionality were established. This includes automated simulation model adaption, data augmentation, piecewise linearization of non-linear behavior, mixed integer linear programming (MILP) based operational optimization, and, live scheduling.

We instantiated the developed services for a packed bed thermal energy storage (PBTES) test rig, acting as the physical entity of the DT, and validated them under consideration of a use case of waste heat recovery in steel production. Under the first experimental operation, we accomplished satisfactory results. The model adaption service proved adequate to keep the high-fidelity simulation model

up to date for accurate and timely replication of the PBTES behavior. The data augmentation service and subsequent linearization service provide robust piecewise linear MILP models of the nonlinear PBTES behavior to be used for operational optimization and control. Thus, the prediction error of the MILP-based optimization compared to the actual operation did not increase, despite a continuously induced degradation of PBTES power. This approach facilitates efficient TES operation and thus contributes to flexible, low-emission industrial operation.

Additionally, we emphasize the advantage of the DT approach during engineering, system observation, and software maintenance. The DT platform facilitates scaling applications and implementing new services. The observation and administration of micro-services during operation proved very simple due to the use of software containers and workflow orchestration.

6.1. Outlook

Regarding the scope of this paper, two main overarching future research directions can be deduced: Further sophistication of DT technology, and, detailed investigations of PBTES integration for waste heat recovery in steel production under harsh operation.

Transferable methods for reliable deviation detection and fault classification will be highly relevant in the future. Additionally, increased automation in initial MILP model creation based on system topology and properties could be futile. For this, generic MILP frameworks are already available (see, e.g., [68], [56], [9]) and the automated simulation model creation based on pipe and instrumentation diagrams has been demonstrated [69, 70]. Fusing these approaches on a DT platform and using the methodology documented in the present paper could further contribute to widespread efficiency improvements.

Acknowledgement

The authors acknowledge funding support of this work through the research project *5DIndustrialTwin* as part of the Austrian Climate and Energy Fund's initiative Energieforschung (e!MISSION) 6th call (KLIEN/FFG project number 881140).

We are grateful for the fruitful collaboration with our project partners evon GmbH, voestalpine Stahl

Donawitz GmbH, and the research unit of Automation Systems at TU Wien. We especially thank evon GmbH for assistance with their product XAM-Control in our test rig SCADA system.

Furthermore, the authors acknowledge TU Wien Bibliothek for financial support through its Open Access Funding program.

CRedit authorship contribution statement

Lukas Kasper: Conceptualization, Methodology, Software, Formal analysis, Experimental investigation, Data curation, Writing – original draft, review & editing, Visualization. **Paul Schwarzmayr:** Methodology, Software, Writing – original draft, review & editing, Visualization. **Felix Birkelbach:** Formal analysis, Writing - review. **Florian Javernik:** Conceptualization, Resources, Writing - review. **Michael Schwaiger:** Conceptualization, Resources, Writing - review. **René Hofmann:** Conceptualization, Writing – review, Supervision, Funding acquisition.

Declaration of Competing Interest

The authors declare that they have no known competing financial interests or personal relationships that could have appeared to influence the work reported in this paper.

Appendix A. Use Case data

Appendix A.1. Evaluation data

Here, the representative input data, used for the use case evaluation, is presented.

Appendix A.1.1. Electronic arc furnace waste heat

For the EAF waste heat, only limited literature data is available. We based our evaluation data on an EAF off-gas profile published by Steinparzer et al. [71], who provided off-gas flow and temperature measurements of one tap-to-tap (TTT) cycle of a 120 t EAF. The profile shows temperature peaks of roughly 1200 °C at typical volume flows of up to 200 000 Nm³/h, but also a sharp drop to 200 °C during the EAF tapping. The authors stated in a later publication that the measurement data of this 120 t EAF could be scaled up to a 150 t EAF, resulting in 244 kWh of waste heat per ton of steel produced [27].

We based our EAF use case data on these measurements and assumptions. Since we only considered absolute power values and no temperature levels in the VES model, we calculated the power profile from temperature and volume flow measurements from Steinparzer et al. [71]. However, we only considered off-gas temperatures above 400 °C as usable, corresponding to a share of 0.944% of its total sensible thermal energy. This resulted in an average usable EAF excess heat of 41,47 MW that was used to scale the given profile. The data was reproduced and modified by a slight statistical fluctuation and then downsampled to 5 minute intervals for the final use case profile. Figure A.1 illustrates the EAF trajectory assumed for the use case evaluation.

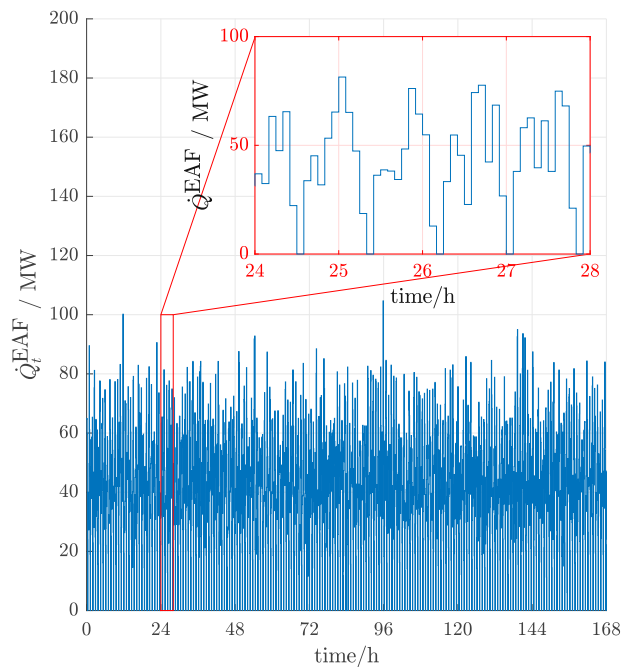


Figure A.1: Assumed EAF waste heat data

Appendix A.1.2. Electricity and gas price

Of course, in day-ahead spot market participation, the quarter-hourly electricity prices are not only known until the price settlement, typically one day ahead. However, based on historical data and the weather forecast, it can be appropriately predicted via forecasting tools [66]. Thus, we assume known prices for a horizon of 48 hours. Weighted average Intra-day spot market prices in 15 minute resolution from February 2023 were considered, retrieved from the European Power Exchange EPEX

². In the chosen time period, starting from Feb. 13, 2023, the electricity price ranged from 92 to 246 €/MWh, while daily spreads of typically more than 80 €/MWh occurred, see Figure A.2. Furthermore, we chose the Austrian wholesale natural gas import price from February 2023 as the representative gas price. It is available at E-Control³ and was valued at 60 €/MWh.

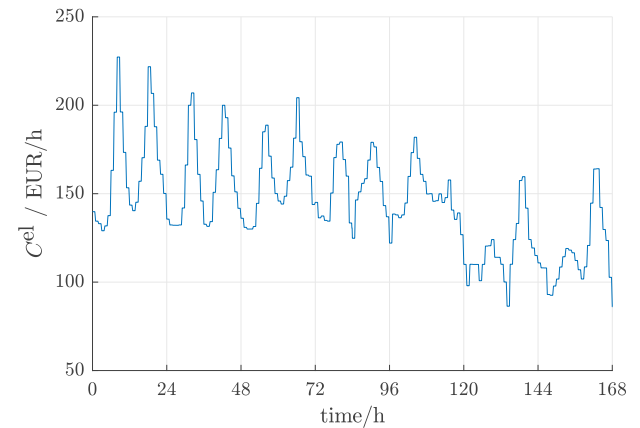


Figure A.2: Electricity price during the use case evaluation period, retrieved from EPEX²

Appendix A.1.3. Steam and heat demand

The saturated steam demand as well as the internal and external heat demand chosen for the use case evaluation are based on measurements from the steel production plant Donawitz (Austria), from a typical winter period. Both steam and heat demand are visualized in Figure A.3. Out of confidentiality, only normalized data can be provided here. The heat demand features a very stable base load but also typical twice-daily spikes. The steam demand features stronger volatility but can be roughly estimated based on the production schedule. The heat demand is about 4 to 5 times larger than the process steam demand.

A typical price for district heating reimbursement was assumed.

Appendix B. Virtual energy system parameters

Table B.1 lists the assumed unit parameters of the UC problem given in Section 3.3. In general, a

²<https://www.epexspot.com/>

³<https://www.e-control.at/industrie/gas/gaspreis/grosshandelspreise>

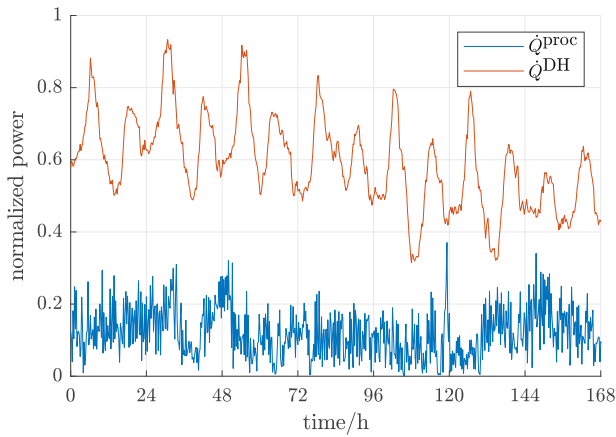


Figure A.3: Process steam demand and heat demand during the use case evaluation period

slightly modified version of the MILP UC formulation presented in that section with additional design variables could be used for the design optimization of the energy system. However, this was not within the scope of this paper.

The system design and parameters were determined in coordination with our project partner and steel production plant operator voestalpine Stahl Donawitz GmbH. The use case, presented in detail in Section 2, corresponds to the current medium-term energy system adaption plans. The RSS system and the steam turbine already exist. We only consider feed-in to the low-pressure part of the turbine, which is mainly fed by the existing steam cycle. This steam cycle is fueled by post-combustion of the carbon monoxide-rich Linz-Donawitz (LD) converter gas from the existing blast furnace and LD converter routes. The auxiliary gas burner (considered to provide backup flexibility) and the SG were designed by empirical knowledge. Typical SG systems are restricted to maximum power ramping of 1-2%/min of the maximum power [72]. A slight iteration of the presented use case could see a second or multiple PBTES installed in parallel. Without the downtime constraints that our PBTES test-rig exhibits, the auxiliary natural gas burner could potentially be spared or used only during start-up and emergency cases.

The slack parameter value used in Equation (22) was chosen as $A^{\text{slack}} = 10^6$. For details on appro-

⁴These values correspond to the upscaled default values of the PBTES test rig. The default values are defined for the initial condition of the test rig. The actual values within the UC problem are retrieved from the virtual entity model.

Table B.1: Assumed optimization problem parameters

Parameter	Value
Auxiliary gas burner	
\dot{Q}_{\min}	0 MW
\dot{Q}_{\max}	50 MW
η_{gas}	0.99
Steam generator (SG)	
\dot{Q}_{\min}	10 MW
\dot{Q}_{\max}	70 MW
$\Delta\dot{Q}_{\text{ramp}}$	70 MW/h
η_{SG}	0.9
Steam turbine	
$\Delta\dot{Q}_{\text{ramp}}$	208 MW/h
$\eta_{\text{turb, el}}$	0.18
$\eta_{\text{turb, out}}$	0.98
Steam storage (RSS)	
\dot{Q}_{\max}	20 MW
γ_{TES}	0.002 %/h
Packed bed thermal energy storage (PBTES)	
S_{\max}^{TES}	112.6 MWh ⁴
$\dot{Q}_{\max}^{\text{PBTES}}$	39.0 MW ⁴
$\dot{Q}_{\min}^{\text{PBTES}}$	100/250 $\dot{Q}_{\max}^{\text{PBTES}}$
γ_{TES}	0.005 %/h

priate slack parameter choice in energy system UC problems, see, e.g., [73].

Appendix C. Virtual energy system operation

Here, an exemplary period of the VES operation during experimental operation is given. Figure C.4 illustrates 12 hours of operation, 2 1/2 days into the experiment. The Figure depicts the heat flows and energy balances at the main conversion points specified in Figure 1 in individual subplots (in the following numbered from top to bottom). The top-most subplot 1 shows the hot off-gas energy balance (equation (13)). Subplot 2 illustrates the PBTES operation. The energy balance within the saturated steam system (equation (18)), holds over subplots 3,4, and 6. Subplot 3 visualizes the total output power of the SG and the ratio of this power that is fed to the saturated steam system and to the superheater for subsequent turbine expansion. Subplot 4 illustrates the fulfillment of the process steam demand with direct saturated steam production and the RSS. The operation of the RSS is given in subplot 5. The decoupled heat from the

turbine and steam system (equation (19)) is illustrated in subplot 6. The electric power output of the steam turbine, as well as the current electricity price, are illustrated in subplot 7.

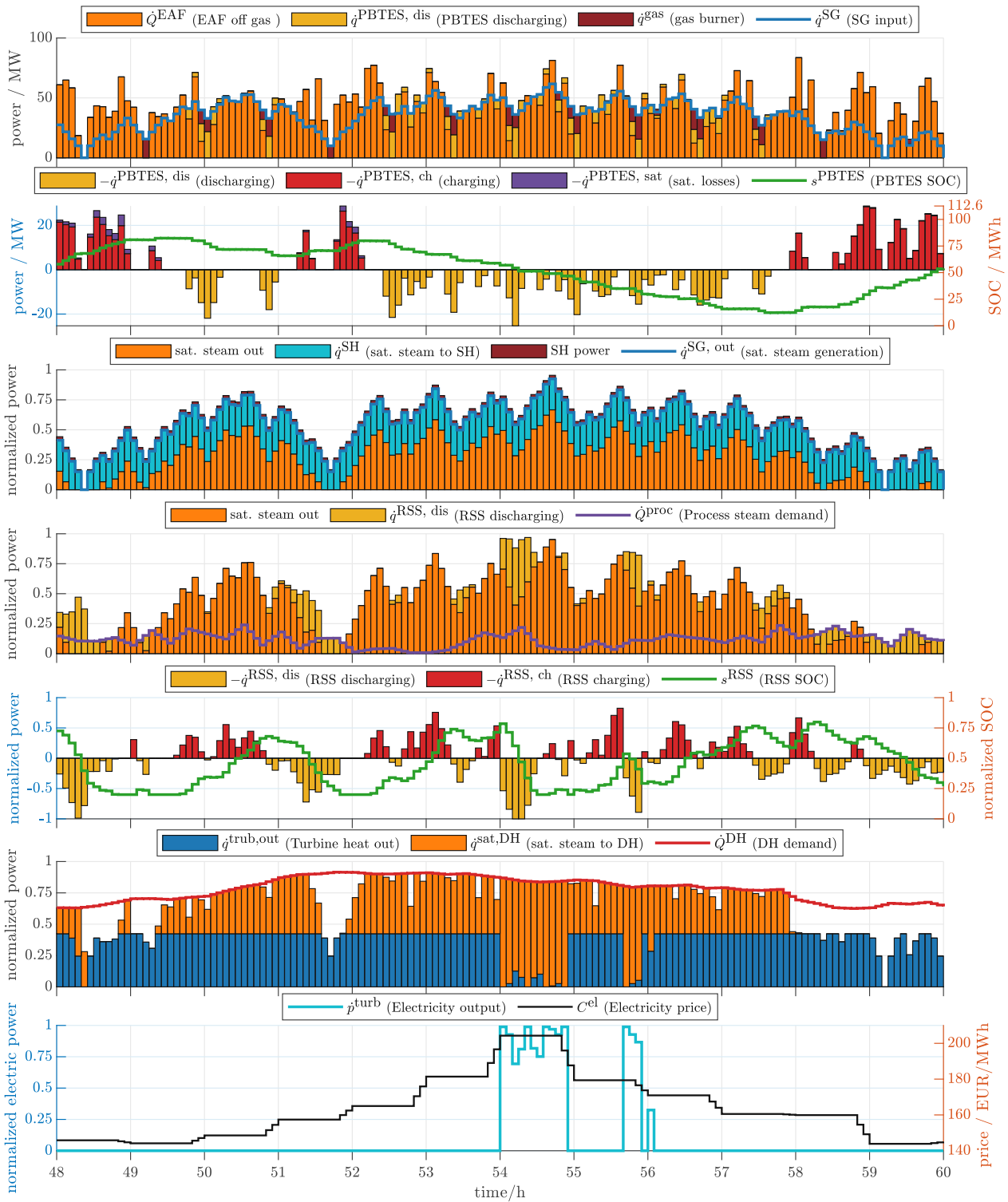


Figure C.4: Exemplary 12 hours of VES operation during the experimental evaluation

References

- [1] Global Carbon Project, Supplemental data of Global Carbon Budget 2019 (Version 1.0) [Data set]. Global Carbon Project, Tech. rep., Global Carbon Project (2019). doi:10.18160/gcp-2019.
- [2] International Energy Agency (IEA), Greenhouse Gas Emissions from Energy Highlights, Available at: <https://www.iea.org/data-and-statistics/data-product/greenhouse-gas-emissions-from-energy-highlights>, licence: Creative Commons Attribution CC BY-NC-SA 4.0 (2022).
- [3] L. Miró, J. Gasia, L. F. Cabeza, Thermal energy storage (TES) for industrial waste heat (IWH) recovery: A review, *Applied Energy* 179 (2016) 284–301. doi:10.1016/j.apenergy.2016.06.147.
- [4] V. Martin, N. J. Chiu, *Industrial Applications of Thermal Energy Storage Systems*, John Wiley & Sons, Ltd, 2022, Ch. 32, pp. 729–747. doi:10.1002/9781119239390.ch32.
- [5] D. Pernsteiner, V. Halmschlager, A. Schirrer, R. Hofmann, S. Jakubek, Efficient Sensitivity-Based Cooperation Concept for Hierarchical Multilayer Process Automation of Steam-Powered Plants, *IEEE Access* 10 (2022) 66844–66861. doi:10.1109/ACCESS.2022.3178436.
- [6] P. Tatjewski, Advanced control and on-line process optimization in multilayer structures, *Annual Reviews in Control* 32 (1) (2008) 71–85. doi:10.1016/j.arcontrol.2008.03.003.
- [7] I. Abdou, M. Tkiouat, Unit Commitment Problem in Electrical Power System: A Literature Review, *International Journal of Electrical and Computer Engineering* 8 (3) (2018) 1357–1372. doi:10.11591/ijece.v8i3.pp1357-1372.
- [8] H. Abdi, Profit-based unit commitment problem: A review of models, methods, challenges, and future directions, *Renewable and Sustainable Energy Reviews* 138 (2021) 110504. doi:10.1016/j.rser.2020.110504.
- [9] A. Moser, D. Muschick, M. Göllles, P. Nageler, H. Schranzhofer, T. Mach, C. Ribas Tugores, I. Leusbrock, S. Stark, F. Lackner, A. Hofer, A MILP-based modular energy management system for urban multi-energy systems: Performance and sensitivity analysis, *Applied Energy* 261 (2020) 114342. doi:10.1016/j.apenergy.2019.114342.
- [10] L. Moretti, E. Martelli, G. Manzolini, An efficient robust optimization model for the unit commitment and dispatch of multi-energy systems and microgrids, *Applied Energy* 261 (2020) 113859. doi:10.1016/j.apenergy.2019.113859.
- [11] D. Muschick, S. Zlabinger, A. Moser, K. Lichtenegger, M. Göllles, A multi-layer model of stratified thermal storage for MILP-based energy management systems, *Applied Energy* 314 (2022) 118890. doi:10.1016/j.apenergy.2022.118890.
- [12] L. Kotzur, L. Nolting, M. Hoffmann, T. Groß, A. Smolenko, J. Priesmann, H. Büsing, R. Beer, F. Kullmann, B. Singh, A. Praktijnjo, D. Stolten, M. Robinius, A modeler's guide to handle complexity in energy systems optimization, *Advances in Applied Energy* 4 (2021) 100063. doi:10.1016/j.adapen.2021.100063.
- [13] C. Milan, M. Stadler, G. Cardoso, S. Mashayekh, Modeling of non-linear CHP efficiency curves in distributed energy systems, *Applied Energy* 148 (2015) 334–347. doi:10.1016/j.apenergy.2015.03.053.
- [14] M. Koller, R. Hofmann, H. Walter, MILP model for a packed bed sensible thermal energy storage, *Computers & Chemical Engineering* 125 (2019) 40–53. doi:10.1016/j.compchemeng.2019.03.007.
- [15] Y. Lu, C. Liu, K. I.-K. Wang, H. Huang, X. Xu, Digital Twin-driven smart manufacturing: Connotation, reference model, applications and research issues, *Robotics and Computer-Integrated Manufacturing* 61 (2020) 101837. doi:10.1016/j.rcim.2019.101837.
- [16] W. Yu, P. Patros, B. Young, E. Klinac, T. G. Walmsley, Energy digital twin technology for industrial energy management: Classification, challenges and future, *Renewable and Sustainable Energy Reviews* 161 (2022) 112407. doi:10.1016/j.rser.2022.112407.
- [17] E. Negri, L. Fumagalli, M. Macchi, A Review of the Roles of Digital Twin in CPS-based Production Systems, *Procedia Manufacturing* 11 (2017) 939–948. doi:10.1016/j.promfg.2017.07.198.
- [18] C. Cimino, E. Negri, L. Fumagalli, Review of digital twin applications in manufacturing, *Computers in Industry* 113 (2019) 103130. doi:10.1016/j.compind.2019.103130.
- [19] M. Liu, S. Fang, H. Dong, C. Xu, Review of digital twin about concepts, technologies, and industrial applications, *Journal of Manufacturing Systems* 58 (2021) 346–361. doi:10.1016/j.jmsy.2020.06.017.
- [20] W. Kritzing, M. Karner, G. Traar, J. Henjes, W. Sihm, Digital Twin in manufacturing: A categorical literature review and classification, *IFAC-PapersOnLine* 51 (11) (2018) 1016–1022. doi:10.1016/j.ifacol.2018.08.474.
- [21] K. Josifovska, E. Yigitbas, G. Engels, Reference Framework for Digital Twins within Cyber-Physical Systems, in: 2019 IEEE/ACM 5th International Workshop on Software Engineering for Smart Cyber-Physical Systems (SEsCPS), Institute of Electrical and Electronics Engineers Inc, 2019, pp. 25–31. doi:10.1109/SEsCPS.2019.00012.
- [22] A. K. Sleiti, J. S. Kapat, L. Vesely, Digital twin in energy industry: Proposed robust digital twin for power plant and other complex capital-intensive large engineering systems, *Energy Reports* 8 (2022) 3704–3726. doi:10.1016/j.egy.2022.02.305.
- [23] Y. Sun, S. Tian, P. Ciaias, Z. Zeng, J. Meng, Z. Zhang, Decarbonising the iron and steel sector for a 2°C target using inherent waste streams, *Nature Communications* 13 (1) (2022) 297. doi:10.1038/s41467-021-27770-y.
- [24] International Energy Agency, *Iron and Steel Technology Roadmap*, Tech. rep., International Energy Agency, Paris, accessed: 2023-06-12 (2020). URL <https://www.iea.org/reports/iron-and-steel-technology-roadmap>
- [25] P. Wang, M. Ryberg, Y. Yang, et al., Efficiency stagnation in global steel production urges joint supply- and demand-side mitigation efforts, *Nature Communications* 12 (2021) 2066. doi:10.1038/s41467-021-22245-6.
- [26] M. Kirschen, V. Risonarta, H. Pfeifer, Energy efficiency and the influence of gas burners to the energy related carbon dioxide emissions of electric arc furnaces in steel industry, *Energy* 34 (9) (2009) 1065–1072. doi:10.1016/j.energy.2009.04.015.
- [27] T. Keplinger, M. Haider, T. Steinparzer, A. Patre-

- jko, P. Trunner, M. Haselgrübler, Dynamic simulation of an electric arc furnace waste heat recovery system for steam production, *Applied Thermal Engineering* 135 (2018) 188–196. doi:10.1016/j.applthermaleng.2018.02.060.
- [28] G. Nardin, A. Meneghetti, F. Dal Magro, N. Benedetti, PCM-based energy recovery from electric arc furnaces, *Applied Energy* 136 (2014) 947–955. doi:10.1016/j.apenergy.2014.07.052.
- [29] A. Inayat, Current progress of process integration for waste heat recovery in steel and iron industries, *Fuel* 338 (2023) 127237. doi:10.1016/j.fuel.2022.127237.
- [30] voestalpine Stahl Donawitz GmbH, greentec steel, accessed: 2023-06-12 (2023). URL <https://www.voestalpine.com/stahldonawitz/en/quality-and-environment/greentec-steel/>
- [31] T. Steinparzer, M. Haider, A. Fleischanderl, A. Hampel, G. Enickl, F. Zauner, Heat exchangers and thermal energy storage concepts for the off-gas heat of steelmaking devices, *Journal of Physics: Conference Series* 395 (1) (2012) 012158. doi:10.1088/1742-6596/395/1/012158.
- [32] F. Dal Magro, S. Savino, A. Meneghetti, G. Nardin, Coupling waste heat extraction by phase change materials with superheated steam generation in the steel industry, *Energy* 137 (2017) 1107–1118. doi:10.1016/j.energy.2017.04.051.
- [33] G. L. Bostick, 14 - Operation and controls, in: V. L. Eriksen (Ed.), *Heat Recovery Steam Generator Technology*, Woodhead Publishing, 2017, pp. 287–319. doi:10.1016/B978-0-08-101940-5.00014-2.
- [34] G. Manente, Y. Ding, A. Sciacovelli, A structured procedure for the selection of thermal energy storage options for utilization and conversion of industrial waste heat, *Journal of Energy Storage* 51 (2022) 104411. doi:10.1016/j.est.2022.104411.
- [35] A. Gautam, R. Saini, A review on sensible heat based packed bed solar thermal energy storage system for low temperature applications, *Solar Energy* 207 (2020) 937–956. doi:10.1016/j.solener.2020.07.027.
- [36] A. Gautam, R. Saini, A review on technical, applications and economic aspect of packed bed solar thermal energy storage system, *Journal of Energy Storage* 27 (2020) 101046. doi:10.1016/j.est.2019.101046.
- [37] B. Xie, N. Baudin, J. Soto, Y. Fan, L. Luo, Chapter 10 - Thermocline packed bed thermal energy storage system: a review, in: M. Jeguirim (Ed.), *Renewable Energy Production and Distribution*, Vol. 1 of *Advances in Renewable Energy Technologies*, Academic Press, 2022, pp. 325–385. doi:10.1016/B978-0-323-91892-3.24001-6.
- [38] T. Bause, F. Campana, L. Filippini, A. Foresti, N. Monti, T. Pelz, Cogeneration with ORC at elbestahlwerke feralpi EAF shop, in: *Proceedings of the iron & steel technology conference and exposition*, Indianapolis, IN, USA, 2014, pp. 5–8, accessed: 2023-06-12. URL http://www.hreii.eu/demo/public/AISTech%202014_Paper_Bause_Cogeneration%20with%20ORC%20at%20Elbe_Stahlwerke%20Feralpi%20EAF%20Shop.pdf
- [39] A.-G. Guézennec, J.-C. Huber, F. Patisson, P. Sessiecq, J.-P. Birat, D. Ablitzer, Dust formation in Electric Arc Furnace: Birth of the particles, *Powder Technology* 157 (1) (2005) 2–11, 4th French Meeting on Powder Science and Technology. doi:10.1016/j.powtec.2005.05.006.
- [40] T. Keplinger, M. Haider, T. Steinparzer, P. Trunner, A. Patrejko, M. Haselgrübler, Modeling, Simulation, and Validation with Measurements of a Heat Recovery Hot Gas Cooling Line for Electric Arc Furnaces, *steel research international* 89 (6) (2018) 1800009. doi:10.1002/srin.201800009.
- [41] A. Reitingner, Construction of a test rig for the characterization of gas-powder two-phase flow in packed bed thermal energy storage systems, Diploma thesis, Technische Universität Wien (2023). doi:10.34726/hss.2023.103589.
- [42] X. Dong, D. Pinson, S. Zhang, A. Yu, P. Zulli, Gas-powder flow and powder accumulation in a packed bed: I. Experimental study, *Powder Technology* 149 (1) (2004) 1–9. doi:10.1016/j.powtec.2004.09.040.
- [43] K. Hollands, H. Sullivan, Pressure drops across rock bed thermal storage systems, *Solar Energy* 33 (2) (1984) 221–225. doi:10.1016/0038-092X(84)90241-X.
- [44] H. Singh, R. Saini, J. Saini, A review on packed bed solar energy storage systems, *Renewable and Sustainable Energy Reviews* 14 (3) (2010) 1059–1069. doi:10.1016/j.rser.2009.10.022.
- [45] K. Knobloch, T. Ulrich, C. Bahl, K. Engelbrecht, Degradation of a rock bed thermal energy storage system, *Applied Thermal Engineering* 214 (2022) 118823. doi:10.1016/j.applthermaleng.2022.118823.
- [46] M. A. Bagherian, K. Mehranzamir, A. B. Pour, S. Rezaania, E. Taghavi, H. Nabipour-Afrouzi, M. Dalvi-Esfahani, S. M. Alizadeh, Classification and Analysis of Optimization Techniques for Integrated Energy Systems Utilizing Renewable Energy Sources: A Review for CHP and CCHP Systems, *Processes* 9 (2) (2021). doi:10.3390/pr9020339.
- [47] G. Steindl, M. Stagl, L. Kasper, W. Kastner, R. Hofmann, Generic Digital Twin Architecture for Industrial Energy Systems, *Applied Sciences* 10 (24) (2020). doi:10.3390/app10248903.
- [48] L. Kasper, F. Birkelbach, P. Schwarzmayr, G. Steindl, D. Ramsauer, R. Hofmann, Toward a Practical Digital Twin Platform Tailored to the Requirements of Industrial Energy Systems, *Applied Sciences* 12 (14), section “Energy Science and Technology”. Special Issue “Industry 4.0 Technologies Supporting the Energy Transition” (2022). doi:10.3390/app12146981.
- [49] P. Schwarzmayr, F. Birkelbach, L. Kasper, R. Hofmann, Development of a Digital Twin Platform for Industrial Energy Systems, in: *Applied Energy Symposium: MIT A+B*, Cambridge, USA, July 5-8, 2022, pp. 1–6. doi:10.46855/energy-proceedings-9974.
- [50] F. Tao, M. Zhang, Nee, A. Y. C., Chapter 3 - Five-Dimension Digital Twin Modeling and Its Key Technologies, in: F. Tao, M. Zhang, A. Y. C. Nee (Eds.), *Digital Twin Driven Smart Manufacturing*, Academic Press, 2019, pp. 63–81. doi:10.1016/B978-0-12-817630-6.00003-5.
- [51] A. Hogan, E. Blomqvist, M. Cochez, C. D’amato, G. D. Melo, C. Gutierrez, S. Kirrane, J. E. L. Gayo, R. Navigli, S. Neumaier, A.-C. N. Ngomo, A. Polleres, S. M. Rashid, A. Rula, L. Schmelzeisen, J. Sequeda, S. Staab, A. Zimmermann, Knowledge Graphs, *ACM Comput. Surv.* 54 (4) (jul 2021). doi:10.1145/3447772.
- [52] T. Bagosi, D. Calvanese, J. Hardi, S. Komla-Ebri, D. Lanti, M. Rezk, M. Rodríguez-Muro, M. Slusnys, G. Xiao, The Ontop Framework for Ontology Based

- Data Access, in: D. Zhao, J. Du, H. Wang, P. Wang, D. Ji, J. Z. Pan (Eds.), *The Semantic Web and Web Science*, Springer Berlin Heidelberg, Berlin, Heidelberg, 2014, pp. 67–77. doi:10.1007/978-3-662-45495-4_6.
- [53] P. Schwarzmayr, F. Birkelbach, H. Walter, R. Hofmann, Standby efficiency and thermocline degradation of a packed bed thermal energy storage: An experimental study, *Applied Energy* 337 (2023) 120917. doi:10.1016/j.apenergy.2023.120917.
- [54] M. Majidi, B. Mohammadi-Ivatloo, A. Anvari-Moghaddam, Optimal robust operation of combined heat and power systems with demand response programs, *Applied Thermal Engineering* 149 (2019) 1359–1369. doi:10.1016/j.applthermaleng.2018.12.088.
- [55] F. Fuhrmann, A. Schirrer, M. Kozek, Model-predictive energy management system for thermal batch production processes using online load prediction, *Computers & Chemical Engineering* 163 (2022) 107830. doi:10.1016/j.compchemeng.2022.107830.
- [56] V. Halmschlager, R. Hofmann, Assessing the potential of combined production and energy management in Industrial Energy Hubs – Analysis of a chipboard production plant, *Energy* 226 (2021) 120415. doi:10.1016/j.energy.2021.120415.
- [57] M. Koller, R. Hofmann, Mixed-Integer Linear Programming Formulation of Combined Heat and Power Units for the Unit Commitment Problem, *Journal of Sustainable Development of Energy, Water and Environment Systems* 6 (4) (2018) 755–769. doi:10.13044/j.sdwes.d6.0207.
- [58] T. Weber, N. Strobel, T. Kohne, et al., Realistic modeling of a combined heat and power plant in the context of mixed integer linear programming, *Energy Informatics* 1 (2018) 27. doi:10.1186/s42162-018-0037-z.
- [59] D. Merkel, Docker: lightweight linux containers for consistent development and deployment, *Linux journal* 2014 (239) (2014) 2.
- [60] J. Lofberg, YALMIP: a toolbox for modeling and optimization in MATLAB, in: 2004 IEEE International Conference on Robotics and Automation (IEEE Cat. No.04CH37508), 2004, pp. 284–289. doi:10.1109/CACSD.2004.1393890.
- [61] P. Schwarzmayr, F. Birkelbach, H. Walter, R. Hofmann, Study on the Standby Characteristics of a Packed Bed Thermal Energy Storage: Experimental Results and Model Based Parameter Optimization, in: *Proceedings of the ASME 2023 Power Conference*, Long Beach, CA, 2023.
- [62] F. Birkelbach, MILPtools, [Gitlab repository]. Available at: <https://gitlab.tuwien.ac.at/iet/public/milptools> (2022).
- [63] F. Fuhrmann, B. Windholz, A. Schirrer, S. Knöttner, K. Schenzel, M. Kozek, Energy management for thermal batch processes with temporarily available energy sources– Laboratory experiments, *Case Studies in Thermal Engineering* 39 (2022) 102473. doi:10.1016/j.csite.2022.102473.
- [64] A. Valibeygi, S. A. R. Konakalla, R. d. Callafon, Predictive Hierarchical Control of Power Flow in Large-Scale PV Microgrids With Energy Storage, *IEEE Transactions on Sustainable Energy* 12 (1) (2021) 412–419. doi:10.1109/TSTE.2020.3001260.
- [65] S. Polimeni, L. Meraldi, L. Moretti, S. Leva, G. Manzolini, Development and experimental validation of hierarchical energy management system based on stochastic model predictive control for Off-grid Microgrids, *Advances in Applied Energy* 2 (2021) 100028. doi:10.1016/j.adapen.2021.100028.
- [66] H. Hadera, I. Harjunkoski, G. Sand, I. E. Grossmann, S. Engell, Optimization of steel production scheduling with complex time-sensitive electricity cost, *Computers & Chemical Engineering* 76 (2015) 117–136. doi:10.1016/j.compchemeng.2015.02.004.
- [67] G. Steindl, T. Frühwirth, W. Kastner, Ontology-Based OPC UA Data Access via Custom Property Functions, in: 2019 24th IEEE International Conference on Emerging Technologies and Factory Automation (ETFA), 2019, pp. 95–101. doi:10.1109/ETFA.2019.8869436.
- [68] U. Krien, P. Schönfeldt, J. Launer, S. Hilpert, C. Kalde-meyer, G. Pleßmann, oemof.solph—A model generator for linear and mixed-integer linear optimisation of energy systems, *Software Impacts* 6 (2020) 100028. doi:10.1016/j.simpa.2020.100028.
- [69] G. Steindl, W. Kastner, Ontology-Based Model Identification of Industrial Energy Systems, in: 2020 IEEE 29th International Symposium on Industrial Electronics (ISIE), 2020, pp. 1217–1223. doi:10.1109/ISIE45063.2020.9152386.
- [70] S. Sierla, M. Azangoo, A. Fay, V. Vyatkin, N. Papanikolaou, Integrating 2D and 3D Digital Plant Information Towards Automatic Generation of Digital Twins, in: 2020 IEEE 29th International Symposium on Industrial Electronics (ISIE), 2020, pp. 460–467. doi:10.1109/ISIE45063.2020.9152371.
- [71] T. Steinparzer, M. Haider, F. Zauner, G. Enickl, M. Michele-Naussed, A. C. Horn, Electric Arc Furnace Off-Gas Heat Recovery and Experience with a Testing Plant, *steel research international* 85 (4) (2014) 519–526. doi:10.1002/srin.201300228.
- [72] R. Hofmann, S. Panuschka, A. Beck, A simultaneous optimization approach for efficiency measures regarding design and operation of industrial energy systems, *Computers & Chemical Engineering* 128 (2019) 246–260. doi:10.1016/j.compchemeng.2019.06.007.
- [73] F. Fuhrmann, A. Schirrer, M. Kozek, MPC for Process Heat Supply Systems: Considering Load Prediction Uncertainty Caused by Human Operators, in: S. Pierucci, F. Manenti, G. L. Bozzano, D. Manca (Eds.), 30th European Symposium on Computer Aided Process Engineering, Vol. 48 of *Computer Aided Chemical Engineering*, Elsevier, 2020, pp. 1219–1224. doi:10.1016/B978-0-12-823377-1.50204-4.

Nomenclature

Acronyms

BPMN	Business Process Model and Notation
DH	District heating
DT	Digital twin
EAF	Electric arc furnace
GDTA	Generic Digital Twin Architecture

IoT	Internet of Things	u	Unit index
LD	Linz-Donawitz	b	bottom
MILP	Mixed-integer linear programming	ch	Superscript - charging
MPC	Model predictive control	$crit$	Superscript - critical value
MQTT	Message Queuing Telemetry Transport	dis	Superscript - discharging
		el	Superscript - electric
OBDA	Ontology-Based Data Access	$fixed$	Superscript - fixed value
OPC UA	Open Platform Communications Unified Architecture	gas	Superscript - gas burner
PBTES	Packed bed thermal energy storage	$init$	Initial value
PID	proportional–integral–derivative (controller)	lat	lateral
		$loss$	Superscript - losses
PLC	Programmable Logic Controller	max	Superscript - maximum value
RSS	Ruths steam storage	min	Superscript - minimum value
SCADA	Supervisory control and data acquisition	out	Superscript - outgoing power
		$proc$	Superscript - process demand
SG	Steam generator	$ramp$	Superscript - ramping parameter
SH	Steam superheater	sat	Superscript - saturation
SOC	State of charge	$slack$	Superscript - slack variable
SPARQL	SPARQL Protocol and RDF Query Language	t	top
		$turb$	Superscript - steam turbine
SQL	Structured Query Language	Parameters and Variables	
TES	Thermal energy storage	Δt	Time step size
TTT	Tap-to-tap (referring to EAF cycle)	\dot{Q}	Parameter - thermal power
UC	Unit commitment	\dot{q}	Continuous variable - thermal power
VES	Virtual energy system	η	efficiency
Indices		γ^{TES}	Thermal loss factor of TES
i	Index in sum	λ_{pb}	effective thermal conductivity of packed bed
j	Time step with fixed electricity values	\mathcal{J}	Set of discrete time steps
k	Index in sum	\mathcal{T}	Set of discrete time steps
n	Number of time steps/ measurement values	\mathcal{U}	Set of units in the UC problem
t	Time step	θ	Parameter array (optimization variables)

$\tilde{\theta}$	Optimized parameters
A^{slack}	slack parameter
C	Parameter - costs
e	Error term
h	Continuous variable - SOC auxiliary variable
J	Objective function
k	heat transfer coefficient
p	Continuous variable - electric power
S	Parameter - state of charge
s	Continuous variable - state of charge
T^{spread}	Temperature spread at the PBTES outlet
w	Weighting factor
x	Binary variable - on/off
z	Binary variable - TES state

Symbols

f	linear function
-----	-----------------

Further publications and other scientific contributions

Parts of my research connected to this thesis were not only published in the presented core publications but were the subject of other dissemination activities. These contributions are listed in this section. A brief description is given, highlighting the most important findings in the context of this thesis. Additionally, my contribution to co-author publications is explicitly presented.

Paper A – Co-author publication

Co-simulation methodology of a hybrid latent-heat thermal energy storage unit

D. Pernsteiner, L. Kasper, A. Schirrer, R. Hofmann and S. Jakubek (2020). “Co-simulation methodology of a hybrid latent-heat thermal energy storage unit”. *Applied Thermal Engineering* 178, 115495. ISSN: 1359-4311. DOI: 10.1016/j.applthermaleng.2020.115495

This journal paper presented the first high-fidelity co-simulation model for the hybrid RSS/LHTES storage introduced in Section 2.1 of this thesis. The one-dimensional RSS model is based on the two-phase equilibrium approach inside the RSS. The two-dimensional high-fidelity PCM cell model, also applied in Paper 1 of the present thesis, includes heat conduction and convection effects. For co-simulation, we developed a thermal coupling concept by wall temperatures and resulting heat flow to ensure energy conservation between the two sub-models. The liquid filling level inside the RSS and the angular position and orientation of the PCM cell can have a significant influence on the melting behavior inside the PCM cell (see Paper 1). To nevertheless reduce the computational effort of the co-simulation, the high number of PCM cells at the circumference of the RSS were aggregated into sectors with one representative cell each. Aggregation criteria were then formulated to optimize the sector partitioning. The aggregation leads to a simulation error reduction from 4.5 % to 0.5 % at the same computational costs, or, at the same accuracy, to a reduction of computational time by up to 73 %. The methods published in this paper serve as a foundation for system analysis, and especially for estimation and control tasks of the hybrid RSS/LHTES storage or similar concepts. Thus, they provided the foundation for the subsequent work on model reduction (Paper B) and storage state estimation (Paper C).

My contribution: Conceptualization. Coupling formulation for the PCM cell sub model. Drafting the paper. Explanation of the PCM cell model in the paper. Evaluation. Review and editing.

Paper B – Co-author publication

Data-based model reduction for phase change problems with convective heat transfer

D. Pernsteiner, A. Schirrer, L. Kasper, R. Hofmann and S. Jakubek (2021). “Data-based model reduction for phase change problems with convective heat transfer”. *Applied Thermal Engineering* 184, 116228. ISSN: 1359-4311. DOI: 10.1016/j.applthermaleng.2020.116228

The motivation for this journal paper was the real-time capability of PCM-based storage simulation, without however neglecting natural convection effects. Such fast but accurate simulation methods are essential for SOC estimation and optimal control for TES, such as the hybrid RSS/LHTES introduced in Section 2.1 of this thesis. The co-simulation methodology developed in Paper A provided a solid foundation for this task, but was still not real-time capable by a factor of more than five, due to the complexity of solving the Navier-Stokes equations. Therefore, a model reduction method was established based on the finding of recurring dominant flow patterns in the PCM enclosures (see Paper 1). The high-fidelity PCM cell model provided the means to train a simplified stream function model of the typical convective flow pattern. The solution-dependent flow domain was transformed via singular value decomposition into a reduced number of dominant modes. Simulation studies with the resulting reduced order model found that computational duration was reduced by up to 44 times while only small errors compared to the neglect of convective effects resulted. The laborious solution of the Navier-Stokes equation could thus be efficiently short-cut and the methodology proved to be perfectly suitable, but not limited to, the state estimation of LHTES.

My contribution: Consultation regarding dominant flow domains in PCM cells. Analysis of PCM simulation studies. Code base review. Review and editing.

Paper C – Co-author publication

State estimation concept for a nonlinear melting/solidification problem of a latent heat thermal energy storage

D. Pernsteiner, A. Schirrer, L. Kasper, R. Hofmann and S. Jakubek (2021). “State estimation concept for a nonlinear melting/solidification problem of a latent heat thermal energy storage”. *Computers & Chemical Engineering* 153, 107444. ISSN: 0098-1354. DOI: 10.1016/j.compchemeng.2021.107444

This journal paper developed a state estimation concept for LHTES based on the previously presented reduced order model in Paper B. The developed observer framework is applicable to any melting/solidification phase change problem with conduction/convection and is able to handle nonlinear distributed-parameter systems. The high-order, nonlinear, but real-time capable PCM model (see Paper B) is used to predict the future states only one time step ahead. It is subsequently linearized around the current trajectory and then reduced via balanced truncation to a low number of dominant modes. The system

matrices of this low-order observer model serve as Jacobians in an extended Kalman filter. The extended Kalman filter computes a state update of the prediction model according to the difference between the measurements and the predicted model outputs. The observer converges well and is in-sensitive against model errors of typical magnitude. Simulation studies showed that the total enthalpy and thus the SOC, as well as the location and shape of the PCM's melting front, can be estimated with high accuracy. Additionally, a mode-shape-based sensor placement criterion by analyzing sensitivities was applied and discussed in this paper.

My contribution: Consultation. Preparation of PCM cell simulation for evaluation in observer framework. Code base review. Review and editing.

Paper D – Co-author publication

Generic Digital Twin Architecture for Industrial Energy Systems

G. Steindl, M. Stagl, L. Kasper, W. Kastner and R. Hofmann (2020). “Generic Digital Twin Architecture for Industrial Energy Systems”. *Applied Sciences* 10(24), 8903. Section “Computing and Artificial Intelligence”. Special Issue “Digital Twins and CPS (Cyberphysical Systems)”. ISSN: 2076-3417. DOI: 10.3390/app10248903

In this journal paper, concepts, architectures, and frameworks for DT in the literature were analyzed, since existing DT implementations were often application-specific solutions. Based on this, a technology-independent generic DT architecture (GDTA) was proposed. Its alignment with the information technology layers of the Reference Architecture Model Industry 4.0 (RAMI4.0) facilitates a common naming and understanding of DT instances. As proof of concept, a prototypical DT based on the architecture and demonstrating the application of semantic web technologies was instantiated. The focus of the implementation was the virtual entity of a TES, consisting of a simulation service in combination with context information as it is a fundamental service of the DT. A base service ontology and an exemplary domain ontology for simulation services were developed, providing references for other service domains. This publication built an architectural guideline for the DT platform presented in Paper 4. There, the generic DT architecture was complemented with specific guidelines for integrating the physical entity and solving technical implementation barriers.

My contribution: Conceptualization of the DT architecture and domain ontology. Preparation of the TES model for the proof of concept. Draft preparation. Review and editing.

Paper E – Co-author publication

Framework for Automated Data-Driven Model Adaption for the Application in Industrial Energy Systems

L. Prendl, L. Kasper, M. Holzegger and R. Hofmann (2021). “Framework for Automated Data-Driven Model Adaption for the Application in Industrial Energy Systems”. *IEEE Access* vol. 9, pp. 113052-113060. ISSN: 2169-3536. DOI: 10.1109/ACCESS.2021.3104058

This journal paper presented an implemented framework for automated data-driven model adaption. Communication in the whole framework is based on OPC UA and SQL. The framework was tested in simulation studies emulating cyclic TES operation under fouling. A grey box model of the TES could be automatically adapted to maintain a high prediction accuracy of TES temperature values and SOC during continuously changing physical behavior. Thus, large prediction errors were prevented. In the presented framework, data storage and handling were performed using proprietary software. Although some capabilities of this software, such as redundancy analysis and event frame classification proved suitable for industrial application, it was discarded in my subsequent work in favor of open-source applications. This paper presented an important cornerstone in evaluating the robustness and speed of the automated grey box model training as well as experience with basic communication infrastructure. In my later work, some of the framework’s elements were adapted or replaced by semantic web technology to provide a more scalable DT platform.

My contribution: Preparation of the physics-based model to emulate the TES test rig. Simulation studies. Evaluation and illustration. Drafting the paper. Contributing to sections of the original draft. Review and editing.

Paper F – Co-author publication

Development of a Digital Twin Platform for Industrial Energy Systems

P. Schwarzmayr, F. Birkelbach, L. Kasper and R. Hofmann (2022). “Development of a Digital Twin Platform for Industrial Energy Systems”. *Applied Energy Symposium: MIT A+B*. July 5-8, 2022. Cambridge, USA. DOI: 10.46855/energy-proceedings-9974

This conference paper presented the specific deployment of the five-dimensional digital twin platform established in Paper 4 to a packed bed thermal energy storage test rig. Furthermore, a use case for the TES integration in steel production processes was outlined. The DT implementation was experimentally evaluated based on the scenario of a temperature sensor failure. Without intervention, such a scenario can lead to significant errors in storage SOC calculation, propagating to other services and rendering efficient operation impossible. To overcome this issue, first, the data dimension was extended by specifying the geometric properties of the test rig while building on reused open-source ontologies.

Second, the DT platform was equipped with three simple services and workflows to interconnect the latter services. In short, the developed DT is able to compensate for a damaged sensor by an automatically created surrogate model, i.e., a soft sensor. Thus, the SOC error due to sensor failure could be reduced from up to 15 % to a maximum of 3 %. Besides the proposed transferable methodology and satisfying quantitative results, this paper also contributed to a qualitative evaluation of DT technology. It showed that the separation of the DT into five dimensions and the encapsulation of domain-specific applications as microservices facilitate cooperation in interdisciplinary teams. Thus, the DT platform presented in Paper 4 proved to be easily scalable.

My contribution: Conceptualization and set-up of the test rig. Conceptualization of the TES use case and DT services. Preparing the basic functionality of the DT platform. Programming of service endpoints and encapsulation scripts. Review and editing.

Paper G – Co-author publication

Operation planning with thermal storage units using MILP: Comparison of heuristics for approximating non-linear operating behavior

F. Birkelbach, L. Kasper, P. Schwarzmayr and R. Hofmann (2022). “Operation planning with thermal storage units using MILP: Comparison of heuristics for approximating non-linear operating behavior”. *ECOS 2023 - THE 36TH INTERNATIONAL CONFERENCE ON EFFICIENCY, COST, OPTIMIZATION, SIMULATION AND ENVIRONMENTAL IMPACT OF ENERGY SYSTEMS June 25-30, 2023. Las Palmas, Spain.*

This conference paper investigated different heuristic approximation methods for nonlinear TES behavior for use in MILP models. Two types of piecewise-linear models were considered: triangulation on a grid and general triangulation. The goal was to find the best approximation with the fewest linear pieces, thus maintaining accuracy while reducing computational complexity. The heuristics were applied to compute piecewise-linear approximations of the nonlinear operating behavior of a TES unit. The performance of these models was compared in a MILP model for the operation planning of a simple energy system. While theoretically, the non-gridded heuristic should be capable of requiring fewer simplices for the same accuracy, this was only observed for low target accuracies. Since much more efficient MILP formulations are available to incorporate gridded models, we concluded that this model type is well suited for deriving data-driven models of non-linear functions with multiple independent variables for MILP problems. I later applied this approach in the linearization service of the DT of a TES presented in Paper 5 since we found that it presents a robust basis for the adaptive virtual entity. Such robust model adaptation methodologies are essential for the accurate operational optimization of industrial energy systems that operate under harsh conditions.

My contribution: Preparing the basis MILP unit commitment formulation. Illustration, review and editing.

Presentations

Referring to the contents of this thesis, three presentations in front of scientific and industrial audiences were given:

L. Kasper, R. Hofmann: “DIGI STEAM - Digitalization and the Digital Twin in the Energy Sector”; Talk: 2. VGB digi-Tag - Umsetzung der strategischen Handlungsfelder in der Digitalisierung, Essen (invited); 2021-02-10.
<http://hdl.handle.net/20.500.12708/95469>

L. Kasper, R. Hofmann: “DIGI STEAM - Digitalization in the field of steam supply systems”; Talk: VGB Summer School Webinar 2021 - Future Energy Technologies, Würzburg (invited); 2021-08-25. <http://hdl.handle.net/20.500.12708/95470>

L. Kasper: “HyStEPs - A novel hybrid thermal energy storage prototype for efficient industrial processes”; Project video presentation on YouTube; 2022-02-12.
<https://youtu.be/DkVHha1Bi4c>

Scientific reports

As part of the IEA IETS Task XVIII on “Digitalization, Artificial Intelligence and Related Technologies for Energy Efficiency and GHG Emissions Reduction in Industry”, I contributed to two scientific reports within the scope of this thesis:

F. Birkelbach, J. Fluch, R. Jentsch, L. Kasper, A. Knapp, S. Knöttner, T. Kurz, D. Paczona, P. Schwarzmayr, E. Sharma, A. J. Tahir, C. R. Tugores and V. Zawodnik (2022). “Digital Twins: Terms & Definitions”. TU Wien. DOI: 10.34726/3802

F. Birkelbach, J. Fluch, R. Jentsch, L. Kasper, A. Knapp, S. Knöttner, T. Kurz, D. Paczona, P. Schwarzmayr, E. Sharma and V. Zawodnik (2022). Existing Digital Twin Solutions: Report on questionnaire. DOI: 10.34726/3803

Furthermore, also within the IEA IETS Task XVIII, I co-organized several scientific workshops and project presentation sessions together with my colleague Felix Birkelbach. These presentations were published on the YouTube channel “Research Unit Industrial Energy Systems - TU Wien”: <https://youtube.com/playlist?list=PLuitK2C8j5-s0PHLDMYRD7GQgNeuSZgw1>

In the course of this thesis, I worked on four additional national and international funded research projects. The public final reports of these research projects are available or can be made available via the corresponding project’s website:

HyStEPs - Hybrid storage for efficient processes; <https://www.nefi.at/de/projekt/hysteps>

DIGI STEAM - Digitalization in the energy sector: Identification of digitalization possibilities in the energy sector especially in the field of steam supply systems; TU Wien, VGB research project P429. https://www.vgbe.energy/fe429_abschlussbericht

5DIndustrialTwin - 5D Digital Twin for Industrial Energy Systems; KLIEN/FFG research project; Grant number 881140; <https://energieforschung.at/projekt/5d-digital-twin-fuer-industrielle-energiesysteme/>

SINFONIES - Sustainability IN Flexibly Operated reNewable Industrial Energy Systems; KLIEN/FFG research project; Grant number 871673; <https://energieforschung.at/projekt/sustainability-in-flexibly-operated-renewable-industrial-energy-systems/>

Supervised theses

In the course of this thesis, I have co-supervised four master's theses that made valuable contributions to my research:

T. Bacher: "Entwicklung eines Anwendungskonzeptes für einen Digitalen Zwilling am Beispiel Dampferzeuger"; Supervisor: R. Hofmann, L. Kasper; E302 - Institut für Energietechnik und Thermodynamik, 2020; final examination: 2020-06-24.
DOI: 10.34726/hss.2020.67700

C. Tubeuf: "Optimal Experimental Design for the Analysis of a Novel Hybrid Steam Storage"; Supervisor: R. Hofmann, L. Kasper, A. Schirrer; E302 - Institut für Energietechnik und Thermodynamik, 2021; final examination: 2021-03-16.
DOI: 10.34726/hss.2021.73107

M. Stagl: "Servitization of 5D-digital twins for industrial energy storage systems"; Supervisor: W. Kastner; Second advisor: R. Hofmann; Assistance: L. Kasper, G. Steindl; Computer Engineering, 2021; final examination: 2021-01-14.
DOI: 20.500.12708/79853

C. Weißegger: "Entwicklung und Anwendung einer neuartigen Methode zur Optimierung des Kautschuk Mischprozesses basierend auf Fingerprint-Diagrammen"; Supervisor: R. Hofmann, L. Kasper; E302 - Institut für Energietechnik und Thermodynamik, 2023; final examination: 2023-07-11.
DOI: 10.34726/hss.2023.105622

Awards

Parts of this work were bestowed with one scientific award:

I was awarded the *vgbe Innovation Award 2022* in the Category *future-oriented* for my work on a digital twin platform tailored to the requirements of industrial energy systems. I received this award from Dr. Georgios Stamatelopoulos, vgbe Chairman, Prof. Dr. Klaus Görner, Science Representative, and Dr. Oliver Then, vgbe Executive Managing Director, at the vgbe congress in Antwerp, September 14, 2022. This award is given by the vgbe Research Foundation for outstanding achievements by young university graduates or young professionals in the field of electricity and heat generation and storage. More information on this award is available on the vgbe website: <https://www.vgbe.energy/vgb-awards/#inno>

Teaching activity

In my function as University Assistant at the Institute of Energy Systems and Thermodynamics at TU Wien, I assisted and lectured in four courses, beginning in the summer term of 2020:

302.022. Modelling and Simulation of Thermodynamic Processes. VO, 3.0 ECTS (2020, 2021, 2022)

302.074. Numerical Process Simulation of Thermal Power Plants. VU, 2.0 ECTS (2020, 2021, 2022)

302.731. Design- and Operational Optimization. VU, 3.0 ECTS (2022)



302.737. Introduction to Industrial Energy Systems and Digital Methods. VO, 2.0 ECTS (2022)

My tasks in these courses included the preparation of lecture and exercise material, giving lectures and exercises, as well as assistance in examinations.

About the author

Lukas Kasper was born in 1994 and grew up in Hollabrunn, Austria. There, he attended secondary school and passed his final exams (Matura) with distinction. Starting in 2012, he entered TU Wien to study Technical Physics and, subsequently, the master's program in Physical Energy and Measurement Engineering. In 2019, he graduated with distinction. Alongside his studies, Lukas Kasper acquired industrial experience through internships at Andritz Hydro and Gas Connect Austria in the areas of control engineering and project management.

His interest in interdisciplinary research in the areas of energy technology, mathematical modelling and informatics led him to pursue a PhD at the Institute for Energy Systems and Thermodynamics at TU Wien, where he started as a research associate (Univ.Ass.) right after his MSc graduation in 2019. His activities in this position included teaching and active participation in national and international research projects such as HyStEPs, DigiSteam, 5DIndustrialTwin, SINFONIES and the IEA IETS Task XVIII. This thesis is based on that research.

An up-to-date list of the author's publications can be found at  <https://orcid.org/0000-0001-9474-3021>. You can follow his professional career on Linked .

